

NUMERICAL STUDY OF THE STABILITY OF A HEATED
WATER BOUNDARY LAYER

Robert Leroy Lowell

NUMERICAL STUDY OF THE STABILITY OF A HEATED,
WATER BOUNDARY LAYER

by
ROBERT L^{eroy} LOWELL, JR.
//

Submitted in partial fulfillment of the requirements
for the Degree of Doctor of Philosophy

Note: Lt. Lowell was a "Burke" scholar
Sponsored by CNET

T156961

Department of Fluid, Thermal and Aerospace Sciences

CASE WESTERN RESERVE UNIVERSITY

January, 1974

NUMERICAL STUDY OF THE STABILITY OF A HEATED,
WATER BOUNDARY LAYER

Abstract

by

ROBERT L. LOWELL, JR.

Numerical solutions are obtained to the sixth order system of disturbance equations describing the hydrodynamic stability of a laminar, heated, flat plate water boundary layer, including all mean and disturbance property variations. The results are compared with those calculated using the fourth order system of Wazzan, Okamura, and Smith [4] (which assumes only mean viscosity variation).

Both systems predict significant boundary layer stabilization (increased minimum critical Reynolds Number, decreased disturbance amplification rates, etc.) with moderate heating, but display a maximum and subsequent decrease as the plate surface-to-free stream temperature difference is further increased. Over the normal liquid range of water, the results of the sixth order calculations show only a slight enhancement of stability over those obtained from the fourth order system. Apparent gains in stability predicted when only disturbance viscosity terms are included in the calculations are offset by the further inclusion of density fluctuation terms.

The insensitivity of stability characteristics to the additional consideration of thermal disturbances is attributed to the

very limited region in which such disturbances are important for fluids of large Prandtl number such as water.

TABLE OF CONTENTS

	<u>Page</u>
ABSTRACT	ii
ACKNOWLEDGEMENTS	iv
TABLE OF CONTENTS	v
LIST OF SYMBOLS	vii
LIST OF FIGURES	xii
LIST OF TABLES	xvi
CHAPTER I. INTRODUCTION	1
CHAPTER II. FORMULATION OF THE STABILITY PROBLEM	8
2.1 Basic Assumptions and Governing Equations	8
2.2 The Mean Flow	12
2.2.1 Mean Flow Equations	14
2.2.2 Mean Flow Boundary Conditions . .	19
2.3 The Disturbance Flow	20
2.3.1 Disturbance Equations	21
2.3.2 Disturbance Boundary Conditions .	33
2.4 Disturbance Field Energy Balance	35
CHAPTER III. NUMERICAL SOLUTION OF THE STABILITY PROBLEM	42
3.1 Thermodynamic Properties and Transport Coefficients	42
3.2 Mean Equations	44
3.3 Disturbance Equations	48
CHAPTER IV. RESULTS	59
4.1 Stability Characteristics	62
4.1.1 Neutral Disturbances ($\alpha_I = 0$) . .	63
4.1.2 Amplified Disturbances ($\alpha_I < 0$) .	69
4.2 Disturbance Amplitude and Energy Dis- tributions	73
CHAPTER V. SUMMARY OF RESULTS AND CONCLUSIONS	87
LIST OF REFERENCES	90
APPENDIX A. DETAILED DERIVATION OF MEAN AND DISTURBANCE FLOW EQUATIONS	94

	<u>Page</u>
APPENDIX B. THERMODYNAMIC AND TRANSPORT COEFFICIENTS AND THEIR TEMPERATURE DERIVATIVES	111
B.1 Curve-Fitting and Derivative Determination	111
B.2 Property Temperature Variation for Water .	117
APPENDIX C. MEAN FLOW SOLUTION VARIABLES	130
APPENDIX D. THE COMPUTER PROGRAM	153
D.1 Program Description	153
D.2 Input	160
D.3 Program Listing	164
APPENDIX E. THE COMPUTER PROGRAM IN OPERATION - SELECTION OF NUMERICAL PARAMETERS	186
E.1 Boundary Layer Edge, n_{\max} , and n_{δ}	188
E.2 Step Size, h	194
E.3 Orthonormalization Angle, Ω	197
E.4 Eigenvalue Estimates, α , ω_{∞} and Re	202

LIST OF SYMBOLES

a_s	Thermal diffusivity of the wall = $\left(\frac{k}{\rho c_p} \right)_s$
B_i	Body force in the i^{th} direction.
c	Nondimensional wave speed = c^*/U
c_p	Specific heat at constant pressure
E	Eckert Number
f	Dimensional frequency.
$f(y)$	Amplitude function of the longitudinal velocity fluctuation.
F	Nondimensional mean flow stream function
\mathcal{F}	Composite amplitude function of the projected longitudinal and transverse velocity fluctuations in the direction of the disturbance wave propagation
g	Gravitational acceleration.
G	Nondimensional transverse (cross) mean flow component
Gr	Grashof Number
h	Step size.
$h(y)$	Amplitude function of the transverse velocity fluctuations
H	Nondimensional mean temperature = $\frac{T - T_\infty}{T_w - T_\infty}$
k	Thermal conductivity
$m(y)$	Amplitude function of viscosity fluctuations.
M	Falkner-Skan parameter = $\frac{x}{u_e} \frac{du_e}{dx}$

P	Mechanical pressure, defined as the negative mean normal stress and related to p_t through equation (2.5).
p_t	Thermodynamic Pressure.
Pr	Free stream Prandtl Number
r(y)	Amplitude function of density fluctuations. $U \xi^*$
Re	Reynolds Number = $\frac{U \delta}{v_\infty}$
t	Time
T	Temperature
U	Reference velocity for stability calculations, defined by equation (2.28).
\bar{u}_δ	Velocity at specified boundary layer edge.
u, v, w	Velocity components in the mutually orthogonal x, y, and z directions, respectively.
w	Composite projection of the longitudinal and transverse mean velocity components in the direction of wave propagation.
x	Longitudinal coordinate direction.
y	Normal coordinate direction
Y_o	Complex, surface-normal admittance (equation (3.19))
z	Transverse coordinate direction.
$z^{(j)}$	j^{th} complex solution vector with individual components $z_i^{(j)}$ identified in equations (2.41).
α	Nondimensional complex wave number = $\alpha^* \delta^*$
$\beta(T)$	Volumetric expansion coefficient, defined in equations (2.5).
δ	Boundary layer thickness
δ^*	Displacement thickness.

δ_{ij}	Kronecker delta
ϵ_{ij}	Rate of strain tensor
η	Density dependent similarity variable, defined in equation (2.14).
η_δ^*	$\frac{\delta^*}{x} \left(\text{Re}_x \right)^{1/2}$
η_δ	Value of η at the boundary layer edge specified for stability calculations.
η_{\max}	Value of η to which the mean boundary layer equations are solved, $\eta_{\max} > \eta_\delta$.
θ	Angle between the x coordinate direction and the direction of wave propagation.
$\kappa(y)$	Amplitude function of thermal conductivity fluctuations.
λ	Second viscosity coefficient
μ	First (dynamic) viscosity coefficient
ν	Kinematic viscosity
ξ_j	Cartesian coordinates of arbitrary orientation
$\pi(y)$	Amplitude function of pressure fluctuations
ρ	Density
σ_{ij}	Stress tensor
$\tau(y)$	Amplitude function of temperature fluctuations.
ϕ	Amplitude function of the normal velocity fluctuation
χ	Angle between the body force (gravity) vector and the y axis.
ψ	Dimensional stream function
ψ	$\tan^{-1} \frac{v_e}{u_e}$

ω	Real frequency = $\alpha c = \omega_\infty Re$
ω_∞	Nondimensional frequency = $\frac{2\pi f v_\infty}{U_\infty^2}$
Ω	Orthonormalization angle criterion

Subscripts

e	Evaluated at the boundary layer edge
I	Imaginary part of a complex quantity
o	Denotes a reference quantity
R	Real part of a complex quantity
w	Evaluated at the wall
∞	Evaluated in the free stream
*	Complex conjugate

Subscripts of a length parameters, unless otherwise identified in this List of Symbols, indicates that length has been used in forming the nondimensional group (e.g. $Re_x = \frac{Ux}{v_\infty}$).

Superscripts

- (1) for the dependent velocity and temperature related variables, denotes a time-averaged (mean) variable defined by equation (A.1)
- (2) for stability parameters, denotes division by n_δ^* (e.g. $\bar{Re} = Re/n_\delta^*$).
- ' Differentiation with respect to n .
- * A dimensional quantity. Unless otherwise specified, all expressions without this symbol are assumed to be nondimensional
- $\hat{}$ Complex fluctuation quantity introduced to simplify the disturbance flow equations.

\sim

A real disturbance quantity (e.g. $\hat{q} = \frac{1}{2} (\hat{q}_+ + \hat{q}_-)$)

\rightarrow

A vector quantity.

LIST OF FIGURES

- Figure 2.1 Coordinate system for the problem.
- 4.1 Mean velocity and temperature profiles for various T_w .
- 4.2 Comparison of neutral stability curves computed with and without thermal disturbances for various T_w (fixed $T_\infty = 60^\circ\text{F}$).
- 4.3 Comparison of $\text{Re}_{\min, \text{crit}}$ computed with and without thermal disturbances as a function of T_w (fixed T_∞).
- 4.4 Details of $\text{Re}_{\min, \text{crit}}$. calculation for $T_w = 90^\circ\text{F}$ ($T_\infty = 60^\circ\text{F}$).
- 4.5 Details of $\text{Re}_{\min, \text{crit}}$. calculation for $T_w = 200^\circ\text{F}$ ($T_\infty = 60^\circ\text{F}$).
- 4.6 Spatial amplification rates for $T_w = 90^\circ\text{F}$ ($T_\infty = 60^\circ\text{F}$).
- 4.7 Maximum amplification rate determination for $T_w = 90^\circ\text{F}$ ($T_\infty = 60^\circ\text{F}$).
- 4.8 Neutral disturbance amplitude profiles for the unheated (Blasius) boundary layer.
- 4.9 Neutral disturbance amplitude profiles for the heated boundary layer: $T_w = 90^\circ\text{F}$ and $T_\infty = 60^\circ\text{F}$.
- 4.10 Neutral disturbance amplitude profiles for the heated boundary layer: $T_w = 200^\circ\text{F}$ and $T_\infty = 60^\circ\text{F}$.
- 4.11 Energy distribution of a neutral disturbance in the unheated (Blasius) boundary layer (lower branch).
- 4.12 Energy distribution of a neutral disturbance in the unheated (Blasius) boundary layer (upper branch).
- 4.13 Energy distribution of a neutral disturbance in the heated boundary layer: $T_w = 90^\circ\text{F}$ and $T_\infty = 60^\circ\text{F}$ (lower branch).
- 4.14 Energy distribution of a neutral disturbance in the heated boundary layer: $T_w = 90^\circ\text{F}$ and $T_\infty = 60^\circ\text{F}$ (upper branch).

- Figure 4.15 Energy distribution of a neutral disturbance in the heated boundary layer: $T_w = 200^{\circ}\text{F}$ and $T_{\infty} = 60^{\circ}\text{F}$ (lower branch).
- 4.16 Energy distribution of a neutral disturbance in the heated boundary layer: $T_w = 200^{\circ}\text{F}$ and $T_{\infty} = 60^{\circ}\text{F}$ (upper branch).
- B.1 First temperature derivative of c_p as a function of temperature as obtained using different procedures.
- B.2 Variations in ρ , c_p , $\rho\mu$, and ρk with temperature.
- B.3 First and second temperature derivatives of ρ as a function of temperature.
- B.4 First and second temperature derivatives of $\rho\mu$ as a function of temperature.
- B.5 First and second temperature derivative of ρk as a function of temperature.
- B.6 Second-to-first viscosity ratio for water as a function of temperature.
- B.7 Deviation between the property-temperature variation of Kaups, et. al. (7) and that specified in Appendix B.2.
- C.1 Relationship between η and $\frac{Y}{\delta^*}$ for various wall temperatures.
- C.2 Variation of η_{δ}^* with changes in the wall temperature.
- C.3 Second velocity derivative evaluated at the wall as a function of the wall temperature.
- C.4 First derivatives of velocity and temperature evaluated at the wall as a function of wall temperature.
- C.5 Specific heat boundary layer profiles for various wall temperatures.
- C.6 Density boundary layer profiles for various wall temperatures.
- C.7 Boundary layer profiles of the first derivative of density for various wall temperatures.

- Figure C.8 Boundary layer profiles of the second derivative of density for various wall temperatures.
- C.9 Boundary layer profiles of the density-viscosity product for various wall temperatures.
- C.10 Boundary layer profiles of the first derivative of the density-viscosity product for various wall temperatures.
- C.11 Boundary layer profiles of the second derivative of the density-viscosity product for various wall temperatures.
- C.12 Boundary layer profiles of the density-thermal conductivity product for various wall temperatures.
- C.13 Boundary layer profiles of the first derivative of the density-thermal conductivity product for various wall temperatures.
- C.14 Boundary layer profiles of the second derivative of the density-thermal conductivity product for various wall temperatures.
- C.15 Boundary layer velocity profiles for various wall temperatures.
- C.16 Boundary layer profiles of the first derivative of velocity for various wall temperatures.
- C.17 Boundary layer profiles for the second derivative of velocity for various wall temperatures.
- C.18 Boundary layer temperature profiles for various wall temperatures.
- C.19 Boundary layer profiles of the first derivative of temperature for various wall temperatures.
- C.20 Boundary layer profiles of the second derivative of temperature for various wall temperatures.
- D.1 Sample input data deck for program BLSTAB.
- E.1 Influence of the Orthonormalization Angle, Ω , on the number of orthonormalizations required per iteration and on the minimum angle encountered in the last boundary layer integration.

Figure E.2 Influence of the step size on the minimum angle encountered between solution vectors on the last eigenvalue iteration for a specified Ω .

LIST OF TABLES

- Table D.1 Description of Program Routines.
- D.2 Description of Input Data for Program BLSTAB.
- E.1 The influence of included disturbance quantities and chosen property variation on an eigenvalue calculation.
- E.2 Convergence history of unknown mean flow boundary conditions, $F''(0)$ and $H'(0)$.
- E.3 Influence of η_{\max} on computed values of $F''(0)$, $H'(0)$, and η_{δ^*} .
- E.4 Influence of the arbitrarily specified boundary layer edge, η_δ , on the eigenvalue computation.
- E.5 Influence of step size, h_m , on the unspecified wall temperature and velocity gradients, $\bar{u}'(0)$ and $H'(0)$.
- E.6 Influence of the step size, h_d , on the computed eigenvalue.
- E.7 Influence of Orthonormalization Angle, Ω , on computed eigenvalue.
- E.8 Convergence history of an eigenvalue search.

CHAPTER I

INTRODUCTION

To gain some insight into the mechanism of laminar-turbulent boundary layer transition, considerable experimental and theoretical effort has been expended in studying the hydrodynamic stability of a laminar boundary layer. This work has revealed that alterations to the mean flow by pressure gradients, boundary roughness and compliancy, suction or blowing, heating and the like can cause significant changes in stability characteristics of the flow. The present study focuses on the influence of heating on the stability of a liquid boundary layer, and is motivated by the favorable effect that surface heating may have on drag reduction of submerged underwater vehicles.

An indication of the qualitative effect of surface heating can be obtained by utilizing the inviscid point-of-inflection criterion (for constant density flows velocity profiles having a point of inflection are unstable). At the surface of a flat plate, the boundary layer equations for a fluid flow with a nonconstant viscosity reduce to

$$\left(\frac{d^2 u}{dy^2} \right)_w = - \frac{1}{\mu_w} \left(\frac{du}{dy} \right)_w \left(\frac{du}{dy} \right)_w \quad (1.1)$$

If the plate is heated (such that $T_w > T_\infty$), then $(dT/dy)_w < 0$. Because the viscosity of a liquid decreases with increasing temperature ($d\mu/dT < 0$), then $(d\mu/dy)_w > 0$. Conversely, for a cooled plate ($T_w < T_\infty$), $(d\mu/dy)_w < 0$. As both μ_w and $(du/dy)_w$ are positive for either case, it follows directly that for $T_w > T_\infty$, $(d^2u/dy^2)_w < 0$. Since the curvature, (d^2u/dy^2) , is vanishingly small but negative as $y \rightarrow \infty$, it follows that if its value at the wall is positive, there must be at least one point of inflection in the boundary layer (i.e., some point at which the curvature is zero). Thus it is anticipated that heating should stabilize and cooling destabilize the liquid laminar boundary layer. This conjecture has been verified theoretically by a number of authors. (Note that it is just opposite to the conclusion reached for gases where viscosity increases with temperature).

DiPrima and Dunn [1] cite unpublished numerical results of McIntosh which indicate that for the two-dimensional Tollmien-Schlichting type of instability in a heated water boundary layer, the minimum critical Reynolds number, $Re_{min.crit.}$, is increased tenfold over the isothermal case for a $50^\circ C$ temperature difference ($T_\infty = 10^\circ C$).

Hauptmann [2] utilizes integral methods and a perturbation procedure to correlate variation in a velocity profile shape factor, arising from small changes in a temperature dependent viscosity, with the stability characteristics for a class of single parameter velocity profiles. His results also predict very strong stabilization

in water for relatively small heating, and are quite compatible with those of McIntosh cited above.

The most extensive study of the stability of a heated and cooled water boundary layer with a Falkner-Skan flow has been conducted by Wazzan, Okamura, and Smith [3,4,5] and Wazzan, Keltner, Okamura, and Smith [6]. For the disturbance equation, assuming explicit fluid property variation in only the mean viscosity and no fluctuating temperature field, they obtain for all their analyses a modified Orr-Sommerfeld equation

$$(\bar{u} - c\chi \phi'' - \alpha^2 \phi) - \bar{u}'' \phi = -\frac{i}{\alpha Re_\delta} [\bar{\mu}(\phi''' - 2\alpha^2 \phi'' + \alpha^4 \phi) + 2\bar{\mu}'(\phi''' - \alpha^2 \phi') + \bar{\mu}''(\phi'' + \alpha^2 \phi)] \quad (1.2)$$

where ' here denotes differentiation with respect to y/δ . In contrast, the variable mean-flow coefficients are obtained by solving the coupled mean momentum and energy boundary layer equations in which all fluid properties are assumed to vary [7]. In general, their results show that while cooling the wall does destabilize the flow, moderate heating very strongly stabilizes it.¹ However, as heating is increased, $Re_{min.crit.}$ reaches a maximum with T_w and then decreases. They explain this behavior as follows [5]:

¹While the results of reference [3] are qualitatively correct, they are quantitatively inaccurate due to an error in the numerical integration of equation (1.2) and subsequently have been corrected [4,5]. The first reference still provides the best explanation of the numerical procedure used.

"As T_w is increased above T_∞ , the velocity profile becomes more stable, whereas the variable viscosity term, $\bar{\mu}(\eta)$, in the modified O-S equation tends to destabilize the flow. However, at moderated rates of heating, the effects of the mean velocity profiles $\bar{u}(\eta)$ and $\bar{u}''(\eta)$ upon $Re_{min.crit.}$ are the dominant ones. As the rate of heating increases, the negative effect of $\bar{\mu}(\eta)$ upon $Re_{min.crit.}$ increases whereas the effect of heating upon $\bar{u}(\eta)$ and $\bar{u}''(\eta)$ and, in turn, their respective stabilizing effects on $Re_{min.crit.}$ begin to level off. $Re_{min.crit.}$ then reaches a maximum at $(T_w)_{crit.}$ where the effects of $\bar{\mu}(\eta)$ and $\bar{u}(\eta)$ and $\bar{u}''(\eta)$ upon $Re_{min.crit.}$ balance out. As T_w is increased beyond $(T_w)_{crit.}$, the destabilizing effect of $\bar{\mu}(\eta)$, becomes dominant and $Re_{min.crit.}$ decreases upon increasing T_w beyond $(T_w)_{crit.}$ ".

Similar results and conclusions are obtained by Potter and Gruber [8] for the stability of Plane Poiseuille water flow with heat transfer. Using for their analysis the same equation as Wazzan, et.al. and neglecting all property variation other than viscosity in the solution of the mean equations, they found that omission of the mean viscosity gradient terms from equation (1.2) indicated increased stability with heating. In contrast, inclusion of these terms show destabilization with increased heating (i.e., a decrease of $Re_{min.crit.}$).

The motivation for the present investigation stems from an attempt to more fully explain the stability anomalies found by Wazzan, Okamura, and Smith through a more complete reformulation

of the problem. Specifically, it is unclear why those authors solve the coupled mean flow system of momentum and energy equations to provide the variable coefficients for the disturbance equation (1.2), and yet neglect a disturbance energy equation coupled with the momentum equation through fluctuating fluid property variation. As an a priori estimate of the relative magnitude of all disturbance quantities and their derivatives is impossible throughout the entire boundary layer, the omission of temperature fluctuations in previously cited investigations is seemingly arbitrary and without justification in a situation involving heat transfer. Accordingly, the complete linearized, parallel flow disturbance equations (excluding only negligible expansion work and viscous dissipation) eventually will be formulated and solved.

A simple illustration substantiates the preceding contention. Assuming for the moment that the only property variation of importance is that of viscosity, it will be shown that the stability equations can be written more completely as

$$\begin{aligned}
 (\bar{u} - c)(\phi'' - \alpha^2 \phi) - \phi \bar{u}'' &= -\frac{i}{\alpha Re} \left[\bar{u} (\phi''' - 2\alpha^2 \phi'' + \alpha^4 \phi) \right. \\
 &\quad \left. + 2\bar{u}' (\phi''' - \alpha^2 \phi') + \bar{u}'' (\phi'' + \alpha^2 \phi) \right] \\
 &- \frac{1}{\alpha Re} \left[(m\bar{u}')'' + \alpha^2 m\bar{u}' \right]
 \end{aligned} \tag{1.3}$$

coupled with a disturbance energy equation

$$\tau(\bar{u} - c) + H' \phi = \frac{1}{\alpha Re Pr} [\tau'' - \alpha^2 \tau] \quad (1.4)$$

through the relation between the viscosity fluctuations, m , and the temperature fluctuations τ . Assuming further that disturbance quantities, m and ϕ , as well as their derivatives, m'' and ϕ'' , are each of comparable magnitude at some point in the boundary layer and realizing that \bar{u}' is of the same magnitude as $\bar{\mu}''$, then terms arising due to the presence of the disturbance viscosity such as $m''\bar{u}'$ and $\alpha^2 m\bar{u}'$ are likewise of comparable magnitude to terms retained by Wazzan, et.al. such as $\phi''\bar{\mu}''$ and $\alpha^2 \phi \bar{\mu}''$, and so should not be discounted in the analysis. Since Wazzan, et.al. attribute much of the stabilization to the mean viscosity gradient terms [5], it would seem as if omission of these terms is "not well justified" and it is not permissible categorically "to assume that $\tilde{T} = 0$ throughout the boundary layer" [3].

Thus the focus of the investigation is upon establishing the difference between the fourth order system of Wazzan, et.al., equation (1.2), and a more complete version of the sixth order system represented by equations (1.3) and (1.4) in which all property variation, mean and disturbance (acceptable within the locally parallel flow and boundary layer assumptions), is considered.

A complete discussion of the assumptions made in formulating the problem considered in this investigation is given in Chapter II. The assumed fluid property-temperature relationships, numerical techniques, and assessment of the numerical errors incurred in the process are discussed in Chapter III. The results of this analysis are presented in Chapter IV, and finally the conclusions drawn from these results are discussed in Chapter V. The Appendices are included to present relevant but nonessential material that would otherwise obscure the primary thrust of this investigation in the text.

CHAPTER II

FORMULATION OF THE STABILITY PROBLEM

This investigation examines the spatial stability to small-scale disturbances of the steady, laminar, boundary layer flow of a viscous, heat-conducting liquid. Since formulation of the problem can easily be made with far greater generality than is eventually required, such a procedure is followed to demonstrate that within the assumptions to be made, the additional complexities fail to significantly alter the resulting stability equations.

Thus while the problem is posed for general Falkner-Skan flows ($u_e = Cx^M$) with constant cross flows ($w_e = \text{constant}$) and arbitrary disturbance orientation, solutions discussed in Chapters VI and V are specifically for two-dimensional, flat plate boundary layers with two-dimensional disturbances. The Falkner-Skan flows are often referred to as "wedge flows" since for $M > 0$ they correspond to a uniform flow over a yawed, rigid, infinite wedge with included angle $\frac{2\pi M}{M+1}$ [9, p 141] at zero angle of attack in the neighborhood of the stagnation point.

2.1 Basic Assumptions and Governing Equations

To describe this flow field mathematically, certain basic assumptions are made concerning the nature of the fluid involved.

- (1) The characteristic scales for mean motion and

disturbances to it must be significantly greater than those associated with molecular motions in the fluid (continuum hypothesis). This permits ascription of meaningful values to fluid and flow parameters "at a point". Further, for disturbance periods ($2\pi/\omega$) much greater than the molecular time scale, say the fluid's structural relaxation time (T_s) (i.e. $\omega T_s \ll 1$), the flow can be considered to be in statistical equilibrium so that molecular transport effects can be represented by transport coefficients (μ , k , etc.).

(2) Once the continuum hypothesis is established, to define the stress relations between fluid elements, it is assumed that the fluid is Newtonian (linear stress variation with rate of strain) and isotropic (no intrinsically preferred elemental spatial orientation).

These two groups of assumptions form the foundation for the Navier-Stokes equations (2.1-2.3). Since there is no experimental evidence to suggest their inadequacy under ordinary conditions, they will be used without reservation in this analysis.

(3) Assuming the fluid to be a liquid, the form for the state equations is defined. The relative pressure independence of all fluid properties permits their expression explicitly as functions of temperature alone.

Thus, (dimensionally)

Continuity: $\frac{D\varrho}{Dt} + \varrho \epsilon_{KK} = 0 \quad (2.1)$

Momentum: $\varrho \frac{Du_i}{Dt} = \varrho B_i + \frac{\partial \sigma_{ij}}{\partial \xi_j} \quad (2.2)$

Energy: $\varrho c_p \frac{DT}{Dt} = \beta T \frac{Dp_t}{Dt} + \lambda \epsilon_{KK} + 2\mu \epsilon_{ij}^2 + \frac{\partial}{\partial \xi_j} (k \frac{\partial T}{\partial \xi_j}) \quad (2.3)$

State: $\varrho, c_p, k, \mu, \lambda = \text{function}(T) \quad (2.4)$

where $\frac{D}{Dt} = \text{material derivative} = \frac{\partial}{\partial t} + u_j \frac{\partial}{\partial \xi_j}$

$$\sigma_{ij} = \text{stress tensor} = -p_t \delta_{ij} + 2\mu \epsilon_{ij} + \lambda \epsilon_{KK} \delta_{ij}$$

$$\epsilon_{ij} = \text{rate-of-strain tensor} = \frac{1}{2} \left(\frac{\partial u_i}{\partial \xi_j} + \frac{\partial u_j}{\partial \xi_i} \right)$$

$B_i = \text{body force}$

$$\beta = \text{volumetric expansion coefficient} = -\frac{1}{\varrho} \left(\frac{\partial \varrho}{\partial T} \right)_P$$

$p - p_t = \text{"mechanical" - thermodynamic pressure}$

$$\text{difference} = -(\lambda + \frac{2}{3}\mu) \epsilon_{KK}$$

This last equation relating the mechanical pressure (negative of the mean normal stress, $-\frac{1}{3} \sigma_{KK}$) and thermodynamic pressure is valid because only the near past is considered (or $\omega T_s \ll 1$ as previously discussed [10]). Note that equations (2.2) reduce to the Navier-Stokes equations if $\frac{\lambda}{\mu} = -\frac{2}{3}$ (Stokes' hypothesis,

valid only for an ideal monatomic gas) or $\epsilon_{KK} = 0$.

For liquid in a heated boundary layer, there is no justification for assuming either statement is valid in general.

Liebermann [11] has shown that for a number of liquids, $\frac{\lambda}{\mu}$ is positive, considerably greater than unity in some cases, and widely different for different liquids. Furthermore, for low frequencies ($\omega T_s \ll 1$), Narasimham [12] notes that the viscosity ratio is independent of disturbance frequency, and almost independent of temperature [13]. (For water, Pinkerton [14] has shown a $\frac{\lambda}{\mu}$ variation of about 16% over the range 0-60°C as compared with a μ variation of 118% over the same range - see Figures B.2 and B.6). Alternatively, for flows with heat transfer (particularly cases with large thermal gradients), when the density is identified as a function of temperature, it will not be constant in that flow field. In such a situation, then ϵ_{KK} will vanish only at a rigid surface for steady flows. Thus if relatively large amplitude density fluctuations were expected in a liquid for which $\frac{\lambda}{\mu}$ was large (e.g., for benzene, this ratio is $0(10^2)$ [11], then there could be a large disparity between mechanical and thermodynamic pressures. It will be shown in Appendix A and Section 2.3.1 that for values of $\frac{\lambda}{\mu}$ of order unity, the stability problem can be solved independently of this quantity.

When the flow is characterized by a single time scale, namely that associated with the frequency of the small, rapid perturbations on the basic flow, each of the flow and transport parameters can

be constructed as the sum of a time-averaged mean and a fluctuating component,

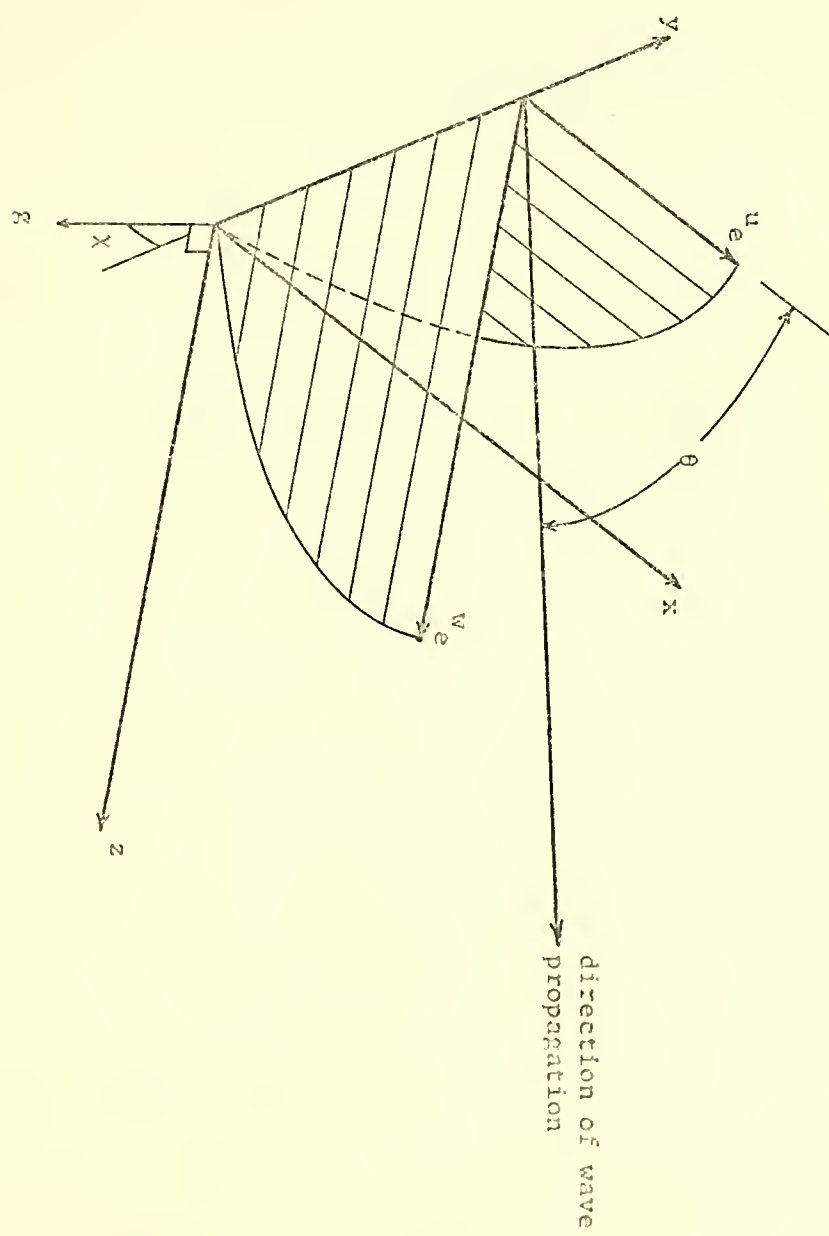
$$Q_i(\xi_j, t) = \bar{Q}_i(\xi_j) + \tilde{Q}_i(\xi_j, t) \quad (2.6)$$

Equations describing the behavior of these components are developed in sections 2.2 and 2.3, respectively.

2.2 The Mean Flow

The mean equations for boundary layer flow over a wedge can be deduced from equations (2.1-2.3) (see Appendix A) after choosing the orthogonal coordinate system shown in figure 2.1 and making the following simplifying assumptions:

- (1) The basic flow is steady but not necessarily spatially homogeneous (eqn. 2.6), so the mean equations evolve from a time-average of the instantaneous equations.
- (2) In the momentum equations for motion parallel to the surface, viscous and inertial forces are of the same order of magnitude. Using the scaling resulting from this requirement and eliminating terms of $O(\text{Re}_\delta^{-1})$ or smaller, boundary layer equations are obtained.
- (3) The wedge is "infinite" in extent in the z direction, so all mean flow variation is independent of the z coordinate.
- (4) Gravity is the only body force present, acting in a plane normal to the z axis at an angle χ to the y axis.



see reference [15]

Figure 2.1 Coordinate system for the stability analysis of a general three-dimensional boundary layer flow.

Additional simplifications leading to exclusion of specific effects on the flow (e.g., dissipation, compression energy, buoyancy) will be made after examining relevant nondimensional coefficients.

2.2.1 Mean Flow Equations

Using the assumptions discussed in section 2.2, equations (2.1-2.3) reduce to the (time-averaged) mean boundary layer equations (dimensionally)

$$\text{Continuity: } \frac{\partial \bar{\rho} \bar{u}}{\partial x} + \frac{\partial \bar{\rho} \bar{v}}{\partial y} = 0 \quad (2.7)$$

$$\begin{aligned} \text{Momentum: } \bar{\rho} \left(\bar{u} \frac{\partial \bar{u}}{\partial x} + \bar{v} \frac{\partial \bar{u}}{\partial y} \right) &= -\bar{\rho} g \sin \chi - \frac{d \bar{P}_t}{dx} \\ &\quad + \frac{\partial}{\partial y} \left(\bar{\mu} \frac{\partial \bar{u}}{\partial y} \right) \end{aligned} \quad (2.8)$$

$$\frac{\partial \bar{P}_t}{\partial y} = 0 \quad (2.9)$$

$$\bar{\rho} \left(\bar{u} \frac{\partial \bar{w}}{\partial x} + \bar{v} \frac{\partial \bar{w}}{\partial y} \right) = \frac{\partial}{\partial y} \left(\bar{\mu} \frac{\partial \bar{w}}{\partial y} \right) \quad (2.10)$$

$$\begin{aligned} \text{Energy: } \bar{\rho} C_p \left(\bar{u} \frac{\partial \bar{T}}{\partial x} + \bar{v} \frac{\partial \bar{T}}{\partial y} \right) &= \bar{\rho} \bar{T} \bar{u} \frac{d \bar{P}_t}{dx} \\ &\quad + \bar{\mu} \left[\left(\frac{\partial \bar{u}}{\partial y} \right)^2 + \left(\frac{\partial \bar{w}}{\partial y} \right)^2 \right] + \frac{\partial}{\partial y} \left(\bar{k} \frac{\partial \bar{T}}{\partial y} \right) \end{aligned} \quad (2.11)$$

Before solving, several modifications are made to the x momentum equation. Evaluation of this equation at the boundary layer edge reveals the nature of the mean pressure variation impressed on the boundary layer (dimensionally)

$$-\frac{d\bar{P}_t}{dx} = \rho_\infty \bar{u}_e \frac{d\bar{u}_e}{dx} + \rho_\infty g \sin \chi \quad (2.12)$$

Further, due to the state equation (2.4), the density can be expanded in a Taylor series in temperature, so dimensionally

$$\bar{\rho}(\bar{T}^*) = \rho_\infty + (\bar{T}^* - T_\infty) \left(\frac{d\bar{\rho}}{dT^*} \right)_{T=T_\infty} + \frac{(\bar{T}^* - T_\infty)^2}{2} \left(\frac{d^2\bar{\rho}}{dT^{*2}} \right)_{T=T_\infty} + \dots$$

or nondimensionally, using the volumetric expansion coefficient, β , defined in equations (2.5),

$$1 - \bar{\rho}(\bar{T}) = \rho_\infty T_\infty (\bar{T} - 1) \left\{ 1 + \frac{(\bar{T} - 1)}{2} \left[\left(\frac{d\beta}{dT} \right)_{T=T_\infty} + \rho_\infty T_\infty \right] + \dots \right\}$$

For small values of $\beta_\infty T_\infty$ and $\frac{T_\infty - 1}{T_\infty}$ (such as is the case for water with moderate temperature differences), this can well be approximated by

$$1 - \bar{\rho}(\bar{T}) = \rho_\infty T_\infty (\bar{T} - 1) \quad (2.13)$$

Thus, with the modifications indicated by equations (2.12) and (2.13), the x momentum equation finally becomes (dimensionally)

$$\begin{aligned} \bar{\rho} \left(\bar{u} \frac{\partial \bar{u}}{\partial x} + \bar{v} \frac{\partial \bar{u}}{\partial y} \right) &= \rho_\infty u_e \frac{du_e}{dx} + \rho_\infty \rho_\infty g \sin \chi (\bar{T} - T_\infty) \\ &\quad + \frac{\partial}{\partial y} \left(\bar{u} \frac{\partial \bar{u}}{\partial y} \right) \end{aligned} \quad (2.8a)$$

Since all fluid properties are assumed to be variable, particularly density, a modified Howarth-Dorotnitsyn transformation is suggested [7], reducing the boundary layer equations to a nearly incompressible form. The required independent variables are

$$\begin{aligned} X &= X \\ \eta &= \sqrt{\frac{U_e}{\nu_\infty X^*}} \int_0^{Y^*} \bar{\rho} dy^* \end{aligned} \quad (2.14)$$

Satisfaction of the continuity equation is accomplished by introducing a dimensional stream function ψ^* such that

$$\bar{\rho}^* \bar{u}^* = \frac{\partial \psi^*}{\partial y^*}$$

$$\bar{\rho}^{*\prime} \bar{u}^* = - \frac{\partial \psi^*}{\partial x^*}$$

and a nondimensional stream function F so that

$$\bar{u}^* = U_e^* F' \quad (2.15)$$

where the two are related by

$$\Psi^* = (\rho_\infty \mu_\infty X^* U_e^*)^{\frac{1}{2}} F$$

Defining the displacement thickness

$$\delta^* = \int_0^\infty (1 - \bar{\rho} \bar{u}) dy^* \quad (2.16)$$

or in transformed variables

$$\delta^* = \sqrt{\frac{V_\infty X^*}{U_e}} \int_0^\infty \left(\frac{1}{\bar{\rho}} - \bar{u} \right) d\eta \quad (2.16a)$$

then

$$\sqrt{\frac{U_e}{V_\infty X}} = \frac{\eta \delta^*}{\delta^*} \quad (2.17)$$

where

$$\gamma_{\delta^*} = \int_0^\infty \left(\frac{1}{\bar{\rho}} - \bar{u} \right) d\eta , \quad (2.18)$$

a constant for specified wall and free stream temperature and wedge angles.

Additionally, defining

$$\begin{aligned} \bar{T}^* &= (T_w - T_\infty) H + T_\infty \\ \bar{w}^* &= w_e G(\eta) \end{aligned}$$

then equations (2.7, 2.8a, 2.10, and 2.11) transform to

$$\begin{aligned} (\bar{\rho} \bar{u} F'')' + M \left(\frac{1}{\bar{\rho}} - F'^2 \right) + \left(\frac{M+1}{2} \right) F F'' + \frac{\bar{G}_r}{\bar{R}_e} \frac{H}{\bar{\rho}} \sin \chi &= 0 \\ (\bar{\rho} \bar{u} G')' + \left(\frac{M+1}{2} \right) F G' &= 0 \\ \left(\bar{\rho} \bar{k} \bar{T}' \right)' + Pr \bar{c}_p \left(\frac{M+1}{2} \right) + Pr E \left\{ \bar{\rho} \bar{u} \left[F''^2 \right. \right. \\ \left. \left. + \left(\frac{w_e}{U_e} \right)^2 G'^2 \right] + \left[\left(\frac{T_\infty}{T_w - T_\infty} \right) \frac{\bar{G}_r}{\bar{R}_e} \sin \chi \right. \right. \\ \left. \left. - (P_w T_\infty) M \right] \frac{\bar{\rho}}{\bar{\rho}} \bar{T} F' \right\} &= 0 \end{aligned} \quad (2.19)$$

where

$$\overline{Re} = \text{Reynolds Number} = \frac{U_e \delta^*}{\nu_\infty \eta_{\delta^*}}$$

$$\overline{Gr} = \text{Grashof Number} = \frac{\beta_\infty g (T_w - T_\infty) \delta^{*3}}{\nu_\infty^2 \eta_{\delta^*}^3}$$

$$E = \text{Eckert Number} = \frac{U_e}{c_{P_\infty} T_\infty}$$

$$Pr = \text{Prandtl Number} = \frac{c_{P_\infty} / \mu_\infty}{K_\infty}$$

$$M = \frac{x}{U_e} \frac{du_e}{dx} = \text{constant since } u_e \text{ is of the form } u_e \propto x^M \text{ for the wedge flow.}$$

At this point an assessment is made of the various force and energy terms of the above equations to determine their influence in establishing the mean velocity and temperature boundary layer profiles, with the following conclusions.

(1) Buoyancy effects can be neglected if $\frac{\overline{Gr}}{\overline{Re}} \sin \chi \ll 1$.

This is easily accomplished analytically by requiring

(a) the surface normal be parallel with the gravity vector so that $\chi = 0$, or

(b) for large χ angles (i.e. $\sin \chi = O(1)$), u_e be sufficiently large that $\frac{\overline{Gr}}{\overline{Re}} \ll 1$, since this parametric group varies inversely with u_e^2 . Thus, except for surface orientations nearly parallel to the gravity vector and low speeds, free convection can be neglected.

(2) Dissipation and expansion (or pressure) work are negligible, requiring that $Pr E \ll 1$. (An estimate of these terms for a water flow indicate that they can never be significant while the boundary layer approximation remains valid).

As a consequence of these assumptions, the boundary layer equations (2.19) are explicitly independent of x . The original set of partial differential equations has been transformed to one of ordinary differential equations, so the velocity and temperature profiles are given by similarity solutions.

The mean flow equations can be written finally as

$$\begin{aligned} \left(\bar{\rho} \bar{\mu} F'' \right)' + M \left(\frac{1}{\bar{\rho}} - F'^2 \right) + \left(\frac{M+1}{2} \right) FF'' &= 0 \\ \left(\bar{\rho} \bar{\mu} G' \right)' + \left(\frac{M+1}{2} \right) FG' &= 0 \\ \left(\bar{\rho} \bar{k} H' \right)' + Pr \bar{C}_P \left(\frac{M+1}{2} \right) FH' &= 0 \end{aligned} \quad (2.20)$$

Note that the z momentum equation is not coupled with the other two; that is, F and H are determined independently of G provided $\bar{\rho}$, $\bar{\mu}$, and \bar{k} are also independent of G .

2.2.2 Mean Flow Boundary Conditions

The boundary layer equations in section 2.2.1 are supplemented with the following boundary conditions:

$$\begin{aligned} \text{at } y = 0 \quad \bar{u}^* &= \bar{w}^* = 0 \quad (\text{no slip at the wall}) \\ \bar{v}^* &= 0 \quad (\text{impermeable wall surface}) \\ \bar{T}^* &= T_w \quad (\text{constant wall temperature}) \end{aligned} \quad (2.21)$$

$$\text{as } y \rightarrow \infty \quad \overline{u}^* \xrightarrow{e} u_e^*(x)$$

$$\overline{w}^* \xrightarrow{e} w_e^*$$

$$\overline{T}^* \xrightarrow{\infty} T_\infty$$

Note that although u_e may vary with x due to a nonzero wedge angle, the free stream temperature (identical with that at the boundary layer edge) is assumed constant.

In terms of the transformed variables, these conditions become

$$\text{at } \eta = 0 \quad F' = G = 0$$

$$F = 0$$

$$H = 1 \quad (2.21a)$$

$$\text{as } \eta \rightarrow \infty \quad F' \rightarrow 1$$

$$G \rightarrow 1$$

$$H \rightarrow 0$$

2.3 The Disturbance Flow

The disturbance equations are obtained as the difference between the instantaneous and mean equations (see Appendix A). Simplification is accomplished by the following considerations.

(1) Consistent with the assumptions of section 2.2, "infinitesimal" disturbance amplitudes permit linearization of the disturbance equations. (Note that all terms of this order vanished in taking the mean). This of course eliminates terms with correlated disturbance quantities (as for the mean equations) and

reduces the disturbance equations to a set of linear, partial differential equations with nonconstant mean flow coefficients.

(2) The mean boundary layer flow is assumed to be locally parallel, so that for a specified distance from the leading edge, x , these coefficients of the disturbance quantities are functions only of the distance normal to the solid surface, y . That is, the stability of a velocity profile at a given x is to be considered independently of the rest of the boundary layer. The requirements necessary to make such an assumption are elucidated in Appendix A and briefly summarized below. When the amplitude of all disturbances and derivatives of disturbances are equal (though not necessarily equal to each other), comparison of the mean flow coefficients in a boundary layer sense indicates that $\bar{v}^* \ll \bar{u}^*$, \bar{w}^* and $\frac{\partial \bar{Q}}{\partial x} \ll \frac{\partial \bar{Q}}{\partial y}$. Furthermore, if disturbance wave lengths are small compared with lengths characterizing changes with x of mean quantities, then these quantities can be considered to be slowly varying functions of x compared with the fluctuations.

Again, the disturbance equations are formulated as generally as possible within the framework of assumptions specified above. Elimination of other terms by examining the magnitudes of their dimensionless coefficients will lead to additional simplifications.

2.3.1 Disturbance Equations

With the assumptions discussed in section 2.3 the disturbance equations for this problem become (dimensionally)

Continuity:

$$\frac{\partial \tilde{\rho}}{\partial t} + \bar{u} \frac{\partial \tilde{\rho}}{\partial x} + \bar{w} \frac{\partial \tilde{\rho}}{\partial z} + \bar{\rho} \left(\frac{\partial \tilde{u}}{\partial x} + \frac{\partial \tilde{v}}{\partial y} + \frac{\partial \tilde{w}}{\partial z} \right) + \tilde{v} \frac{d\bar{\rho}}{dy} = 0 \quad (2.22)$$

Momentum:

$$\begin{aligned} \bar{\rho} \left(\frac{\partial \tilde{u}}{\partial t} + \bar{u} \frac{\partial \tilde{u}}{\partial x} + \tilde{v} \frac{d\bar{u}}{dy} + \bar{w} \frac{\partial \tilde{u}}{\partial z} \right) &= \tilde{\rho} g \sin \chi - \frac{\partial \tilde{p}_t}{\partial x} \\ &+ \frac{\partial}{\partial x} \left[2\bar{\mu} \frac{\partial \tilde{u}}{\partial x} + \bar{\lambda} \left(\frac{\partial \tilde{u}}{\partial x} + \frac{\partial \tilde{v}}{\partial y} + \frac{\partial \tilde{w}}{\partial z} \right) \right] \\ &+ \frac{\partial}{\partial y} \left[\bar{\mu} \frac{d\bar{u}}{dy} + \bar{u} \left(\frac{\partial \tilde{u}}{\partial y} + \frac{\partial \tilde{v}}{\partial x} \right) \right] + \bar{\mu} \frac{\partial}{\partial z} \left[\frac{\partial \tilde{u}}{\partial z} + \frac{\partial \tilde{w}}{\partial x} \right] \end{aligned} \quad (2.23)$$

$$\begin{aligned} \bar{\rho} \left(\frac{\partial \tilde{v}}{\partial t} + \bar{u} \frac{\partial \tilde{v}}{\partial x} + \bar{w} \frac{\partial \tilde{v}}{\partial z} \right) &= \tilde{\rho} g \cos \chi - \frac{\partial \tilde{p}_t}{\partial y} \\ &+ \bar{\mu} \frac{\partial}{\partial x} \left[\frac{\partial \tilde{u}}{\partial y} + \frac{\partial \tilde{v}}{\partial x} \right] + \frac{\partial}{\partial y} \left[2\bar{\mu} \frac{\partial \tilde{v}}{\partial y} + \bar{\lambda} \left(\frac{\partial \tilde{u}}{\partial x} + \frac{\partial \tilde{v}}{\partial y} + \frac{\partial \tilde{w}}{\partial z} \right) \right] \\ &+ \frac{d\bar{u}}{dy} \frac{\partial \tilde{u}}{\partial x} + \frac{d\bar{w}}{dy} \frac{\partial \tilde{u}}{\partial z} + \bar{\mu} \frac{\partial}{\partial z} \left[\frac{\partial \tilde{v}}{\partial z} + \frac{\partial \tilde{w}}{\partial y} \right] \end{aligned} \quad (2.24)$$

$$\begin{aligned} \bar{\rho} \left(\frac{\partial \tilde{w}}{\partial t} + \bar{u} \frac{\partial \tilde{w}}{\partial x} + \tilde{v} \frac{d\bar{w}}{dy} + \bar{w} \frac{\partial \tilde{w}}{\partial z} \right) &= - \frac{\partial \tilde{p}_t}{\partial z} \\ &+ \bar{\mu} \frac{\partial}{\partial x} \left[\frac{\partial \tilde{w}}{\partial x} + \frac{\partial \tilde{u}}{\partial z} \right] + \frac{\partial}{\partial y} \left[\bar{\mu} \frac{d\bar{w}}{dy} + \bar{u} \left(\frac{\partial \tilde{u}}{\partial z} + \frac{\partial \tilde{w}}{\partial y} \right) \right] \\ &+ \frac{\partial}{\partial z} \left[2\bar{\mu} \frac{\partial \tilde{w}}{\partial z} + \bar{\lambda} \left(\frac{\partial \tilde{u}}{\partial x} + \frac{\partial \tilde{v}}{\partial y} + \frac{\partial \tilde{w}}{\partial z} \right) \right] \end{aligned} \quad (2.25)$$

Energy:

$$\begin{aligned}
 & \bar{\rho} \bar{c}_P \left(\frac{\partial \tilde{T}}{\partial t} + \bar{u} \frac{\partial \tilde{T}}{\partial x} + \tilde{v} \frac{d \tilde{T}}{dy} + \bar{w} \frac{\partial \tilde{T}}{\partial z} \right) \\
 &= \bar{\rho} \bar{T} \left(\frac{\partial \tilde{P}_t}{\partial t} + \bar{u} \frac{\partial \tilde{P}_t}{\partial x} + \bar{w} \frac{\partial \tilde{P}_t}{\partial z} \right) + \tilde{u} \left[\left(\frac{d \bar{u}}{dy} \right)^2 + \left(\frac{d \bar{w}}{dy} \right)^2 \right] \\
 &+ 2\bar{u} \left[\frac{d \bar{u}}{dy} \left(\frac{\partial \tilde{v}}{\partial x} + \frac{\partial \tilde{u}}{\partial y} \right) + \frac{d \bar{w}}{dy} \left(\frac{\partial \tilde{w}}{\partial y} + \frac{\partial \tilde{v}}{\partial z} \right) \right] \\
 &+ \bar{K} \left(\frac{\partial^2 \tilde{T}}{\partial x^2} + \frac{\partial^2 \tilde{T}}{\partial z^2} \right) + \frac{\partial}{\partial y} \left(\bar{K} \frac{\partial \tilde{T}}{\partial y} + \tilde{K} \frac{d \tilde{T}}{dy} \right)
 \end{aligned} \tag{2.26}$$

Notice that by virtue of the parallel flow assumptions, the mean flow coefficients of all disturbance terms are functions of y only, so these equations are now separable in terms of solutions of the form

$$\hat{Q} = \hat{g} e^{i \alpha^* (x^* \cos \Theta + z^* \sin \Theta - c^* t^*)}$$

Noting that the assumed disturbance form is complex (with complex amplitude function \hat{g}) while the disturbance equations (2.22-2.26) are not, physical quantities can later be recovered by taking the real part of the complex solution. Thus, the disturbances are assumed to be sinusoidal waves of frequency $\omega^* = \alpha^* c^*$ propagating at an angle Θ to the x axis. For this spatial analysis, ω^* is assumed real and α^* complex to admit solutions which are temporally only oscillatory but spatially amplified ($\alpha_I^* < 0$), neutral ($\alpha_I^* = 0$),

or damped ($\alpha_I^* > 0$).

Such a formulation will reduce the set of disturbance equations from partial differential equations to ordinary ones in \bar{y} . Thus introducing

$$\left. \begin{array}{l} \hat{u}^* = u_e f(\bar{y}) \\ \hat{v}^* = U \frac{\alpha^* \delta^*}{\eta^*} \phi(\bar{y}) \\ \hat{w}^* = w_e h(\bar{y}) \\ \hat{p}^* = \rho_\infty U^2 \pi(\bar{y}) \\ \hat{p}_t^* = \rho_\infty U^2 \pi_t(\bar{y}) \\ \hat{T}^* = (T_w - T_\infty) \tau(\bar{y}) \\ \hat{\mu}^* = \mu_\infty m(\bar{y}) \\ \hat{r}^* = \rho_\infty r(\bar{y}) \\ \hat{K}^* = K_\infty K(\bar{y}) \end{array} \right\} \cdot \exp [i \alpha^* (x^* \cos \theta + z^* \sin \theta - c^* t^*)] \quad (2.27)$$

where

$$U = u_e(x) \cos \theta + w_e \sin \theta \quad (2.28)$$

and defining for the mean and disturbance velocities parallel to the surface, respectively,

$$f = \frac{f(\bar{y}) + h(\bar{y}) \tan \psi \tan \theta}{1 + \tan \psi \tan \theta} \quad (2.29)$$

and

$$W = \frac{\bar{u}(\bar{y}) + \bar{w}(\bar{y}) \tan \psi \tan \theta}{1 + \tan \psi \tan \theta} \quad (2.30)$$

where $\tan \Psi = \frac{\frac{w}{e}}{\frac{u}{e}}$ and θ is the angle between the x axis and the direction of wave propagation, then the disturbance equations become:

Continuity

$$\frac{i\tau(w-c)}{\bar{\rho}} + i\mathcal{F} + (\bar{\rho}\phi)' = 0 \quad (2.31)$$

Momentum

$$\begin{aligned} i\mathcal{F}(w-c) + (\bar{\rho}\phi)w' &= -\frac{\overline{Gr}}{\bar{\alpha}\overline{Re}^2}\bar{\rho}\tau \sin\chi \cos\theta \\ &- \frac{i\pi_t}{\bar{\rho}} + \frac{i\bar{\alpha}}{\overline{Re}\bar{\rho}} \left[2i\mathcal{F}\bar{u} + \bar{\lambda}(i\mathcal{F} + \bar{\rho}\phi') \right] \\ &+ \frac{1}{\bar{\alpha}\overline{Re}} \left[\bar{\rho}^m w' + \bar{\rho}\bar{u} \left(\mathcal{F}' + \frac{i\bar{\alpha}^2(\bar{\rho}\phi)}{\bar{\rho}^2} \right) \right]' \end{aligned} \quad (2.32)$$

and

$$\begin{aligned} i\bar{\alpha}^2(\bar{\rho}\phi)w-c &= -\frac{\overline{Gr}}{\overline{Re}^2}\bar{\rho}\bar{\rho} \cos\chi \tau - \bar{\rho}\pi'_t \\ &+ \frac{i\bar{\alpha}}{\overline{Re}} \bar{\rho}\bar{u} \left[\mathcal{F}' + \frac{i\bar{\alpha}^2(\bar{\rho}\phi)}{\bar{\rho}^2} \right] + \frac{i\bar{\alpha}}{\overline{Re}} \bar{\rho}^m w' \\ &+ \frac{\bar{\alpha}}{\overline{Re}\bar{\rho}} \left[2\bar{\rho}\bar{u}\phi' + \bar{\lambda}(i\mathcal{F} + \bar{\rho}\phi') \right]' \end{aligned} \quad (2.33)$$

Energy

$$\bar{c}_p \left[i(w-c)\tau + (\bar{\rho}\phi)H' \right] = -(\rho_\infty T_\infty) E i \bar{\rho} \bar{T} \frac{(w-c)}{\bar{\rho}} \pi_t \\ + \frac{E}{\bar{\alpha} \bar{R}_e} \left\{ \bar{\rho}^m \left[\left(\frac{U_e}{U} \right)^2 \bar{U}'^2 + \left(\frac{W_e}{U} \right)^2 \bar{W}'^2 \right] + 2\bar{\rho} \bar{U} \left[\left(\frac{U_e}{U} \right)^2 \bar{U}' f' + \left(\frac{W_e}{U} \right)^2 \bar{W}' h' \right. \right. \\ \left. \left. + \frac{i\bar{\alpha}^2}{\bar{\rho}^2} (\bar{\rho}\phi) w' \right] \right\} + \frac{1}{\bar{\alpha} \bar{R}_e \bar{P}_r} \left\{ \left[\bar{\rho} \bar{k} \tau' + \bar{\rho} \kappa H' \right]' - \frac{\bar{\alpha}^2}{\bar{\rho}^2} \bar{\rho} \bar{k} \tau \right\} \quad (2.34)$$

where differentiation is again with respect to η to permit information obtained from the mean equations to be used directly in the numerical solution of the disturbance equations, and where all fluid property variation is of the form

$$\hat{g} = \frac{g_\infty}{T_\infty} \frac{d\bar{Q}}{dT} \hat{\tau} = g_\infty \frac{d\bar{Q}}{dH} \tau e^{i\alpha^*(x^* \cos \theta + z^* \sin \theta - c^* t^*)} \quad (2.35)$$

The dimensionless wave number and Reynolds number are defined by

$$\bar{\alpha} = \frac{\alpha^* \delta^*}{\eta_{\delta^*}}$$

and

$$\bar{R}_e = \frac{U \delta^*}{V_\infty \eta_{\delta^*}}$$

Note that the composite $x-z$ momentum equation is obtained by multiplying the transformed x and z momentum equations by $\cos \theta$ and $\sin \theta$, and then adding. Furthermore, dilatary expansion energy

drops out of the energy equation with linearization, and so must be considered a second order effect for this problem.

To simplify these equations further, the assumptions made in section 2.2.1 regarding buoyancy, dissipation and expansion energy are used again, with some interesting implications.

(1) Neglect of the dissipation energy terms (for $\frac{\bar{E}}{\alpha \bar{R}_e} \ll 1$) permits the energy equation to be written as a function of \mathcal{F} and W rather than f , h , \bar{u} , and \bar{w} , thereby reducing the order of the system of equations by two from eight to six. In other words, when viscous dissipation is negligible in the disturbance energy equation then "the stability of a three-dimensional boundary layer to a plane-wave disturbance of arbitrary orientation reduces to a two-dimensional stability problem governed by the boundary-layer profile in the direction of wave propagation and by the mean temperature profile"[15]. Thus, alterations of the external flow due to changes in pressure gradient or cross flow would be manifest as changes to the variable coefficients in the disturbance equations.

(2) When the expansion energy is negligible ($\beta_\infty T_\infty E \ll 1$), variation of the thermodynamic pressure appears only in the momentum equations. Under these circumstances, explicit inclusion of the second viscosity coefficient, $\bar{\lambda}$, in the momentum equations can be avoided by using the "mechanical" rather than thermodynamic pressure. Such a change would not affect the mean pressure, for using equation (2.5) and the "parallel-flow" and linearity assumptions, $\bar{P}_t = \bar{p}$; however, it would result in a difference between the two

fluctuation pressures $\tilde{p} - \tilde{p}_t = (\bar{\lambda} + \frac{2}{3}\bar{\mu})(\frac{\partial \tilde{u}}{\partial x} + \frac{\partial \tilde{v}}{\partial y} + \frac{\partial \tilde{w}}{\partial z}) \neq 0$

or, in terms of equations (2.27)

$$\Pi - \Pi_t = \frac{\bar{\alpha}}{\bar{R}e} / \bar{\mu} \left[\frac{\bar{\lambda}^*}{\bar{\mu}^*} + \frac{2}{3} \right] \left(\frac{\bar{\rho}'}{\bar{\epsilon}} \bar{\rho} \phi + i r \frac{(w - c)}{\bar{\epsilon}} \right) \quad (2.36)$$

As noted before, for the large Reynolds and small wave numbers anticipated, this pressure difference could only be significant for large values of $\bar{\lambda}^*/\bar{\mu}^*$.

On the other hand, if the expansion energy is not negligible (say, $(\beta_\infty T_\infty)E \sim 0(1)$), the appearance of λ can still be avoided in the momentum equations. Elimination of the thermodynamic pressure fluctuations between the two momentum equations (2.33) yields a vorticity equation - an Orr-Sommerfeld type equation modified by the inclusion of fluid property terms - in which terms containing λ identically cancel [16]. However, this procedure would require evaluation of higher order temperature derivatives of the fluid properties. Since the equations will ultimately be reduced to a system of first order equations for solution, such a step should be avoided if possible.

In short, the second viscosity coefficient should influence only the disturbance thermodynamic pressure distribution. For water flow, it has already been noted that E must be very much less than unity, so the first procedure for eliminating λ is utilized for this analysis.

(3) Buoyancy effects are negligible ($-\frac{\bar{G}_r}{\bar{\alpha} \bar{R}e^2} \ll 1$).

Since the assumption was made in solving for the mean equations that buoyancy terms of order $\bar{Gr}/\bar{Re} \ll 1$, it is certainly reasonable to assume that the body force influence with terms now of order $(\bar{Gr}/\bar{\alpha}\bar{Re})^2$ is even less significant. If buoyant effects were to be included, their contribution would appear indirectly through modifications to the mean velocity and temperature profiles. Although it is known that for flows driven primarily by body forces, heating from above stabilizes while heating from below destabilizes the flow through the influence of thermal instabilities, this effect will not be considered herein.

Thus with the assumptions discussed above, the disturbance equations finally become:

Continuity: $\frac{i r (W - c)}{\bar{\rho}} + i \mathcal{F} + (\bar{\rho} \phi)' = 0 \quad (2.37)$

Momentum:

$$i \mathcal{F}(W - c) + (\bar{\rho} \phi) W' = -i \frac{\pi}{\bar{\rho}} + \frac{i \bar{\alpha}}{\bar{\alpha} \bar{R}_e} \left\{ 2i \mathcal{F} + \frac{2}{3} \left[i r \left(\frac{W - c}{\bar{\rho}} + \frac{\bar{\rho}'}{\bar{\rho}} (\bar{\rho} \phi) \right) \right] \right\} + \frac{1}{\bar{\alpha} \bar{R}_e} \left\{ \bar{\rho}^m W' + \bar{\rho} \bar{\mu} \left[\mathcal{F}' + \frac{i \bar{\alpha}^2 (\bar{\rho} \phi)}{\bar{\rho}^2} \right] \right\} \quad (2.38)$$

$$i \bar{\alpha}^2 (\bar{\rho} \phi) (W - c) = -\bar{\rho} \pi' + i \frac{\bar{\alpha}}{\bar{R}_e} \left\{ \bar{\rho} \bar{\mu} \left[\mathcal{F}' + \frac{i \bar{\alpha}^2 (\bar{\rho} \phi)}{\bar{\rho}^2} \right] + \bar{\rho}^m W' \right\} + \bar{\rho} \frac{\bar{\alpha}}{\bar{R}_e} \left\{ \bar{\mu} \left(-2i \mathcal{F} - \frac{4}{3} \left[\frac{i r (W - c)}{\bar{\rho}} + \frac{\bar{\rho}'}{\bar{\rho}} (\bar{\rho} \phi) \right] \right) \right\}' \quad (2.39)$$

Energy:

$$\bar{c}_p \left[i(W-c)\tau + (\bar{\rho}\phi)H' \right] = \frac{1}{\bar{\alpha}RePr} \left\{ (\bar{\rho}\bar{k}\tau' + \bar{\rho}\kappa H')' - \frac{\bar{\alpha}^2}{\bar{\rho}^2} (\bar{\rho}\bar{k})\tau \right\} \quad (2.40)$$

Since these equations are not in a form suitable for numerical integration, they are rearranged and recast as a system of six, first-order equations. Denoting the dependent variables as

$$\begin{aligned} Z_1 &= \bar{\rho}\phi & Z_4 &= \pi \\ Z_2 &= \mathcal{F} & Z_5 &= \mathcal{F}' \\ Z_3 &= \tau & Z_6 &= \tau' \end{aligned} \quad (2.41)$$

the six equations can be written as

$$Z_j' = \sum_{k=1}^6 C_{jk} Z_k \quad (2.42)$$

where C_{jk} is a 6×6 coefficient matrix with the following nonzero terms:

$$C_{12} = -i$$

$$C_{13} = -i \frac{d\bar{\rho}}{dH} \frac{(W-c)}{\bar{\rho}}$$

$$C_{25} = 1$$

$$c_{36} = 1$$

$$c_{41} = - \frac{i\bar{\alpha}^2(W-c)}{\bar{e}} + \frac{\bar{\alpha}}{\bar{R}_e/\bar{\mu}} \left\{ \frac{4}{3} \left[2 \left(\frac{\bar{e}'}{\bar{e}} \right)^2 - \left(\frac{\bar{e}'}{\bar{e}} \right) \left(\frac{\bar{e}\bar{u}}{\bar{e}\bar{u}} \right)' - \frac{\bar{e}''}{\bar{e}} \right] - \frac{\bar{\alpha}^2}{\bar{e}^2} \right\}$$

$$c_{42} = \frac{i\bar{\alpha}}{\bar{R}_e/\bar{\mu}} \left[\frac{10}{3} \frac{\bar{e}'}{\bar{e}} - 2 \left(\frac{\bar{e}\bar{u}}{\bar{e}\bar{u}} \right)' \right]$$

$$c_{43} = \frac{i\bar{\alpha}}{\bar{R}_e/\bar{\mu}} \left\{ \frac{4}{3} \left[\frac{1}{\bar{e}} \frac{d\bar{e}}{dH} \left(3 \frac{\bar{e}'}{\bar{e}} - \left(\frac{\bar{e}\bar{u}}{\bar{e}\bar{u}} \right)' \right) - \frac{1}{\bar{e}} \frac{d^2\bar{e}}{dH^2} H' \right] (W-c) \right.$$

$$\left. + \left[-\frac{4}{3} \frac{1}{\bar{e}} \frac{d\bar{e}}{dH} + \frac{1}{\bar{e}\bar{u}} \frac{d\bar{e}\bar{u}}{dH} \right] W' \right\}$$

$$c_{45} = - \frac{i\bar{\alpha}}{\bar{R}_e/\bar{\mu}}$$

$$c_{46} = - \frac{4}{3} \frac{i\bar{\alpha}}{\bar{R}_e/\bar{\mu}} \frac{d\bar{e}}{dH} (W-c)$$

$$c_{51} = \frac{\bar{\alpha} \bar{R}_e}{\bar{e}\bar{u}} W' + \frac{i\bar{\alpha}^2}{\bar{e}^2} \left[\frac{4}{3} \frac{\bar{e}'}{\bar{e}} - \left(\frac{\bar{e}\bar{u}}{\bar{e}\bar{u}} \right)' \right]$$

$$c_{53} = -\frac{1}{3} \frac{\bar{\alpha}^2}{\bar{\rho}^3} \frac{d\bar{\rho}}{dH} (W - c) - \frac{1}{\bar{\rho}^4} \left(\frac{d^2 \bar{\rho} \bar{u}}{dH^2} H' W' + \frac{d\bar{\rho} \bar{u}}{dH} W'' \right)$$

$$c_{54} = \frac{i \bar{\alpha} \bar{R}_e}{\bar{\rho} (\bar{\rho} \bar{u})}$$

$$c_{55} = - \frac{(\bar{\rho} \bar{u})'}{\bar{\rho} \bar{u}}$$

$$c_{56} = - \frac{1}{\bar{\rho} \bar{u}} \frac{d \bar{\rho} \bar{u}}{dH} W'$$

$$c_{61} = \frac{\bar{\alpha} \bar{R}_e P_r \bar{C}_P}{\bar{\rho} \bar{K}} H'$$

$$c_{63} = \frac{i \bar{\alpha} \bar{R}_e P_r \bar{C}_P}{\bar{\rho} \bar{K}} (W - c) + \frac{\bar{\alpha}^2}{\bar{\rho}^2} - \frac{(\bar{\rho} \bar{K})''}{\bar{\rho} \bar{K}}$$

$$c_{66} = -2 \frac{(\bar{\rho} \bar{K})'}{\bar{\rho} \bar{K}}$$

Z'_5 is obtained from the composite x-z momentum equation; Z'_1 , from the continuity equation; Z'_6 , from the energy equation; and Z'_4 , from the y momentum equation.

2.3.2 Disturbance Boundary Conditions

The disturbance velocity boundary conditions used in this analysis are easily obtained by requiring that there be no relative motion between the fluid and the solid surface at this interface (no slip), and that the velocity normal to the surface must also vanish there (impermeability). In notational form, at $y = 0$,

$$\tilde{U}^* = \tilde{W}^* = 0 \quad (\text{no slip})$$

$$\tilde{V}^* = 0 \quad (\text{impermeability})$$

or at $n = 0$, $\mathcal{F} = \phi = 0$ (2.43)

The thermal boundary condition at the wall requires more careful consideration (see also discussion by Dunn and Lin [17]). The scaling procedure used in Appendix A indicates that for a region very close to the surface ($y/\delta \ll 1$), the energy equation reduces to the one-dimensional, unsteady conduction equation (dimensionally)

$$\bar{\rho} \bar{c}_p \frac{\partial \bar{T}}{\partial t} = \frac{\partial}{\partial y} \left(\bar{k} \frac{\partial \bar{T}}{\partial y} + \bar{\kappa} \frac{d \bar{T}}{dy} \right)$$

The important point to note is that longitudinal temperature fluctuations are negligible in this region. Thus, solving this equation in the solid and requiring that disturbance temperatures

and heat fluxes be continuous at the liquid - solid interface ($y = 0$), the thermal boundary condition becomes

$$\tau'(0) - \left[\beta_s \frac{k_s^*}{k^*} - \frac{(\bar{\rho} \bar{k})'}{\bar{\rho} \bar{k}} \right]_w \tau(0) = 0$$

where

$$\beta_s^2 = -i \frac{\omega_\infty \bar{R}e^2}{\bar{\rho}^2} \frac{\nu_\infty}{\alpha_s^*}$$

and the subscript "s"
denotes properties of the
solid.

It is simple enough analytically to require that the thermal inertial of the solid be sufficiently large that thermal fluctuations die out in the solid very close to the surface. Under these conditions, the appropriate boundary condition would be $\tau(0) = 0$ (i.e., $\left[\beta_s \frac{k_s^*}{k^*} - \frac{(\bar{\rho} \bar{k})'}{\bar{\rho} \bar{k}} \right] \gg 1$). Realistically, however, the full boundary condition should be closely scrutinized when applying this analysis to a particular solid, at a specified frequency, etc. For this analysis, the condition

$$\tau(0) = 0 \quad (2.44)$$

is chosen.

Further it is assumed that all disturbances are bounded at large distances from the surface

$$y \rightarrow \infty \quad \tilde{u}^*, \tilde{v}^*, \tilde{w}^*, \tilde{T}^* \rightarrow 0 \quad (2.45)$$

or

$$\eta \rightarrow \infty \quad \phi, \mathcal{F}, \tau \rightarrow 0$$

2.4 Disturbance Field Energy Balance

Although mathematically the stability characteristics of the disturbance flow field can be completely described (within the framework of specified assumptions) by the equations formulated in the three preceding sections, it is instructive also to develop the theory on a more physical foundation as well. Insight into the physical mechanisms at work in the boundary layer is thus sought by examining the production, dissipation and transfer of the disturbance energies.

The appropriate equations are obtained by first multiplying each of the x, y, and z disturbance momentum equations (2.23-2.25) by its corresponding disturbance velocity, u, v, and w, and then summing the three. After some algebraic manipulation, a meaningful equation is obtained and expressed (dimensionally) as:

$$\begin{aligned}
 & \underbrace{D \left[\frac{\bar{\rho}}{2} (\tilde{u}^2 + \tilde{v}^2 + \tilde{w}^2) \right]}_{(1)} = - \bar{\rho} \left(\tilde{u} \tilde{v} \frac{d\tilde{u}}{dy} + \tilde{v} \tilde{w} \frac{d\tilde{w}}{dy} \right) \\
 & - \tilde{\mu} \left(\tilde{\tau}_z \frac{d\tilde{u}}{dy} + \tilde{\tau}_x \frac{d\tilde{w}}{dy} \right) - \tilde{\rho} \left[D \tilde{\rho} + \tilde{v} \frac{d\tilde{\rho}}{dy} \right] \\
 & + 2 \frac{d\tilde{u}}{dy} \left(\tilde{u} \frac{\partial \tilde{v}}{\partial x} + \tilde{w} \frac{\partial \tilde{v}}{\partial z} - \tilde{v} \frac{\partial \tilde{u}}{\partial x} - \tilde{v} \frac{\partial \tilde{w}}{\partial z} \right) - \tilde{\mu} \tilde{\xi} \cdot \tilde{\xi} \\
 & - \frac{4}{3} \frac{\bar{\mu}}{\bar{\rho}^2} \left(D \tilde{\rho} + \tilde{v} \frac{d\tilde{\rho}}{dy} \right)^2 + \left\{ \nabla \cdot \left[-\tilde{\rho} \tilde{u} + \tilde{u} \times \tilde{\rho} \tilde{\xi} \right] \right. \\
 & \left. - \frac{4}{3} \frac{\bar{\mu}}{\bar{\rho}} \left(D \tilde{\rho} + \tilde{v} \frac{d\tilde{\rho}}{dy} \right) \tilde{u} + \tilde{u} \tilde{v} \frac{d\tilde{u}}{dy} \right\} + \frac{\partial}{\partial y} \left(\tilde{u} \tilde{u} \cdot \frac{d\tilde{u}}{dy} \right) \quad (2.46)
 \end{aligned}$$

where $\bar{V} = 0$

$$D \equiv \frac{\partial}{\partial t} + \bar{U} \frac{\partial}{\partial x} + \bar{W} \frac{\partial}{\partial z}$$

$$\tilde{\tau}_z = \left(\frac{\partial \tilde{u}}{\partial y} + \frac{\partial \tilde{v}}{\partial x} \right)$$

$$\tilde{\xi}_x = \left(\frac{\partial \tilde{w}}{\partial y} - \frac{\partial \tilde{v}}{\partial z} \right)$$

$$\tilde{\tau}_x = \left(\frac{\partial \tilde{w}}{\partial y} + \frac{\partial \tilde{v}}{\partial z} \right)$$

$$\tilde{\xi}_y = \left(\frac{\partial \tilde{u}}{\partial z} - \frac{\partial \tilde{w}}{\partial x} \right)$$

$$\tilde{\xi}_z = \left(\frac{\partial \tilde{v}}{\partial x} - \frac{\partial \tilde{u}}{\partial y} \right)$$

Assuming only two-dimensional mean and disturbance flows,

equation (2.46) reduces to:

$$\begin{aligned}
 & \overbrace{D \left[\frac{\bar{\rho}}{2} (\tilde{u}^2 + \tilde{v}^2) \right]}^{(1)} = \overbrace{- \bar{\rho} \tilde{u} \tilde{v} \frac{d \bar{u}}{dy}}^{(2)} - \overbrace{\bar{\mu} \tilde{\tau}_z \frac{d \bar{u}}{dy}}^{(3)} \\
 & - \overbrace{\frac{\tilde{p}}{\bar{\rho}} (D \tilde{\rho} + \tilde{v} \frac{d \bar{\rho}}{dy})}^{(4)} + \overbrace{2 \frac{d \bar{u}}{dy} \left(\tilde{u} \frac{\partial \tilde{v}}{\partial x} - \tilde{v} \frac{\partial \tilde{u}}{\partial x} \right)}^{(5)} - \overbrace{\bar{\mu} \tilde{\xi}_z^2}^{(6)} \\
 & - \overbrace{\frac{4}{3} \bar{\mu} \frac{\bar{\rho}}{\bar{\rho}^2} (D \tilde{\rho} + \tilde{v} \frac{d \bar{\rho}}{dy})}^{(7)} + \overbrace{\frac{\partial}{\partial x} \left[- \tilde{p} \tilde{u} + \bar{\mu} \tilde{v} \tilde{\xi}_z \right]}^{(8)} \\
 & - \overbrace{\frac{4}{3} \bar{\mu} \frac{\bar{\rho}}{\bar{\rho}} (D \tilde{\rho} + \tilde{v} \frac{d \bar{\rho}}{dy}) \tilde{u} + \bar{\mu} \tilde{v} \frac{d \bar{u}}{dy}}^{(9)} + \overbrace{\frac{\partial}{\partial y} \left[- \tilde{p} \tilde{v} - \bar{\mu} \tilde{u} \tilde{\xi}_z \right]}^{(10)} \\
 & - \overbrace{\frac{4}{3} \bar{\mu} \frac{\bar{\rho}}{\bar{\rho}} (D \tilde{\rho} + \tilde{v} \frac{d \bar{\rho}}{dy}) \tilde{v} + \bar{\mu} \tilde{u} \frac{d \bar{u}}{dy}}^{(11)}
 \end{aligned} \tag{2.47}$$

The time-averaged version of equation (2.47) written nondimensionally in terms of disturbance amplitude functions (see equations (2.27) is:

$$\begin{aligned}
 & \overline{\alpha_I} \bar{R}e \bar{\rho} \bar{u} \left[\overline{f f_*} + \frac{\bar{\alpha} \bar{\alpha}_* (\bar{\rho} \phi)(\bar{\rho} \phi)_*}{\bar{\rho}^2} \right] = - \bar{\rho} \bar{u}' \bar{R}e (\bar{\alpha} \bar{\rho} \phi f_*)_R^{(1)} \\
 & - \bar{\rho} \bar{u}' \left[(\bar{\rho} m f'_*)_R^{(2)} + \left(\frac{\bar{\alpha}_*^2}{\bar{\rho}^2} (\bar{\rho} \phi)_* \bar{\rho} m \right)_I^{(3)} \right] = - \bar{R}e \tilde{z}(\pi)^{(4)} \\
 & - 4 \bar{\alpha}_R \bar{u}' (\bar{\alpha} \bar{\rho} \phi f_*)_I^{(5)} - \bar{\rho}^2 \bar{u} \left[\frac{\bar{\alpha}^2 \bar{\alpha}_*^2}{\bar{\rho}^4} (\bar{\rho} \phi)(\bar{\rho} \phi)_* + f' f'_* \right]_I^{(6)} \\
 & + 2 \left(\frac{\bar{\alpha}^2}{\bar{\rho}^2} \bar{\rho} \phi f'_* \right)_I^{(7)} - \frac{4}{3} \bar{u} \tilde{z} \left(\frac{i r (\bar{u} \bar{\alpha} - \bar{\omega})}{\bar{\rho}} + \bar{\rho}' \bar{\alpha} \bar{\rho} \phi \right) \\
 & + \bar{R}e \left[2 \alpha_I (\pi_* f)_R - \bar{\rho} \frac{d}{d\eta} (\pi_* \frac{\bar{\alpha}}{\bar{\rho}} \bar{\rho} \phi)_R \right]^{(8)} \\
 & + 2 \bar{\alpha}_I \bar{u} \left[\bar{\alpha}_I \frac{\bar{\alpha} \bar{\alpha}_*}{\bar{\rho}^2} (\bar{\rho} \phi)(\bar{\rho} \phi)_* + (\bar{\alpha} \bar{\rho} \phi f'_*)_R \right] \\
 & + \bar{\rho} \frac{d}{d\eta} \left\{ \bar{\rho} \bar{u} \left[\left(\frac{\bar{\alpha}^2}{\bar{\rho}^2} \bar{\rho} \phi f_* \right)_I + (f f')_R \right] \right\} + \frac{8}{3} \alpha_I \bar{u} \tilde{z}(f) \\
 & - \frac{4}{3} \bar{\rho} \frac{d}{d\eta} \left[\tilde{z} \left(\frac{\bar{\alpha}}{\bar{\rho}} \bar{\rho} \phi \right) \right] - 2 \bar{\alpha}_I \bar{u}' \left\{ m_* \bar{\alpha} \bar{\rho} \phi \right\}_R + \bar{\rho} \frac{d}{d\eta} \left\{ \bar{\sigma}' (\bar{\rho} m f'_*)_R \right\}^{(2.48)}
 \end{aligned}$$

where

$$\tilde{z}(g) = - \left[g_* \frac{r (\bar{u} \bar{\alpha} - \bar{\omega})}{\bar{\rho}} \right]_I + \bar{\rho}' \left[g_* \bar{\alpha} \bar{\rho} \phi \right]_R, \quad \bar{\omega} = \bar{\alpha} c,$$

and * denotes the complex conjugate.

It is instructive to examine each term at this point to identify the physical process it represents and assess its relative importance. Thus, the indicated terms represent:

- (1) the rate of change in kinetic energy of the disturbance field. Note that for a neutral disturbance, the averaged value is zero so there is no net energy change in the boundary layer.

(2) the energy drawn from the mean motion by the working of Reynolds stresses against the gradients of the mean velocity. As this is the only source of energy for the disturbance field of the unheated flow, it can also be expected to be significant when there is heat transfer. Furthermore, it is expected to be greatest and positive in the region roughly between the wall and the critical point, signifying energy transfer from the mean to the disturbance flow, but small and quite possibly negative from there to the boundary layer edge.

(3) the energy extracted from the mean flow due to the working of the disturbance viscous stresses against the mean velocity gradients. By and large, it is expected to have the same sign as term (2) and so should represent primarily a source of energy for the disturbance field. It should be most significant in regions where temperature fluctuations are largest since the viscosity and temperature fluctuations are proportional.

(4) the rate at which the pressure fluctuations do work.

Physically this energy is produced by two different mechanisms:

(a) the periodic expansion and dilation of each fluid element (caused by density fluctuations) in the presence of a disturbance pressure field, and (b) the movement of this same fluid element along a mean density gradient also in the presence of the disturbance pressure. Note from equation (2.48) that for a neutral disturbance, the contribution from the first mechanism will vanish at both the wall and the critical layer.

(5) change in energy resulting from a nonzero mean viscosity gradient. As may be seen from equation (2.48), this term is of order $\frac{4\alpha_R}{Re}$ times that of the major production terms (2). Since the general order of α_R decreases and Re increases with moderate heating, it is expected that this term should be of negligible significance.

(6) mechanical energy lost from the disturbance field by viscous friction. This loss is manifest physically as a heat source which in turn produces minute changes in the disturbance temperature (and so density) level. Since the term is negative definite, it will always represent a dissipation and should be most important near the wall.

(7) energy dissipation from thermal fluctuations. Specifically, this is the energy lost associated with the dilation of the fluid elements due to their expansion and contraction with changes in density (caused by changes in temperature). This effect should be small in liquid boundary layers where the amplitude of disturbance density fluctuations is relatively small, even with significant mean thermal gradients.

(8) rate of transfer of pressure and dilatory energy, vorticity, and disturbance viscous shear stress. If the disturbance field is neutral ($\alpha_I = 0$), no energy is transferred parallel to the plate. Further, if this term is integrated from the wall to some large distance ($n \rightarrow \infty$), the remaining energy contributions will vanish identically due to the homogeneous boundary conditions. Thus,

the term acts only to transfer energy from one position in the boundary layer to another, and for a neutral disturbance makes no contribution to the net energy.

Two examples are now examined to more clearly identify the terms of interest in this investigation. First, equation (2.48) is reduced to a form compatible with the assumptions made by Wazzan, et.al; namely in the disturbance equations, $\bar{\rho} = \text{constant}$ (but variable in the mean flow), $\bar{\mu} = \bar{\mu}(y)$, and $\tau = 0$ (so $\tilde{\rho} = \tilde{\mu} = 0$). Thus, for a neutral disturbance, the y -integrated, nondimensional, energy equation is composed of only the production and dissipation contributions:

$$0 = \overbrace{-\bar{\alpha}_R \bar{R}_e \bar{u}' (\bar{\rho} \phi f_*)_R}^{(2)} - \overbrace{4 \bar{\alpha}_R^2 \bar{\mu}' (\bar{\rho} \phi f_*)_I}^{(5)} - \overbrace{-\bar{\rho}^2 \bar{\nu} \left[\frac{\bar{\alpha}_R^4}{\bar{\rho}^4} (\bar{\rho} \phi)(\bar{\rho} \phi)_* + f' f'_* + 2 \frac{\bar{\alpha}_R^2}{\bar{\rho}^2} (\bar{\rho} \phi f'_*)_I \right]}^{(6)} \quad (2.49)$$

(Note that the variable $\bar{\rho}$ still appears in this equation since differentiation is with respect to η ; i.e. $\frac{d}{d(\gamma^*/\delta^*)} = \eta_{\delta^*} \bar{\rho} \frac{d}{d\eta}$).

Secondly, assuming for this analysis all mean and disturbance

quantities may vary, the equivalent equation becomes

$$\begin{aligned}
 O = & \underbrace{-\bar{\rho} \bar{u}' \bar{\alpha}_R \bar{Re} (\bar{\rho} \phi f_*)_R}_{(2)} - \underbrace{-\bar{\rho} \bar{u}' [\bar{(\bar{\rho} m f'_*)}_R + \frac{\bar{\alpha}_R^2}{\bar{\rho}^2} (\bar{\rho} m \bar{\rho} \phi'_*)_I]}_{(3)} \\
 & - \underbrace{\bar{Re} \tilde{\approx} (\pi)}_{(4)} - \underbrace{4 \bar{\alpha}_R^2 \bar{u}' (\bar{\rho} \phi f'_*)_I}_{(5)} \\
 & - \underbrace{-\bar{\rho}^2 \bar{u} \left[\frac{\bar{\alpha}_R^4}{\bar{\rho}^4} (\bar{\rho} \phi) (\bar{\rho} \phi)_R + f' f''_* + 2 \frac{\bar{\alpha}_R^2}{\bar{\rho}^2} (\bar{\rho} \phi f'_*)_I \right]}_{(6)} \\
 & - \underbrace{-\frac{4}{3} \bar{u} \approx \left[\frac{i \bar{\alpha}_R r (\bar{u} - c_R)}{\bar{\rho}} + \frac{\bar{\phi}'}{\bar{\rho}} \bar{\alpha}_R (\bar{\rho} \phi) \right]}_{(7)} \quad (2.50)
 \end{aligned}$$

where $\tilde{\approx} (q)$ is here slightly simplified to

$$\tilde{\approx} (q) = - \left[\frac{g_* \bar{\alpha}_R r (\bar{u} - c_R)}{\bar{\rho}} \right]_I + \frac{\bar{\rho}'}{\bar{\rho}} \left[g_* \bar{\alpha}_R \bar{\rho} \phi \right]_R$$

CHAPTER III

NUMERICAL SOLUTION OF THE STABILITY PROBLEM

3.1 Thermodynamic Properties and Transport Coefficients

Before numerical boundary layer integration can be performed for either the mean or disturbance equations, values for the thermodynamic and transport properties of the liquid and their required derivatives must be specified at each step. Consistent with assumptions made thus far that the property variations are independent of pressure (also for the boundary layer approximation, the mean pressure is constant in the boundary layer anyway), these quantities can depend on position only through values of the mean temperature. For the mean flow, such temperature dependence couples the momentum and energy equations. More specifically, for the stability problem, accurate information is needed not only for the variable properties of the mean flow, but for the disturbance quantities r , m , and κ as well (see equations (2.20 and 2.35)).

Since the solution process for the mean flow equations requires changes of the temperature at a particular physical position both during the iterative search for unknown wall boundary conditions (discussed in section 3.2) and later with the choice of step size for the converged solution, discrete input to a numerical scheme of required fluid properties and derivatives is impossible. That is to say, this information is available in general only by

interpolating tabulated experimental data at each step. It follows, then, that the temperature derivatives must be obtained by numerical differentiation of the discrete set of data points, and so must be interpolated as well.

Water is chosen as the representative liquid for numerical purposes to maximize applicability of the results of this investigation (in which thermal fluctuations are considered) to situations occurring in nature, but primarily to enable comparison with the results of the fourth order stability analysis of Wazzan, et.al. [4]. In general to obtain the "best" information available, values for c_p , ρ , μ , and k are taken from recently published measurements and/or evaluations of preexisting data. Temperature derivatives of these properties are obtained directly by analytically differentiating the empirical property-temperature relationship proposed for each. Note that this procedure is in contradistinction to first estimating derivatives directly from the data (with the method of cubic splines, for example) and then smoothing any spurious fluctuations.

A more extensive discussion of the sources and accuracy of input property data, alternate means considered for curve-fitting tabulated data and obtaining high quality derivatives, and graphical presentation of the properties and temperature derivatives for water are given in Appendix B.

3.2 Mean Equations

The equations describing the mean two-dimensional, boundary-layer flow over a heated, flat plate are obtained directly from equations (2.20) as

$$(\bar{\rho} \bar{u} F'')' + \frac{1}{2} FF'' = 0 \quad (3.1)$$

and.

$$(\bar{\rho} \bar{k} H')' + \frac{\bar{c}_p \bar{P}_r}{2} F H' = 0$$

with boundary conditions specified by equations (2.21)

$$\begin{aligned} \eta=0 : \quad F' &= F = 0, \quad H = 1 \\ \text{and} \quad \eta \rightarrow \infty : \quad F' &\rightarrow 1, \quad H \rightarrow 0 \end{aligned} \quad (3.2)$$

The numerical solution to these equations introduced several difficulties characteristic of a boundary value problem, in addition to those associated with the nonlinearity and coupling through fluid property variation. The method of Nachtsheim and Swigert [18] adopted for this analysis is found to satisfactorily deal with all difficulties, especially: determination of where to stop the integration for the un converged solution, and approximation and refinement of initial conditions.

First, to obtain a unique solution of these equations,

external conditions must be "satisfied" for an undetermined, but finite $\eta = \eta_{\max} > \eta_\delta$. Asymptotic convergence (where, $F' \rightarrow 1$ and $H \rightarrow 0$ as $\eta \rightarrow \infty$ becomes $F' = 1$ and $H = 0$ at $\eta = \eta_{\max}$) is assured simply by requiring velocity and temperature gradients vanish at the "truncated infinity" ($F'' = H' = 0$ at $\eta = \eta_{\max}$). Note from equations (3.1) that these additional conditions cause all higher derivatives to vanish there as well. However, the value of η_{\max} (or equivalently, that η beyond which no appreciable change is observed in the solution) still remains unknown. If the a priori specification of η_{\max} is too small, boundary layer integration is terminated too soon and boundary conditions cannot be satisfied; if η_{\max} is chosen too large, computation time becomes excessive.

Secondly, numerical integration of the mean flow equations requires specification of as many conditions at the wall as there are conditions to be satisfied at the boundary layer edge. Since the required additional wall conditions (F''_w and H'_w) are initially unknown, they must be first estimated and then iteratively adjusted until the asymptotic conditions can be satisfied, or

$$F'(F''_w, H'_w, \eta_{\max}) = 1$$

$$H(F''_w, H'_w; \eta_{\max}) = 0 \quad (3.3)$$

with the supplemental conditions

$$F''(F''_w, H'_w; \eta_{\max}) = 0$$

$$H'(F''_w, H'_w; \eta_{\max}) = 0$$

In other words, the system of equations is solved as an initial

value problem with the wall gradients as the specified initial values. Due to the extreme sensitivity of equations (3.1) to values of F''_w and H'_w , even fair estimates of these parameters are likely to cause the numerical boundary layer integration to "blow up" prior to reaching the prescribed value of η_{\max} . Thus no means would be available for refining initial estimates of the wall gradients.

The mean equations are thus solved in the following fashion. With an estimate of initial conditions, F''_w and H'_w , Runge-Kutta and Adams-Moulton integration techniques are applied over an abbreviated η range. At the end of this range, the initial conditions are refined by determining the least-square solution for discrepancies between the computed variables and the proper asymptotic values. When successive iterations over this interval fail to appreciably change the initial conditions, an error estimate E , the sum of the squares of the deviation of computed quantities from their asymptotic values, is evaluated:

$$E = (1 - F')^2 + H^2 + F''^2 + H'^2 \quad (3.4)$$

If this error is sufficiently small, then the solution is considered to be found. If such is not the case, then the η range is increased and the above procedure repeated. The boundary layer is thus traversed in a stepwise fashion until errors are within acceptable limits. The last η range then determines η_{\max} automatically.

In summary, this method yielded relatively rapid, unique convergence to the proper solution and seemed to be insensitive to

initial estimates of the wall gradients.

Once solution of the mean flow equations is accomplished, the variable coefficients for the disturbance equations can be computed directly and the latter solved in the manner described in the next section. However, other incidental calculations can easily be performed as well. For example, to find η_{δ}^* for the unheated case (or more specifically, when density is considered constant), from equation (2.18)

$$\eta_{\delta}^* = \int_0^\infty (1 - \bar{U}) d\eta \approx \int_0^{\eta_{\max}} (1 - F') d\eta = \eta_{\max} - F(\eta_{\max})$$

For the heated case, though, the solution is not immediately available from variables computed in the boundary layer integration:

$$\eta_{\delta}^* \approx \int_0^{\eta_{\max}} \frac{1}{\bar{\rho}} d\eta - F(\eta_{\max}) \quad (3.4)$$

Instead, using stored values of $\bar{\rho}(\eta)$ and the composite Simpson's Rule formula [19, p.79], the required integral is determined numerically. Computed values of η_{δ}^* are tabulated in Table E.3 and plotted in Figure C.2. An analysis in section E.1 indicates an $\eta_{\max} = 10$ to be adequate for the boundary layer integration of the mean equations.

Conversion back to physical coordinates must be similarly computed. From equations (2.16a) and (2.17)

$$\frac{y^*}{\delta^*} = \frac{1}{\eta_{\delta^*}} \int_0^\eta \frac{d\eta}{\bar{\epsilon}} \quad (3.5)$$

so that

$$\frac{\delta}{\delta^*} = \frac{1}{\eta_{\delta^*}} \int_0^{\eta_{\delta^*}} \frac{d\eta}{\bar{\epsilon}} \quad (3.6)$$

a constant, once the mean flow equations are solved and the boundary layer edge is specified. A plot of the $\frac{y^*}{\delta^*}$: η and $\frac{\delta}{\delta^*}$ relationships for the mean flows analyzed is given in Figure C.1.

3.3 Disturbance Equations

The equations describing the hydrodynamic spatial stability of two-dimensional disturbances in a two-dimensional, heated, liquid boundary layer are obtained from equations (2.37-2.40) by setting $\theta = 0$ and $\psi = 0$ (see equations (2.29 and 2.30)), and requiring that Re and $\omega = \alpha c$ be real and α be complex. Thus,

Continuity:

$$\frac{i r (\bar{u} - c)}{\bar{\rho}} + i f + (\bar{\rho} \phi)' = 0$$

Momentum:

$$\begin{aligned} i f (\bar{u} - c) + (\bar{\rho} \phi) \bar{u}' &= - \frac{i \pi}{\bar{\rho}} + \frac{i \bar{\alpha}}{\bar{R} e} \left\{ \bar{\mu} \left[2 i f + \frac{2}{3} \left(\frac{i r (\bar{u} - c)}{\bar{\rho}} \right) \right] \right. \\ &\quad \left. + \frac{\bar{\rho}'}{\bar{\rho}} (\bar{\rho} \phi) \right\} + \frac{1}{\bar{\alpha} \bar{R} e} \left\{ \bar{\rho} m \bar{u}' + \bar{\rho} \bar{u} \left[f' + \frac{i \bar{\alpha}^2 \bar{\rho} \phi}{\bar{\rho}^2} \right] \right\}' \end{aligned} \quad (3.6)$$

$$\begin{aligned} i \bar{\alpha}^2 (\bar{\rho} \phi) (\bar{u} - c) &= - \bar{\rho} \pi r' + \frac{i \bar{\alpha}}{\bar{R} e} \left\{ \bar{\rho} m \bar{u}' + \bar{\rho} \bar{u} \left[f' + \frac{i \bar{\alpha}^2 \bar{\rho} \phi}{\bar{\rho}^2} \right] \right\} \\ &\quad - \bar{\rho} \frac{\bar{\alpha}}{\bar{R} e} \left\{ \bar{\mu} \left(2 i f + \frac{4}{3} \left[\frac{i r (\bar{u} - c)}{\bar{\rho}} + \frac{\bar{\rho}'}{\bar{\rho}} (\bar{\rho} \phi) \right] \right) \right\}' \end{aligned}$$

Energy:

$$\bar{c}_p [i(\bar{u} - c)\tau + \bar{\rho}\phi H'] = \frac{1}{\alpha \bar{R}e \bar{P}r} \left\{ \left[\bar{\rho}\bar{k}\tau + \bar{\rho}kH' \right]' - \frac{\bar{\omega}^2}{\bar{\rho}^2} \bar{\rho}\bar{k}\tau \right\}$$

which satisfy a set of homogenous boundary conditions obtained from equations (2.43-2.45),

$$\eta = 0: \quad f = \phi = \tau = 0$$

and

(3.7)

$$\eta \rightarrow \infty: \quad f, \phi, \tau \rightarrow 0$$

Since these equations and boundary conditions are insufficient to establish a nontrivial solution, the system is cast as an eigenvalue problem (i.e., nonzero solutions satisfying boundary conditions are obtainable only for selected combinations of the parameters α , ω , and Re).

Since the complexity of the equations precludes exact analytical solutions within the boundary layer, numerical techniques are applied. Of numerous possible methods previously utilized for solving this type of problem, the orthonormalized, differential method used for this investigation seems to be one of the most efficient and general [20]. Schematically, the employed scheme has the following steps:

- (1) estimate an eigenvalue;
- (2) starting from solutions valid in external region, integrate numerically to the wall and try to satisfy the specified boundary conditions there as well;
- (3) refine the initial eigenvalue estimate and reintegrate as in (2).

The final two steps are repeated until "satisfaction" of wall boundary conditions is attained. Although this procedure is conceptually quite straightforward, its implementation is not. The ensuing discussion elaborates on the difficulties associated with each of the steps enumerated above.

As noted previously, there are four parameters associated with this eigenvalue problem, α_R , α_I , ω , and Re . In subsequent discussion, "the eigenvalue" should be interpreted as those two real parameters which are iteratively adjusted to satisfy the real and imaginary parts of a wall boundary condition. The choice of the two fixed parameters is determined by information sought from the analysis; for example, to obtain curves of constant amplification, it is found convenient to fix α_I and Re , and then search for the proper values of α_R and ω . Although inclusion of a fluctuating temperature field for this investigation is expected to somewhat modify the existing results of Wazzan, Okamura, and Smith [4] (in which no such field was considered), the initial eigenvalue estimate for a specified T_w and T_∞ is taken from the latter. Once several "exact" eigenvalues are determined, these can be extrapolated to estimate others in the same neighborhood.

With all pertinent parameters specified, the eigenvalue problem is now converted to a boundary value problem. Thus it remains to mathematically describe the asymptotic condition specified for the boundary layer edge. Since the mean flow coefficients in the disturbance equations are all assumed to be constant outside the boundary layer, an exact solution can be obtained for $\eta \geq \eta_e$. Specifically, equations (2.42) reduce to

$$\bar{Z}'_1 = -i \bar{Z}_2 - i \left(\frac{d\bar{\rho}}{d\bar{H}} \right)_e (1-c) \bar{Z}_3$$

$$\bar{Z}'_2 = \bar{Z}_5$$

$$\bar{Z}'_3 = \bar{Z}_6$$

$$\begin{aligned} \bar{Z}'_4 &= - \left[i \bar{\alpha}^2 (1-c) + \frac{\bar{\alpha}^3}{\bar{R}_e} \right] \bar{Z}_1 - \frac{i \bar{\alpha}}{\bar{R}_e} \bar{Z}_5 \\ &\quad - \frac{4}{3} i \frac{\bar{\alpha}}{\bar{R}_e} \left(\frac{d\bar{\rho}}{d\bar{H}} \right)_e (1-c) \bar{Z}_6 \end{aligned} \tag{3.8}$$

$$\bar{Z}'_5 = \left[i \bar{\alpha} \bar{R}_e (1-c) + \bar{\alpha}^2 \right] \bar{Z}_2 - \frac{1}{3} \bar{\alpha}^2 \left(\frac{d\bar{\rho}}{d\bar{H}} \right)_e (1-c) \bar{Z}_3 + i \bar{\alpha} \bar{R}_e \bar{Z}_4$$

$$\bar{Z}'_6 = \left[\bar{\alpha}^2 + i \bar{\alpha} \bar{R}_e \text{Pr} (1-c) \right] \bar{Z}_3$$

or after some manipulation

$$\bar{Z}_1''' - (\bar{\alpha}^2 + \gamma^2) \bar{Z}_1'' + \bar{\alpha}^2 \gamma^2 \bar{Z}_1 + i \left(\frac{d\bar{\rho}}{d\bar{H}} \right)_e (1-c) [\bar{Z}_3''' - \gamma^2 \bar{Z}_3''] = 0 \tag{3.9}$$

and

$$\bar{Z}_3'' - \dot{\rho} \bar{Z}_3 = 0 \tag{3.10}$$

where

$$\begin{aligned}\gamma^2 &= \bar{\alpha}^2 + i\bar{\alpha} \overline{R}_e (1-c) \\ \beta^2 &= \bar{\alpha}^2 + i\bar{\alpha} \overline{R}_e P_r (1-c)\end{aligned}\quad (3.11)$$

From Eqn. (3.10) it is easily shown that to satisfy the external boundary conditions (equation (3.7)), for the j^{th} solution vector

$$Z_3^{(j)} = C_3^{(j)} e^{-\beta(\eta - \eta_e)} \quad \text{for } \eta \geq \eta_e \text{ and real } \beta > 0 \quad (3.12)$$

Thus equation (3.9) is an ordinary, nonhomogeneous differential equation with constant coefficients which when satisfying the same conditions of boundedness has the solution

$$Z_1^{(j)} = C_1^{(j)} e^{-\bar{\alpha}(\eta - \eta_e)} + C_2^{(j)} e^{-\gamma(\eta - \eta_e)} + \frac{i\beta \left(\frac{d\bar{P}}{dH_e} \right) (1-c)}{(\beta^2 - \bar{\alpha}^2)} Z_3^{(j)} \quad (3.13)$$

for $\eta > \eta_e$ and real $\alpha, \gamma > 0$.

From equation (3.8) and (3.13)

$$\begin{aligned}Z_2^{(j)} &= -i\bar{\alpha} C_1^{(j)} e^{-\bar{\alpha}(\eta - \eta_e)} - i\gamma C_2^{(j)} e^{-\gamma(\eta - \eta_e)} \\ &\quad + \frac{\bar{\alpha}^2}{\beta^2 - \bar{\alpha}^2} \left(\frac{d\bar{P}}{dH_e} \right) (1-c) Z_3^{(j)}\end{aligned}\quad (3.14)$$

for $\eta > \eta_e$ and real $\alpha, \gamma > 0$.

The values for Z_4 , Z_5 , and Z_6 can be expressed in terms of Z_1 , Z_2 , and Z_3 as

$$\begin{aligned} Z_4^{(j)} &= \frac{\gamma + \bar{\alpha}}{Re} \left[\gamma Z_1^{(j)} - i Z_2^{(j)} \right] - \frac{i}{Re} \left(\frac{d\bar{\rho}}{dH_e} \right) (1-c) \left[\frac{4}{3} \bar{\alpha} + \gamma \frac{(\bar{\alpha} + \gamma)}{(\bar{\alpha} + \beta)} \right] Z_3^{(j)} \\ Z_5^{(j)} &= -i \bar{\alpha} \gamma Z_1^{(j)} - (\bar{\alpha} + \gamma) Z_2^{(j)} + \frac{\bar{\alpha}(\bar{\alpha} + \gamma)}{(\bar{\alpha} + \beta)} \left(\frac{d\bar{\rho}}{dH_e} \right) (1-c) Z_3^{(j)} \\ Z_6^{(j)} &= -\beta Z_3^{(j)} \end{aligned} \quad (3.15)$$

As indicated, the three acceptable, linearly independent fundamental solutions $e^{-\bar{\alpha}(\eta-\eta_e)}$, $e^{-\gamma(\eta-\eta_e)}$, and $e^{-\beta(\eta-\eta_e)}$ can be combined to obtain a general solution to the simplified disturbance equations outside the boundary layer.

With an eigenvalue estimate and specified values for the three linearly independent solution vectors $Z^{(j)}$ at the boundary layer edge (obtained from eqns. (3.12-3.15) by setting $c_i^{(j)} = \delta_{ij}$, $i, j = 1, 2, 3$), a fourth order Runge-Kutta method is implemented to numerically integrate simultaneously the disturbance equation solution vectors to the wall, $\eta = 0$. After each integration step, however, the original linear independence is found to be so greatly diminished that the solution vectors become computationally dependent before reaching the wall. Thus, insufficient information is available there to satisfy boundary conditions.

In complex vector space, this can be viewed as a rotation of one or more of the solution vectors from an orthogonal to a colinear configuration, or a reduction of the included angle from ninety to zero degrees. The difficulty is explained as follows. Although the exponentially growing solutions to equations (3.16) can be excluded from the boundary conditions in a mathematically exact way, their influence cannot be eliminated from the numerical integration inside the boundary layer. Here, truncation or round-off errors provide suitable initial conditions for subsequent integration steps. As the computer will allow the most general solution, the rapidly growing portion eventually dominates the three solution vectors (parasitic error). To avoid this difficulty, an orthonormal basis is reestablished whenever complete loss of linear independence is imminent. Gersting and Jankowski [20, 21] contrast this "near-orthonormalized integration" to the "fully-orthonormalized integration" used by Wazzan, et. al. [3], in which solution vectors are kept orthonormal at each step.

Integration thus proceeds in the following manner. The three basic solution vectors $z^{(j)}$ are integrated using a Runge-Kutta scheme with a fixed step size from the boundary layer edge toward the wall until, at mesh point η_1 , the attendant parasitic error reduces the angle between any two solution vectors below a specified limit, or

$$\min \cos^{-1} \left| \frac{(z^{(i)}, z^{(j)})}{\{(z^{(i)}, z^{(i)}) (z^{(j)}, z^{(j)})\}^{1/2}} \right| < \Omega \quad i, j = 1, 2, 3 \quad (3.16)$$

$$\quad \quad \quad i \neq j$$

where $(z^{(i)}, z^{(j)})$ represents the complex inner product of the vectors i and j . There, the Gram-Schmidt algorithm for orthonormalizing a set of vectors is applied [22]. When eigenfunctions are to be recovered, the orthonormalizing matrix, available as a nonessential by-product of the orthonormalization process, is also computed and stored for later use. The integration is then continued from η_1 using as initial conditions the orthonormalized basis vectors, $\bar{Z}^{(j)}$, until at mesh point η_2 , the angle between any two solution vectors is again less than Ω . This procedure is repeated until the wall is reached, at which point a final orthonormalization is performed.

An evaluation of the proper step size, h_d , and orthonormalization angle criterion, Ω , required for this integration is given in sections E.2 and E.3 of Appendix E respectively. Based on that evaluation, the values of $h_d \leq .02$ and $\Omega = 45^\circ$ were used to generate the results presented in Chapter IV. (Since the integration scheme used requires computation of derivatives at half-step intervals, the mean equations thus must be integrated with step size $h_m = 1/2 h_d$).

At the wall, the three independent solution vectors are linearly combined in an attempt to satisfy the homogeneous boundary conditions, equations (3.7), for that particular eigenvalue estimate. In general, such satisfaction is not achieved immediately unless the eigenvalue is "exact," and so some iterative correction scheme must be implemented. Thus, for the vector components

$$\bar{Z}_i(o) = \sum_{j=1}^3 C_j \bar{Z}_i^{(j)}(o) \quad (3.17)$$

it is required that (see also [23])

$$\bar{Z}_2(o) + B_1 \bar{Z}_1(o) = 0$$

and

(3.18)

$$\bar{Z}_3(o) = 0$$

where specification of the arbitrary constant $B_1 = \bar{u}''(0)$ is found to give good eigenvalue convergence using the search procedures discussed below. Following Wazzan, et. al. [23], the quantity actually used to clearly distinguish an eigensolution from all others is the complex, surface-normal, boundary layer admittance

$$Y_o(\omega, \alpha, Re) = \frac{\bar{Z}_1(o)}{\bar{Z}_4(o)} \quad (3.19)$$

for, the smaller the "zero" components of the eigensolution ($\bar{Z}_1(o)$, $\bar{Z}_2(o)$, and $\bar{Z}_3(o)$) are than the nonzero ones ($\bar{Z}_4(o)$, $\bar{Z}_5(o)$, and $\bar{Z}_6(o)$), the more accurate will be the eigenvalue [24, p. 280]. Requiring both the real and imaginary parts of Y_o vanish establishes two real equations in the two adjustable parameters (or the complex

"eigenvalue").

For iterative refinement of the eigenvalues (i.e., finding the zero(s) of Y_o), two schemes were employed: the plane fit of Wazzan, et.al [23], and the quadratic complex curve fit of Muller [25]. In the former, a plane of the form

$$\text{"eigenvalue"} = a_o + a_1 Y_{oR} + a_2 Y_{oI}$$

is fitted to three successive eigenvalue estimates and their corresponding computed admittances. The corrected eigenvalue estimate for the next iteration is then simply a_o . When Y_o is sufficiently small, Muller's method is used to expedite eigenvalue convergence. This scheme fits a quadratic curve in complex space, also through the last three eigenvalue estimates and computed admittances, of the form

$$Y_o = b_o + b_1 (\text{eigenvalue}) + b_2 (\text{eigenvalue})^2$$

Setting $Y_o = 0$, this equation can be inverted using the standard quadratic formula to give an eigenvalue estimate for the next iteration. Note that both techniques have the advantage that no derivative of Y_o and only one evaluation of Y_o is required per iteration (in contrast, say, to Newton's method). A complete discussion of the more subtle applications of these two procedures for an efficient eigenvalue search is relegated to section E.4.

When the "eigenvalue" is determined to within desired accuracy, the eigenfunctions can be recovered using the stored orthonormalizing matrix and solution vectors [22]. For standardization, the magnitude of these eigenfunctions are adjusted so as to

make the amplitude of the pressure fluctuation equal to unity at the wall. If desired, energy production, dissipation and transfer terms can then be evaluated directly (see section 2.4).

CHAPTER IV

RESULTS

The hydrodynamic stability of the boundary layer formed on a heated, constant-temperature flat plate ($M = 0$) in two-dimensional water flow and with two-dimensional disturbances ($\psi = 0$ and $\theta = 0$) is examined and the results presented in this section. Specific comparison is sought with the results of Wazzan, et.al [4] who analyzed this same configuration, but who assumed only isothermal disturbances of the mean variables.

Rather than regenerating in this investigation the stability characteristics for the entire range of wall temperatures considered by Wazzan, et.al., selective checks are made to compare the results of the two. Accordingly, since those authors found that increased surface heating at first stabilized and then destabilized the boundary layer flow (i.e., peaking of $Re_{min.crit.}$ - that value of Re below which disturbances are damped for all wave numbers and frequencies), with the extreumums occurring at about $T_w = 140^\circ F$ ($T_\infty = 60^\circ F$), the numerical calculations herein will be limited primarily to wall temperatures within the normal liquid range of water and including that temperature range where the peaking occurs: specifically, $T_w = 90^\circ, 150^\circ$, and $200^\circ F$ with $T_\infty = 60^\circ F$. When detailed characteristic behavior is to be illustrated, the case of $T_w = 90^\circ F$ will be used, as this is conceivably within the range of

temperatures for which experimental comparison can be made.

An accurate solution to the mean flow equations is essential for solving the disturbance equations. The procedure and results for the mean flow solution are described in Section 3.2 and Appendix C. In the latter both detailed boundary layer distributions of all the mean properties and their derivatives required for the coefficients of the disturbance equations, and variations of surface velocity and temperature gradients with the wall temperature are graphically presented.

The mean velocity and temperature boundary layer profiles to be examined in this section are repeated in Figure 4.1. Note that the temperature boundary layer is much thinner than that of the velocity boundary layer so thermal influences are restricted to regions close to the wall. This observation is related to the later understanding of the relative importance of thermal disturbances in boundary layer stability calculations.

Keeping in mind the role that a linear stability analysis should play in only suggesting those conditions which might enhance or delay the onset of laminar-turbulent transition (there is no definitive link between the point of instability predicted by such an analysis and the point of transition), this investigation is restricted to regions which could conceivably still be laminar. Thus, although determination of stability characteristics for excessively large Re might be an interesting numerical or mathematical exercise, the results are not of interest if transition has

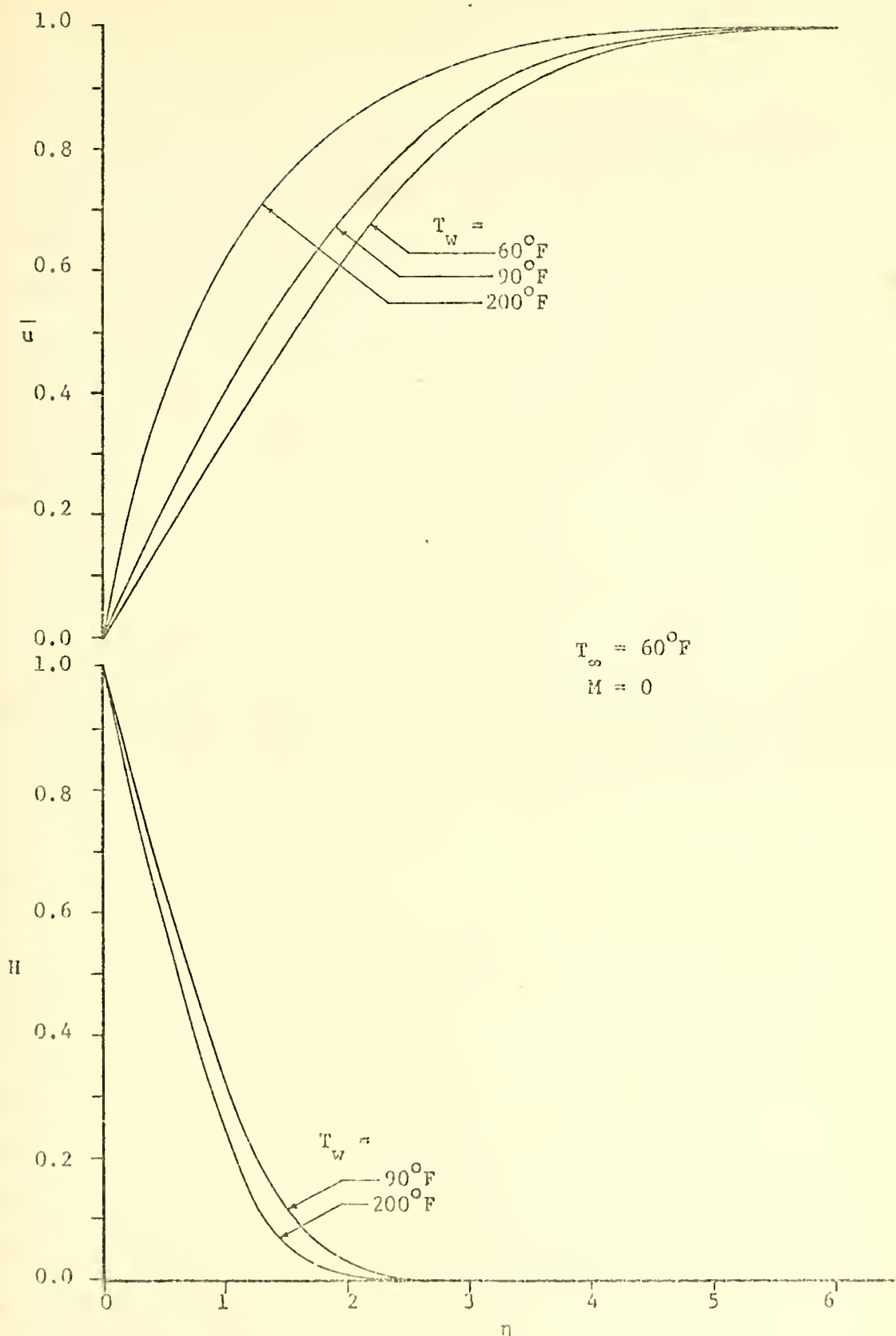


Figure 4.1 Mean velocity and temperature profiles for various T_w ($T_\infty = 60^{\circ}\text{F}$).

occurred.

Much of this investigation was conducted neglecting the effects of a fluctuating density field ($r = 0$); that is, only fluctuations of viscosity $\mu(y)$ and thermal conductivity $\kappa(y)$ were included in the disturbance momentum and energy equations, respectively. Such an assumption seemed reasonable due to the relative constancy of the density of water over the normal liquid range. Subsequent calculations with variable density nevertheless were made and their results are included.

Unless otherwise indicated, the property-temperature variation for water is that specified in Appendix B.2. Although this variation differed slightly from that of Kaups and Smith [7] (used by Wazzan, et.al. in their analysis) as shown in Figure B.7, there is a marked effect on some of the calculated stability characteristics, as will be shown presently.

4.1 Stability Characteristics

As suggested in previous discussion, for a specified set of mean flow parameters (T_w , T_∞ , and M), the eigensolutions to the homogeneous disturbance equations and their boundary conditions describe a surface in the four-dimensional parameter space (α_R , α_I , ω_∞ , and Rc). It is of interest to locate minima and maxima on this surface and to trace the path followed by an actual disturbance as it propagates through the boundary layer (e.g., to ascertain whether an amplification region ($\alpha_I < 0$) is traversed,

and if so, the rate of amplification expected). The stability characteristics associated with neutral and amplified disturbances are discussed below.

4.1.1 Neutral Disturbances ($\alpha_I = 0$)

Perhaps the most obvious quantitative guide to the effect of heating on boundary layer stabilization is the amount with which neutral curves are shifted with changes in the wall-to-free stream temperature difference. The movement of these stability loops is characterized by changes in the minimum critical Reynolds number,

$Re_{min.crit}$, the maximum wave number $a_{R_{max}}$, and the maximum frequency, ω_{∞} (above which all disturbances are damped). As may be seen from Figures 4.2 and 4.3, with only moderate heating, both the fourth order system of equations of Wazzan, et.al. [4] and the sixth order system of this investigation (without density fluctuations, however) predict a significant delay in the onset of boundary layer instability (evidenced by the increased $Re_{min.crit}$) and a reduced range of frequencies and wave numbers which could become unstable. As the wall-to-free stream temperature difference is further increased, however, both the fourth and sixth order systems consistently indicate a peaking and subsequent decrease of $Re_{min.crit}$. Based on these calculations for water at the indicated temperature levels, the following conclusions may be drawn.

- (1) It would be impossible to achieve complete boundary layer stabilization by indefinitely increasing the heat rate;

All curves are for $T_{\infty} = 60^{\circ}\text{F}$ using the property-temperature relationships of Kays, et.al.[7].

— Present investigation ($r = 0$)
- - - Wazzan, et.al. [4]

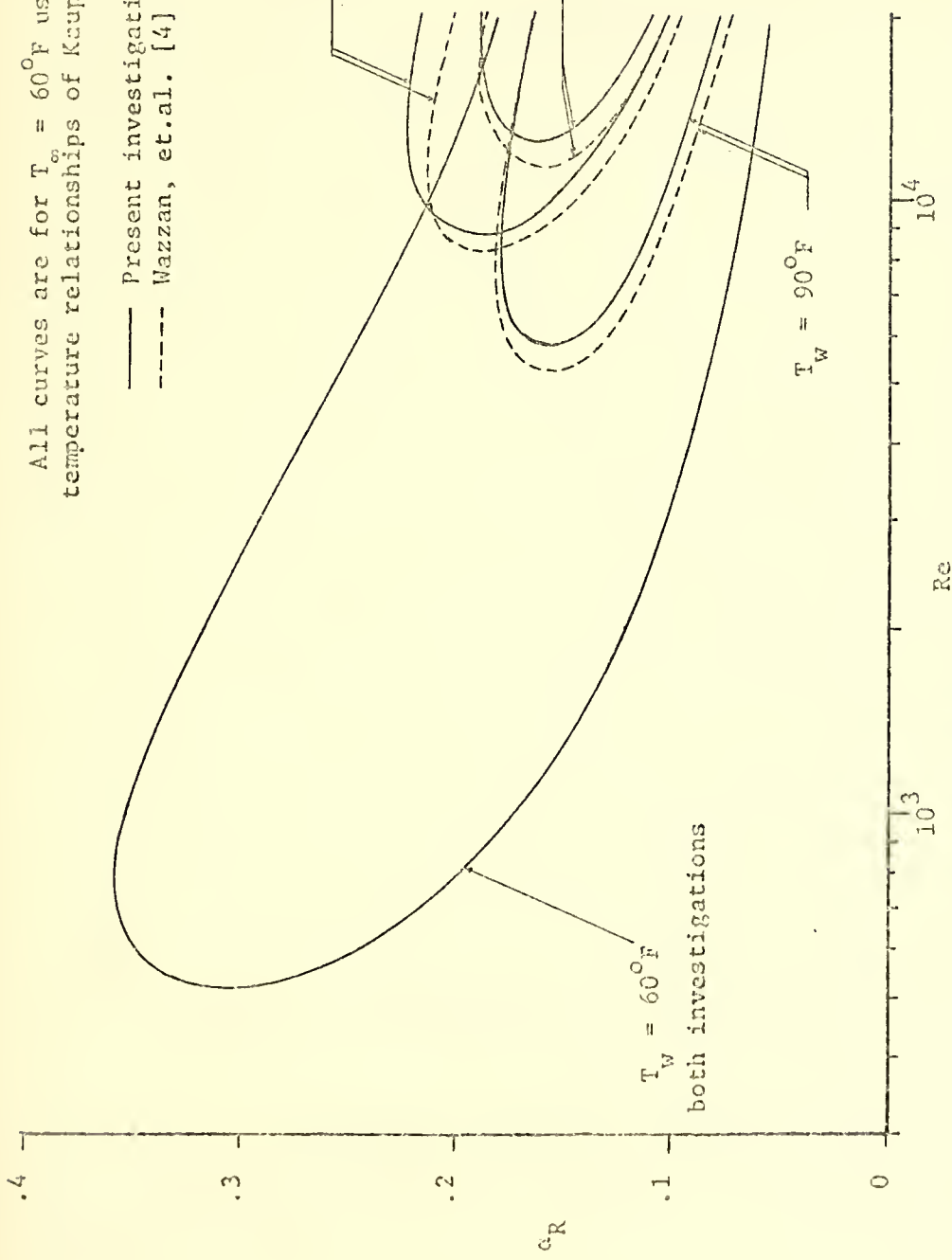


Figure 4.2 Comparison of neutral stability curves computed with and without thermal disturbances for various wall temperatures.

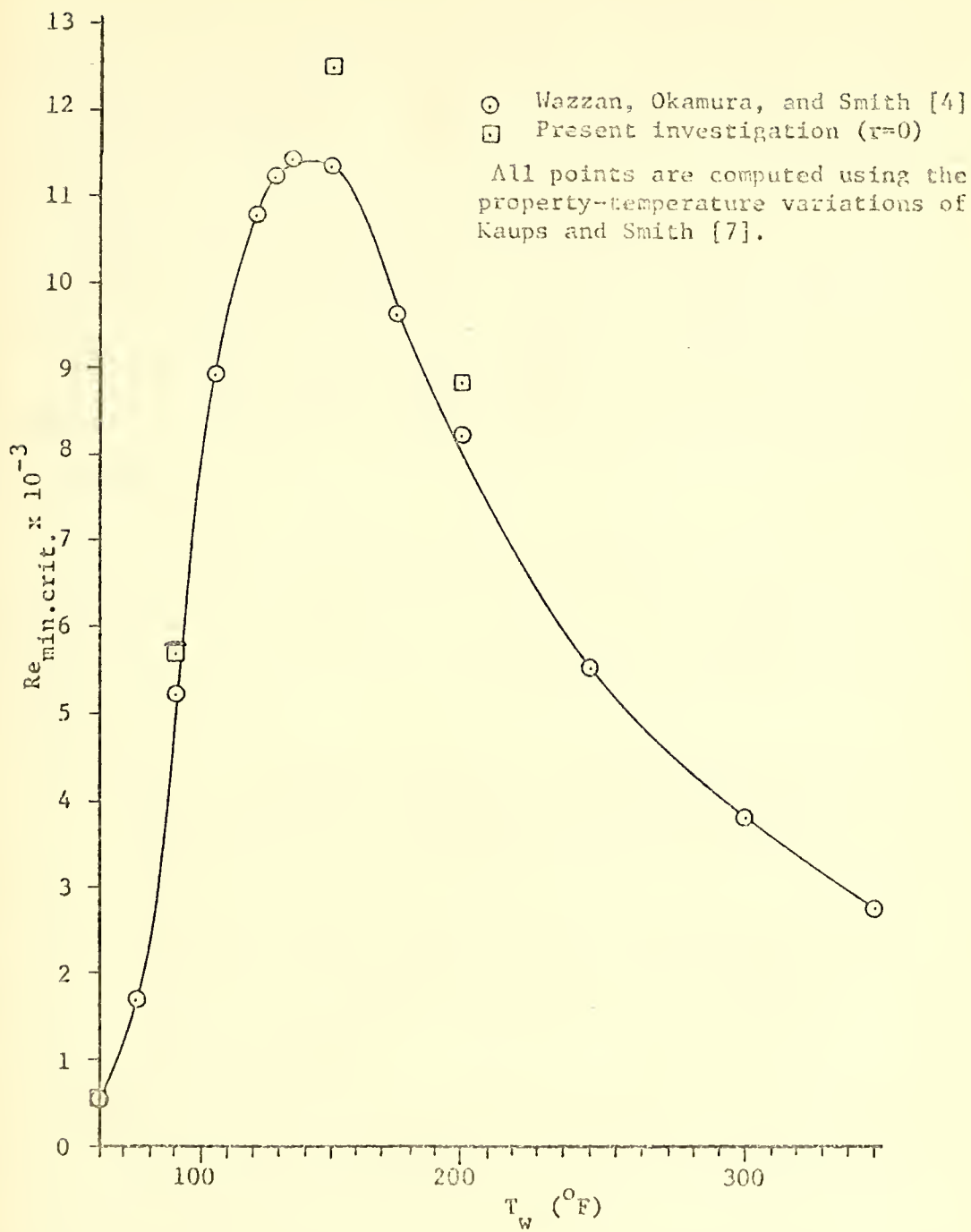


Figure 4.3 Comparison of $Re_{min,crit.}$ computed with and without thermal disturbances as a function of T_w (fixed $T_\infty = 60$ °F).

(2) While the calculations which include thermal disturbances do predict slightly larger values of $Re_{min.crit.}$, the qualitative variation of this quantity with T_w (for fixed $T_\infty = 60^\circ F$) is not altered.

The values of $Re_{min.crit.}$ are easily obtained for specified mean flow parameters by fixing $\alpha_I = 0$ and α_R , then adjusting estimates of Re and ω_∞ until boundary conditions can be satisfied. An example of this procedure is shown in Figure 4.4 and 4.5 for several different cases.

For no other calculation is the influence of the chosen property-temperature relationship or assumed property fluctuations more pronounced than in this one. For example, from these two figures it may be seen that:

- (1) use of the property variation of Kaups and Smith [7] effects a shift of $Re_{min.crit.}$ first above ($T_w = 90^\circ F$) and then below ($T_w = 200^\circ F$) that computed with the variation specified in Appendix B.2;
- (2) for either property variation, calculations including thermal disturbances (but with $r = 0$) predict a $Re_{min.crit.}$ roughly 10% greater than that computed using the fourth order equation of Wazzan, et.al. (equation (1.2));
- (3) inclusion of density fluctuations in the calculations as well, offsets the gains in stability predicted above in (2) as T_w is increased.

An explanation for the relatively pronounced influence of density fluctuations on $Re_{min.crit.}$ calculations is found in the distribution of disturbance properties in the stability equations. Although the density fluctuations may be comparatively small (by

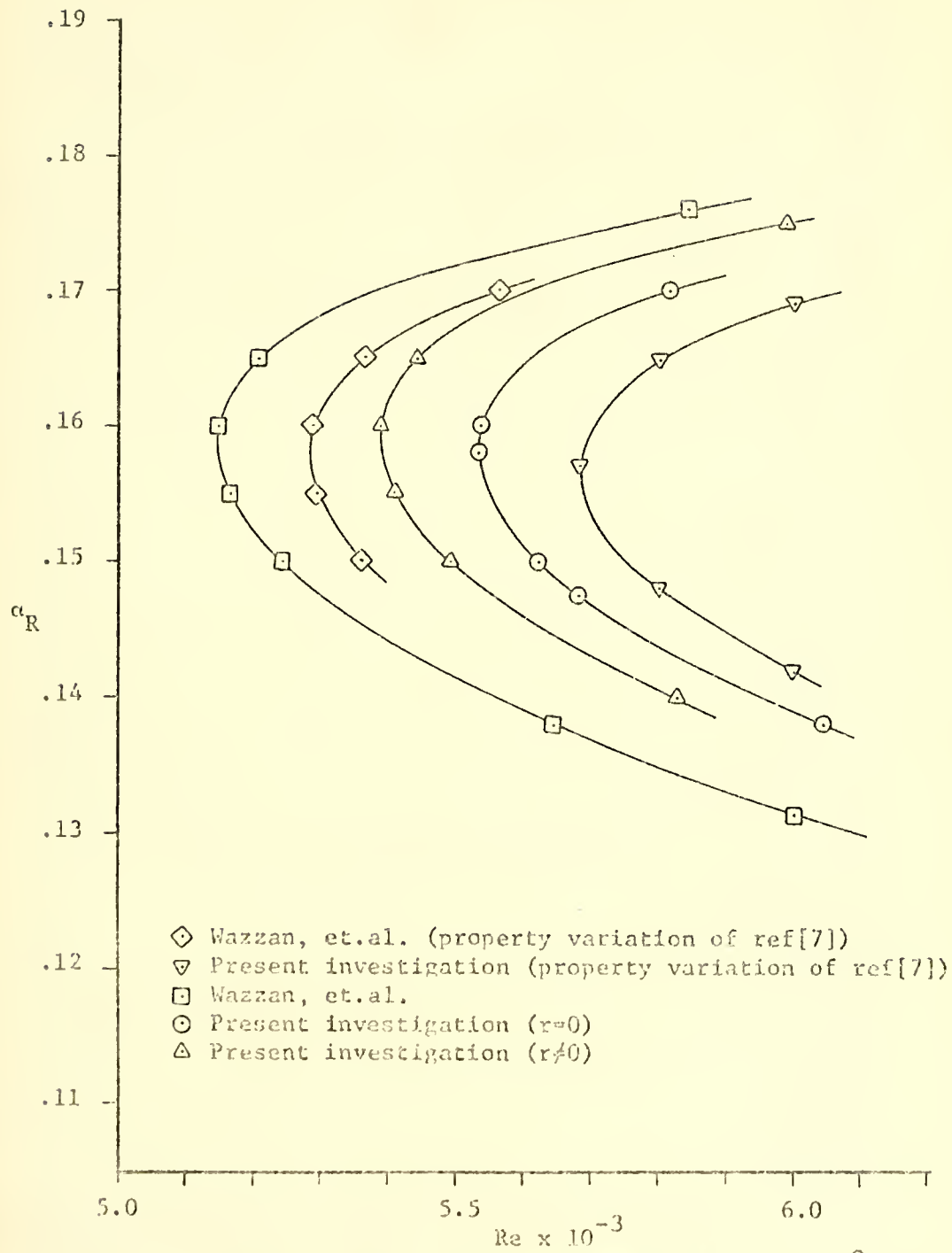


Figure 4.4 Details of $Re_{min.crit.}$ calculation for $T_w = 90^{\circ}\text{F}$ ($T_\infty = 60^{\circ}\text{F}$)

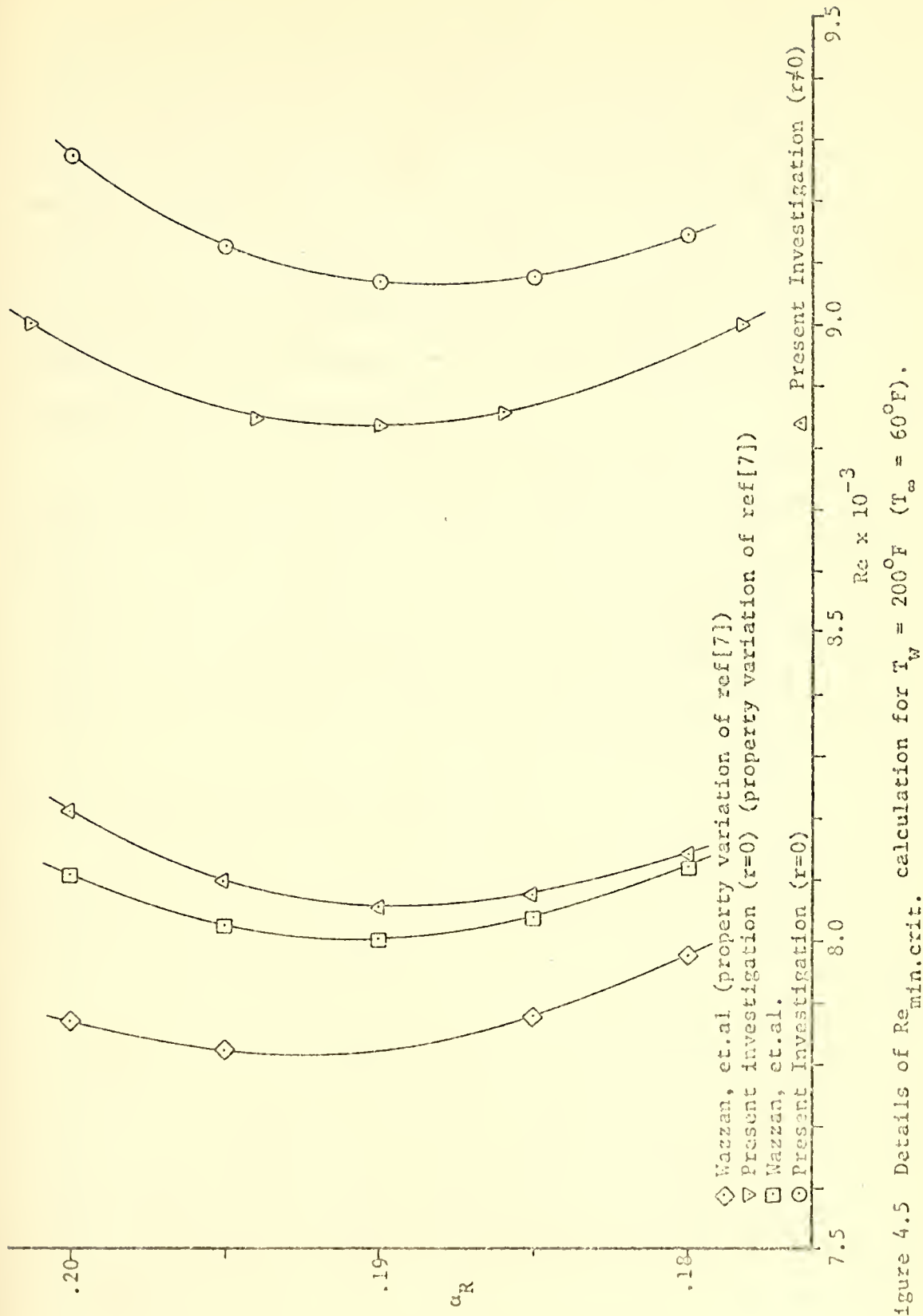


Figure 4.5 Details of $Re_{min.crit.}$ calculation for $T_w = 200^{\circ}\text{F}$ ($T_\infty = 60^{\circ}\text{F}$).

as much as several orders of magnitude less than the viscosity fluctuations - see Figures 4.9 and 4.10, for example), they do appear in both the inviscid and viscous parts of the stability equations, whereas viscosity fluctuations are restricted only to the latter. As temperatures are increased, the disparity between the two disturbance quantities diminishes; eventually, disturbance density contributions dominate those from all other property fluctuations in the calculations.

However, as shown in Figures 4.4 and 4.5, while the fluctuating viscosity terms tend to enhance stability, the density terms degrade it. It is important to note that over the normal liquid range of water, results from the sixth order system of equations (even including density disturbances) predict a slightly more stable boundary layer than does the fourth order system for which $\tau(y) \geq 0$.

4.1.2 Amplified Disturbances ($\alpha_I < 0$)

The tendency to transition is also a function of amplification rates and so attention will now be given to the amplified portion of the stability loop ($\alpha_I < 0$).

A typical set of stability curves illustrating the topological nature of the eigenvalue variation for $T_w = 90^\circ\text{F}$, $T_\infty = 60^\circ\text{F}$, and $M = 0$ ($r = 0$) is shown in Figure 4.6. These curves are similar in general shape to those for the unheated Blasius boundary layer although dramatically different in magnitude (see reference [26, p.90] for example).

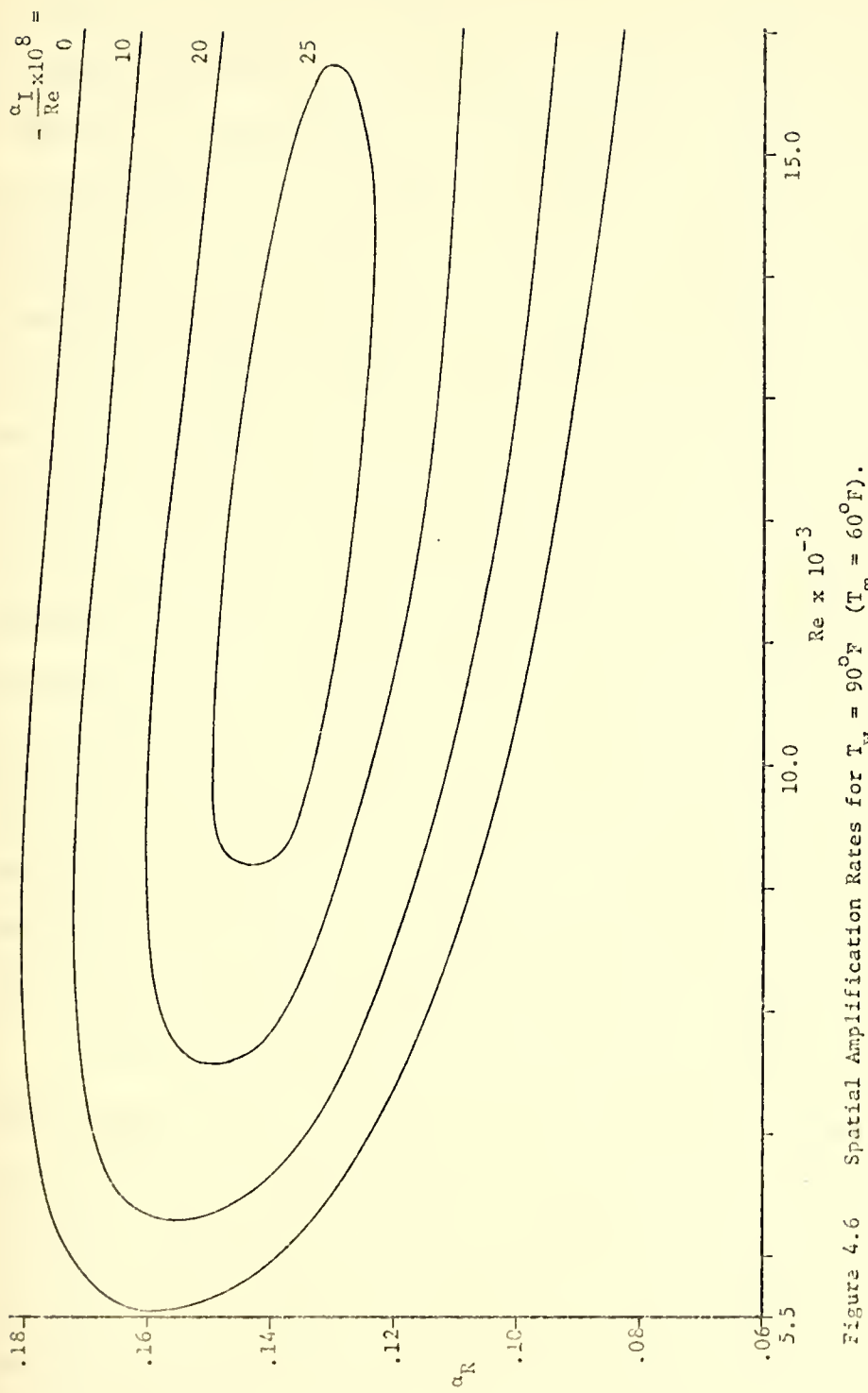


Figure 4.6 Spatial Amplification Rates for $T_w = 90^{\circ}\text{F}$ ($T_{\infty} = 60^{\circ}\text{F}$).

A much more significant indication of boundary layer stabilization by heating than $Re_{min.crit.}$ is given by the maximum amplification rate, $-(\alpha_I/Re)_{max}$, established for specified mean flow conditions. The parametric location at which this maximum occurs is determined by a more involved procedure than that for finding $Re_{min.crit.}$, as illustrated in Figure 4.7. More specifically, the amplification rates for specified Re are computed and individual local maxima determined. Following the locus of these individual maxima, the largest value attained is designated the maximum amplification rate and its associated wave number (and frequency) are obtained graphically. While the flatness of this locus curve in the neighborhood of $-(\alpha_I/Re)_{max}$ allows relatively accurate evaluation of that quantity, it does, however, preclude similar accuracy for α_R (and ω_∞) there. Physically this implies that there is effectively a band of wave numbers (and frequencies) which will receive nearly maximum amplification. To complete the eigenvalue set, Re can be determined from Figure 4.6 by again following the locus of individual maxima until the required value of α_R is reached.

Due to the numerical effort required to compute the maximum amplification rate, only one set of calculations was made for $T_w = 90^\circ F$ and $T_w = 200^\circ F$ ($T_\infty = 60^\circ F$), using the presumably more accurate property-temperature relationships of Appendix B.2 (assuming $r = 0$). Values obtained for $-(\alpha_I/Re)_{max} \times 10^3$ of 26.6 for the former and 19.5 for the latter can be compared with the corresponding values tabulated by Wazzan, et.al. [4] of 28 and 20, and the value

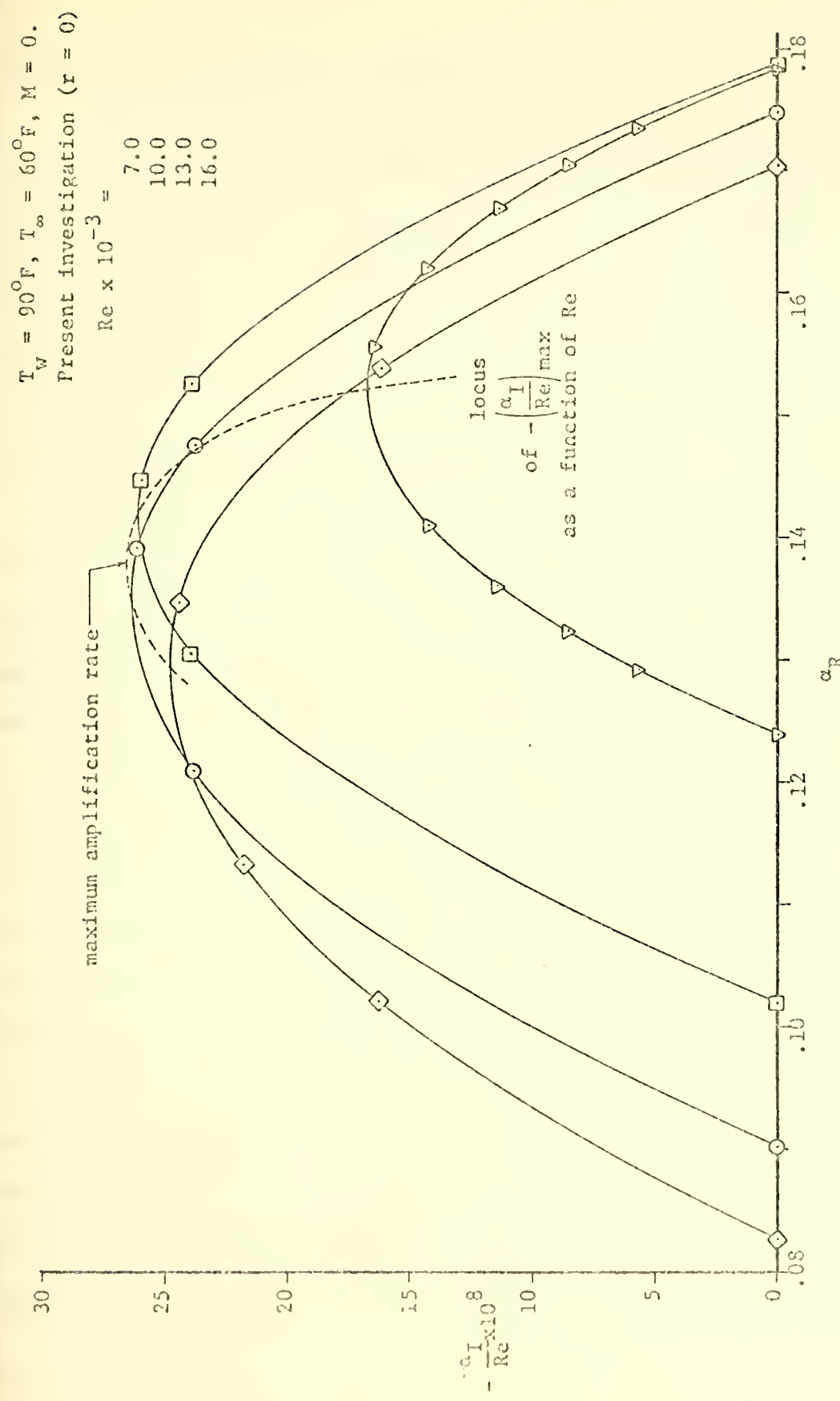


Figure 4.7 Maximum Amplification Rate determination for $T_w = 90^{\circ}\text{F}$ ($T_\infty = 60^{\circ}\text{F}$).

for the unheated (Blasius) boundary of 740.

Thus, not only is the onset of disturbance instability delayed and the range of disturbance wave numbers and frequencies receiving amplification reduced as pointed out in the preceding section, but the amplification rates to which disturbances will be subjected are also dramatically reduced. These features all point to a more stable boundary layer flow.

4.2 Disturbance Amplitude and Energy Distributions

Finding no major modifications to the stability characteristics of a heated, water boundary layer by including in the calculations the effects of a disturbance temperature field, an explanation is sought from the boundary layer distribution of disturbance quantities and the energies produced or dissipated by them.

Due to the homogeneity of the equations and boundary conditions, solutions to the disturbance equations are independent of an absolute amplitude (see section 2.3.1). Thus, as a comparison is sought between disturbance levels for both the same and different mean thermal boundary conditions, it is necessary to resort to some physical reasoning to determine a normalizing quantity that would remain virtually constant in the comparison. Since there is no streamwise pressure gradient (i.e., $M = 0$ for all Re), the mean pressure within the boundary layer is assumed constant, and the disturbance pressure is nonzero and slowly varying throughout (see Figures 4.8 through 4.10, for example), the amplitude of the

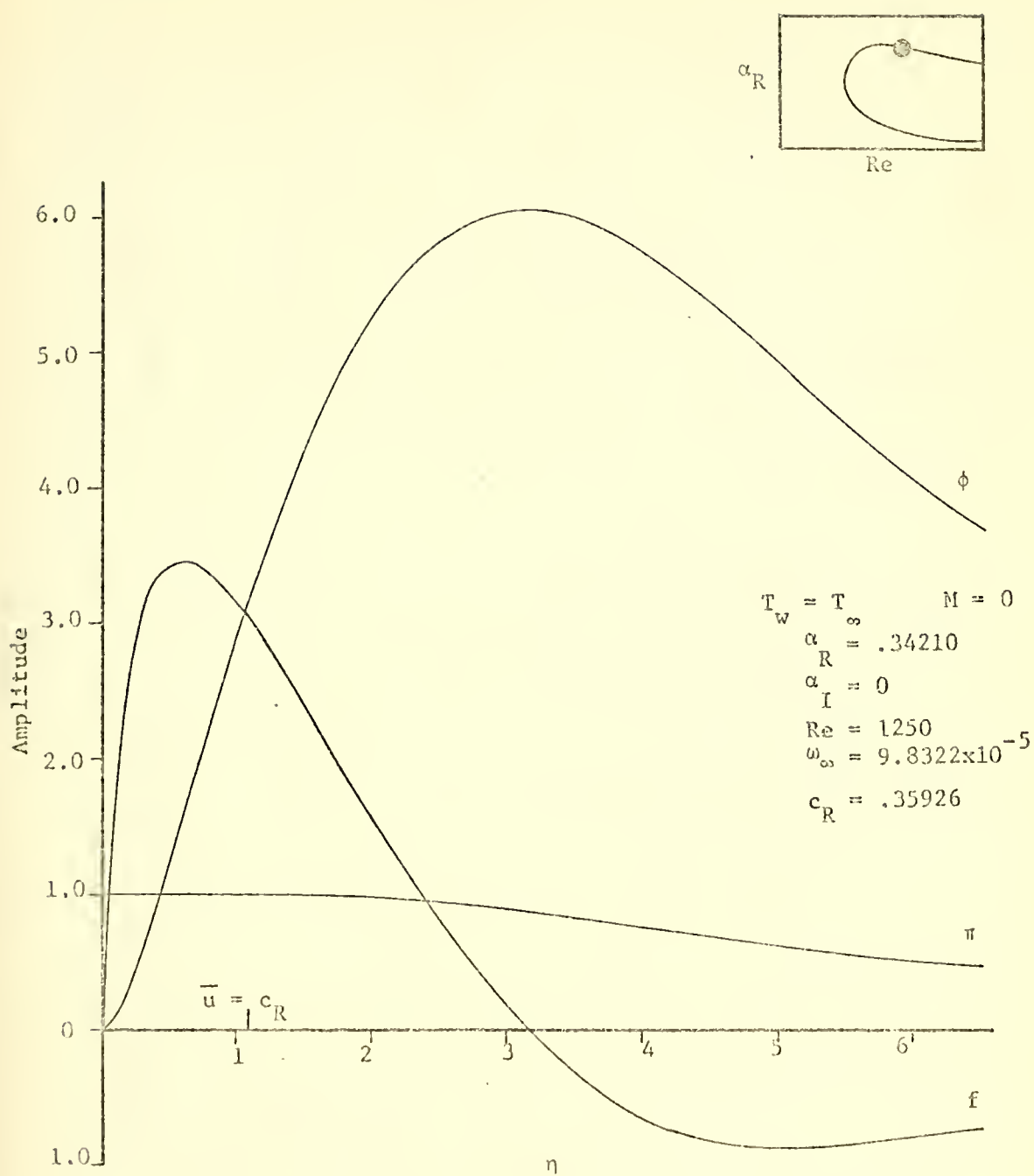


Figure 4.8 Neutral disturbance amplitude profiles for the unheated (Blasius) boundary layer.

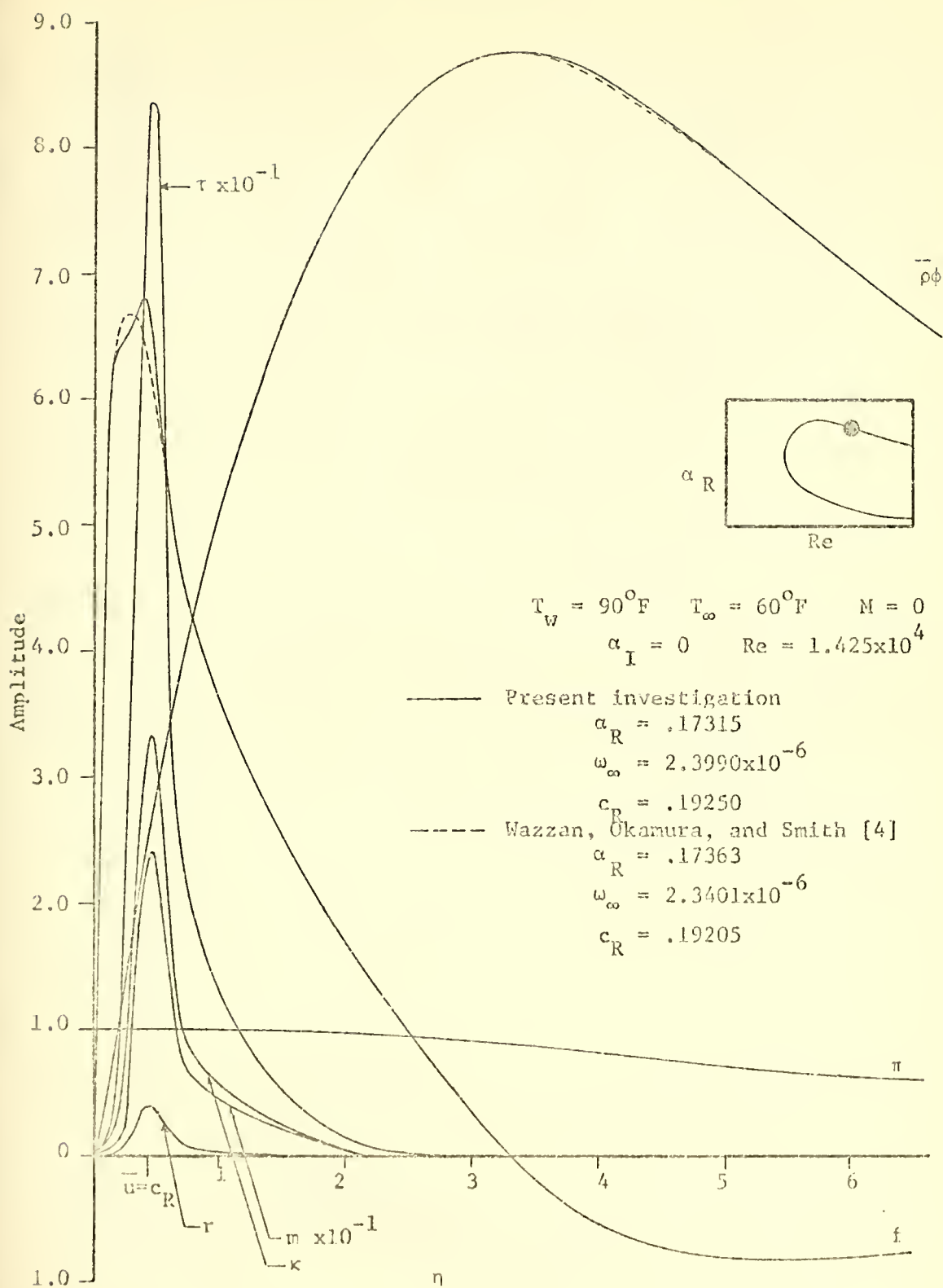


Figure 4.9 Neutral disturbance amplitude profiles for the heated boundary layer: $T_w = 90^{\circ}\text{F}$ and $T_\infty = 60^{\circ}\text{F}$.

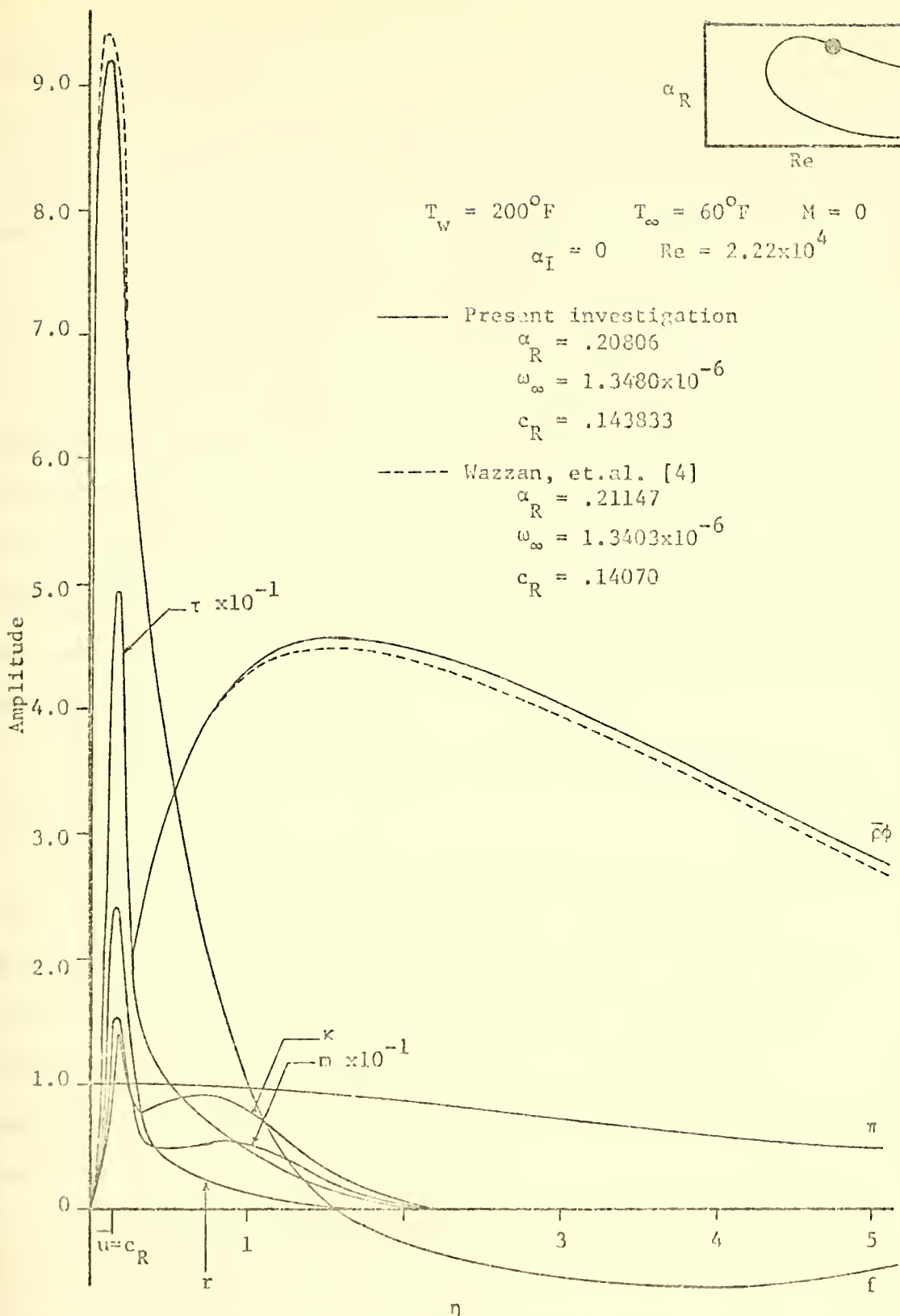


Figure 4.10 Neutral disturbance amplitude profiles for the heated boundary layer: $T_w = 200^{\circ}\text{F}$ and $T_\infty = 60^{\circ}\text{F}$.

disturbance pressure at the wall, $|\pi(0)|$, was chosen to normalize all disturbance quantities. Thus all comparisons made between different eigensolutions in the remainder of this section are predicated on this assumption.

To further investigate the importance of density fluctuations, they are included in all calculations made in this section.

Typical amplitudes of disturbance quantities found in this analysis are presented in Figures 4.8 through 4.10 for wall temperatures $T_w = 60^\circ$, 90° , and 200°F ($T_\infty = 60^\circ\text{F}$), respectively. For standardization, the eigenvalues associated with each set of eigenfunctions are all located on the upper branch of their respective neutral stability curves at frequencies near that receiving maximum amplification.

After studying these figures, the following observations are made.

(1) As anticipated from the relatively large Pr for water (i.e., such that the thermal boundary layer thickness is much less than the velocity one), in the temperature range considered, thermal effects are restricted to a region very close to the wall. Since thermal fluctuations must vanish at the wall, even within this region, they attain fairly large amplitudes only within a far narrower range.

(2) By far the most dominant property disturbance amplitude is that of viscosity. However, for relatively small surface heating ($T_w = 90^\circ\text{F}$), even the thermal conductivity disturbance amplitudes is

commensurate with that of the normal velocity in some regions.

For large heating ($T_w = 200^\circ\text{F}$), when density fluctuations are significant, they are seen to be larger in amplitude than both the thermal conductivity and normal velocity disturbances.

(3) With increased heating, the ratio of $|f|_{\max} / |\bar{\rho} \phi|_{\max}$ increases significantly. Further, assuming that the disturbance wall pressure amplitude is relatively insensitive to changes in T_w within the range $60^\circ \leq T_w \leq 200^\circ\text{F}$, $|f|_{\max}$ increases monotonically with T_w while $|\bar{\rho} \phi|_{\max}$ exhibits a maximum.

(4) Just as the stability characteristics are only slightly modified by the inclusion of thermal disturbances in the analysis, so too are the disturbance velocity and pressure amplitude profiles. Even the disparity shown (except in the region where thermal disturbances obviously dominate) can be attributed in part to the difference between the neutral eigenvalues required to satisfy the fourth and sixth order systems.

Once the eigenvalues and eigenfunctions are obtained by the procedure outlines in section 2.3.1, it is a simple matter to compute the energy balance developed in section 2.4. However, for ease of analysis, only those terms contributing a net increase or decrease of energy of a neutral disturbance are evaluated (i.e., all terms of equation (2.50)). The results of such calculations are presented in Figures 4.11 through 4.16. For each of the cases $T_w = 60^\circ, 90^\circ, 200^\circ\text{F}$ ($T_\infty = 60^\circ\text{F}$), the eigenvalues selected from the upper and lower branches of the neutral stability curves (see

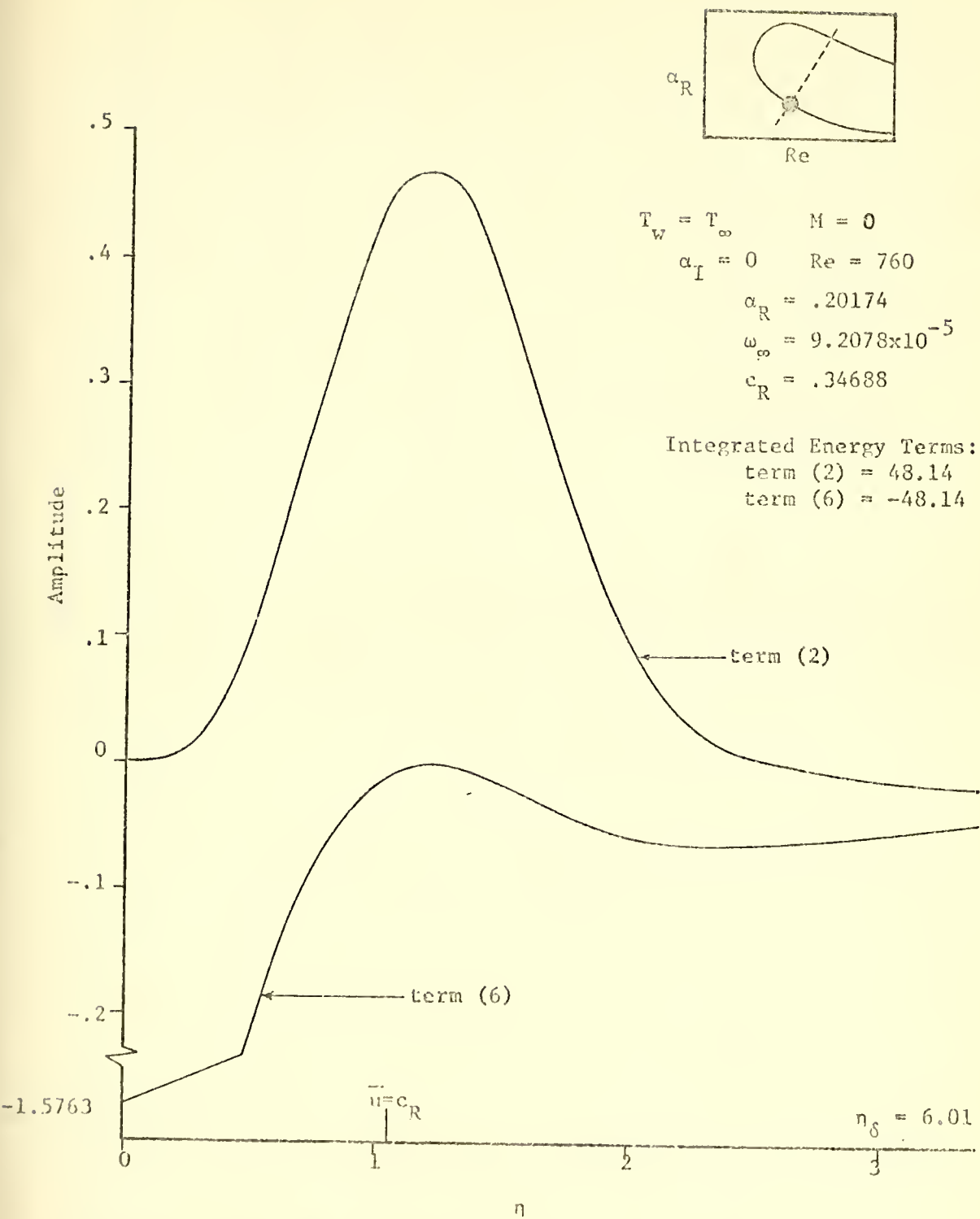


Figure 4.11 Energy distributions of a neutral disturbance in the unheated (Blasius) boundary layer (lower branch).

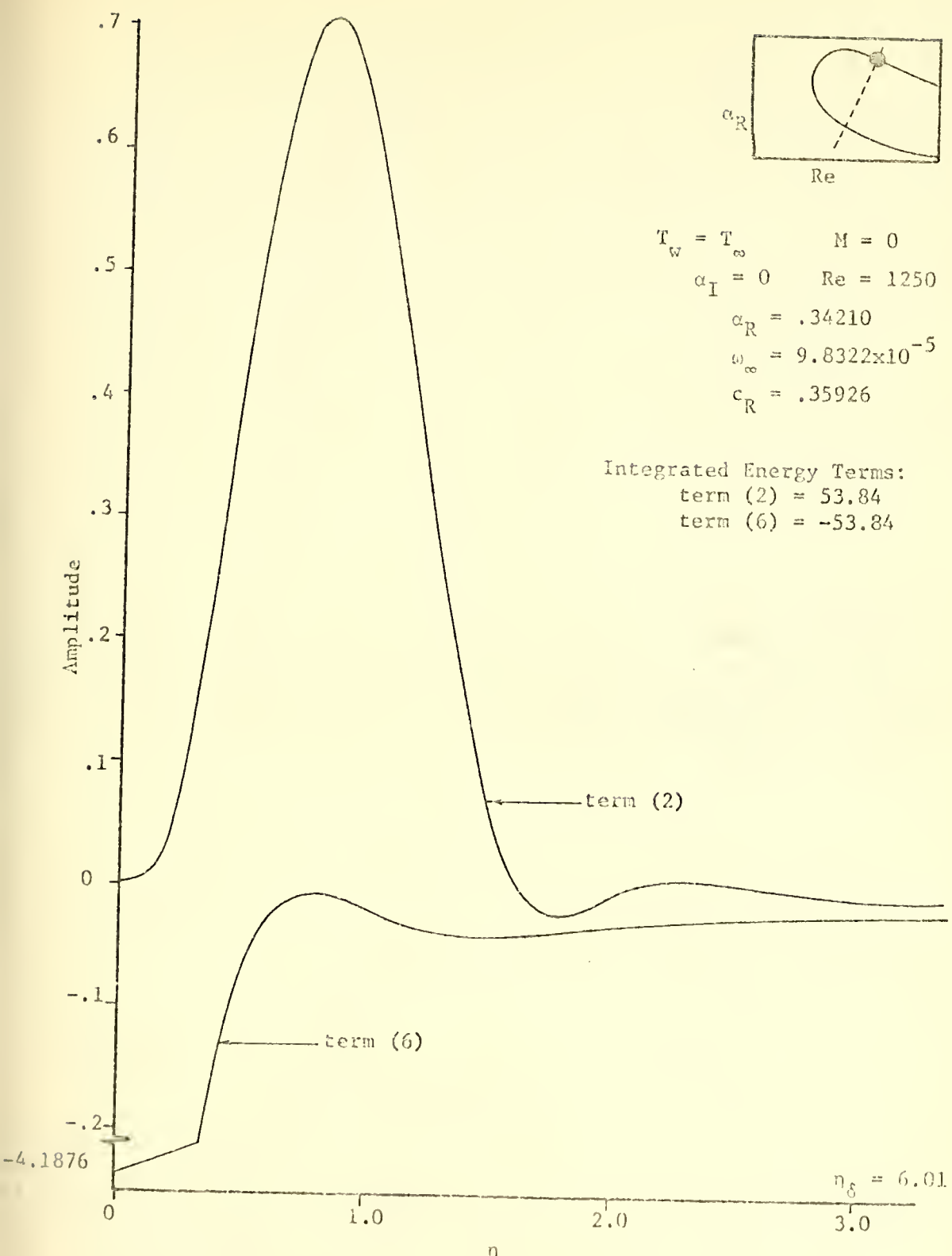


Figure 4.12 Energy distributions of a neutral disturbance in the unheated (Blasius) boundary layer (upper branch).

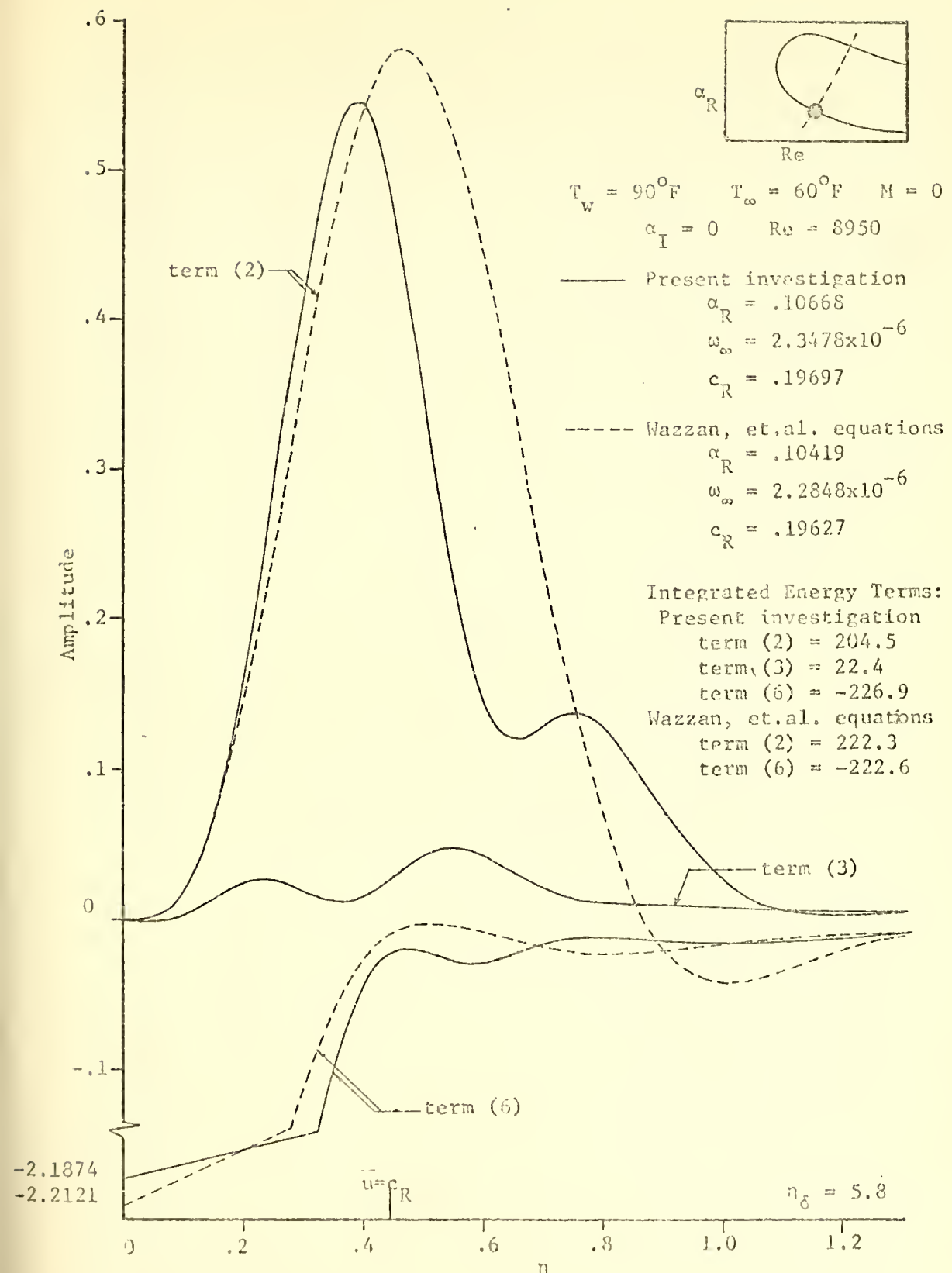


Figure 4.13 Energy distributions of a neutral disturbance in the heated boundary layer: $T_w = 90^{\circ}\text{F}$ and $T_\infty = 60^{\circ}\text{F}$ (lower branch).

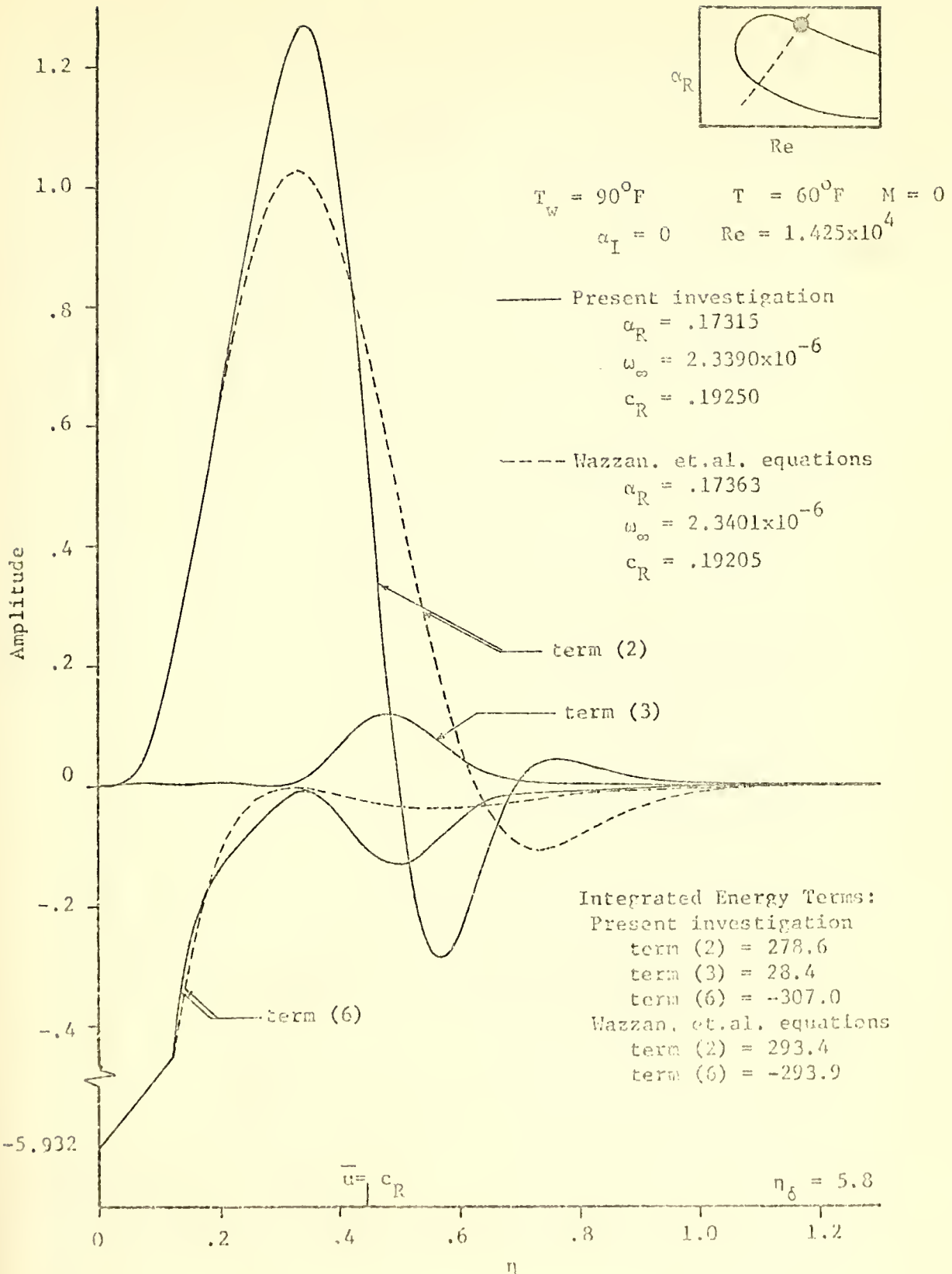


Figure 4.14 Energy distribution of a neutral disturbance in the heated boundary layer: $T_w = 90^{\circ}\text{F}$ and $T_\infty = 60^{\circ}\text{F}$ (upper branch).

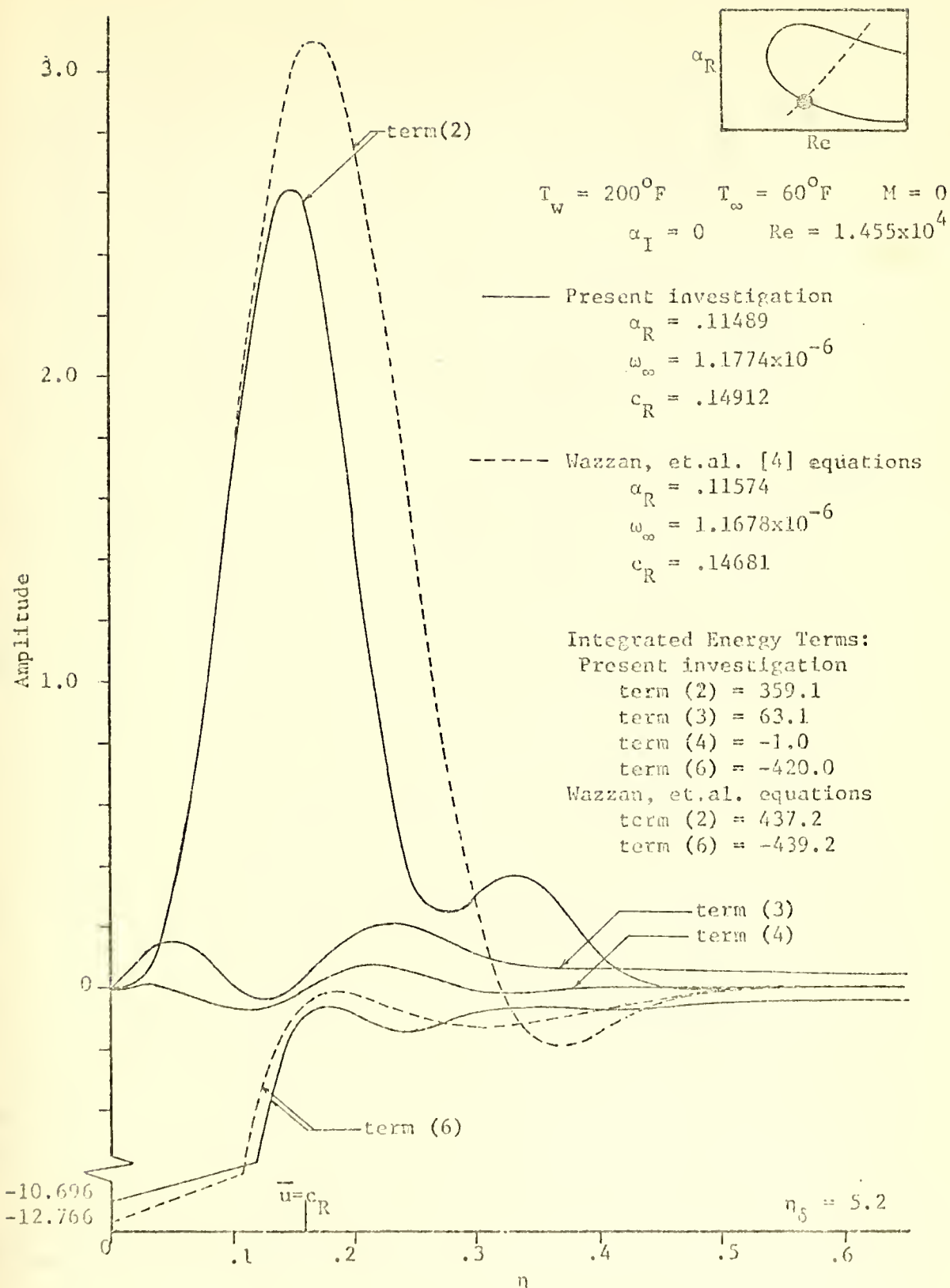


Figure 4.15 Energy distributions of a neutral disturbance in the heated boundary layer: $T_w = 200^{\circ}\text{F}$ and $T_\infty = 60^{\circ}\text{F}$ (lower branch).

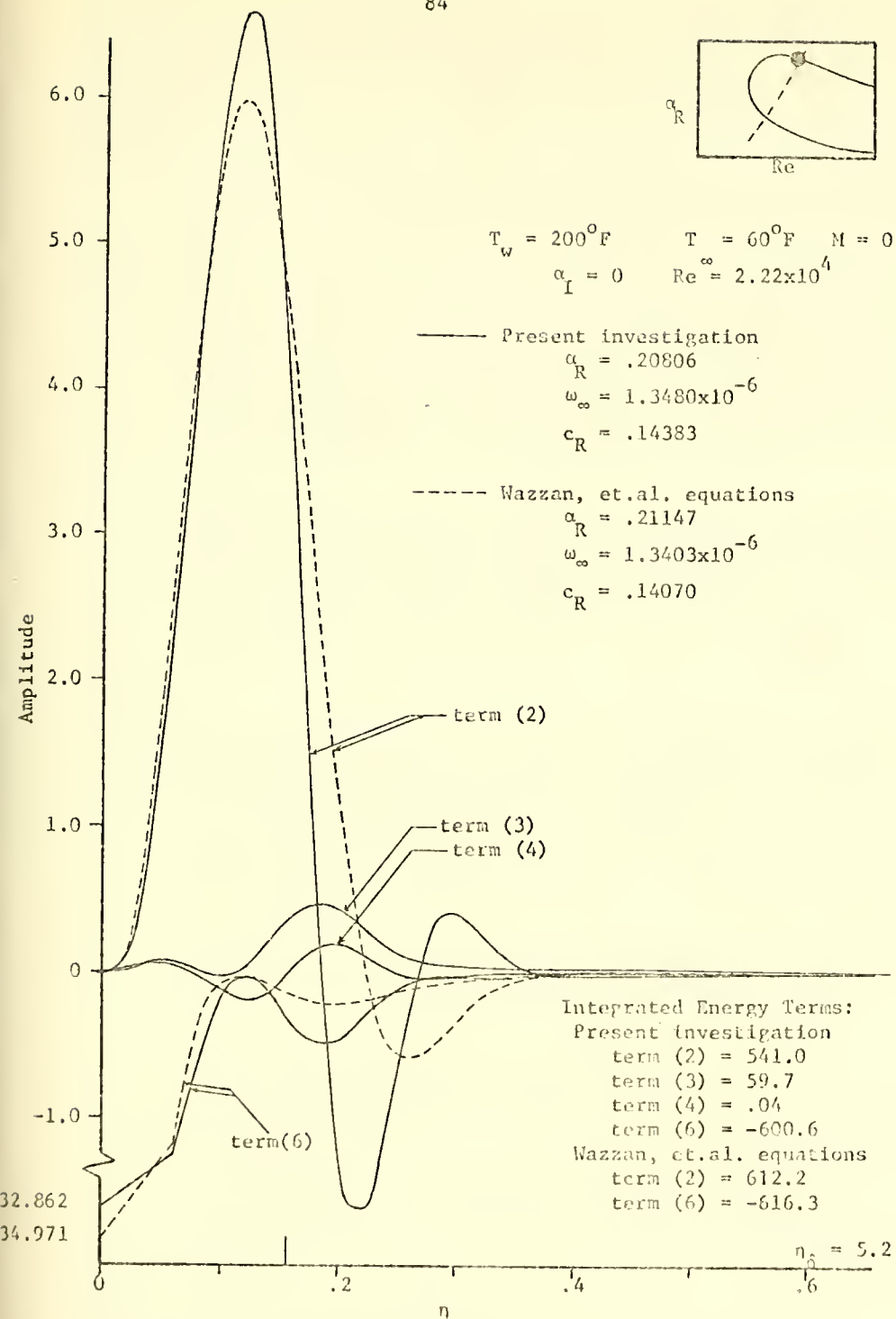


Figure 4.16 Energy distributions of a neutral disturbance in the heated boundary layer: $T_w = 200^{\circ}\text{F}$ and $T_\infty = 60^{\circ}\text{F}$ (upper branch).

Figure 4.1) again are for frequencies for which disturbances are subjected to approximately maximum amplification when traversing the loop.

From these six figures, the following observations are made. The "terms" referred to are those designated in equation (2.50).

- (1) The dominant terms in the neutral disturbance energy balance are the traditional ones: The Reynolds stress production (term (2)) in the region between the wall and the neighborhood of $u = c_R$, balanced by the dissipation (term (6)) which is extremely large near the wall.
- (2) Dissipation due to a nonuniform mean disturbance density (term (7)) is always negligible. Although not nearly as small, energy production due to a mean viscosity gradient (term (5)) is also insignificant. Neither are large enough to appear in Figures 4.11 -- 4.16.
- (3) The disturbance shear stress (term (3)), although dissipative in some regions, represents primarily energy production for the disturbance field. In all the cases examined, it produced roughly 10% of the energy, with the Reynolds stress production (term (2)) supplying the rest. Recall that this is approximately the same amount that $Re_{min.crit.}$ was increased for sixth order system calculations ($r = 0$) beyond that calculated with the fourth order system (see Figures 4.4 and 4.5).
- (4) Pressure production (term (4)), also resulting from density nonuniformities, primarily gives rise to production for $u > c_R$ and dissipation for $u < c_R$. Since its integrated value over the boundary layer is nearly zero, this term is not thought to be of significance in the stability of this flow.

To check the accuracy of the computed energy production and dissipation terms, each was first numerically integrated from the wall to the boundary layer edge and then the resultant summed. Within the accuracy sought, this sum was zero as required by

equation (2.50). Furthermore, it was found that the percent of positive or negative energy contribution from the production terms (such as the Reynolds stress) remained virtually unchanged with changes in the wall temperature level.

It is especially important to note the extent of the region in which significant energy contributions take place. For the heated boundary layer, in contrast to the unheated one, all energetics are restricted to a region very close to the wall. Outside of that region, energy terms tend to vanish, signifying that there is very little correlation between disturbance quantities over most of the boundary layer.

CHAPTER V

SUMMARY OF RESULTS AND CONCLUSIONS

This investigation has examined the sixth order system of equations describing the hydrodynamic stability of infinitesimal disturbances in a heated, flat plate, water boundary layer flow. Throughout, comparison has been made with the fourth order analysis of this same problem as previously done by Wazzan, Okamura, and Smith [4].

The time-averaged (mean) equations of laminar flow are simplified by making the usual boundary layer assumptions, and by neglecting buoyancy forces, viscous dissipation and expansion energy. They are then transformed from partial to ordinary differential equations using Howarth-Dorodnitsyn type similarity variables and their resultant solutions used to provide the velocity, temperature, and other profiles required for the disturbance equations. The latter are found as the linearized difference between the instantaneous and mean equation, after neglecting here as well buoyancy, dissipation, and expansion energy terms, assuming the flow to be locally parallel, and finally using a normal modes analysis to obtain ordinary, linear differential equations. The two sets of equations, mean and disturbance, thus derived differ from those of Wazzan, et.al. by the inclusion of a disturbance energy equation coupled to the other disturbance equations. This permits density,

viscosity, and thermal conductivity fluctuation effects to be considered in the stability problem.

Both the fourth order system of Wazzan, et.al. and the sixth order system of the present investigation predict significant boundary layer stabilization with moderate heating, but display a maximum and subsequent stability decrease as the plate surface-to-free stream temperature difference is further increased. The computed stability characteristics (minimum critical Reynolds Number, maximum amplification rate, maximum wave number and frequency subject to amplification, etc.) obtained from each system differ only slightly, however. In particular, the peaking of each characteristic with wall temperature (at about $T_w = 140^{\circ}\text{F}$ with fixed $T_\infty = 60^{\circ}\text{F}$) is neither eliminated nor significantly altered by the higher order system. Thus, complete stabilization apparently cannot be achieved by indefinitely increasing boundary layer heating.

The insensitivity of these results to the additional consideration of thermal disturbances is attributed to the extremely limited region in which such disturbances are important. Due to the relatively large Prandtl Number for water and homogeneous disturbance boundary conditions, the boundary layer distributions of thermal disturbance amplitudes "spike" very close to the wall.

In all cases considered, the sixth order stability system is found to predict a slightly more stable flow than the fourth order system, as evidenced by larger values of the minimum critical Reynolds Number and reduced values of the maximum amplification rate.

However, it is postulated that for wall temperatures beyond the normal liquid range of water (with $T_\infty = 60^\circ\text{F}$), the presence of density fluctuations will eventually negate the increased stability predicted with only viscosity fluctuations assumed, and actually degrade the degree of stability predicted by the fourth order system. That is, when thermal disturbances are assumed, it is necessary to include all property disturbances to obtain an accurate assessment of the boundary layer stability.

The admission of thermal fluctuations also has revealed the existence of several energy production and dissipation terms not present in an energy balance equation for the fourth order system. Of particular note is the disturbance shear stress production, $-\tilde{\rho} \left(\frac{\partial \tilde{u}}{\partial y} + \frac{\partial \tilde{v}}{\partial x} \right) \frac{d\tilde{u}}{dy}$, a source which accounts for about 10% of the energy extracted from the mean and supplied to the disturbance flow. In contrast, when only isothermal disturbances are assumed, energy is supplied completely by the Reynolds stress production,

In summary, the fourth order system of equations used by Wazzan, et.al. [4] seems to adequately describe the stability of a heated, water boundary layer flow in the temperature ranges considered. This may not be true, however, for other liquids, particularly those with $\text{Pr} < 1$, where it is conjectured that calculations will be much more sensitive to the influence of thermal disturbances.

REFERENCES

1. DiPrima, R. C., and Dunn, D. W. "The Effect of Heating and Cooling on the Stability of the Boundary-Layer Flow of a Liquid over a Curved Surface." J. Aero. Sci., Vol 23, No. 10 (1965), 913-916.
2. Hauptmann, E. G. "The Influence of Temperature Dependent Viscosity on Laminar Boundary-Layer Stability." Int. J. Heat Mass Trans., Vol. 11 (1968), 1049-52.
3. Wazzan, A. R., Okamura, T. T., and Smith, A. M. O. "The Stability of Water Flow over Heated and Cooled Flat Plates." J. Heat Trans., Vol. 90, No. 1 (1968), 109-14.
4. Wazzan, A. R., Okamura, T. T., and Smith, A. M. O. "The Stability of Incompressible Flat Plate Laminar Boundary Layer in Water with Temperature Dependent Viscosity." Proc. Sixth Southeastern Seminar on Thermal Sciences, 184-202, (April, 1970).
5. Wazzan, A. R., Okamura, T. T., and Smith, A. M. O. "The Stability and Transition of Heated and Cooled Incompressible Laminar Boundary Layers." Proc. Fourth International Heat Transfer Conference, ed. U. Grigull and E. Hahne, Vol. 2, FC 1.4, Amsterdam: Elsevier Publishing Company, 1970.
6. Wazzan, A. R., Keltner, G., Okamura, T. T., and Smith, A. M. O. "Spatial Stability of Stagnation Water Boundary Layer with Heat Transfer." Phy. Fluids, Vol. 15, No. 12 (December, 1972), 2114-18.
7. Kaups, K., Smith, A. M. O. "The Laminar Boundary Layer in Water with Variable Properties." ASME-AIChE Heat Trans. Conf., Seattle, Wash., Paper 67-HT-69, August, 1967.
8. Potter, M. C., and Graber, E. "Stability of Plane Poiseuille Flow with Heat Transfer." Phys. Fluids, Vol. 15, No. 3 (March, 1972), 387-391.
9. Schlichting, H. Boundary-Layer Theory. Sixth edition. New York: McGraw-Hill Book Company, 1968.
10. Tisza, L. "Supersonic Absorption and Stokes' Viscosity Relation." Phys. Rev., Vol. 61 (April, 1942), 531-536.

11. Liebermann, L. N. "The Second Viscosity of Liquids." Phys. Rev., Vol. 75, No. 9 (May, 1949), 1415-1422.
12. Narasimham, A. V. "A Model for the Bulk Viscosity of a Liquid." IEE Trans. on Sonics and Ultrasonics, Vol. SU-16, No. 4 (October, 1969), 182-189.
13. Narasimham, A. V. "The Bulk Viscosity Coefficient of a Liquid." Mater. Sci. Eng., Vol. 6, No. 6 (Dec. 1970), 351-360.
14. Pinkerton, J. M. M. "A Pulse Method for the Measurement of Ultrasonic Absorption in Liquids: Results for Water." Nature, Vol. 160, No. 4056 (July, 1947), 128-129.
15. Reshotko, E. "Stability of Three-Dimensional Compressible Boundary Layers." NASA TN D-1220, 1962.
16. Reshotko, E. "Stability of the Compressible Boundary Layer." GALCIT Hypersonic Res. Project, Memo. No. 52, 1960.
17. Dunn, D. W., and Linn, C. C. "On the Stability of the Laminar Boundary Layer in a Compressible Fluid." J. Aero. Sci., Vol. 22, No. 7 (July, 1965), 455-77.
18. Nachtsheim, P. R. and Swigert, P. "Satisfaction of Asymptotic Boundary Conditions in Numerical Solution of Systems of Nonlinear Equations of Boundary-Layer Type." NASA TN D-3004, 1965.
19. Carnahan, B., Luther, H. A., and Wilkes, J. O. Applied Numerical Methods. New York: John Wiley and Sons, Inc., 1969.
20. Gersting, J. M., and Jankowski, D. F. "Numerical Methods for Orr-Sommerfeld Problems." Intern. J. for Numer. Meth. in Engng., Vol. 4 (March, 1972), 195-206.
21. Gersting, J. M., and Jakowski, D. F. "The Hydrodynamic Stability of Two Axisymmetric Flows." Developments in Mechanics, Vol. 6, Proceedings of the 12th Midwestern Mechanics Conference, 179-192. Notre Dame, Indiana: University of Notre Dame Press, August, 1971.
22. Boehman, L. I. "Recalculation of Brown's Stability Results." Proc. Boundary Layer Transition Workshop held 3-5 Nov. 1971. Aerospace Rept. No. TOR-0172(52816-16)-5, Dec. 1971.
23. Wazzan, A. R., Okamura, T. T., and Smith A. M. O. "Stability of Laminar Boundary Layers at Separation." Phys. Fluids, Vol. 10 No. 12 (December, 1967), 2540-45.

24. Mach, L. M. "Computation of the Stability of the Laminar Compressible Boundary Layer." Methods in Computational Physics, Volume 4, ed. B. Alder, S. Fernbach, and M. Rotenburg, 247,299. New York: Academic Press, 1965.
25. Mulier, D. E. "A Method for Solving Algebraic Equations Using an Automatic Computer." Math. Tables Aids Comput., Vol. 10, (1956), 208-215.
26. Betchov, R., and Criminale, W.O., Jr. Stability of Parallel Flows. New York: Academic Press, 1967.
27. Mack, L. M. "Boundary Layer Stability Theory." JPL Tech. Rept. 900-277 Rev. A, Jet Propulsion Laboratory, California Institute of Technology, Pasadena, California, November 1959.
28. Theilheimer, F., and Starkweather, W. "The Fairing of Ship Lines on a High-Speed Computer." Math. of Comp., Vol. 15, No. 76(1961), 338-355.
29. Walsh, J. L., Ahlberg, J. H., and Nilson, E. N. "Best Approximation Properties of the Spline Fit." J. Math. Mech., Vol. 11, No. 2 (1962), 225-234.
30. Touloukian, Y. S., and Makita, T. Thermophysical Properties of Matter, Volume 6, p. 102. New York: IFI/Plenum Data Corp., 1970.
31. Osborne, N. S., Stimson, H. F., and Ginnings, D. C. "Measurements of Heat Capacity and Heat of Vaporization of Water in the Range 0° to 100° C." J. Res. Nat. Bur. Stand., Vol. 23, (August, 1939) 238.
32. Powell, R. W. "Thermal Conductivities and Expansion Coefficients of Water and Ice." Adv. in Phys., Vol. 7, No. 26 (April, 1958), 276-297.
33. Touloukian, Y. S., Liley, P. E., and Saxena, S. C. Thermophysical Properties of Matter, Volume 3, p. 120. New York: IFI/Plenum Data Corp., 1970.
34. Gildseth, W., Habenschuss, A., and Spedding, F. G. "Precision Measurements of Densities and Thermal Dilation of Water between 5° and 80° C." J. Chem. and Engng. Data, Vol. 17, No. 4 (October, 1972), 402-409.
35. Stott, V., and Bigg, P. H. "Density and Specific Volume of Water." International Critical Tables, Volume 3, 24-26. New York: McGraw-Hill Book Co., Inc., 1933.

36. Korosi, A., and Fabuss, B. M. "Viscosity of Liquid Water from 25° to 150° C Measurements in Pressurized Glass Capillary Viscometer." Anal. Chem., Vol. 40, No. 1 (January, 1968), 157-162.
37. Herzfeld, K. F., and Litovitz, T. A. Absorption and Dispersion of Ultrasonic Waves. New York: Academic Press, 1959.
38. Univac 1108 FORTRAN V, Manual CHI-1002, second edition. Cleveland, Ohio: CHI Corporation, April 1973.
39. Conte, S. D. "The Numerical Solution of Linear Boundary Value Problems." SIAM Rev., Vol. 8, No. 3 (July, 1966), 309-321.
40. Okamura, T. T. "A Method for Calculating Laminar Boundary-Layer Profiles and Their Spatial Stability Properties for Two-Dimensional or Axisymmetric Bodies." Douglas Aircraft Company Rept. No. MDC-J0097, December 1971.
41. Funderlic, R. E. The Programmer's Handbook: A Compendium of Numerical Analysis Utility Programs. Detroit, Michigan: American Data Processing.

APPENDIX A

Detailed Derivation of Mean and Disturbance Flow Equations

In accordance with the discussion in section 2.1, it can be assumed that the flow field is describable by the set of conservation equations (2.1-2.3). Mean and fluctuating behavior are deduced from these equations in the following fashion.

The instantaneous value of each quantity can be decomposed into a mean and fluctuating component.

$$Q_i = \bar{Q}_i(\xi_j) + \tilde{Q}_i(\xi_j, t) \quad (2.6)$$

where \bar{Q}_i is the time-averaged mean

$$\bar{Q}_i(\xi_j) = \lim_{T \rightarrow \infty} \frac{1}{T} \int_t^{t+T} Q_i(\xi_j, \tau) d\tau \quad (A.1)$$

and where the time-averaged value of any fluctuating component is defined to be zero.

$$\bar{\tilde{Q}}_i = \lim_{T \rightarrow \infty} \frac{1}{T} \int_t^{t+T} \tilde{Q}_i(\xi_j, \tau) d\tau = 0$$

For a time average to be meaningful, mean quantities must be time-independent as already denoted by the argument of \bar{Q}_i in equation (A.1). The use of time- rather than space-averaged means

corresponds to observed boundary layer behavior where disturbances grow or decay spatially rather than temporally.¹

Thus, substituting equations (A-1) into equations (2.1-2.3) and performing a time average, the mean equations become (dimensionally)

Continuity:

$$\frac{\partial}{\partial \xi_j} (\bar{u}_j + \tilde{u}_j) = 0 \quad (\text{A.2})$$

Momentum:

$$\begin{aligned} & \bar{\rho} \left(\bar{u}_j \frac{\partial \bar{u}_i}{\partial \xi_j} + \tilde{u}_j \frac{\partial \tilde{u}_i}{\partial \xi_j} \right) + \bar{\rho} \left[\frac{\partial \tilde{u}_i}{\partial t} + (\bar{u}_j + \tilde{u}_j) \frac{\partial \tilde{u}_i}{\partial \xi_j} + \tilde{u}_j \frac{\partial \bar{u}_i}{\partial \xi_j} \right] \\ &= \bar{\rho} B_i - \frac{\partial}{\partial \xi_j} (\bar{p} + \bar{\lambda} \bar{\epsilon}_{KK} + \tilde{\lambda} \tilde{\epsilon}_{KK}) + 2 \frac{\partial}{\partial \xi_j} (\bar{u} \bar{\epsilon}_{ij} + \tilde{u} \tilde{\epsilon}_{ij}) \quad (\text{A.3}) \end{aligned}$$

Energy:

$$\begin{aligned} & (\bar{\rho} \bar{c}_P + \tilde{\rho} \tilde{c}_P) \bar{u}_j \frac{\partial \bar{T}}{\partial \xi_j} + (\bar{\rho} \tilde{c}_P + \bar{\rho} \bar{c}_P + \tilde{\rho} \tilde{c}_P) \left[\frac{\partial \tilde{T}}{\partial t} + (\bar{u}_j + \tilde{u}_j) \frac{\partial \tilde{T}}{\partial \xi_j} + \tilde{u}_j \frac{\partial \bar{T}}{\partial \xi_j} \right] \\ &+ \bar{\rho} \bar{c}_P \tilde{u}_j \frac{\partial \bar{T}}{\partial \xi_j} = (\bar{\rho} \bar{T} + \tilde{\rho} \tilde{T}) \bar{u}_j \frac{\partial \bar{p}}{\partial \xi_j} + \bar{\rho} \bar{T} \tilde{u}_j \frac{\partial \tilde{p}}{\partial \xi_j} \\ &+ (\bar{\rho} \tilde{T} + \tilde{\rho} \bar{T} + \tilde{\rho} \tilde{T}) \left[\frac{\partial \tilde{p}}{\partial t} + (\bar{u}_j + \tilde{u}_j) \frac{\partial \tilde{p}}{\partial \xi_j} + \tilde{u}_j \frac{\partial \bar{p}}{\partial \xi_j} \right] + 2 \bar{\rho} (\bar{\epsilon}_{ij}^2 + \tilde{\epsilon}_{ij}^2) \\ &+ 2 \tilde{u} (2 \bar{\epsilon}_{ij} \tilde{\epsilon}_{ij} + \tilde{\epsilon}_{ij}^2) + \bar{\lambda} (\bar{\epsilon}_{KK}^2 + \tilde{\epsilon}_{KK}^2) + \tilde{\lambda} (2 \bar{\epsilon}_{KK} \tilde{\epsilon}_{KK} + \tilde{\epsilon}_{KK}^2) \\ &+ \frac{\partial}{\partial \xi_j} \left(\bar{K} \frac{\partial \bar{T}}{\partial \xi_j} + \tilde{K} \frac{\partial \tilde{T}}{\partial \xi_j} \right) \quad (\text{A.4}) \end{aligned}$$

¹ Eventually (see section 2.3), to reduce the disturbance differential equations from partial to ordinary ones, disturbances of the form $\tilde{Q}_i = g(y) \exp[(i\alpha_k - \alpha_i)(x \cos \theta + z \sin \theta) - i\omega t]$ will be considered. Clearly the time average of this disturbance is zero, whereas a space average is not (except for a neutral disturbance where $\alpha_i = 0$).

To avoid the closure problem characteristic of turbulent flows, it is desirable that this set of equations be solved independently of correlated disturbance quantities. Thus, a set of new nondimensional independent variables is defined

$$\xi_j = \left(1 - \frac{l_j}{L_j} \right) X_j + \frac{l_j}{L_j} x_j \quad (\text{A.5})$$

where L_j and l_j are length scales in the j th direction characteristic of mean and fluctuating flow behavior, respectively. For example, at a given position, L_x might represent a length characteristic of the boundary layer development, specifically the distance from the body's leading edge, while l_x would correspond to the disturbance wave length at that point. When characteristic length scales are comparable so that $\frac{l_j}{L_j} = O(1)$, then equation (A.5) reduces to $\xi_j = x_j$. Here x_j must be considered a measure of both large and small scale variations in the j th direction, since both scales are in fact identical, or formally $\xi_j = X_j = x_j$. Such a situation typically arises in this analysis where transverse boundary layer scales L_y and l_y are equivalent (exception to be noted later) and equal to the boundary layer or displacement thickness, for example, so that $y = Y$.

If it can be argued that variations in the mean motion be independent of small scale disturbances in each direction (i.e., mean equations can be solved independently of disturbance

correlations), or that the mean flow with sufficiently small disturbances behaves as an undisturbed flow, then \bar{Q}_i must be independent of x_j (unless, of course, $l_j/L_j = O(1)$). With this assumption (dimensionally)

$$\bar{Q}_i(\xi_j, t) = \bar{Q}_i(X_j) + \tilde{Q}_i(X_j, x_j, t) \quad (\text{A.6})$$

and the mean equations become (nondimensionally)

Continuity:

$$\left(\frac{U_0 L_x}{U_0 L_j} \right) \frac{\partial \bar{\rho} \bar{u}_j}{\partial X_j} + \left(\frac{L_x \bar{\rho}_0 \tilde{u}_j}{\ell_j \bar{\rho}_0 U_0} \right) \frac{\partial \bar{\rho} \tilde{u}_j}{\partial \xi_j} = 0 \quad (\text{A.7})$$

Momentum:

$$\begin{aligned} & \bar{\rho} \left[\left(\frac{U_0 U_{0i} L_x}{U_0^2 L_j} \right) \bar{u}_j \frac{\partial \bar{u}_i}{\partial X_j} + \left(\frac{\tilde{u}_0 \tilde{u}_{0i} L_x}{U_0^2 \ell_j} \right) \bar{u}_j \frac{\partial \tilde{u}_i}{\partial \xi_j} \right] + \left(\frac{\bar{\rho}_0 L_x}{\bar{\rho}_0 \ell_x} \right) \tilde{\rho} \frac{\partial \tilde{u}_i}{\partial t} \\ &= \frac{\bar{\rho} B_i L_x}{U_0^2} - \left(\frac{L_x \bar{\rho}_0}{L_i \bar{\rho}_0 U_0^2} \right) \frac{\partial \bar{\rho}}{\partial X_i} \\ &+ \left(\frac{\nu_0 L_x}{U_0 L_y^2} \right) \left[\frac{L_y}{L_j} \frac{\partial}{\partial X_j} \left(2 \bar{\mu} \bar{\epsilon}_{ij} + \frac{\lambda_0 L_y}{\mu_0 L_x} \bar{\lambda} \bar{\Delta} \delta_{ij} \right) \right. \\ &+ \left. \frac{2 \tilde{\mu}_0 L_y^2}{\mu_0 \ell_y \ell_j} \frac{\partial}{\partial \xi_j} \bar{\mu} \bar{\epsilon}_{ij} \right] \end{aligned} \quad (\text{A.8})$$

Energy:

$$\begin{aligned}
 & (\bar{\rho} \bar{c}_P + \frac{\tilde{\rho}_0 \tilde{c}_{P0}}{\rho_0 c_{P0}} \bar{\rho} \bar{c}_P) \frac{u_{0j} L_x}{u_0 L_j} \bar{u}_j \frac{\partial \bar{T}}{\partial X_j} + \frac{\tilde{u}_{0j} \tilde{T}_0}{u_0 T_0} \frac{L_x}{\ell_j} \bar{\rho} \bar{c}_P \bar{\tilde{u}} \frac{\partial \bar{T}}{\partial \xi_j} \\
 & + \left(\frac{\tilde{c}_{P0}}{c_{P0}} \bar{\rho} \bar{c}_P + \frac{\tilde{\rho}_0}{\rho_0} \bar{\rho} \bar{c}_P + \frac{\tilde{\rho}_0 \tilde{c}_{P0}}{\rho_0 c_{P0}} \bar{\rho} \bar{c}_P \right) \frac{L_x}{\ell_x} \frac{\partial \bar{T}}{\partial t} \\
 & = \left(\beta_0 T_0 \right) \left(\frac{u_0^2}{c_{P0} T_0} \right) \left(\frac{P_0}{\rho_0 u_0^2} \right) \left\{ \left(\bar{\rho} \bar{T} + \frac{\tilde{\rho}_0 \tilde{T}_0}{\rho_0 T_0} \bar{\rho} \bar{T} \right) \frac{u_{0j}}{u_0} \frac{L_x}{L_j} \bar{u}_j \frac{\partial \bar{p}}{\partial X_j} \right. \\
 & + \left(\frac{\tilde{T}_0}{T_0} \bar{\rho} \bar{T} + \frac{\tilde{\rho}_0}{\rho_0} \bar{\rho} \bar{T} + \frac{\tilde{\rho}_0 \tilde{T}_0}{\rho_0 T_0} \bar{\rho} \bar{T} \right) \frac{L_x}{\ell_x} \frac{\partial \tilde{p}}{\partial t} + \frac{\tilde{u}_{0j}}{u_0} \frac{\tilde{\rho}_0}{P_0} \frac{L_x}{\ell_j} \bar{\rho} \bar{T} \bar{u}_j \frac{\partial \tilde{p}}{\partial \xi_j} \right\} \\
 & + \left(\frac{u_0^2}{c_{P0} T_0} \right) \left(\frac{v_0 L_x}{u_0 L_y^2} \right) \left\{ 2 \bar{\mu} \left[\bar{\epsilon}_{ij}^2 + \frac{L_y^2}{L_x^2} \tilde{\epsilon}_{ij}^2 \right] + 2 \frac{\tilde{u}_0}{u_0} \bar{\mu} \left[2 \frac{L_y}{L_x} \bar{\epsilon}_{ij} \tilde{\epsilon}_{ij} + \frac{L_y^2}{L_x^2} \tilde{\epsilon}_{ij}^2 \right] \right. \\
 & \left. + \frac{\lambda_0}{\mu_0} \left[\bar{\lambda} \left(\frac{L_y^2}{L_x^2} \bar{\Delta}^2 + \frac{L_y^2}{L_x^2} \tilde{\Delta}^2 \right) + \frac{\tilde{\lambda}_0}{\lambda_0} \bar{\lambda} \left(2 \frac{L_y}{L_x} \bar{\Delta} \tilde{\Delta} + \frac{L_y^2}{L_x^2} \tilde{\Delta}^2 \right) \right] \right\} \quad (A.9) \\
 & + \left(\frac{K_0}{C_{P0} \mu_0} \right) \left(\frac{v_0 L_x}{u_0 L_y^2} \right) \left\{ \frac{L_y^2}{L_j^2} \frac{\partial}{\partial X_j} \left(\bar{K} \frac{\partial \bar{T}}{\partial X_j} \right) + \frac{\tilde{K}_0}{K_0} \frac{\tilde{T}_0}{T_0} \frac{L_y^2}{\ell_j^2} \frac{\partial}{\partial \xi_j} \left(\bar{K} \frac{\partial \bar{T}}{\partial \xi_j} \right) \right\}
 \end{aligned}$$

where now

$$\begin{aligned}
 \tilde{\epsilon}_{ij} &= \frac{1}{2} \left(\frac{\tilde{u}_{0i}}{u_0} \frac{\ell_y}{\ell_j} \frac{\partial \tilde{u}_i}{\partial \xi_j} + \frac{\tilde{u}_{0j}}{u_0} \frac{\ell_y}{\ell_i} \frac{\partial \tilde{u}_j}{\partial \xi_i} \right) \\
 \bar{\epsilon}_{ij} &= \frac{1}{2} \left(\frac{u_{0i}}{u_0} \frac{L_y}{L_j} \frac{\partial \bar{u}_i}{\partial X_j} + \frac{u_{0j}}{u_0} \frac{L_y}{L_i} \frac{\partial \bar{u}_j}{\partial X_i} \right) \\
 \bar{\Delta} &= \frac{\tilde{u}_{0k}}{u_0} \frac{\ell_y}{\ell_k} \frac{\partial \tilde{u}_k}{\partial \xi_k} \\
 \tilde{\Delta} &= \frac{u_{0k}}{u_0} \frac{L_x}{L_k} \frac{\partial \bar{u}_k}{\partial X_k} \\
 \frac{\partial \tilde{Q}_i}{\partial t} &= \frac{\tilde{Q}_{0i}}{Q_0} \left[\left(\frac{\ell_x}{u_0 \ell_0} \right) \frac{\partial \tilde{Q}_i}{\partial t} + \left(\frac{u_{0j}}{u_0} \bar{u}_j + \frac{\tilde{u}_{0j}}{u_0} \tilde{u}_j \right) \frac{\ell_x}{\ell_j} \frac{\partial \tilde{Q}_i}{\partial \xi_j} \right] \\
 &+ \frac{Q_{0i}}{Q_0} \frac{\tilde{u}_{0i}}{u_0} \frac{\ell_x}{L_j} \bar{u}_j \frac{\partial \bar{Q}_i}{\partial X_j}
 \end{aligned}$$

$$\frac{\partial \bar{x}_j}{\partial \xi_j} = \begin{cases} \left(\frac{l_j}{L_j - l_j} \right) \frac{\partial}{\partial \bar{X}_j} + \frac{\partial}{\partial x_j} & \text{for } \frac{l_j}{L_j} \ll 1 \\ \frac{\partial}{\partial x_j} = \frac{\partial}{\partial \bar{X}_j} & \text{for } \frac{l_j}{L_j} = O(1) \end{cases}$$

From these equations, several interesting observations can be made.

(1) Two reference mean quantities are left unspecified by any physical or geometric considerations: v_o , a reference normal velocity; and L_y , a characteristic normal length scale. The former can be found from the continuity equation by requiring that a nontrivial two-dimensional solution be obtainable, so

$$v_o = u_o \frac{L_y}{L_x}$$

The latter is found by comparing the relative magnitudes of terms in either the momentum or energy equations. In the velocity boundary layer, viscous and inertial terms of the momentum equations are assumed equal, indicating that

$$\frac{L_x}{L_y} = \frac{u_o L_y}{v_o} = Re_{L_y}$$

Alternatively, equating conduction and convection terms of the energy equation in the thermal boundary layer

$$\frac{L_x}{L_y} = Re_{L_y} Pr_o$$

Since attention herein is to be focused on the stability of a flow field, the length scale characterizing the velocity boundary layer is chosen.

(2) For the assumption that the mean behavior be independent of small scale variation, $\bar{Q} = \bar{Q}(x_j)$, to be consistent, from the momentum equations, the criterion

$$\left(\frac{\tilde{Q}_o}{Q_o}\right)^2 \left(\frac{L_x}{L_y} \right) \left(\frac{L_y}{l_x}\right) \ll 1$$

must be satisfied, where the amplitude of all disturbances, have been assumed equal. If l_x represents a characteristic wave length, then

$$\left|\frac{\tilde{Q}_o}{Q_o}\right| \ll O\left[\left(\alpha_{L_y} Re_{L_y}\right)^{-\frac{1}{2}}\right]$$

where $\alpha_{L_y} Re_{L_y} \gg 1$. Analytically, the amplitude can be assumed as small as is necessary to satisfy this criterion; experimentally, control of the amplitude is quite a different story.

Thus, formally assuming that:

- (1) mean flow is steady;
- (2) viscous and inertial effects are equal in magnitude, so that attention is focused on the behavior of a velocity boundary layer, and

$$\frac{L_x}{L_y} = Re_{L_y} \gg 1$$

- (3) all disturbance amplitudes are of the same order of magnitude and sufficiently small that correlated disturbance quantities need not be considered in solving for mean variations, or specifically

$$\left| \frac{\tilde{Q}_o}{Q_o} \right| \ll O \left[(\alpha_{Ly} Re_{Ly})^{-\frac{1}{2}} \right]$$

- (4) flow quantities are independent of the z coordinate or the body is "infinite" in the z direction, so that

$$\frac{L_x}{L_z} \ll 1 \quad \text{and} \quad B_z = 0$$

- (5) $\left(\frac{w_o}{U_o} \right) \leq O(1)$ and $\left(\frac{l_x}{L_z} \right) = O(1)$ but $l_x / L_x \ll 1$, the last condition implying that the disturbance wave length is small compared with a length characterizing changes in mean quantities;

$$(6) \left(l_y / L_y \right) = O(1) \text{ and } \left(l_x / L_y \right)^{-1} = O(\alpha_{Ly});$$

$$(7) \frac{\lambda_o}{\mu_o} = O(1)$$

- (8) dynamic pressure is a good measure of the system pressure, so $p_o = \rho_o U_o^2$

the mean equations to $O(Re_{Ly}^{-1})$ can be written as

Continuity:

$$\frac{\partial \bar{\rho} \bar{U}}{\partial X} + \frac{\partial \bar{\rho} \bar{V}}{\partial Y} = 0 \quad (\text{A.10})$$

Momentum:

$$\bar{\rho} \left(\bar{u} \frac{\partial \bar{u}}{\partial X} + \bar{v} \frac{\partial \bar{u}}{\partial Y} \right) = \bar{\rho} \frac{B_x L_x}{U_o^2} - \frac{\partial \bar{p}}{\partial X} + \frac{\partial}{\partial Y} \left(\bar{u} \frac{\partial \bar{u}}{\partial Y} \right) \quad (\text{A.11a})$$

$$\sigma = \frac{\partial \bar{p}}{\partial Y} \quad (\text{A.11b})$$

$$\bar{\rho} \left(\bar{u} \frac{\partial \bar{w}}{\partial X} + \bar{v} \frac{\partial \bar{w}}{\partial Y} \right) = \frac{\partial}{\partial Y} \left(\bar{u} \frac{\partial \bar{w}}{\partial Y} \right) \quad (\text{A.11c})$$

Energy:

$$\begin{aligned} \bar{\rho} \bar{c}_P \left(\bar{u} \frac{\partial \bar{T}}{\partial X} + \bar{v} \frac{\partial \bar{T}}{\partial Y} \right) &= \left(\beta_0 T_0 \right) \left(\frac{U_o^2}{C_{P_0} T_0} \right) \bar{\rho} \bar{T} \bar{u} \frac{\partial \bar{p}}{\partial X} \\ &+ \left(\frac{U_o^2}{C_{P_0} T_0} \right) \left[\left(\frac{\partial \bar{u}}{\partial Y} \right)^2 + \left(\frac{W_o}{U_o} \right)^2 \left(\frac{\partial \bar{w}}{\partial Y} \right)^2 \right] + \left(\frac{k_o}{C_{P_0} \mu_o} \right) \left[\frac{\partial}{\partial Y} \left(\bar{K} \frac{\partial \bar{T}}{\partial Y} \right) \right] \end{aligned} \quad (\text{A.12})$$

Formally, the disturbance equations are obtained as the difference between the instantaneous and mean equations. Performing such an operation with equations (2.1-2.3) and (A.3-A.5), the complete set of disturbance equations can be written non-dimensionally as

Continuity:

$$\frac{\partial \tilde{\rho}}{\partial t} + (\bar{\rho} + \frac{\tilde{\rho}_o}{\rho_o} \tilde{v}) \tilde{\Delta} + \frac{\tilde{\rho}_o}{\rho_o} \tilde{v} \frac{\ell_x}{L_x} \bar{\Delta} - \frac{\tilde{\rho}_o}{\rho_o} \frac{\tilde{u}_{ij}}{u_{ij}} \frac{\ell_x}{\ell_j} \frac{\partial}{\partial \xi_{ij}} (\bar{\rho} \tilde{u}_j) = 0 \quad (A.13)$$

Momentum:

$$\begin{aligned} & \left(\bar{\rho} + \frac{\tilde{\rho}_o}{\rho_o} \tilde{v} \right) \frac{\partial \tilde{u}_i}{\partial t} + \frac{\tilde{\rho}_o}{\rho_o} \frac{u_{ij} u_{oi}}{U_o^2} \frac{\ell_x}{L_j} \tilde{v} \bar{u}_j \frac{\partial \bar{u}_i}{\partial X_j} - \bar{\rho} \frac{\tilde{u}_{ij} \tilde{u}_{oi}}{U_o^2} \frac{\ell_x}{\ell_j} \bar{u}_j \frac{\partial \tilde{u}_i}{\partial \xi_{ij}} \\ & - \frac{\tilde{\rho}_o}{\rho_o} \tilde{v} \frac{\partial \tilde{u}_i}{\partial t} = \frac{\tilde{\rho}_o}{\rho_o} \frac{B_i \ell_x}{U_o^2} \tilde{v} - \frac{\tilde{\rho}_o}{\rho_o} \frac{P_o}{\rho_o U_o^2} \frac{\ell_x}{\ell_{x_i}} \frac{\partial \tilde{p}}{\partial \xi_i} \\ & + \frac{v_o \ell_x}{U_o \ell_y^2} \left\{ \delta_{ij} \frac{\lambda_o}{\mu_o} \left[\frac{\tilde{\lambda}_o}{\lambda} \frac{\ell_y}{L_x} \frac{\ell_y}{\ell_j} \left(\bar{\Delta} \frac{\partial \tilde{\lambda}}{\partial \xi_j} + \frac{\ell_j}{\ell_j} \tilde{\lambda} \frac{\partial \bar{\Delta}}{\partial X_i} \right) + \frac{\ell_y}{\ell_j \ell_x} \left(\bar{\mu} \frac{\partial \tilde{\epsilon}_{ij}}{\partial \xi_{ij}} \right. \right. \right. \\ & \left. \left. \left. + \frac{\ell_j}{L_j} \tilde{\epsilon}_{ij} \frac{\partial \bar{u}}{\partial X_j} \right) + \frac{\tilde{\lambda}_o}{\lambda_o} \frac{\ell_y^2}{\ell_x \ell_j} \frac{\partial}{\partial \xi_{ij}} (\tilde{\lambda} \bar{\Delta} - \bar{\tilde{\lambda}} \bar{\Delta}) \right] \right\} \\ & + 2 \left[\frac{\tilde{\mu}_o}{\mu_o} \frac{\ell_y^2}{\ell_j L_y} \left(\tilde{\epsilon}_{ij} \frac{\partial \tilde{u}}{\partial \xi_j} + \frac{\ell_j}{L_j} \tilde{\mu} \frac{\partial \bar{\epsilon}_{ij}}{\partial X_j} \right) + \frac{\ell_y}{\ell_j} \left(\bar{\mu} \frac{\partial \tilde{\epsilon}_{ij}}{\partial \xi_{ij}} + \frac{\ell_j}{L_j} \tilde{\epsilon}_{ij} \frac{\partial \bar{u}}{\partial X_j} \right) \right] \\ & + \left. \left. \left. \frac{\tilde{\mu}_o}{\mu_o} \frac{\ell_y}{\ell_j} \frac{\partial}{\partial \xi_{ij}} (\tilde{\mu} \tilde{\epsilon}_{ij} - \bar{\mu} \bar{\tilde{\epsilon}}_{ij}) \right] \right\} \end{aligned} \quad (A.14)$$

Energy

$$\begin{aligned}
& \left(\frac{\tilde{\rho}_o}{\rho_o} \tilde{\rho} \bar{c}_P + \frac{\tilde{c}_{P_o}}{c_{P_o}} \bar{\rho} \tilde{c}_P + \frac{\tilde{\rho}_o \tilde{c}_{P_o}}{\rho_o c_{P_o}} \tilde{\rho} \tilde{c}_P \right) \left[\frac{\partial \tilde{T}}{\partial t} + \frac{u_o j}{u_o} \frac{\ell_x}{L_j} \bar{u}_j \frac{\partial \bar{T}}{\partial X_j} \right] \\
& + \bar{\rho} \bar{c}_P \frac{\partial \tilde{T}}{\partial t} - \frac{\tilde{\rho}_o \tilde{c}_{P_o}}{\rho_o c_{P_o}} \frac{u_o j}{u_o} \frac{\ell_x}{L_j} \bar{\rho} \tilde{c}_P \bar{u}_j \frac{\partial \bar{T}}{\partial X_j} - \frac{\tilde{u}_o j}{u_o} \frac{\tilde{T}_o}{T_o} \frac{\ell_x}{\ell_j} \bar{\rho} \bar{c}_P \tilde{u}_j \frac{\partial \tilde{T}}{\partial \xi_j} \\
& - \left(\frac{\tilde{\rho}_o}{\rho_o} \tilde{\rho} \bar{c}_P + \frac{\tilde{c}_{P_o}}{c_{P_o}} \bar{\rho} \tilde{c}_P + \frac{\tilde{\rho}_o \tilde{c}_{P_o}}{\rho_o c_{P_o}} \tilde{\rho} \tilde{c}_P \right) \frac{\partial \tilde{T}}{\partial t} = (\beta_o T_o) \left(\frac{P_o}{\rho_o u_o^2} \right) \left(\frac{u_o^2}{c_{P_o} T_o} \right) \left\{ \bar{\rho} \bar{T} \frac{\partial \tilde{p}}{\partial t} \right. \\
& + \left(\frac{\tilde{T}_o}{T_o} \bar{\rho} \tilde{T} + \frac{\tilde{\beta}_o}{\beta_o} \bar{\beta} \bar{T} + \frac{\tilde{\rho}_o \tilde{T}_o}{\rho_o T_o} \tilde{\rho} \tilde{T} \right) \left[\frac{\partial \tilde{p}}{\partial t} + \frac{u_o j}{u_o} \frac{\ell_x}{L_j} \bar{u}_j \frac{\partial \bar{p}}{\partial X_j} \right] \\
& - \frac{\tilde{\rho}_o \tilde{T}_o}{\rho_o T_o} \frac{u_o j}{u_o} \frac{\ell_x}{L_j} \bar{\rho} \tilde{T} \bar{u}_j \frac{\partial \bar{p}}{\partial X_j} - \frac{u_o j}{u_o} \frac{\ell_x}{\ell_j} \frac{\tilde{p}_o}{P_o} \bar{\rho} \tilde{T} \tilde{u}_j \frac{\partial \tilde{p}}{\partial \xi_j} \\
& - \left. \left(\frac{\tilde{\beta}_o}{\beta_o} \bar{\beta} \tilde{T} + \frac{\tilde{T}_o}{T_o} \bar{\rho} \tilde{T} + \frac{\tilde{\rho}_o \tilde{T}_o}{\rho_o T_o} \tilde{\rho} \tilde{T} \right) \frac{\partial \tilde{p}}{\partial t} \right\} \\
& + \left(\frac{u_o^2}{c_{P_o} T_o} \right) \left(\frac{v_o \ell_x}{u_o \ell_y^2} \right) \left(\frac{\ell_y}{L_y} \right) \left\{ \frac{\lambda_o}{\mu_o} \left[\bar{\lambda} \left(2 \frac{\ell_y L_y}{\ell_x L_x} \bar{\Delta} \tilde{\Delta} + \frac{\ell_y L_y}{\ell_x^2} (\tilde{\Delta}^2 - \bar{\Delta}^2) \right) \right. \quad (A.15) \\
& + \frac{\tilde{\lambda}_o}{\lambda_o} \frac{\ell_y L_y}{\ell_x^2} \left(\tilde{\lambda} \left(\frac{\ell_x}{L_x} \bar{\Delta} + \tilde{\Delta} \right)^2 - \frac{\tilde{\lambda}}{2} \left(2 \frac{\ell_x}{L_x} \bar{\Delta} \tilde{\Delta} + \tilde{\Delta}^2 \right) \right] + 2 \bar{\mu} \left[2 \tilde{\epsilon}_{ij} \bar{\epsilon}_{ij} \right. \\
& \left. + \frac{L_y}{\ell_y} \left(\tilde{\epsilon}_{ij}^2 - \bar{\epsilon}_{ij}^2 \right) \right] + 2 \frac{\tilde{\mu}_o}{\mu_o} \left[\frac{\ell_y}{L_y} \tilde{\mu} \left(\bar{\epsilon}_{ij} + \frac{L_y}{\ell_y} \tilde{\epsilon}_{ij} \right)^2 - \tilde{\mu} \left(2 \bar{\epsilon}_{ij} \tilde{\epsilon}_{ij} + \frac{L_y}{\ell_y} \tilde{\epsilon}_{ij}^2 \right) \right] \\
& + \left(\frac{k_o}{c_{P_o} \mu_o} \right) \left(\frac{v_o \ell_x}{u_o \ell_y^2} \right) \left\{ \frac{\tilde{T}_o}{T_o} \frac{\ell_y^2}{\ell_j^2} \left[\tilde{K} \frac{\partial^2 \tilde{T}}{\partial \xi_j^2} + \frac{\ell_j}{L_j} \frac{\partial \tilde{K}}{\partial X_j} \frac{\partial \tilde{T}}{\partial \xi_j} \right] + \frac{\tilde{k}_o}{k_o} \frac{\ell_y^2}{\ell_j L_j} \left[\frac{\partial \tilde{K}}{\partial \xi_j} \frac{\partial \bar{T}}{\partial X_j} \right. \\
& \left. + \frac{\ell_j}{L_j} \tilde{K} \frac{\partial^2 \bar{T}}{\partial X_j^2} \right] + \frac{\tilde{k}_o \tilde{T}_o}{K_o T_o} \frac{\ell_y^2}{\ell_j^2} \frac{\partial}{\partial \xi_j} \left[\tilde{K} \frac{\partial \tilde{T}}{\partial \xi_j} - \tilde{K} \frac{\partial \tilde{T}}{\partial \xi_j} \right] \right\}
\end{aligned}$$

To make this set of equations tractable, the equations are linearized through the assumption of "infinitesimal" disturbance amplitudes. The linearized disturbance equations are,

Continuity:

$$\begin{aligned} \left(\frac{\ell_x}{U_0 t_0} \right) \frac{\partial \tilde{\rho}}{\partial t} + \bar{u} \frac{\partial \tilde{\rho}}{\partial x} + \frac{w_0}{U_0} \frac{\ell_x}{\ell_z} \bar{w} \frac{\partial \tilde{\rho}}{\partial z} + \frac{\ell_x}{L_y} \tilde{v} \frac{\partial \bar{u}}{\partial y} \\ + \tilde{\rho} \left[\frac{\partial \tilde{u}}{\partial x} + \frac{\ell_x}{L_y} \frac{\partial \tilde{v}}{\partial y} + \frac{\ell_x}{\ell_z} \frac{\partial \tilde{w}}{\partial z} \right] = 0 \end{aligned} \quad (\text{A.16})$$

Momentum:

$$\begin{aligned} \tilde{\rho} \left[\left(\frac{\ell_x}{U_0 t_0} \right) \frac{\partial \tilde{u}}{\partial t} + \bar{u} \frac{\partial \tilde{u}}{\partial x} + \frac{w_0 \ell_x}{U_0 \ell_z} \bar{w} \frac{\partial \tilde{u}}{\partial z} + \frac{\ell_x}{L_y} \tilde{v} \frac{\partial \bar{u}}{\partial y} \right] = \tilde{\rho} \frac{B_x \ell_x}{U_0^2} \\ - \frac{\partial \tilde{p}}{\partial x} + \frac{w_0 \ell_x}{U_0 \ell_y^2} \left\{ \frac{\ell_y^2}{\ell_x^2} \left[\frac{\lambda_0}{\mu_0} \bar{\lambda} \frac{\partial}{\partial x} \left(\frac{\partial \tilde{u}}{\partial x} + \frac{\ell_x}{L_y} \frac{\partial \tilde{v}}{\partial y} + \frac{\ell_x}{\ell_z} \frac{\partial \tilde{w}}{\partial z} \right) + 2 \bar{u} \frac{\partial^2 \tilde{u}}{\partial x^2} \right] \right. \\ + \frac{\ell_y^2}{\ell_z^2} \bar{\mu} \frac{\partial}{\partial z} \left(\frac{\partial \tilde{u}}{\partial z} + \frac{\ell_z}{\ell_x} \frac{\partial \tilde{w}}{\partial x} \right) + \frac{\ell_y}{L_y} \left(\frac{\partial \tilde{u}}{\partial y} \frac{\partial \bar{u}}{\partial y} + \frac{\ell_y}{L_y} \tilde{v} \frac{\partial^2 \bar{u}}{\partial y^2} \right) \\ \left. + \left[\bar{u} \frac{\partial}{\partial y} \left(\frac{\partial \tilde{u}}{\partial y} + \frac{\ell_y}{\ell_x} \frac{\partial \tilde{v}}{\partial x} \right) + \frac{\ell_y}{L_y} \left(\frac{\partial \tilde{u}}{\partial y} + \frac{\ell_y}{\ell_x} \frac{\partial \tilde{v}}{\partial x} \right) \frac{\partial \bar{u}}{\partial y} \right] \right\} \end{aligned} \quad (\text{A.17})$$

$$\begin{aligned} \tilde{\rho} \left[\left(\frac{\ell_x}{U_0 t_0} \right) \frac{\partial \tilde{v}}{\partial t} + \bar{u} \frac{\partial \tilde{v}}{\partial x} + \bar{w} \frac{w_0}{U_0} \frac{\ell_x}{\ell_z} \frac{\partial \tilde{v}}{\partial z} \right] = \tilde{\rho} \frac{B_y \ell_x}{U_0^2} - \frac{\ell_x}{L_y} \frac{\partial \tilde{p}}{\partial y} \\ + \frac{w_0 \ell_x}{U_0 \ell_y^2} \left\{ \frac{\ell_y}{\ell_x} \left[\bar{\mu} \frac{\partial}{\partial x} \left(\frac{\ell_y}{\ell_x} \frac{\partial \tilde{v}}{\partial x} + \frac{\partial \tilde{u}}{\partial y} \right) + \frac{\ell_y}{L_y} \frac{\partial \tilde{u}}{\partial x} \frac{\partial \bar{u}}{\partial y} \right] \right. \\ + \frac{\ell_y}{\ell_x} \frac{\lambda_0}{\mu_0} \left[\bar{\lambda} \frac{\partial}{\partial y} \left(\frac{\partial \tilde{u}}{\partial x} + \frac{\ell_x}{L_y} \frac{\partial \tilde{v}}{\partial y} + \frac{\ell_x}{\ell_z} \frac{\partial \tilde{w}}{\partial z} \right) + \frac{\ell_y}{L_y} \left(\frac{\partial \tilde{u}}{\partial x} + \frac{\ell_x}{L_y} \frac{\partial \tilde{v}}{\partial y} \right) \right. \\ \left. + \frac{\ell_x}{\ell_z} \frac{\partial \tilde{w}}{\partial z} \right] \frac{\partial \bar{\lambda}}{\partial y} + 2 \left[\bar{u} \frac{\partial^2 \tilde{v}}{\partial y^2} + \frac{\ell_y}{L_y} \frac{\partial \tilde{v}}{\partial y} \frac{\partial \bar{u}}{\partial y} \right] \\ \left. + \frac{\ell_x}{\ell_z} \left[\bar{u} \frac{\partial}{\partial z} \left(\frac{\ell_y}{\ell_z} \frac{\partial \tilde{v}}{\partial z} + \frac{\partial \tilde{w}}{\partial y} \right) + \frac{\ell_y}{L_y} \frac{w_0}{U_0} \frac{\partial \bar{w}}{\partial y} \frac{\partial \tilde{u}}{\partial z} \right] \right\} \end{aligned} \quad (\text{A.18})$$

$$\begin{aligned}
& \bar{\rho} \left[\left(\frac{\ell_x}{U_0 t_0} \right) \frac{\partial \tilde{w}}{\partial t} + \bar{u} \frac{\partial \tilde{w}}{\partial x} + \frac{w_0}{U_0} \frac{\ell_x}{\ell_z} \bar{w} \frac{\partial \tilde{w}}{\partial z} + \frac{w_0}{U_0} \frac{\ell_x}{L_y} \tilde{v} \frac{\partial \tilde{w}}{\partial y} \right] = - \frac{\ell_x}{\ell_z} \frac{\partial \tilde{p}}{\partial z} \\
& + \frac{v_0 \ell_x}{U_0 \ell_y^2} \left\{ \frac{\ell_y^2}{\ell_x^2} \left[\bar{u} \frac{\partial}{\partial x} \left(\frac{\partial \tilde{w}}{\partial x} + \frac{\ell_x}{\ell_z} \frac{\partial \tilde{u}}{\partial z} \right) \right] + \frac{w_0}{U_0} \frac{\ell_y}{L_y} \left[\frac{\partial \bar{w}}{\partial y} \frac{\partial \tilde{u}}{\partial y} \right. \right. \\
& + \frac{\ell_y}{L_y} \tilde{u} \frac{\partial^2 \bar{w}}{\partial y^2} \left. \right] + \left[\bar{u} \frac{\partial}{\partial y} \left(\frac{\partial \tilde{w}}{\partial y} + \frac{\ell_y}{\ell_z} \frac{\partial \tilde{v}}{\partial z} \right) \right. \\
& + \frac{\ell_y}{L_y} \left(\frac{\partial \tilde{w}}{\partial y} + \frac{\ell_y}{\ell_z} \frac{\partial \tilde{v}}{\partial z} \right) \frac{\partial \bar{u}}{\partial y} \left. \right] + \frac{\ell_y^2}{\ell_z^2} \left[2 \bar{u} \frac{\partial^2 \tilde{w}}{\partial z^2} \right. \\
& \left. \left. + \frac{\lambda_0}{\mu_0} \frac{\ell_z}{\ell_x} \bar{\lambda} \frac{\partial}{\partial z} \left(\frac{\partial \tilde{u}}{\partial x} + \frac{\ell_x}{\ell_y} \frac{\partial \tilde{v}}{\partial y} + \frac{\ell_x}{\ell_z} \frac{\partial \tilde{w}}{\partial z} \right) \right] \right\}
\end{aligned}$$

(A.19)

Energy:

$$\begin{aligned}
& \bar{\rho} \bar{c}_p \left[\left(\frac{\ell_x}{U_0 t_0} \right) \frac{\partial \tilde{T}}{\partial t} + \bar{u} \frac{\partial \tilde{T}}{\partial x} + \frac{w_0}{U_0} \frac{\ell_x}{\ell_z} \bar{w} \frac{\partial \tilde{T}}{\partial z} + \frac{\ell_x}{L_y} \tilde{v} \frac{\partial \tilde{T}}{\partial y} \right] \\
& = (\beta_0 T_0) \left(\frac{P_0}{\rho_0 U_0^2} \right) \left(\frac{U_0^2}{C_p T_0} \right) \bar{\rho} \bar{T} \left[\left(\frac{\ell_x}{U_0 t_0} \right) \frac{\partial \tilde{p}}{\partial t} + \bar{u} \frac{\partial \tilde{p}}{\partial x} + \frac{w_0}{U_0} \frac{\ell_x}{\ell_z} \bar{w} \frac{\partial \tilde{p}}{\partial z} \right] \\
& + \left(\frac{U_0^2}{C_p T_0} \right) \left(\frac{v_0 \ell_x}{U_0 \ell_y^2} \right) \left(\frac{\ell_y}{L_y} \right) \left\{ 2 \bar{u} \left[\frac{\partial \bar{u}}{\partial y} \left(\frac{\partial \tilde{u}}{\partial y} + \frac{\ell_y}{\ell_x} \frac{\partial \tilde{v}}{\partial x} \right) \right. \right. \\
& + \frac{\partial \bar{w}}{\partial y} \left(\frac{\partial \tilde{w}}{\partial y} + \frac{\ell_y}{\ell_z} \frac{\partial \tilde{v}}{\partial z} \right) \frac{w_0}{U_0} \left. \right] + \frac{\ell_y}{L_y} \tilde{u} \left[\left(\frac{\partial \bar{u}}{\partial y} \right)^2 + \left(\frac{w_0}{U_0} \right)^2 \left(\frac{\partial \bar{w}}{\partial y} \right)^2 \right] \left. \right\} \\
& + \left(\frac{K_0}{C_p \mu_0} \right) \left(\frac{v_0 \ell_x}{U_0 \ell_y^2} \right) \left\{ \frac{\ell_y^2}{\ell_x^2} \bar{K} \frac{\partial^2 \tilde{T}}{\partial x^2} + \bar{K} \frac{\partial^2 \tilde{T}}{\partial y^2} + \frac{\ell_y^2}{\ell_z^2} \bar{K} \frac{\partial^2 \tilde{T}}{\partial z^2} \right. \\
& \left. + \frac{\ell_y}{L_y} \left[\frac{\partial \bar{K}}{\partial y} \frac{\partial \tilde{T}}{\partial y} + \frac{\partial \tilde{K}}{\partial y} \frac{\partial \bar{T}}{\partial y} + \frac{\ell_y}{L_y} \bar{K} \frac{\partial^2 \tilde{T}}{\partial y^2} \right] \right\}
\end{aligned}$$

(A.20)

Note that the resulting equations are those of a parallel flow.

It can be shown by this analysis that the omitted "non-parallel" terms of the boundary layer equations are of order $(\alpha_{L_y}^{-1/2} Re_{L_y})$, so that if small values of $\alpha_{L_y}^{-1/2} Re_{L_y}$ were expected, it would be necessary to retain these terms. However, since it is expected that heating will increase stability [1 - 7], larger values of this parameter are expected than for the unheated case, and the parallel flow assumptions will be even more accurate for this boundary layer flow.

From this analysis, several interesting observations may be made:

(1) To the linear order considered, there is no provision to account for thermal fluctuations of specific heat, second viscosity coefficient, or coefficient of thermal expansion (however slight they may be).

(2) Additional length scales encountered in boundary layer stability can be easily derived from dimensional considerations.

Consider a region very close to the boundary (viscous sublayer) with a characteristic velocity u_{ob} and length l_{yb} such that $u_{ob} \ll u_o$ and $l_{yb} \ll L_y$ (all other conditions remaining as previously specified). If the boundary can be approached so closely that

$$\frac{u_o}{u_{ob}} \gg \frac{l_x}{L_y} = \frac{2\pi}{\alpha_{L_y}}, \text{ then equating viscous and inertia terms}$$

of the momentum equation requires that

$$\frac{l_{y_b}}{L_y} = \sqrt{\frac{2\pi}{\alpha_{L_y} Re_{L_y}}}$$

Incidentally, the pressure terms is also of the same order, so the full momentum equation is approximated in this region by Prandtl's equation [27, p 6-9]

$$\frac{\partial \tilde{u}}{\partial t} = - \frac{\partial \tilde{p}}{\partial x} + \frac{1}{Re_{L_y}} \bar{\mu} \frac{\partial^2 \tilde{u}}{\partial y^2}$$

If another characteristic velocity, u_{oc} , and length l_{yc} are chosen so that $l \ll \frac{u_o}{u_{oc}}$ $\ll \frac{2\pi}{\alpha_{L_y}}$ and still $l_{yc} \ll L_y$, then in this region, equating the inertia and viscous terms gives

$$1 = \frac{2}{\alpha_{L_y} Re_{L_y}} \left(\frac{L_y}{l_y} \right)^3 \frac{u_o l_{yc}}{u_{oc} l_x}$$

But from continuity $\frac{u_o l_{yc}}{u_{oc} l_x} = 1$ so that

$$\frac{l_{yc}}{L_y} = \sqrt[3]{\frac{2\pi}{\alpha_{L_y} Re_{L_y}}}$$

This region corresponds to the "critical layer" where the wave speed and mean velocity are equal (e.g., $\bar{u} = c_R$ for a two-dimensional flow).

For example, specifying $T_w = 90^\circ\text{F}$, $T_\infty = 60^\circ\text{F}$ for a two-dimensional flat plate boundary layer, a solution to equations (A.16-A.20) with homogeneous boundary conditions is found to be (see Appendix E)

$$\begin{aligned}\text{Re}_\delta &= 7000 \\ \alpha_R &= .122347 \\ \alpha_I &= 0 \\ \omega_\infty &= 3.68283 \times 10^{-6} \\ C_R &= .210709 \\ C_I &= 0\end{aligned}$$

$$\text{where } c_R = \bar{u} \text{ at } y_c = .31852$$

Thus for the length and velocity scales with the reference length L_y chosen as the displacement thickness, δ^*

$$\frac{u_o}{u_{ob}} \gg 51.355 \gg \frac{u_o}{u_{oc}} = 4.7459 \gg 1$$

and

$$\frac{1}{\delta^*} y_b = .085653$$

$$\frac{1}{\delta^*} y_c = .19431$$

In the viscous sublayer $0 \leq y \leq \frac{1}{\delta^*}$, so that $\infty > \frac{u_o}{u} \geq 16.865$ whereas from the continuity equation

$$\frac{u_o}{u_{o_b}} = \sqrt{\frac{2\pi Re_{L_y}}{\alpha_{L_y}}} = 599.57$$

In the critical layer, $y_c - \frac{1}{2\delta^*} \leq y \leq y_c + \frac{1}{2\delta^*}$, so that $6.6978 \geq \frac{u_o}{u} \geq 3.7104$ and as pointed out previously, at the critical point, $\frac{u}{u_c} = 4.7459$.

Thus all the length and velocity scales derived from dimensional considerations seem to be in accord with derived solutions. Note that these two length scales, representing regions in which viscosity plays a dominant role, are also consistent with those derived from asymptotic analyses (see Mack [27, pp. 4-4, 4-5] for example).

Appendix B

Thermodynamic and Transport Coefficients and Their Temperature Derivatives

B.1 Curve-Fitting and Derivative Determination

Selection of the curve-fitting technique used in this investigation is predicated both on the method's capability of closely approximating tabulated data and for predicting high quality derivatives, with particular emphasis on the latter. In the ensuing discussion, no exhaustive analysis of all available techniques for achieving this objective is intended or attempted; remarks will be limited only to procedures considered.

Of course, a given set of data can easily be "fit" as closely as desired by using a least-squares polynomial of sufficiently high degree. However, if the degree is too large, small scale oscillations about the primary variation will be evident in the resulting curves due to truncation and scatter of data information. Utilization of these curves to generate derivatives, then, will naturally indicate even more conspicuous but completely fictitious "wiggles" in the computed derivatives. For a lower degree polynomial, not only may data be poorly approximated but variations in higher order derivatives might not even be seen. For both the method of least squares and other such empirical formulations considered (see relationships for ρ and μ in section B.2, for example) it is significant to note for later reference that property variation over the entire temperature range is described by a single,

analytic, continuous function. Thus interpolation is not between "exact" tabulated experimental data points, but between approximate values (which presumably are within acceptable experimental error limits). Derivatives are then available immediately simply by analytically differentiating the indicated equation.

As an alternative to least-squares polynomial curve fits, the method of mathematical splines can partially satisfy the previously established selection criteria (assuming availability of a sufficient quantity and quality of data information). In general, a spline function is composed of piecewise polynomial arcs of degree n (where n is a positive integer, $n \geq 3$) which are joined at prescribed points such that derivatives up to and including order $n-1$ are everywhere continuous. Obviously such a function provides continuity of the greatest number of derivatives consistent with the use of polynomials of lower degree than would be required to fit all data points exactly by a single polynomial. Since the curvature of a mathematical spline is most easily controlled when $n = 3$, or a cubic spline, the use of simple cubics seems to be an attractive way to interpolate (in the strictest sense) experimental data points representing some physical relationship. As applied to this investigation, an explicit formula for this "piecewise cubic" is given by

$$S(T) = a + bT + cT^2 + A_1 T^3 + \sum_{j=2}^{J-1} A_j (T - T_j)_+^3$$

where the T_j and the J ($J \geq 3$) distinct temperatures over the normal liquid range for water

$$0^\circ\text{C} = T_1 < T_2 < T_3 < \dots < T_{J-1} < T_J = 100^\circ\text{C}$$

at which tabulated property data (denoted as P_j) are specified

$$P_1, P_2, \dots, P_J$$

and where,

$$(T - T_j)_+^3 = \begin{cases} 0 & \text{for } T \leq T_j \\ (T - T_j)^3 & \text{for } T > T_j \end{cases}$$

The $J+2$ coefficients $a, b, c, A_1, \dots, A_{J-1}$ are then determined by requiring $s(T_j) = P_j$, $j = 1, \dots, J$ and specifying first or second derivatives at the ends of the temperature interval, T_1 or T_J [28].

The method as suggested should work perfectly if data points were exact. Not only would this data be exactly satisfied at the endpoints of each polynomial segment, but the methods minimization of the curvature and relaxation of the overall requirement of analyticity would ensure first derivatives of high quality [29]. For reasons intimated above, however, it is unreasonable to expect that data information should be satisfied exactly. Consequently, the procedure outlined above is modified to permit departures from the prescribed data within specified tolerances while excluding unwanted changes in curvature. Numerically, the smoothing is accomplished by

minimizing

$$\sum_{j=1}^J [s(\tau_j) - P_j]^2 + C \sum_{j=2}^{J-1} \left[\frac{d^2 s}{d\tau^2}(\tau_j) - r_j \right]^2$$

where C is a positive proportionality constant and r_j is the second difference at the j th point defined by

$$r_j = \frac{2}{\tau_{j+1} - \tau_{j-1}} \left[\frac{P_{j+1} - P_j}{\tau_{j+1} - \tau_j} - \frac{P_j - P_{j-1}}{\tau_j - \tau_{j-1}} \right]$$

Note that if $C = 0$, then only the first sum would be minimized, and the procedure then corresponds to the method of least squares. For large C , primarily the second sum would be minimized in an attempt to eliminate undesired fluctuations [28]. Further note that in contrast to the first methods discussed in which temperature derivatives were obtained after smoothing data, this one computes accurate first derivatives while fitting the spline function to the specified data.

For the present application, the problem is thus one of mathematically approximating tabulated fluid property data sufficiently well that all physically realistic variation is retained, but spurious fluctuations are smoothed out. Note that failure

to accomplish the latter should certainly be revealed by evaluating higher order derivatives. As the order of the required derivative is increased, the more difficult this problem is to satisfy. It is just this difficulty that determined the form of the disturbance equation adopted for this analysis (see section 2.3.1).

As an example of the methods discussed, Figure B.1 compares the temperature variation of the first derivative of c_p obtained from various sources by various techniques. Specifically, included are derivatives obtained both analytically from least-square polynomial fits of Touloukian, et.al. [30] and Kaups, et.al. [7], and numerically using a cubic spline fit with smoothing to the data of Osborne, et.al. [31]. Consistent with previous discussions, the latter category should indicate the more accurate general trend. However, it was not used for direct input to the numerical program; the following discussion explains some of the considerations dictating this decision.

(1) Even with smoothing, questionable oscillations in derivatives are indicated - specifically, those attributed to data uncertainty. In short, with no unusual property-temperature variation appearing in the normal liquid range of water (e.g., numerous changes in slope and curvature), data can be well approximated by a least-square polynomial of relatively low degree.

(2) Since the amplitude of a fluctuating fluid property at a given mean temperature is assumed directly proportional to the first temperature derivative there (see eqn. (2.35)), it is essential

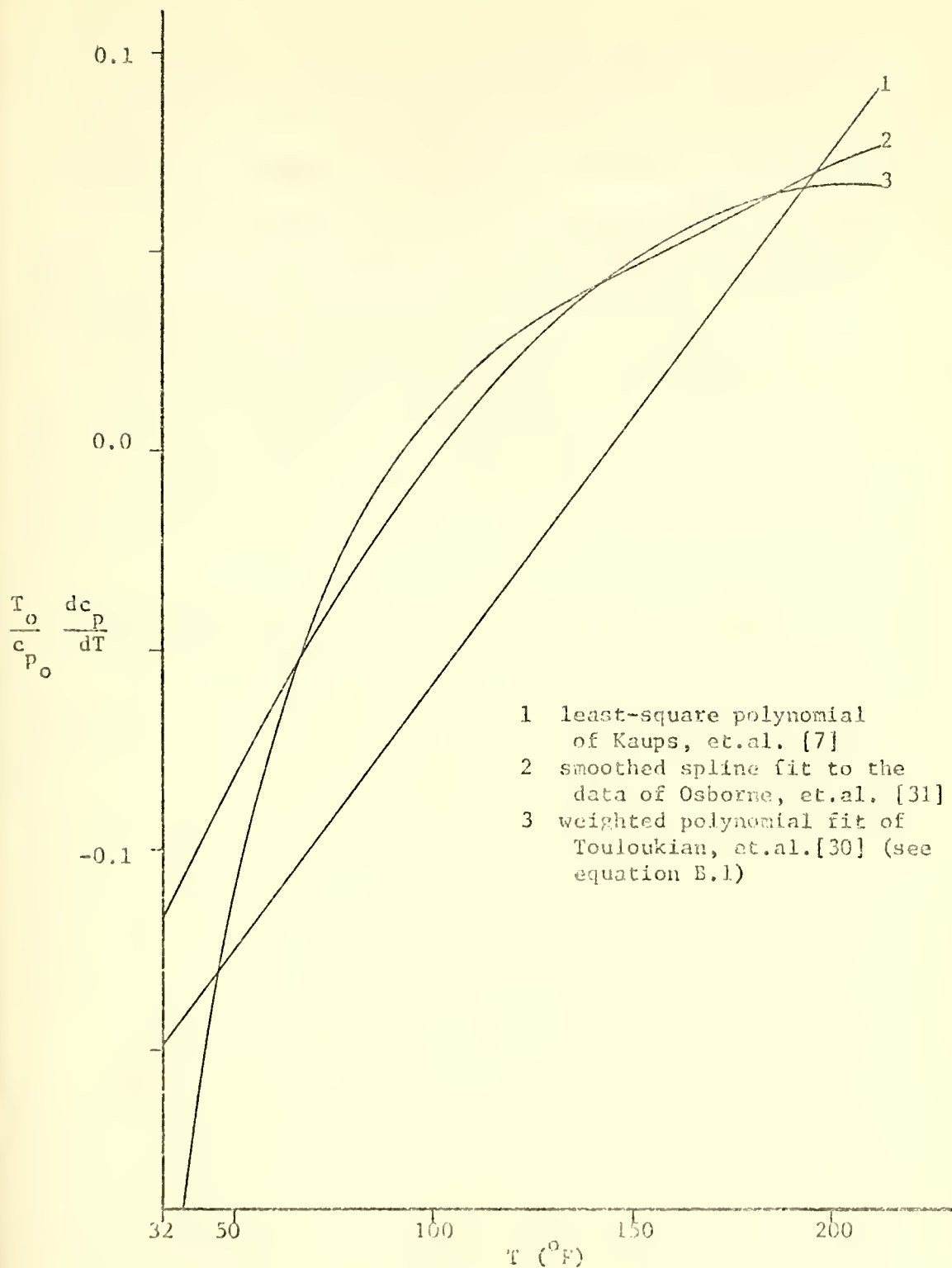


Figure B.1 First temperature derivative of c_p as a function of temperature as obtained using different procedures.

to know whether and where erratic behavior in this derivative occurs. Only in this way can logical explanations be advanced for aberrations in eigenfunctions, Reynolds stresses, dissipation, etc.

(3) For simplicity of evaluation and conservation of data storage, it is more efficient to use a low degree least-square polynomial or empirical curve fit.

Similar analyses were conducted for the three other fluid properties, ρ , k , and μ . The results suggested the property-temperature relationships for use in this stability study and are discussed in section B.2.

B.2 Property-Temperature Variation for Water

Since a major contention of this study is that a fluid's property-temperature variation plays an important part in establishing its flow stability characteristics in a heated boundary layer, accurate values for thermodynamic and transport properties is considered essential. The literature survey prompted by a search for the "best" available property information for water led to the following results and conclusions.

(1) Rather than digressing on an extensive evaluation of data (which would entail an analysis of experimental techniques and the quality of information available from each, assessment of systematic error limits in reported data, correlation of the information judged most reliable, etc.), recourse is made to recent studies of such a nature. Although, as evidenced by Figure B.2, by

far the largest property variation with temperature is by the viscosity, equal care is exercised in specifying the behavior of each of the properties. In this way, discrepancies between the results obtained in this numerical study and those occurring in nature are less likely to be attributed to inaccurate property information. It should be noted that, of the sources encountered in the literature survey, published data measurements found subsequent to those used herein agree to within experimental error.

(2) Since some of the "best" data available are generated by polynomial correlations of numerous sets of data (see below for c_p and k), concern was experienced regarding the capability of a low degree polynomial to be able to predict accurately the behavior of higher order derivatives. For example, while a second degree polynomial equation might adequately fit a set of data, the constant second derivative analytically derived from it may not be realistic. Erratic behavior in the derivatives can also be expected if the degree chosen is too large. Evidence of these two cases has already been presented in Figure B.1. Using the smoothed cubic spline as an approximate standard with the data set of Osborne, et.al. [31] (judged to be one of the most reliable [30]), and knowing that only the first derivative, $\frac{dc_p}{dT}$, is required for this analysis, one can see that the third degree polynomial of Touloukian, et.al.[30] adequately approximates the required behavior over the temperature range of interest. When second derivatives are required as well (such as is the case for ρ , ν , and k), the above procedure remains

basically the same, although more involved. For example, again using as an indicator the smoothed cubic spline with data recommended by Powell [32] (also judged to be among the most reliable available for k [33]), first and second derivative behavior is found to be best approximated when thermal conductivity is defined by a third degree polynomial.

In short, when an analysis of existing data uses polynomial correlations which would obviously not predict behavior of higher derivatives needed herein, information characteristic of that obtained from the polynomial fit is used instead.

(3) Regarding the required property variation of water, the following information is relevant:

Specific heat, c_p . An analysis is made by Touloukian, et.al [30] of twenty sets of data for the isobaric specific heat of liquid water. For the saturated liquid, recommended values are computed from

$$c_p \text{ (cal g}^{-1}\text{K}^{-1}) = 2.13974 - 9.68137 \times 10^{-3}T + 2.68536 \times 10^{-5}T^2 \\ - 2.42139 \times 10^{-8}T^3 \quad (T \text{ in } ^\circ\text{K}) \quad (\text{B.1})$$

for $273^\circ \leq T \leq 410^\circ\text{K}$. This equation is found to fit the data analyzed with a mean deviation of .14% and a maximum deviation of 1.83% (for one data set - all others differ by no more than .5%). Of particular interest for this study, reference [30] indicates that c_p as calculated from the above equation "should be substantially correct to within one percent" below 400°K . The ability of this

cubic to predict first derivative behavior has already been discussed.

Density, ρ . Four previous works are evaluated by Gildseth, et.al. [34] and compared with their experimental results. Recommended values for the density of air free water are generated for $0^\circ \leq T \leq 80^\circ\text{C}$ by a modified form of the Tilton and Taylor equation (i.e., the inclusion of the exponential term which is negligible for $T \leq 40^\circ\text{C}$)

$$\rho(\text{g/ml}) = 1 - \frac{(T - 3.9863)^2(T + 288.9414)}{508929.2(T + 68.12963)} + 0.011445 \exp(-\frac{374.3}{T}) \quad (\text{T in } ^\circ\text{C}) \quad (\text{B.2})$$

to fit experimental data with a mean absolute deviation of $.7 \times 10^{-6}$ g/ml. While the authors do specify these values to be uncertain in the seventh decimal place for the lower temperatures, they do indicate that at least above 40°C uncertainty is in the sixth place and increases with temperature. Since this equation does reproduce the densities tabulated in the International Critical Tables [35] for the range $80^\circ \leq T \leq 100^\circ\text{C}$ (to within the indicated uncertainty), it is extrapolated in this study to cover the full temperature range, $0^\circ - 100^\circ\text{C}$.

Dynamic viscosity, μ . The experimental measurements of Korosi, et. al. [36] are compared with ten previous, similar sets of data. The authors propose a correlation

$$\log \mu = -1.64779 + \frac{262.37}{T - 133.98} \quad (\mu \text{ in cp and } T \text{ in } ^\circ\text{K})$$

to fit their data over the temperature range $20^\circ \leq T \leq 150^\circ\text{C}$ with an average deviation of 0.17% and a maximum deviation of 0.49% at 40°C . However, since this data seems to be characteristic of the mean of the other compared data for a specified temperature, an alternate formulation is used. Interpolated data is generated instead by using (for the same temperature range) an equation recommended by R. E. Manning in reviewing the paper:

$$\log \left(\frac{\mu_{20^\circ\text{C}}}{\mu} \right) = \frac{1.37023(T - 20) + 8.36 \times 10^{-4}(T - 20)^2}{109 + T} \quad (\text{B.3})$$

$$(T \text{ in } ^\circ\text{C and } \mu(20^\circ\text{C}) = 1.002 \text{ cp})$$

This equation is found to represent Korosi's experimental data to within 0.05% average deviation.

Thermal Conductivity, k. Of the more than sixty sets of experimental data available on the thermal conductivity of liquid water, Touloukian, et.al. [33] evaluate seven as being the most reliable. They then correlate these and generate recommended values for $273.16^\circ \leq T \leq 413.16^\circ\text{K}$ with the second degree polynomial

$$10^6 k \text{ (cgsu)} = -1390.53 + 15.1937T - 0.0190398T^2 \quad (T \text{ in } ^\circ\text{K})$$

This equation is found to fit the data considered with a mean deviation of 0.24% and a maximum deviation of 0.82%. As indicated in previous discussion, however, a second degree polynomial appears

to be inadequate to describe the behavior of the second derivative in the temperature range considered. Thus, for application in this stability study, a third degree, least-square polynomial is fit to an earlier correlation of thermal conductivity data by Powell [32] with the following result

$$k \text{ (mwatts cm}^{-1}\text{K}^{-1}) = -9.901090 + .1001982T - 1.873892 \times 10^{-4} T^2 \\ + 1.039570 \times 10^{-7} T^3 \quad (T \text{ in } ^\circ\text{K}) \quad (B.4)$$

Values generated by this equation deviate from the preceding one by no more than .25%.

Due to the nature of the formulation of the mean and disturbance equations, it was found convenient to calculate the product of the density with the viscosity and thermal conductivity, $\rho \mu$ and ρk , rather than these properties individually (see equation 2.20 for example). Thus temperature variations of c_p , ρ , $\rho \mu$, and ρk as well as their temperature derivatives required for this analysis are shown in figures B.1 through B.5. The ratio of the second to the first viscosity coefficients is computed using equation 3.3 of reference [37, p.47] and the data of Pinkerton [14] and is included for reference in figure B.6 (see section 2.1).

Since the stability characteristics are found to be sensitive to assumed property variation with temperature (see Chapter IV), a comparison is made between fluid properties calculated by equations (B.1 - B.4) (those used for this investigation) and by the least-square polynomial fits of Kaups and Smith [7] (used by Wazzan et.al.)

Deviation of the latter from the former (of the form $\left[\frac{(\rho)}{\rho_0} \right]_{KAUPs, et.al.} - \left[\frac{(\rho)}{\rho_0} \right]_{eqn\beta_2} \times 100$, for example, where ρ_0 is the reference quantity evaluated at $T_0 = 32^\circ F$) is shown in Figure B.7.

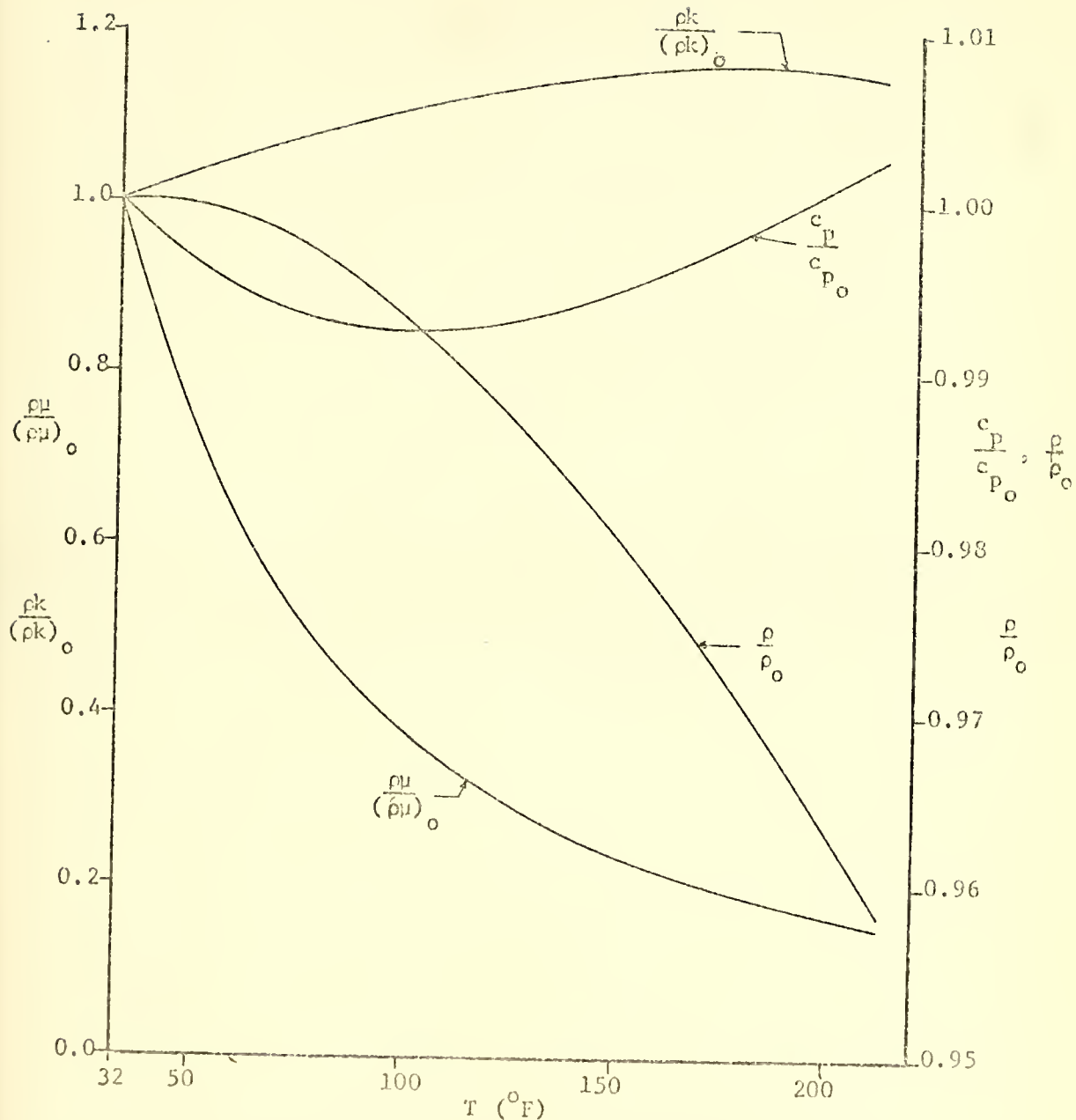


Figure B.2 Variations in ρ , c_p , μ , and ρk with temperature.

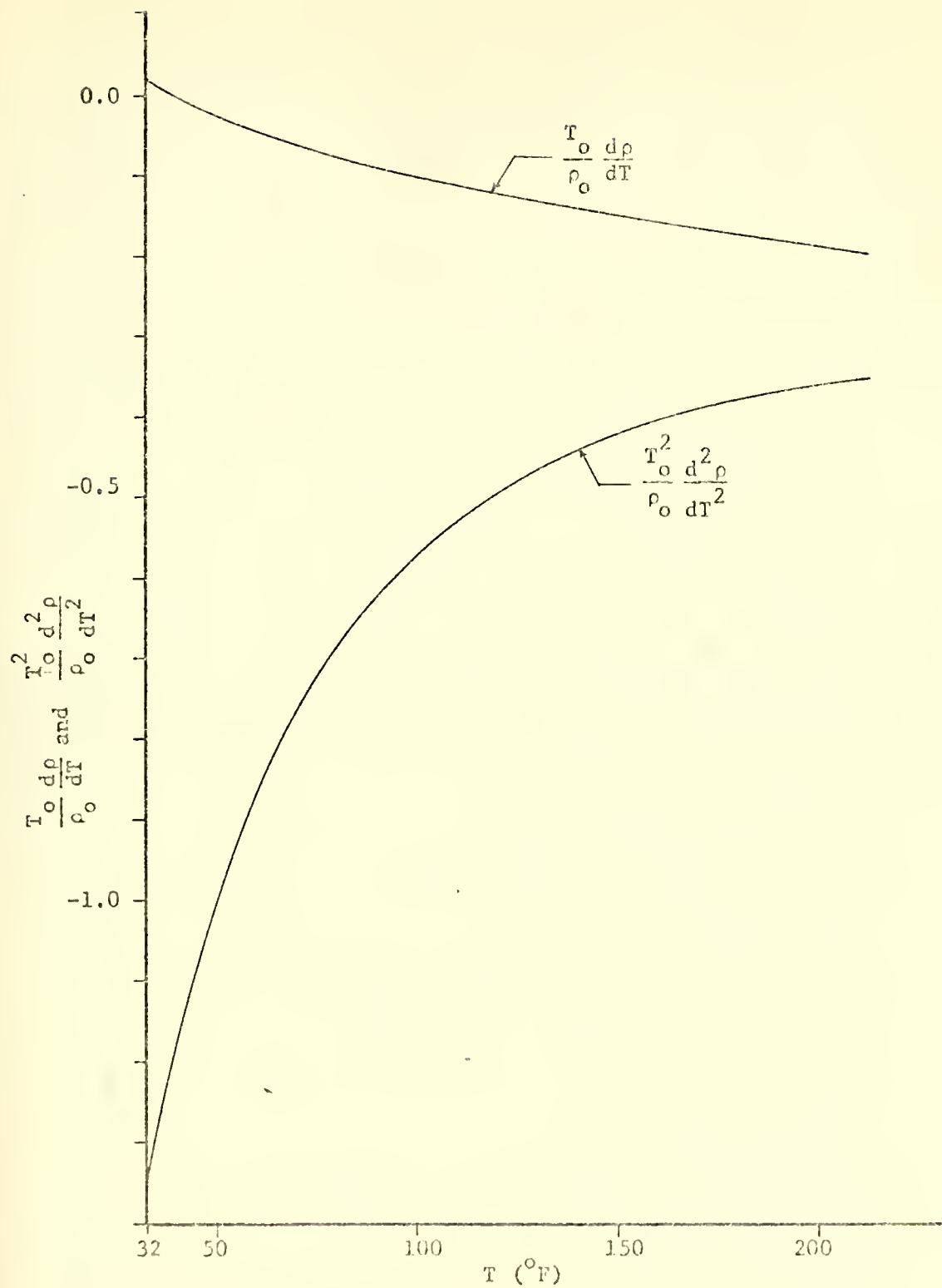


Figure B.3 First and second temperature derivatives of ρ as a function of temperature.

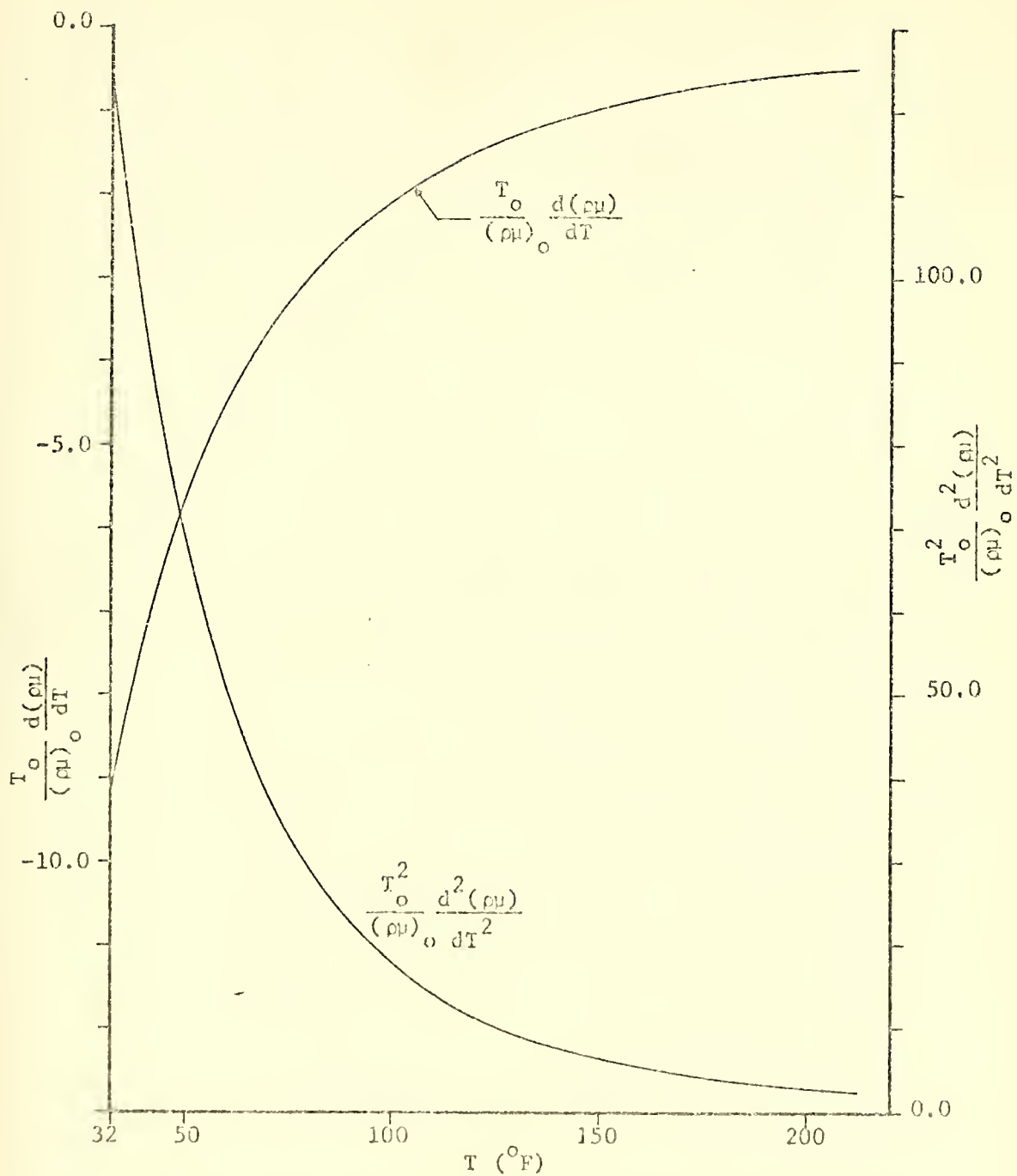


Figure B.4 First and second temperature derivatives of μ as a function of temperature.

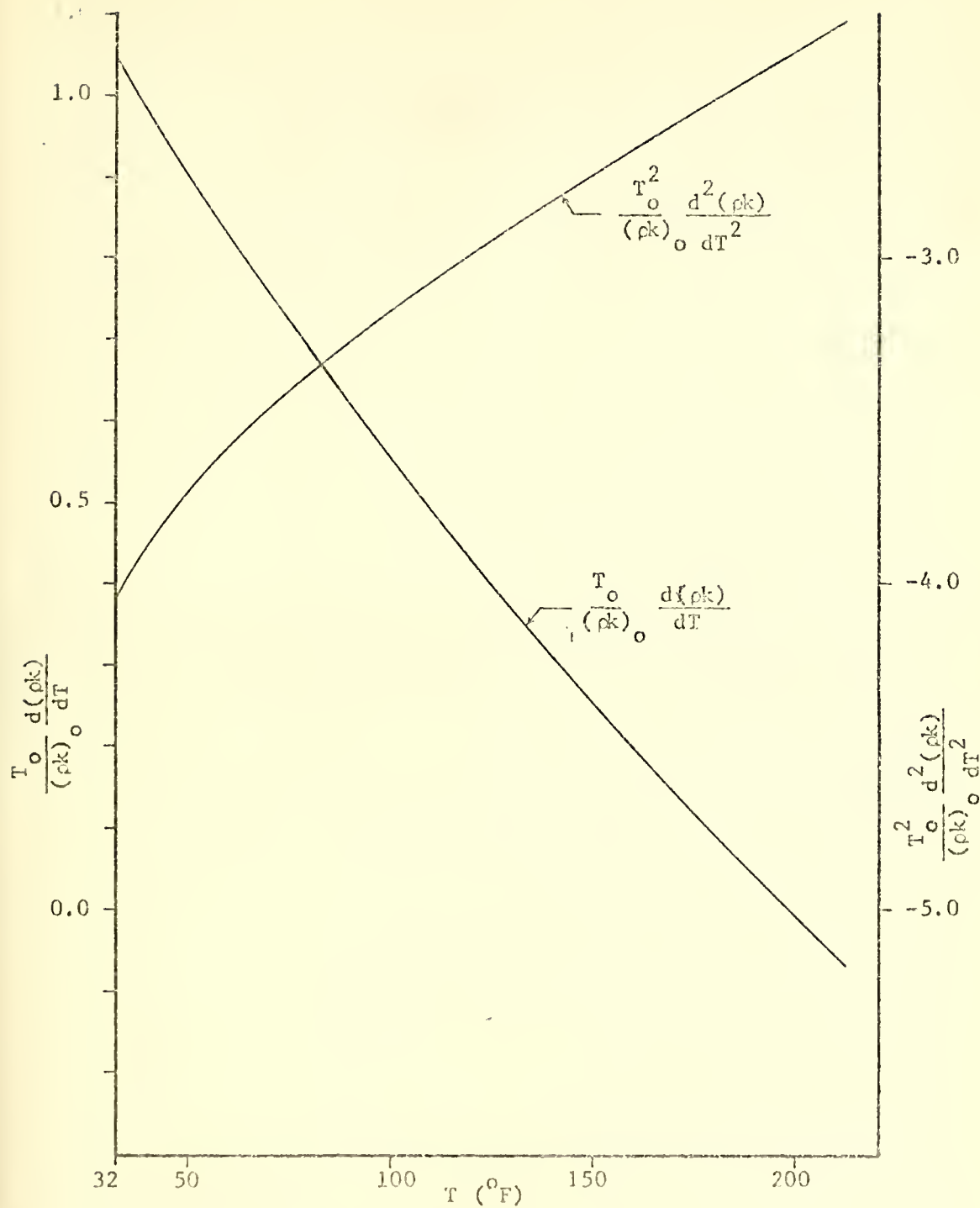


Figure B.5 First and second temperature derivative of ρ_k as a function of temperature.

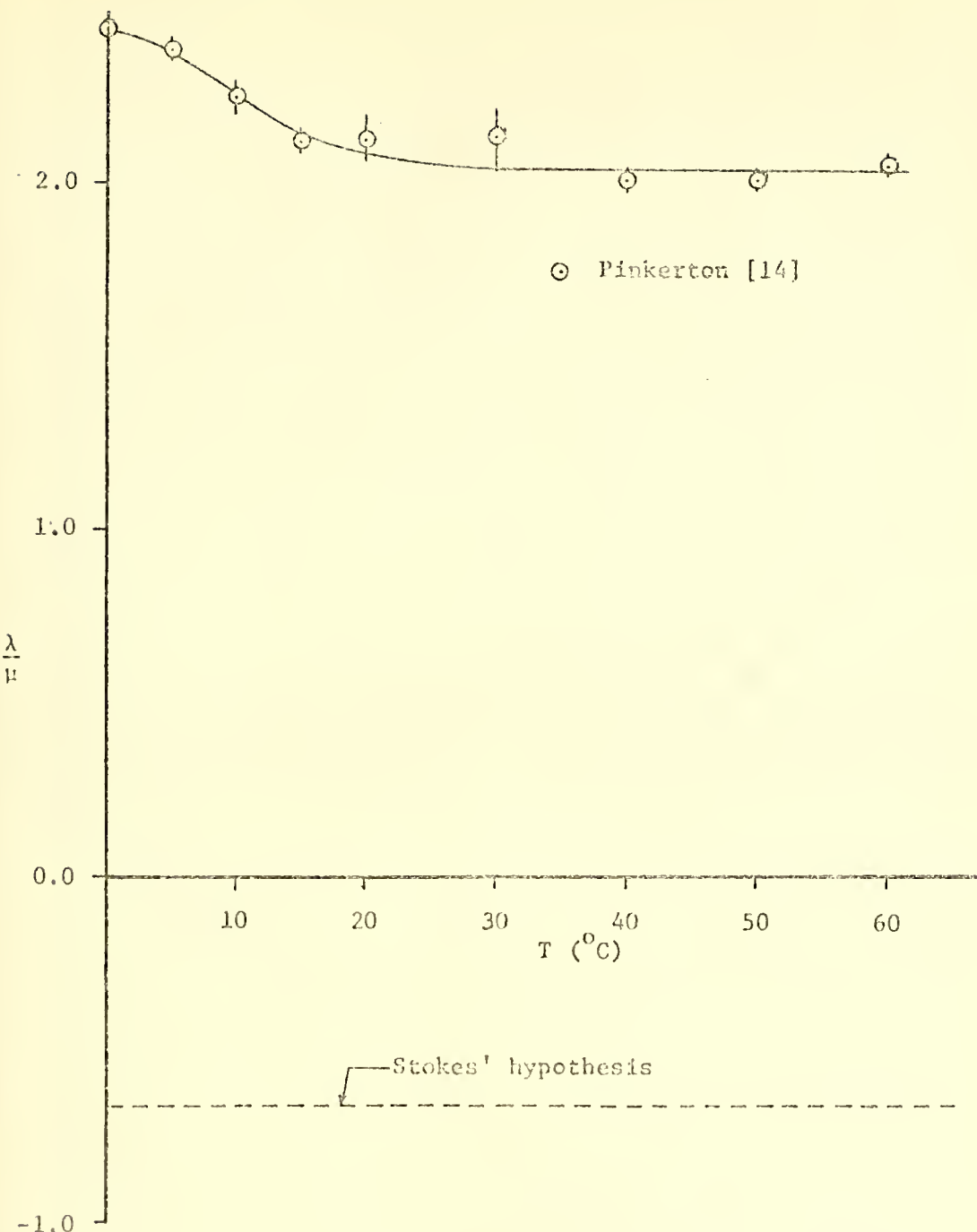


Figure B.6 Second-to-first viscosity ratio for water as a function of temperature.

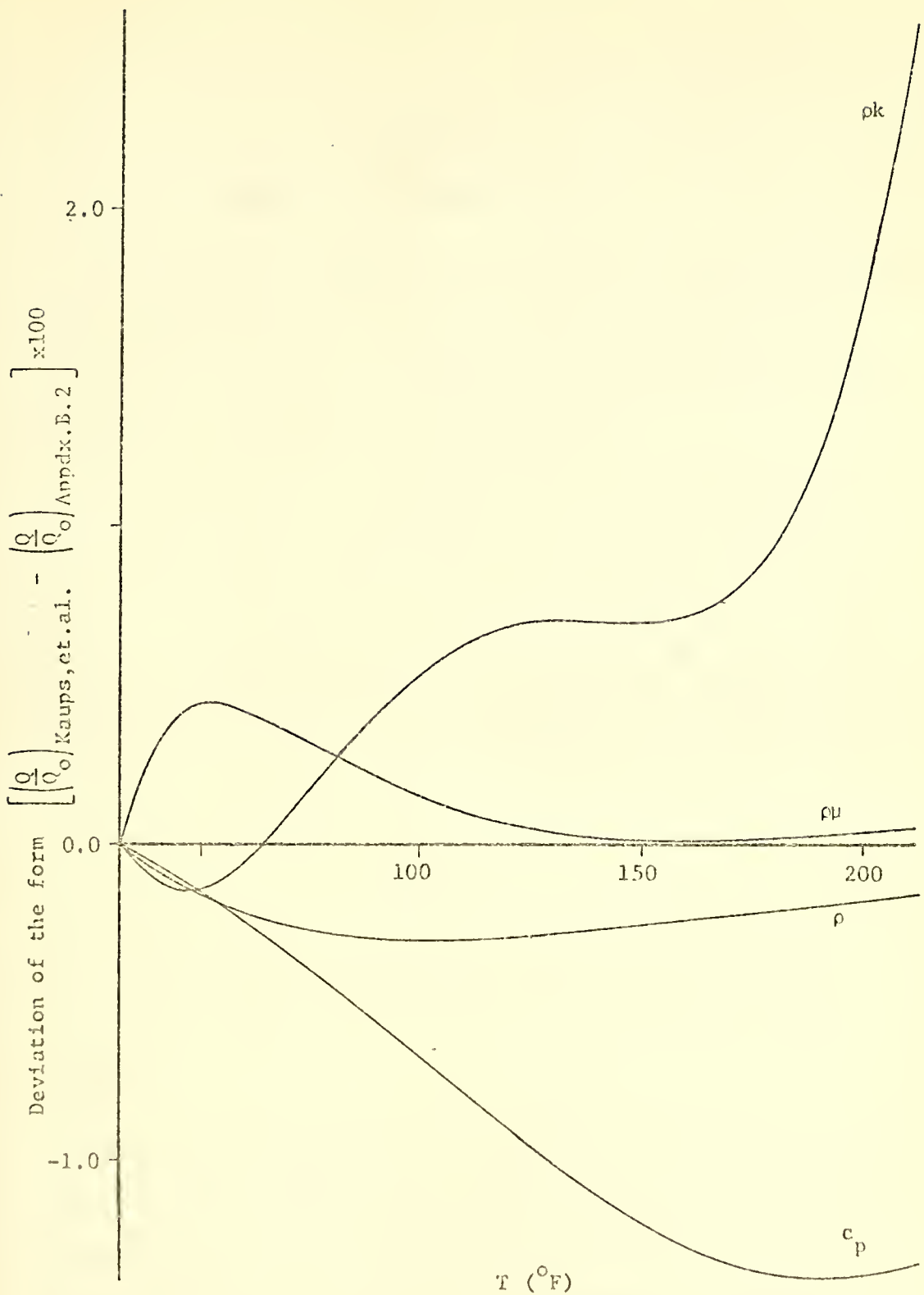


Figure B.7 Deviation between the property-temperature variation of Kaups, et.al [7] and that specified in Appendix B.2.

APPENDIX C

MEAN FLOW SOLUTION VARIABLES

For reference purposes, the mean velocity, temperature and property variation through the boundary layer, as well as their derivatives computed by the program are plotted in this appendix for the flows considered in this investigation.

To transform this information from the η coordinate system to a more physical one, Figure C.1 has been included. If, for example, the reference normal scale is denoted as y_o (i.e. $y = \frac{y}{y_o}$), then

$$\frac{dy}{d\eta} = \frac{y_o}{\delta^*} \eta_{\delta^*} \bar{\rho} \frac{d}{d\eta}$$

or

$$d\eta = \frac{y_o}{\delta^*} \eta_{\delta^*} \bar{\rho} dy$$

In this formulation the advantages and disadvantages of using η (rather than y) as the independent variable may clearly be seen.

Advantages

(1) Using the mean density variation, the physical step size is "automatically" adjusted within regions where the temperature is significantly different from its free stream value. This means that although the η step size remains fixed throughout the entire integration range, the actual distance traversed will be varied

constantly within the thermal boundary layer. The larger the wall-to-free stream temperature difference (and so, the more severe the thermal gradients near the wall), then the smaller will be the initial steps from the wall. Admittedly, liquid water's density variation with temperature is not as significant as might be desired for such a formulation, but for large temperature differences, it is still sufficient to permit selection of a constant step size outside the thermal boundary layer while adequately describing variation within it.

(2) If information obtained from solution of the mean flow equations (2.20) is to be used directly in defining the variable coefficients for the disturbance equations, then both must be expressed in terms of the same independent variable. If the latter is to be solved instead with y as the independent variable (to compensate for the first disadvantage discussed below), then a constantly varying step

$$\Delta y = \frac{\delta^*}{Y_0} \frac{1}{\eta_s^*} \int_{\eta_i}^{\eta_{i+1}} \frac{d\eta}{\bar{\rho}}$$

must be used within the thermal boundary layer. It would seem to be inconsistent (particularly for large temperature differences) to solve the mean flow equations in terms of the Howarth-Dorotnitsyn variables (eqn. (2.14)) and then assume the mean density to be constant ($\bar{\rho} \equiv 1$) to solve the disturbance equations (as apparently

Wazzan et.al. [3-5] have). Such an assumption should raise questions concerning the accuracy of the variable coefficients for the latter, especially in the wall region where density changes are greatest.

Disadvantages

(1) Outside the thermal boundary layer, the η step size is times that of the equivalent "y" one. For the temperature range considered η_{δ^*} is always greater than unity ($T_w \leq 213^{\circ}\text{F}$ with $T_\infty = 60^{\circ}\text{F}$, $\beta = 0$ for $\eta_{\delta^*} \leq 1$) so even when the displacement thickness is chosen as the reference length ($y_0 = \delta^*$), a larger η step would actually be required than for a comparable y integration. This means to obtain the same accuracy, more steps would be required with η as the independent variable.

(2) An extra calculation is required to transform back from the η to y coordinate system.

It was decided that the advantages outweighed the disadvantages and so the problem was formulated and solved using η as the independent variable.

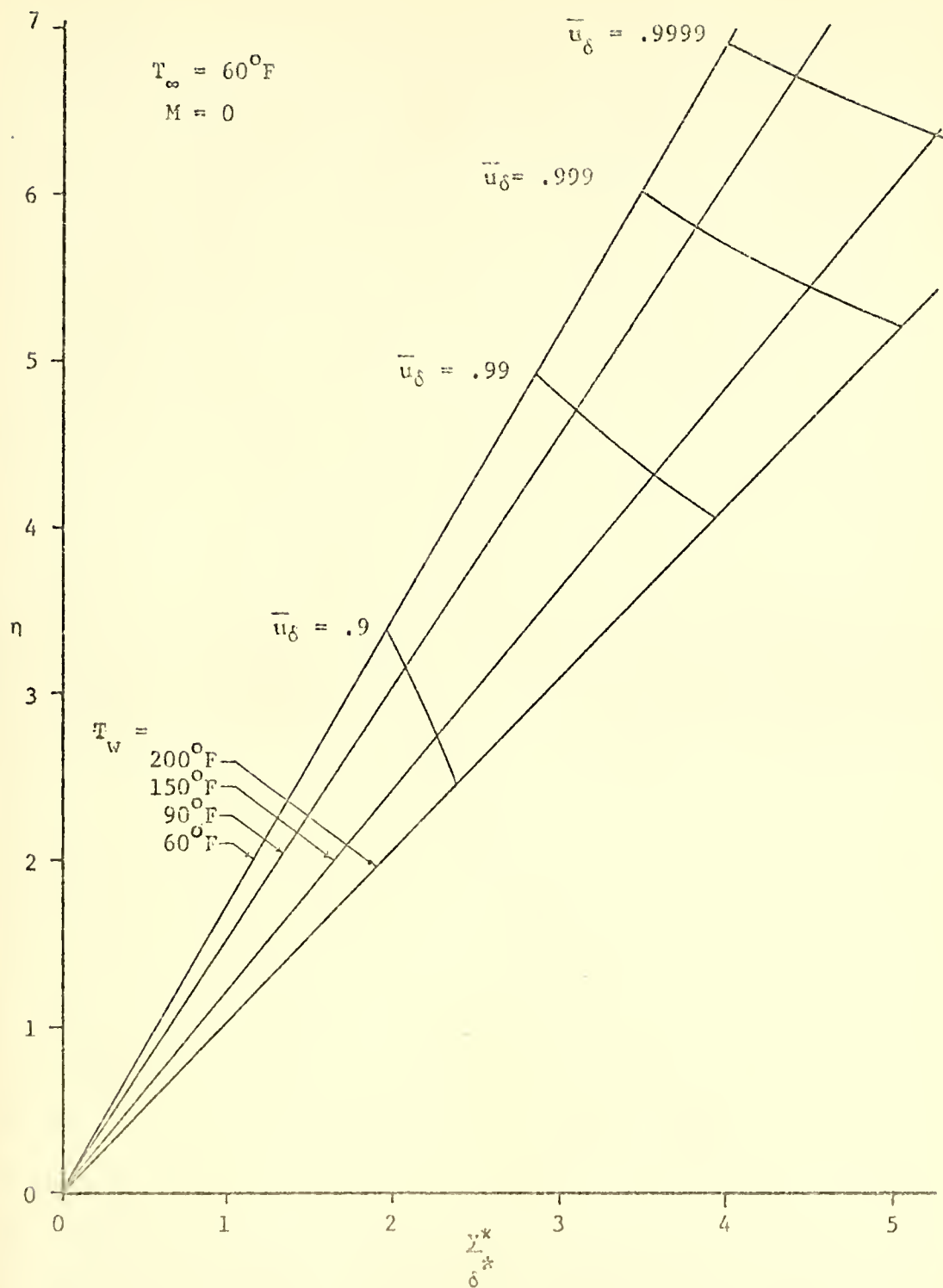


Figure C.1 Relationship between η and $\frac{y^*}{\delta^*}$ for various wall temperatures.

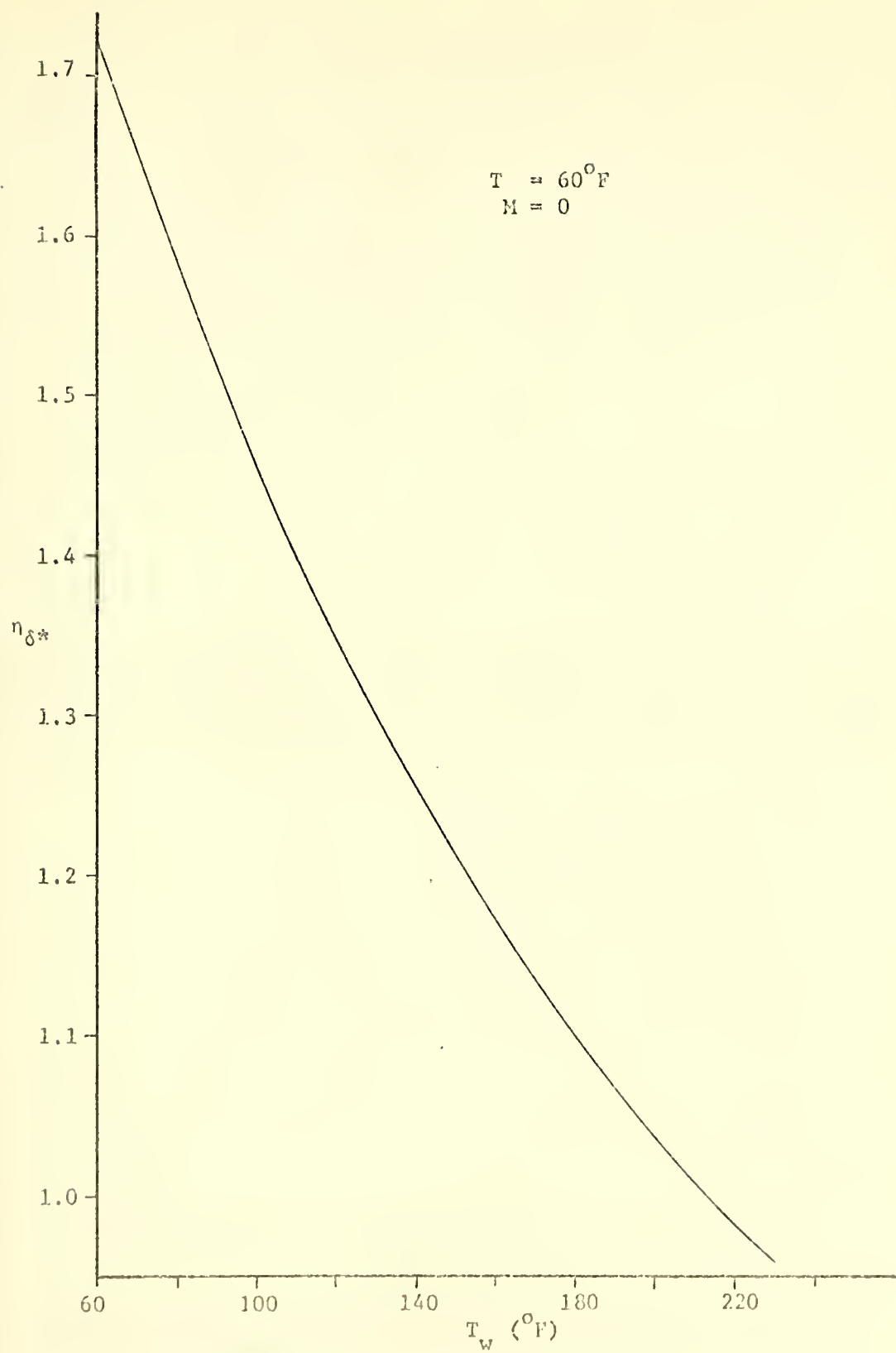


Figure C.2 Variation of $n_{\delta*}$ with changes in the wall temperature.

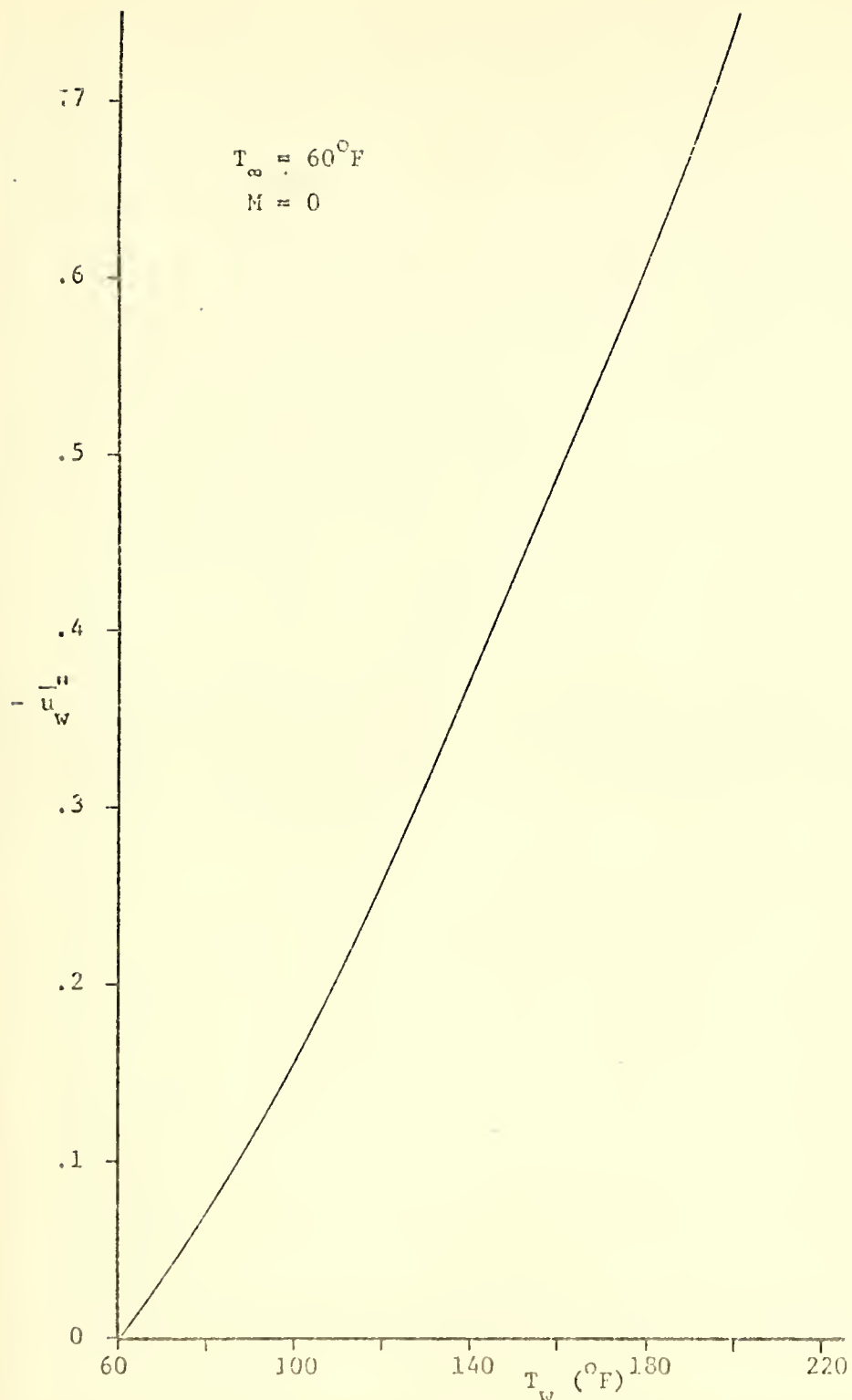


Figure C.3 Second velocity derivative evaluated at the wall as a function of the wall temperature.

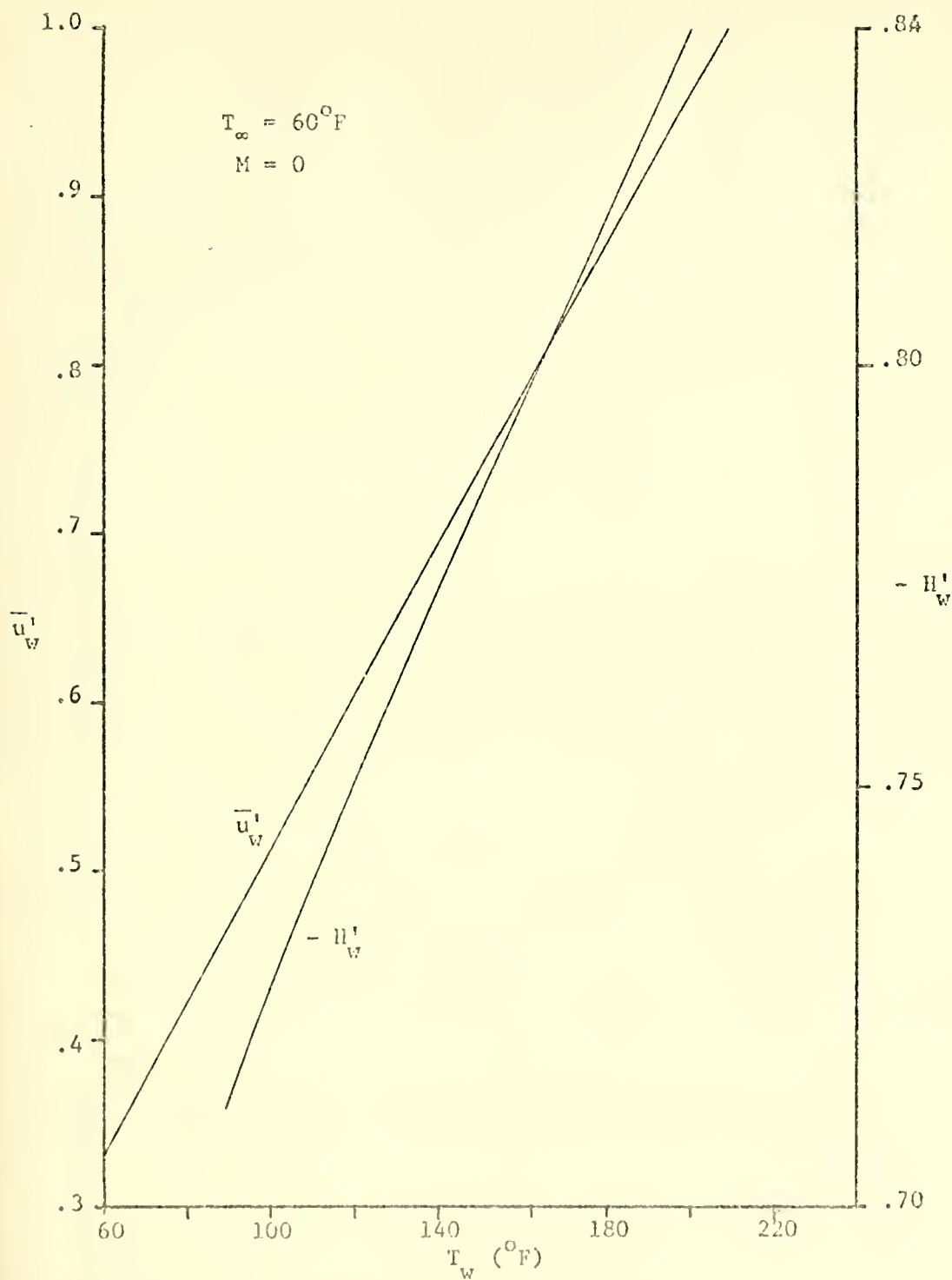


Figure C.4 First derivatives of velocity and temperature evaluated at the wall as a function of wall temperature.

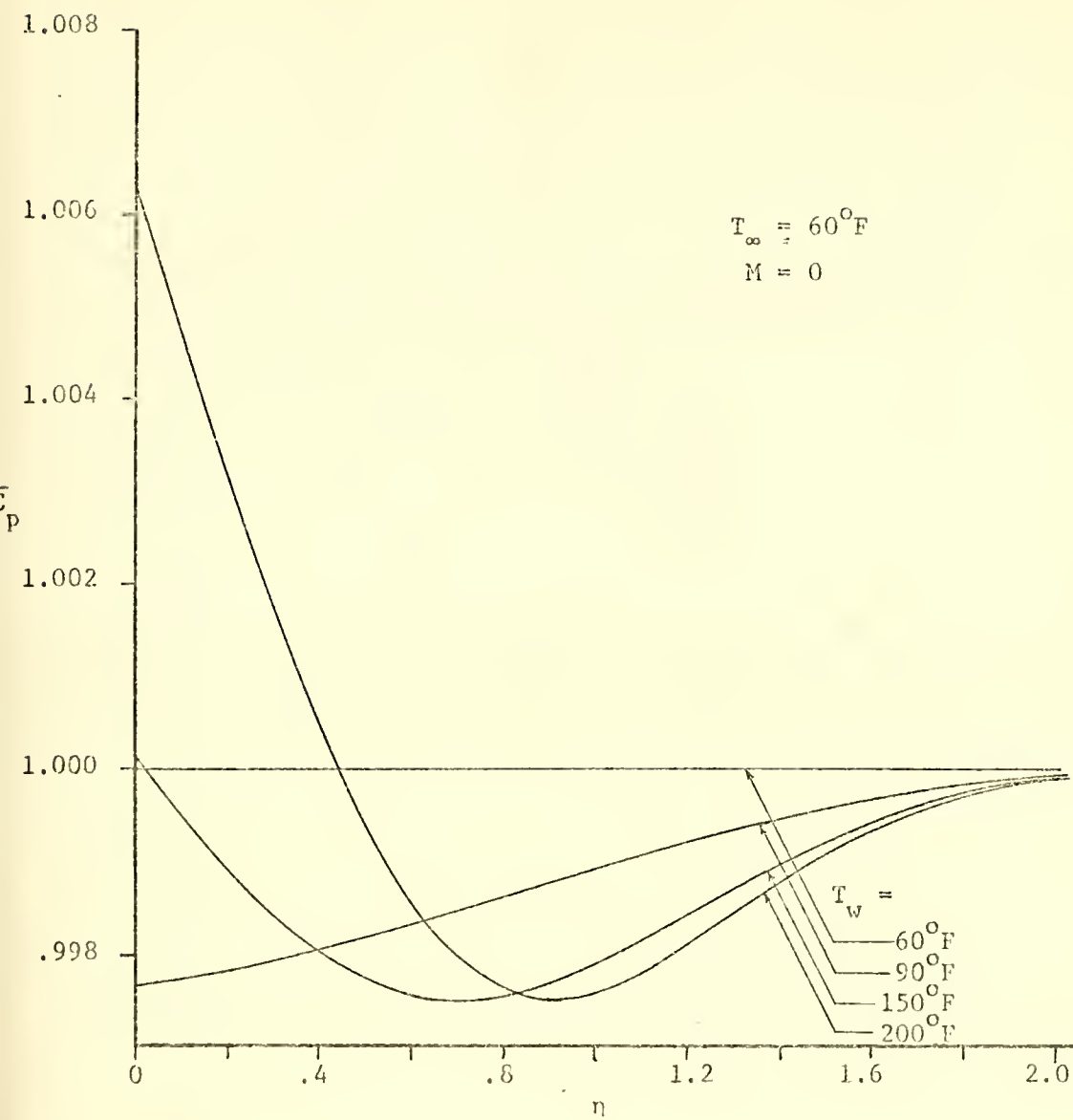


Figure C.5 Specific heat boundary layer profiles for various wall temperatures.

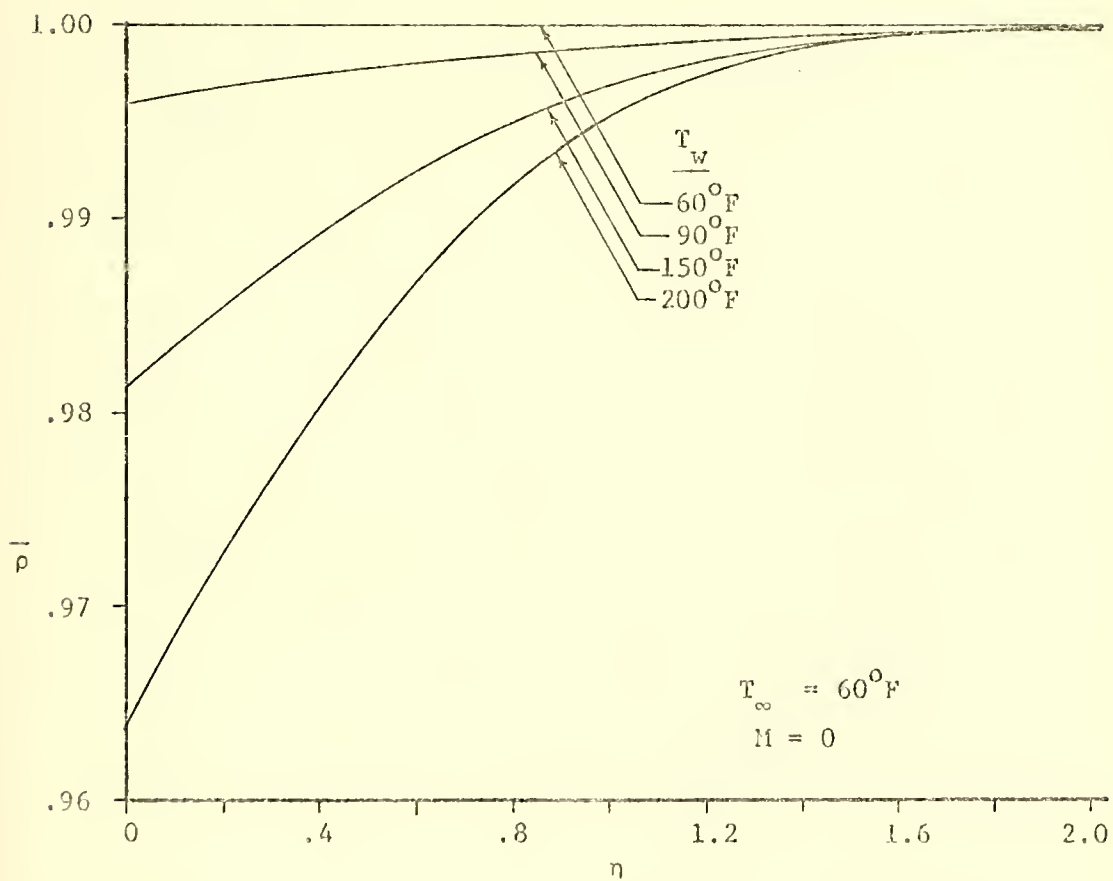


Figure C.6 Density boundary layer profiles for various wall temperatures.

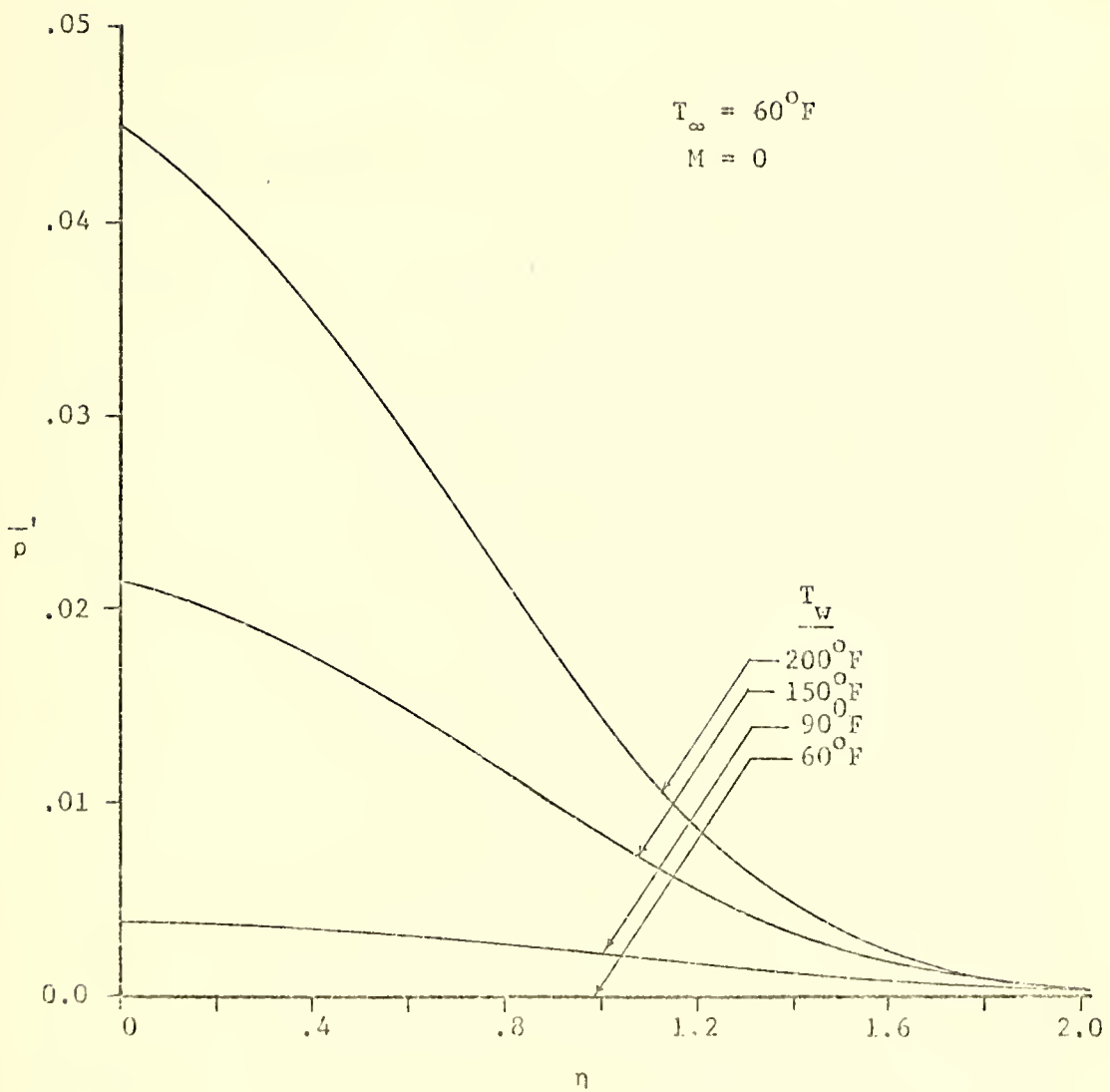


Figure C.7 Boundary layer profiles of the first derivative of density for various wall temperatures.

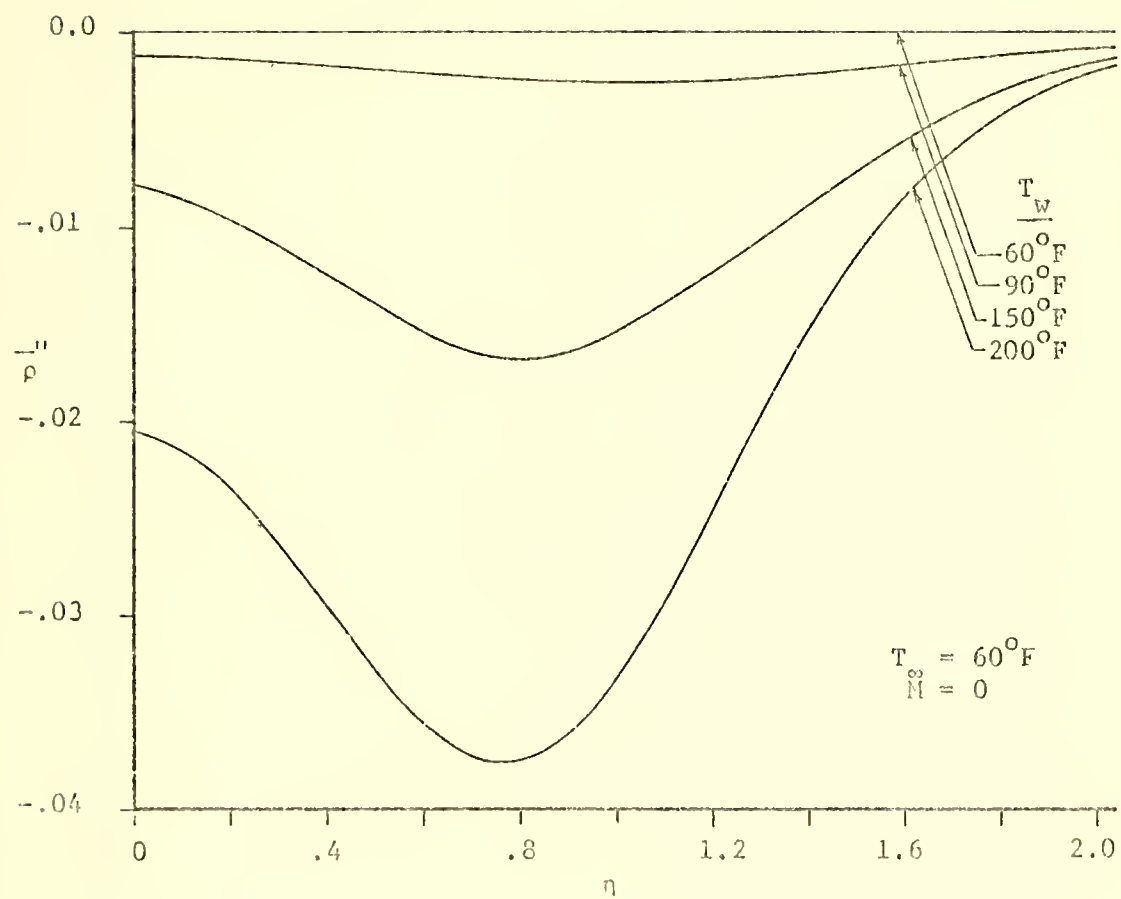


Figure C.8 Boundary layer profiles of the second derivative of density for various wall temperatures.

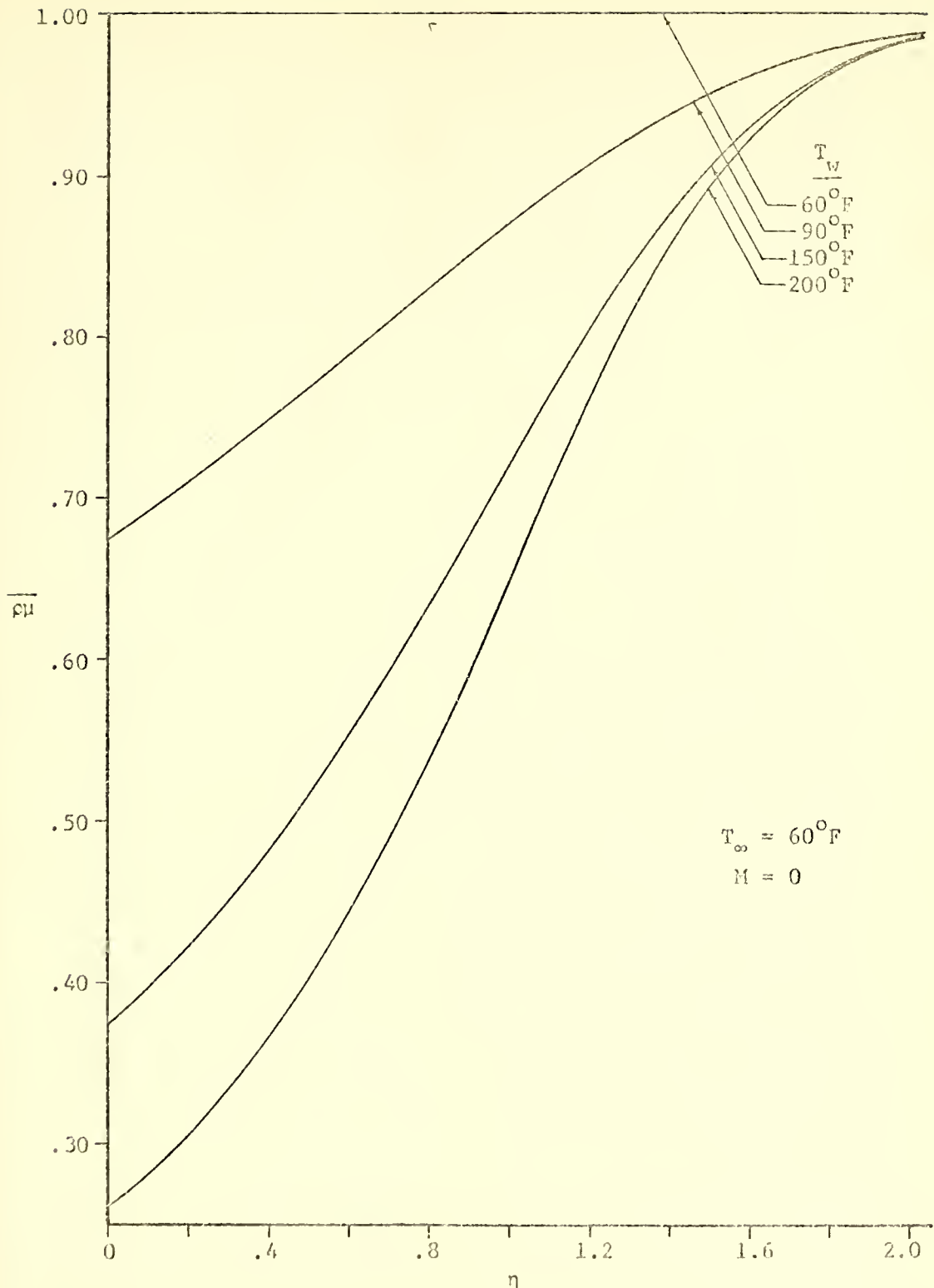


Figure C.9 Boundary layer profiles of the density-viscosity product for various wall temperatures.

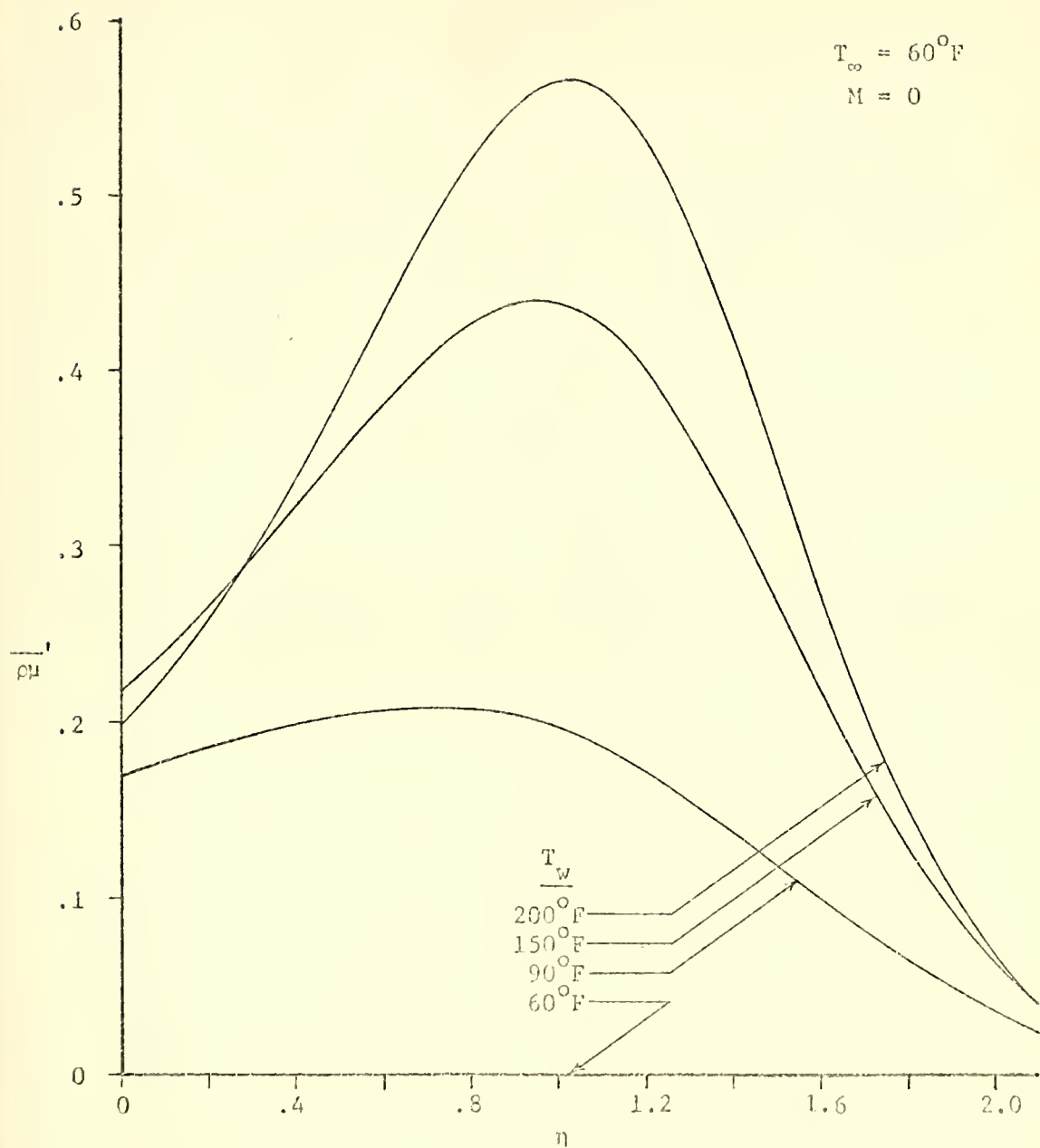


Figure C.10 Boundary layer profiles of the first derivative of the density-viscosity product for various wall temperatures.

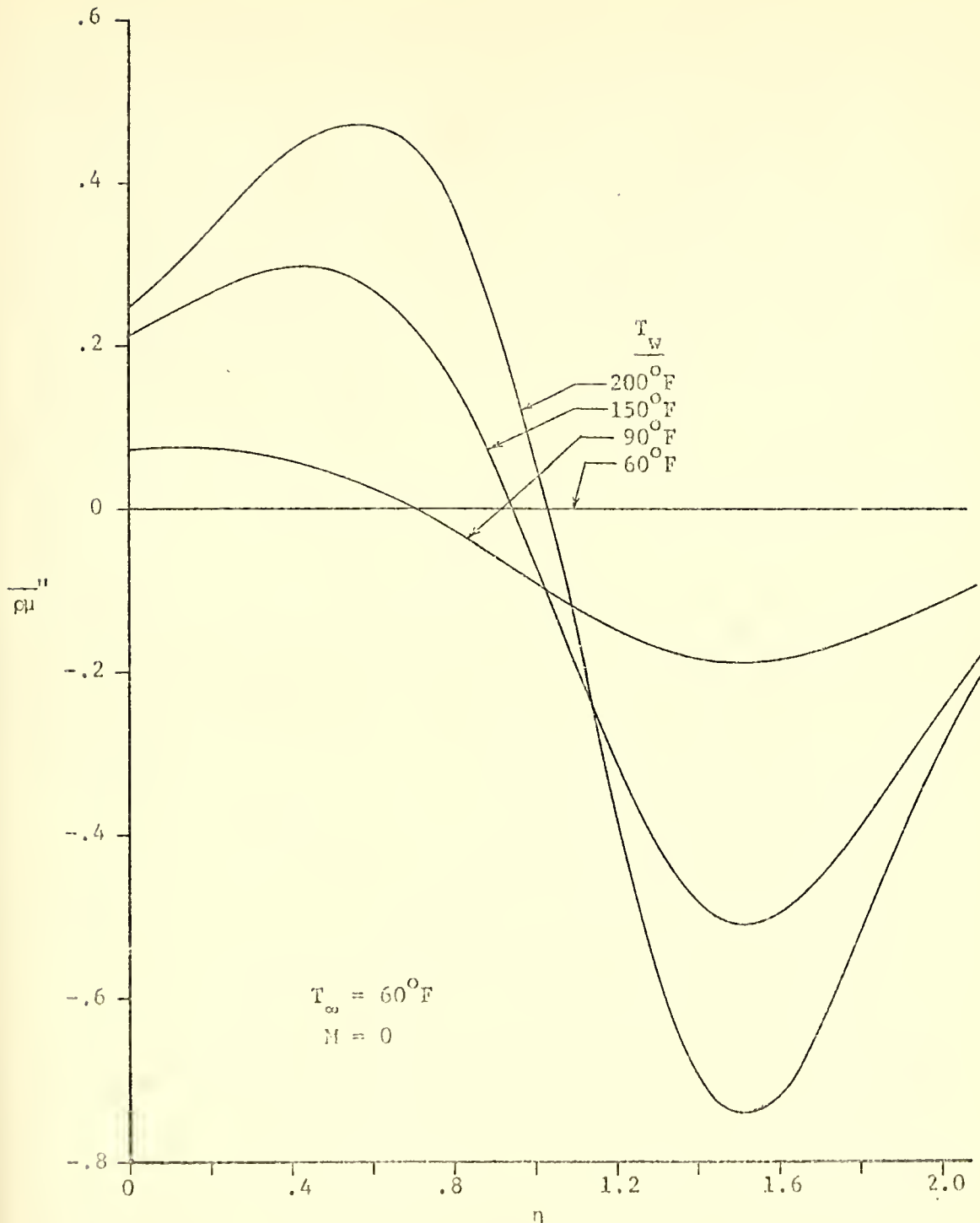


Figure C.11 Boundary layer profiles of the second derivative of the density-viscosity product for various wall temperatures.

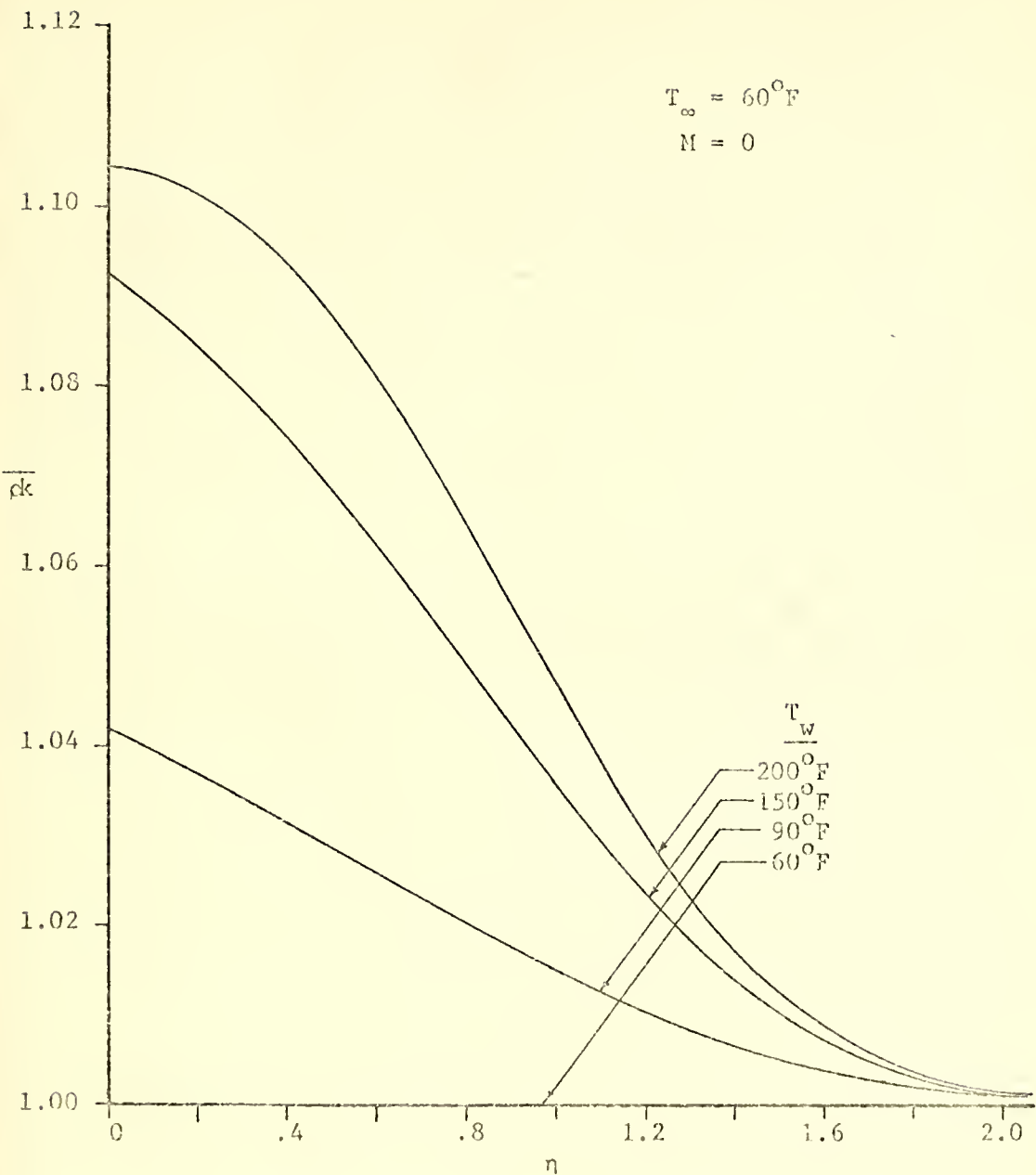


Figure C.12 Boundary layer profiles of the density-thermal conductivity product for various wall temperatures.

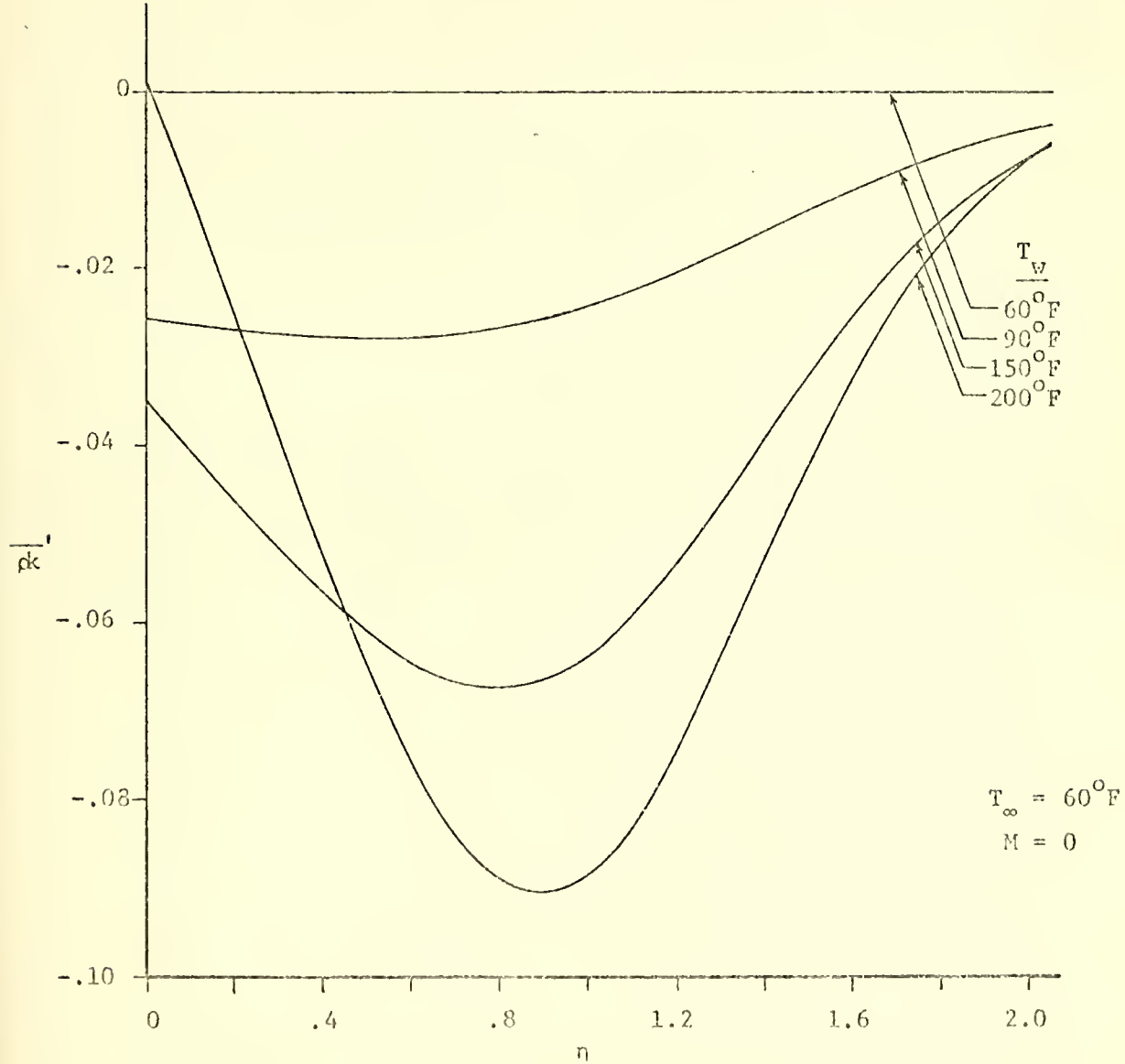


Figure C.13 Boundary layer profiles of the first derivative of the density-thermal conductivity product for various wall temperatures.

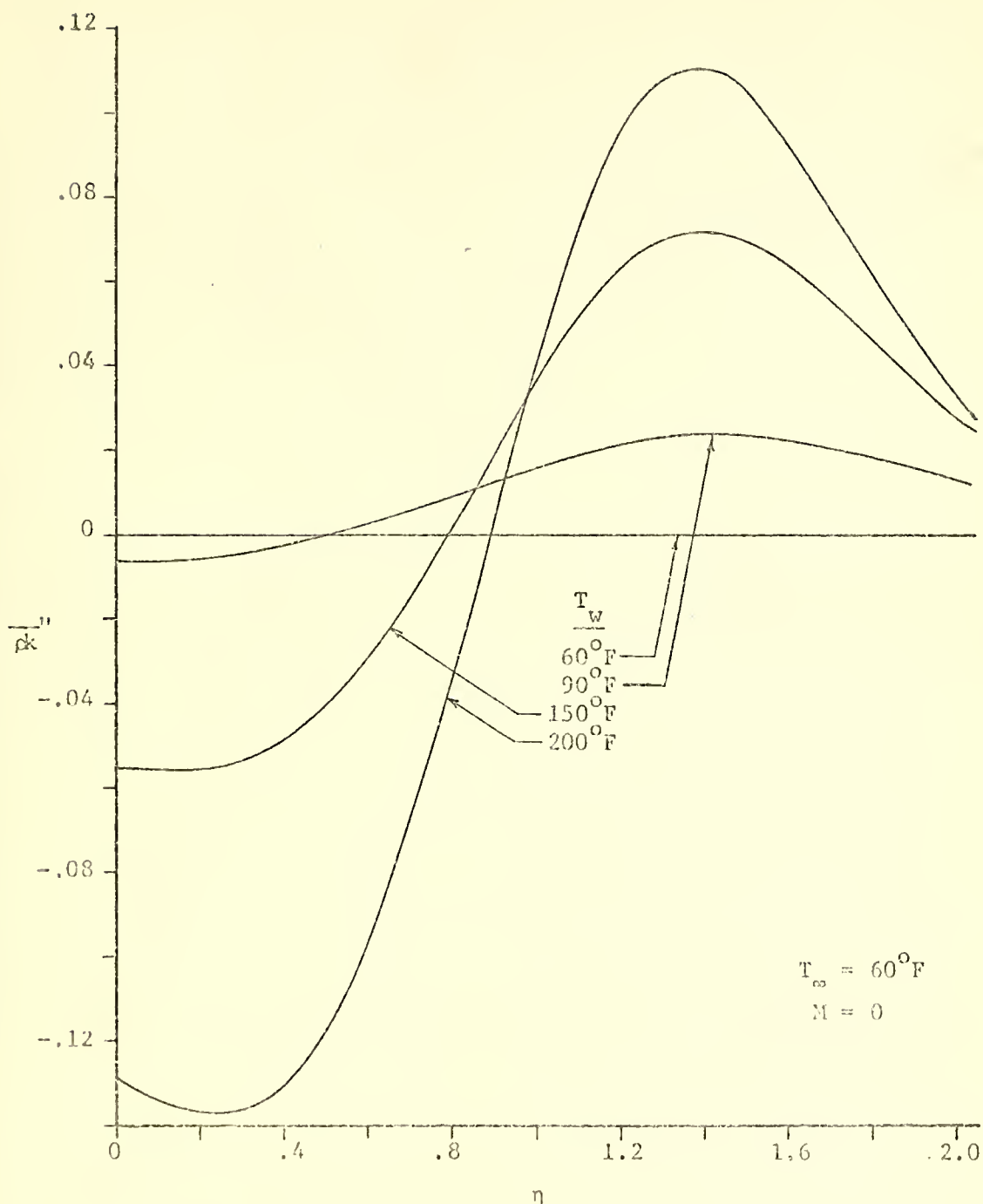


Figure C.14 Boundary layer profiles of the second derivative of the density-thermal conductivity product for various wall temperatures.

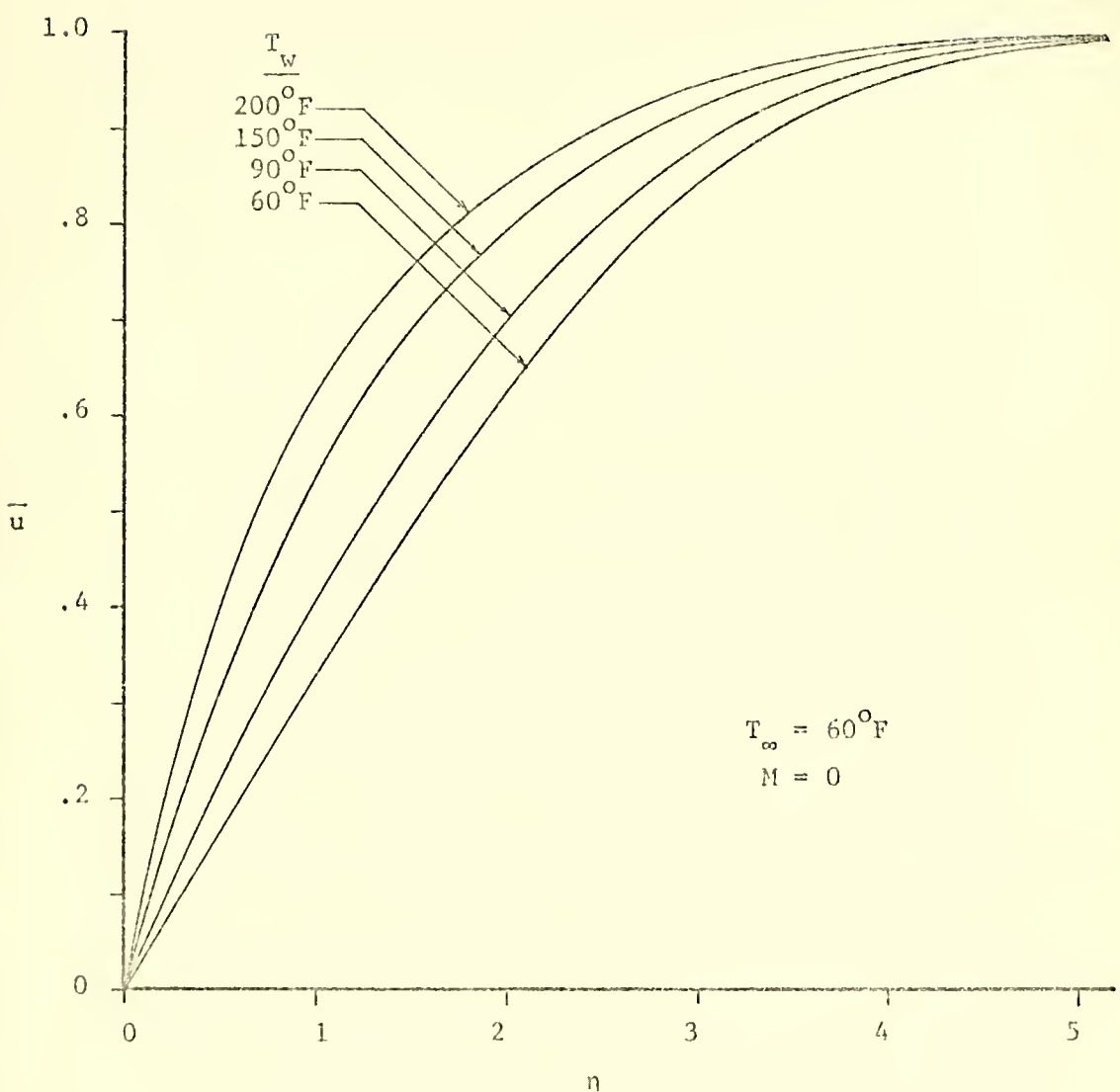


Figure C.15 Boundary layer velocity profiles for various wall temperatures.

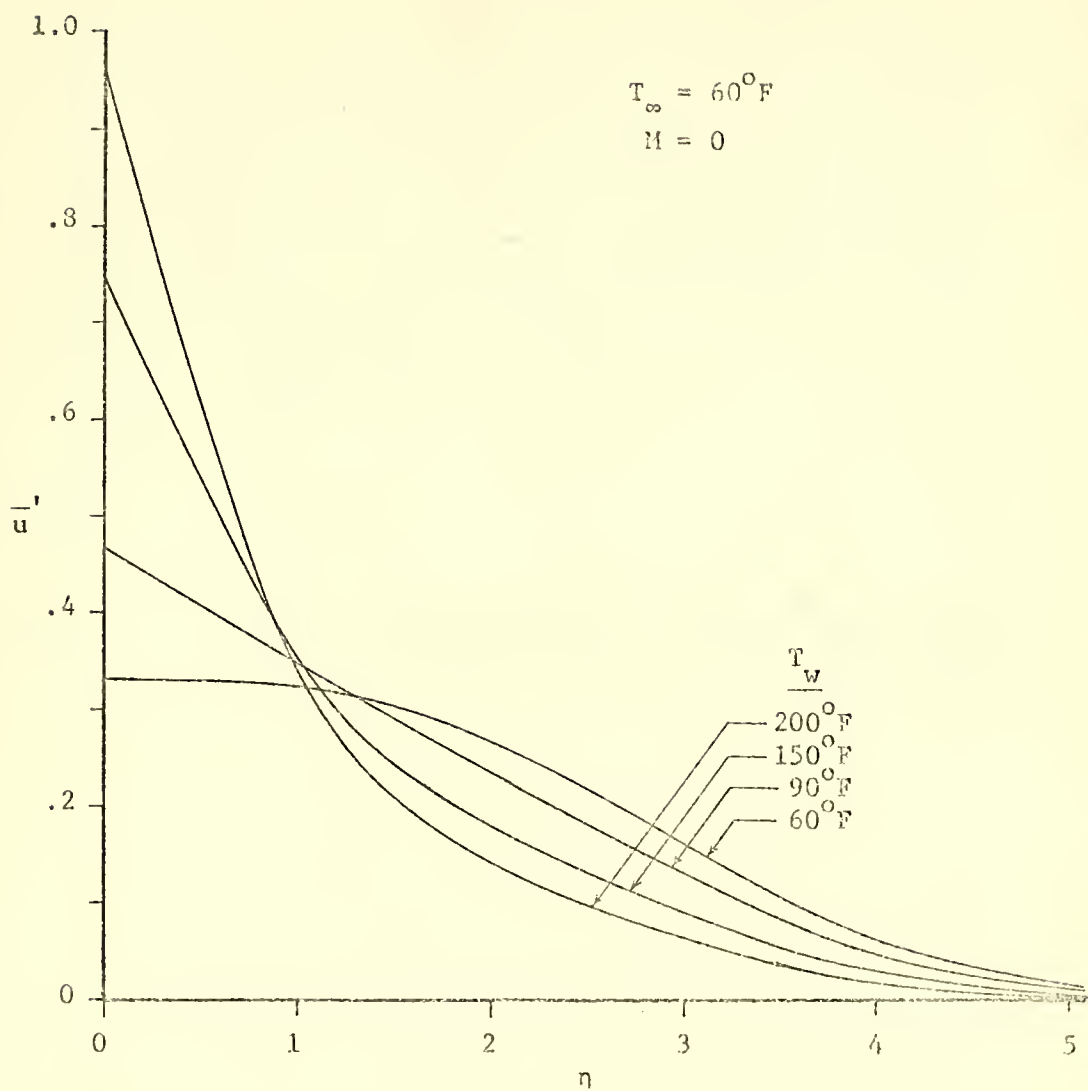


Figure C.16 Boundary layer profiles of the first derivative of velocity for various wall temperatures.

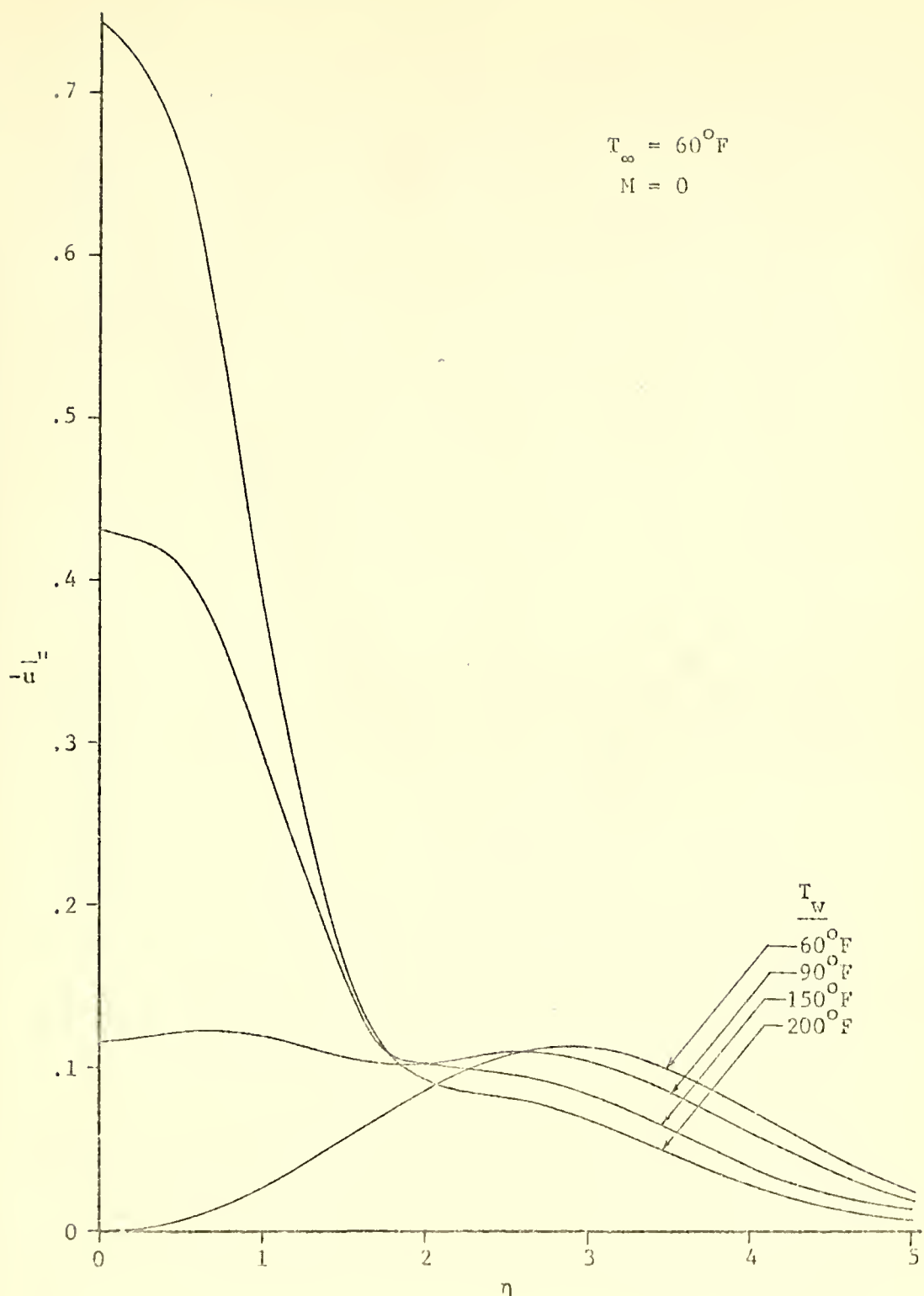


Figure C.17 Boundary layer profiles for the second derivative of velocity for various wall temperatures.

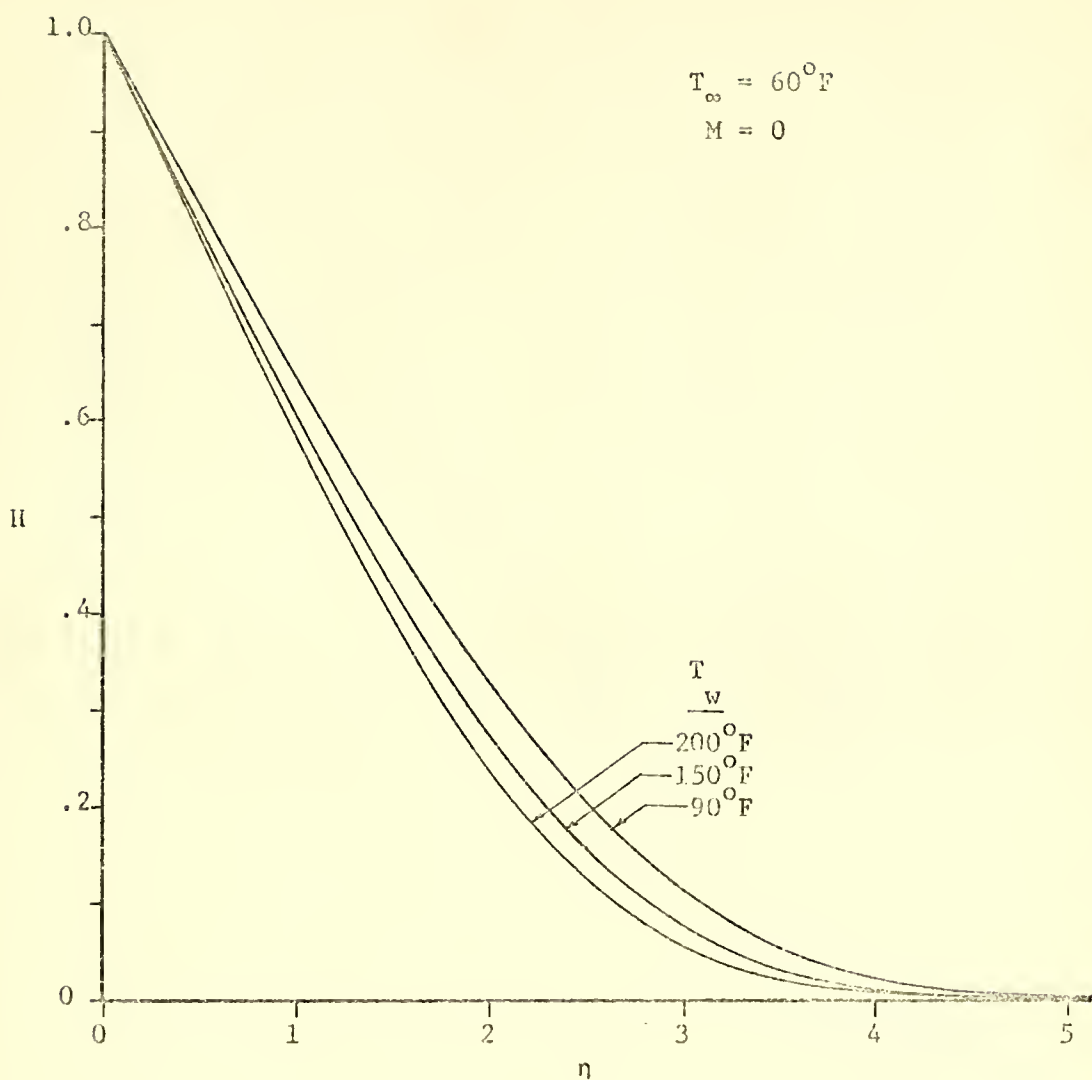


Figure C.18 Boundary layer temperature profiles for various wall temperatures.

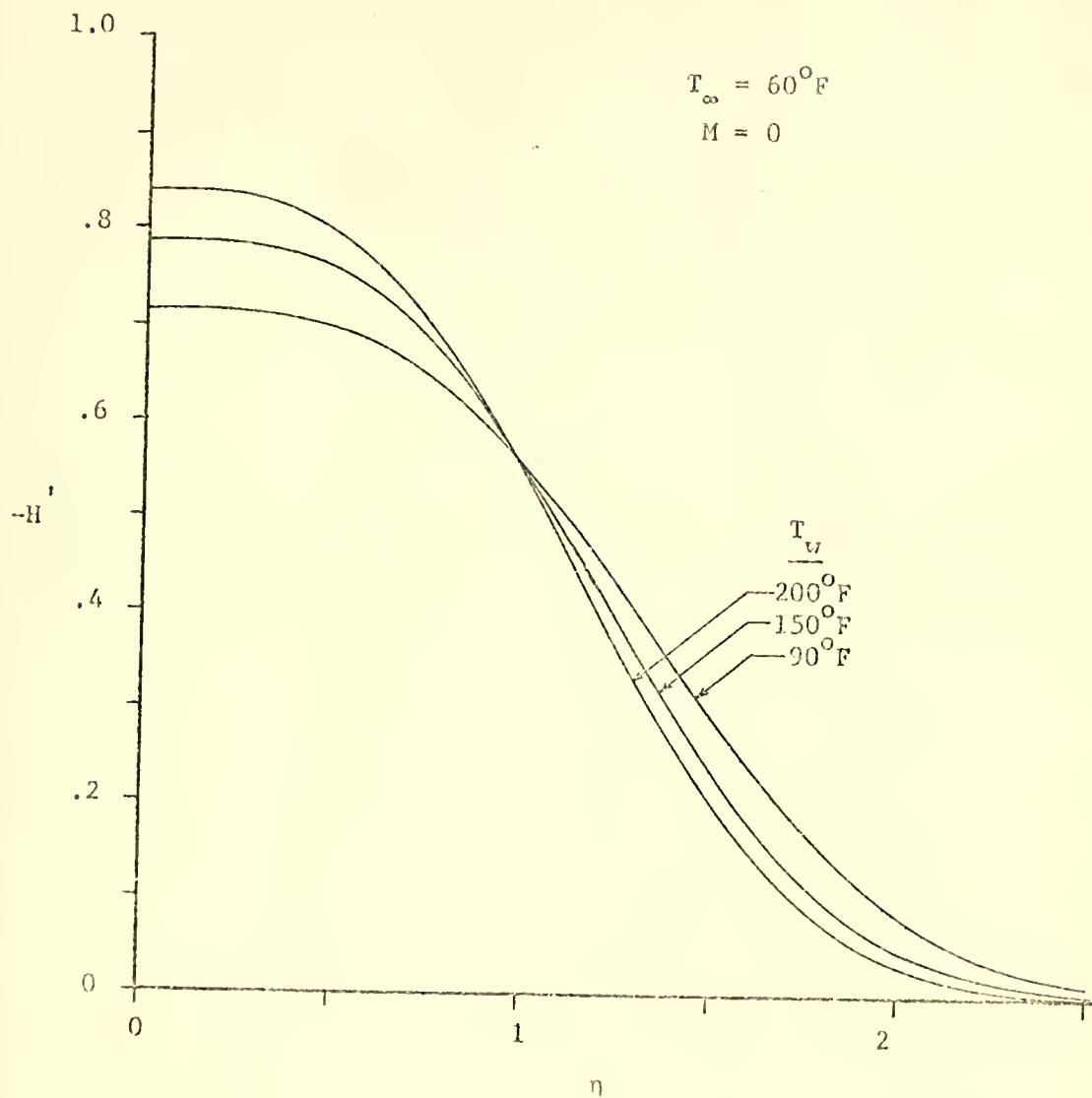


Figure C.19 Boundary layer profiles of the first derivative of temperature for various wall temperatures.

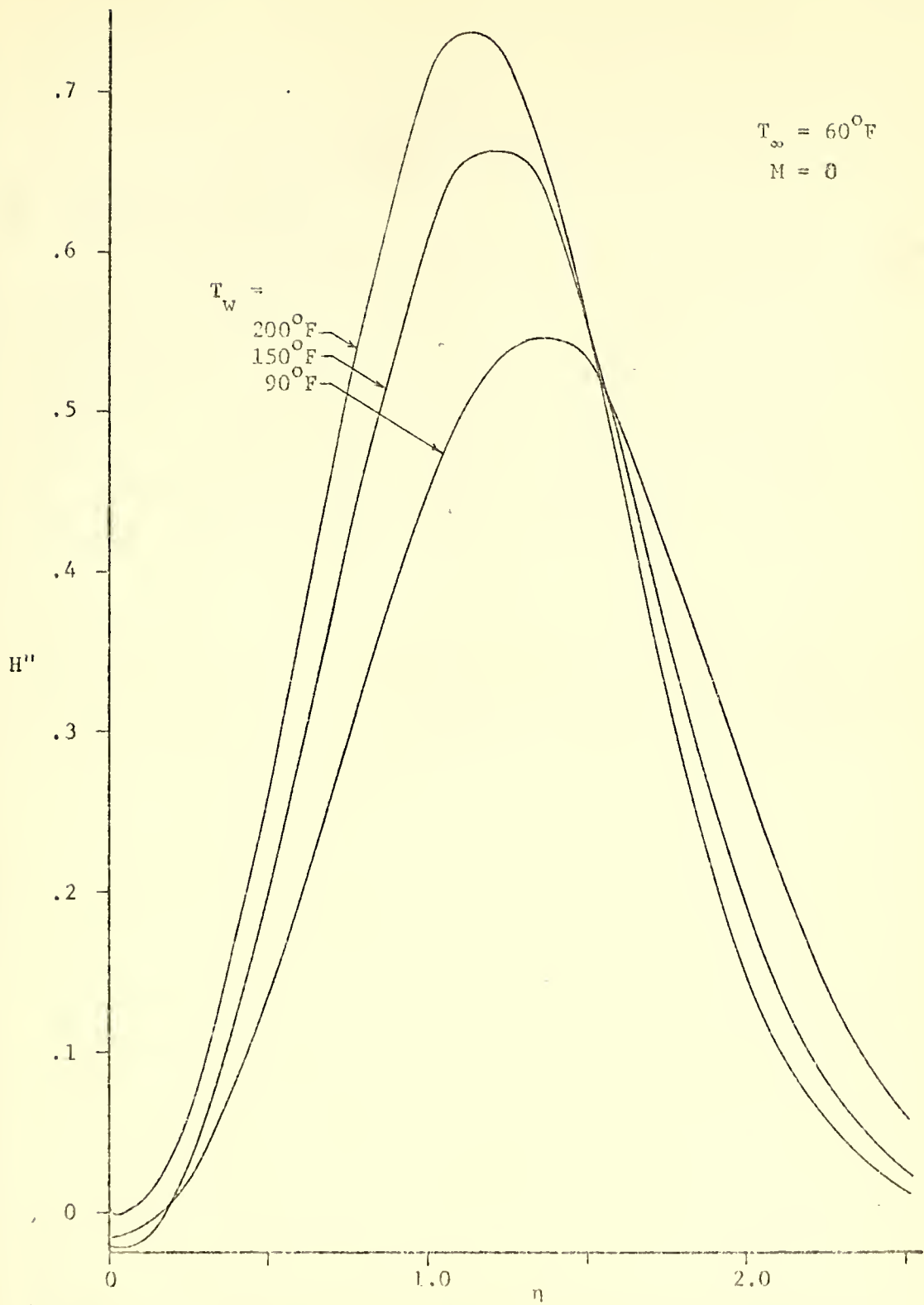


Figure C.20 Boundary layer profiles of the second derivative of temperature for various wall temperatures.

Appendix D

The Computer Program

D.1 Program Description

The program written to solve the stability problem formulated in Chapter II consists of a mapping processor (BLSMAP), the main program (BLSTAB), and eleven subroutines, all of which are coded in FORTRAN V. A brief description of each, along with its role in the overall computational scheme and references to numerical procedures (where applicable), is given in Table D.1.

Routine	Numerical References	Purpose	Description
BLSMAP	[38]	reduce overall storage requirements	This mapping routine dictates only the storage allocation of the program and is nonessential for its capability to function as designed.
BLSTAB (Main program)		control overall execution of the program	Calculation of mean flow quantities, MM sets of stability characteristics, or both (as specified by the logical variables NOTE (I)) are all regulated by this, the main program. If the mean flow variables BLPAR (I,K) and coefficients C(I,K) have been previously calculated and stored in unit 8, then their recalculation is bypassed and the information read directly before attempting solution of the disturbance equations. If stability characteristics are evaluated and eigenfunctions formed, it can calculate property fluctuations, FLUCT (I,K), and energy production and dissipation terms, FUNC (I,K), for a neutral disturbance (ALFA1 = 0).

TABLE D.1 Description of Program Routines

Routine	Numerical References	Purpose	Description
MFEQN	[18] [19]	control solution of mean flow equations and computation of disturbance equation coefficients	This routine initializes dependent variables Y(I), then calls ADAMS to integrate mean flow equations from ETA = 0 to ETAEND (I). It computes corrections DELX and DELZ to the unknown wall velocity and temperature gradients X and Z, and then assesses whether both the corrections and asymptotic error, E, are sufficiently small. If such is the case, one more boundary layer integration is performed to evaluate mean flow variables B(I,K) and variable coefficients C(I,K) at each step required for the integration of the disturbance equations. Using the composite Simpson's Rule formula, the integral required to obtain displacement thickness ratios, ERADLS, is found. When required, the relationship between y/δ^* and η is computed.
DIFF		evaluate first order differential mean equations	With calls to TEMVAR to evaluate required mean property derivatives, the system of first order, differential, mean flow equations is calculated.

TABLE D.1 Continued

Routine	Numerical References	Purpose	Description
TEMPVAR	[7]	input property temperature variation for water	<p>For INDEX > 0, the routine evaluates water's nondimensional properties, G(I) and their first two "logarithmic" derivatives, GP(I) =</p> $\frac{1}{G(I)} \frac{dG(I)}{dTTEMP} \text{ and } GPP(I) = \frac{1}{G(I)} \frac{d^2G(I)}{dTTEMP^2}, \text{ at}$ <p>temperature TEMP = $\frac{T - T_{ref}}{T_v - T_\infty}$ for either the data formulation of Kaups and Smith or that specified in Appendix B.2.</p> <p>If INDEX = 0, free stream fluid property values, GINF(I) are computed (except for Kaups, et.al. data which computes nondimensional ratio of free stream values to those at $T_{ref} = 32^\circ\text{F}$).</p>
ADAMS	[18]	integrate mean flow equations	<p>This integration routine is designed to use single step Runge-Kutta procedures alone or in combination with the multistep Adams-Moulton predictor-corrector scheme. With calls to DIFF, it integrates the mean flow equations in double precision.</p>

TABLE D.1 Continued

Routine Reference	Numerical References	Purpose	Description
DISTEQ		control solution of disturbance equations and stability characteristics	After initializing the three solution vectors, Z(J,I,KP), at the boundary layer edge, KP = KPTOT, this routine directs the integration of the disturbance equations by calls to DIFFEQ and then checks the linear independence of the solution vectors after each step with calls to ORTHCR. Upon completion of the integration, it linearly combines solution vectors at the wall, KP = 1, with coefficients X(J), and evaluates the complex admittance, F(ITER), for the ITERth estimate of the eigenvalue, EV(ITER). If the estimate is inadequate, EVEST is called for a refined value, EV(ITER+1), for use in the next iteration. If it is sufficiently accurate and eigenfunctions are also required, a call is made to ECNFCN. When the maximum allowed number of iterations, ITRMAX, is exceeded, the most accurate estimate of the eigenvalue, EV(NITR), is returned to the main program.
STABEQ		evaluate first order differential, disturbance equations	The system of complex, first order, differential equations for the disturbance flow is evaluated. A determination is made whether the equations of Wazzan, et.al. or those formulated in this investigation are to be used. For the latter, a further determination specifies the fluctuating quantities to be omitted from the calculations.

TABLE D.1 Continued

Routine	Numerical References	Purpose	Description
EGNFCN	[22]	recover eigenfunctions	Using the stored orthonormalizing matrix, $P(I,J,K)$, solutions vectors, $Z(J,I,K)$, and combining coefficients, $X(J)$, this routine reforms the eigenfunctions, $Y(I,K)$.
GSORTII	[22]	orthonormalize solution vectors	When called, this routine applies the Gram-Schmidt orthonormalization routine to the three solution vectors, $Z(J,I,K)$ at position K . If eigenfunctions are to be recovered, the orthonormalizing matrix $P(I,J,K)$ is also computed.
EVEST	[23,40] [25,41]	provide eigenvalue estimate for next iteration	On the initial call, when complex, surface admittances, $F(ITER)$, have been determined for the three estimated eigenvalues, $EV(ITER)$, the routine first determines the best estimate, $EV(NITR)$, then uses the plane fitting technique of Wazzan, et.al. to predict an eigenvalue for the next iteration, $EV(ITER+1)$. Averaging that value with $EV(NITR)$, it returns to DISTEQ . On subsequent calls, the same procedure is repeated except that no averaging is performed unless the eigenvalue search is nonuniformly converging, $F(ITER) \neq F(NITR)$. When the denominator required for this technique, $Z1+Z2+Z3$, is sufficiently small, then Muller's scheme is employed (unless it was used to compute the previous eigenvalue estimate or if the magnitude difference between the two components of the eigenvalue is too great).

TABLE D.1 Continued

Routine Reference	Numerical References	Purpose	Description
ORTHCR		evaluate degree of orthogonality between solution vectors	At boundary layer position K, this routine computes the angle, GAMMA, between solution vectors, $Z(J,I,K)$. If it is less than the specified orthonormalization angle, ANGLE, or the wall is reached, the routine makes its 11th call to GSORTH and records the position as KORTH(II). The smallest angle between solution vectors encountered during the boundary layer integration is identified as ASMIN.
DIFFEQ	[19]	integrate disturbance flow equations	This routine integrates the complex, first order, ordinary, differential disturbance equations using the Kutta integration scheme and calls to STABEQ.

TABLE D.1 Continued

D.2 Input

A description of data required to successfully execute the program described previously is now given in Table D.2. Further, the required format for this data is illustrated by a sample data deck in Figure D.1. Note that data input is arranged so that the first card lists only the logical control variables for the program; the second, all mean-flow related information; and, the remaining, disturbance flow and stability related information. If only the mean flow solution is sought, then only the first two cards are required; all others will be ignored by the computer.

Figure D.1 Sample Input Data Deck for Program BLSIB

Card	Field	Program Variable	Description
<u>Program Control Parameters</u>			
1	1 - 30	NOTE(I)	A series of logical variables identified in BLSTAB which controls the operation and output of the program.
<u>Mean Flow Parameters</u>			
2	1	TWALL	Wall temperature, T_w (specified in degrees Fahrenheit).
2	2	TINF	Free stream temperature, T_∞ (specified in degrees Fahrenheit).
2	3	BETA	Falkner-Skan parameter, $M = \frac{x}{u_e} \frac{du_e}{dx}$
2	4	EPSILN	Specified boundary layer edge parameter, where $\bar{u}_\delta = 1 - EPSILN$.
2	5	H	Step size for mean flow equation calculations, h_m . It is half that used for the disturbance equation integration, h_d , and must be greater than or equal to $\eta_\delta / 700$ where η_δ is the position defined as the boundary layer edge.
<u>Stability Parameters</u>			
3	1	ITERMAX	Maximum number of iterations permitted to compute an eigenvalue.
3	2	ANGLE	An orthonormal basis is reformed if the angle between any two solution is degraded to less than this quantity.

TABLE D.2 Description of Input Data for Program BLSTAB.

Card	Field	Program Variable	Description
<u>Stability Parameters (cont.)</u>			
3	3	EPSLN	Indicates the degree of refinement of eigenvalue estimate. Iteration is terminated when $ F(ITER) $,
			$ 1 - \frac{RE(EV(ITER))}{RE(EV(ITER+1))} $, and
			$ 1 - \frac{AIMAG(EV(ITER))}{AIMAG(EV(ITER+1))} $
			are all less than EPSLN.
3	4	NEV	Specifies which stability parameters are to be fixed and which are to be varied as the complex eigenvalue, EV.
		NEV	
		1	EV(ALFAR, OMEGA)
		2	EV(ALFAR, ALFAI)
		3	EV(ALFAR, RE)
		4	EV(OMEGA, RE)
		5	EV(OMEGA, ALFAI)
		6	EV(RE, ALFAI)
4	1	MM	Number of eigenvalues to be computed (maximum of 10)
5-14	1	REDLS(I)	Reynolds number, Re_δ^* .
5-14	2	ARDLS(I)	Real part of the wave number, $\alpha_R^* \delta^*$
5-14	3	AIDLS(I)	Imaginary part of the wave number, $\alpha_I^* \delta^*$.
5-14	4	FREQ(I)	Frequency, ω_∞ . All of the four preceding quantities are the best estimate of the Ith eigenvalue to be computed.

TABLE D.2 Continued

D.3 Program Listing

A complete listing of the FORTRAN V source deck used to generate the results in this investigation is given in this section. Note that where possible, the routines have been written in general so that application to systems of order greater than six is possible immediately with perhaps merely a change in the DIMENSION statements. This is particularly obvious in the routines associated with boundary layer integration, ADAMS and DIFFEQ, and with the Gram-Schmidt Orthonormalization algorithm, GSORTH, EGNFCN, and ORTHCR.

BLSTAB
1

SEG BLSTAB-* (REFCON, DISTEON-* (DIFFEQ-STABEQ-ORTHOR-EVEST, EGNFCN))

BLSTAB

```

1      DIMENSION C(14,701),BLPAR(7,701),Y(6,351),EV(50),
2      1RECLS(10),APCLS(10),ATDLS(10),FREQ(10),ZDIST(3,6,351),P(3,3,351),
3      2FLUCTG(3,351),FUNC(6,351)
4      DOUBLE PRECISION ALPHA
5      COMPLEX Y, EV, FLUCTG, ZDIST, P
6      LOGICAL NOTE, H20VAR
7      EQUIVALENCE (P,FLUCTG), (ZDIST,FUNC)
8      COMMON /BLK1/ALPHA,BETA,PRINF/BLK2/R,S,GINF(4)*C2/BLK3/G(4),
9      1GP(4),GPP(4)/BLK4/BLPAR,C/BLKS/N,N,KTOT,KMAX2/BLK7/ALFAR,
10     2ALFA,RE,CEGA/BLK8/NOTE(30)
11     READ (5,200) (NOTE(I),I=1,30)
12     WRITE (6,116) (NOTE(I),I=1,30)
13     116 FORMAT (1X,30L1)
14     200 FORMAT (30L1)
15 C IF LOGICAL VARIABLES NOTE(I) = TRUE, THE FOLLOWING ACTION IS TAKEN:
16 C NOTE(1) TERMINATE PROGRAM EXECUTION AFTER CALCULATING AND STORING
17 C IN UNIT 8 MEAN FLOW PARAMETERS AND STABILITY EGN COEFS.
18 C NOTE(2) CALCULATE ONLY EIGENVALUE. IF FALSE, EIGENFUNCTIONS ALSO
19 C COMPUTED.
20 C NOTE(3) WRITE ETA, VELOCITY, TEMPERATURE, AND THEIR ETA DERIVATIVES
21 C NOTE(4) WRITE KTOT AND ETADL
22 C NOTE(5) WRITE C(I,K)'S = STABILITY EQUATION COEFFICIENTS
23 C NOTE(6) WRITE ANGLE, ITMAX, EPSLN
24 C NOTE(7) WRITE ETADL'S AND RATIO OF U.L. TO DISPL. THICKNESS
25 C NOTE(8) WRITE EIGENVALUES
26 C NOTE(9) WRITE MEAN FLOW BOUNDARY LAYER STEP SIZE, TNALL, TINF, ETC.
27 C NOTE(10) WRITE GUESSES OF MEAN TEMP AND VELOC GRAD AT WALL AND
28 C TRIP INCREMENTS; WRITE ASYMPTOTIC ERROR IN SOLUTION, E.
29 C NOTE(11) READ MEAN FLOW AND STABILITY EGN COEFS INFORMATION FROM
30 C STORAGE UNIT 8. IF FALSE, PROGRAM RECOMPUTES THIS INFO
31 C PRIOR TO PROCEEDING TO EIGENVALUE PROBLEM.
32 C NOTE(12) COMPUTE AND WRITE RELATIONSHIP BETWEEN ETA AND
33 C Y/(DISPLACEMENT THICKNESS)
34 C NOTE(13) WRITE SPECIFIC INT.DENSITY, (DENSITY*VISCOSITY),
35 C (DENSITY*HEAT CONDUCTIVITY) AND THEIR ETA DERIVATIVES.
36 C NOTE(14) WRITE ITER/EV(ITER), GA, MA, SIGMA, Z(J,I,EPTOT)'S
37 C NOTE(15) COMPUTE DENSITY, VISCOSITY, AND THERMAL COND FLUCTUATIONS
38 C NOTE(16) COMPUTE REYNOLDS STRESS
39 C NOTE(17) WRITE ITEM # 10. OF ORTHONORMALIZATIONS REQUIRED.
40 C NOTE(18) WRITE X(J,I)'S = COORDINATE COEFFICIENTS
41 C NOTE(19) WRITE Y(I,1)'S = EIGENFUNCTION'S VALUE AT WALL
42 C NOTE(20) WRITE F(ITR) AND ABS(F(ITR))
43 C NOTE(21) INDICATE THAT ITMAX EXCEEDED AND BEST EST OF EIGENVALUE
44 C IN ITMAX EXCEEDED, WRITE ALL EV(ITER) AND F(ITER)
45 C NOTE(22) WRITE KGRD(I,I) = POSITIONS OF ORTHONORMALIZATIONS
46 C NOTE(23) USE PROPERTY VARIATION G(1)-G(4) OF: TOULOUKIAN ET AL.;  

47 C CHALCOTT ET AL., PROKOSHET AL., AND POSSLE. IF FALSE, USE
48 C THAT OF KARS & SMITH (1971). IF NOTE(30) FALSE
49 C NOTE(24) WRITE ABS(F(I,I)) = VALUE AND POSITION OF BEST SOLUTION
50 C NOTE(25) INDICATE USE OF STOCHASTIC FINITE ELEMENTS IN SOLUTION
51 C NOTE(27) INCLUDE THERMAL FLUCTUATIONS IN SOLUTION (ASSUMING
52 C NOTE(30)=TRUE). IF FALSE, NO TEMP FLUC ARE ASSUMED.
53 C

```



```

54 C NOTE(29) PRINT ANGLE BETWEEN SOLN VECTORS ON FIRST ITERATION
55 C NOTE(30) USE LOVELL'S EQUATIONS. IF FALSE, USE EQUATIONS OF WAZZAN,
56 C OKAMURA, AND SMITH.
57      M = 6
58      N = 3
59      KMAX = 701
60      READ (5,201) TWALL,TINF,BETA,EPISLN,H
61 201 FORMAT (SF10.2,L16.2,D10.2)
62 C KMAX = MAX NO. OF STEPS ALLOWED
63 C H > CR = ETABEL/(KMAX-1) OR DIMENSION STMTS MUST BE CHANGED FOR KMAX
64      TALL = TWALL + 459.69
65      TINF = TINF + 459.69
66      ALPHA = (BETA + 1.0)/2.0
67      R = TINF/491.69
68      S = (TWALL-TINF)/491.69
69      C2 = (TALL-TINF)*5./9.
70      CALL TEFVAR(0,0,0)
71      IF (NOTE(9)) WRITE (6,109) H,BETA,TWALL+459.69,TINF+459.69,PRINF,
72 11,-EPISLN
73 109 FORMAT (' STEP SIZE =',D16.8/' FALKNER-SKAN PARAMETER =',F10.4/
74     1' WALL TEMPERATURE =',F10.4/' FREE STREAM TEMPERATURE =',F10.4/
75     2' FREE STREAM PRANDTL NO. =',F10.6/' BOUNDARY LAYER EDGE DETERMINE
76     3D BY U =',F11.7)
77      IF (NOTE(11)) .AND. (.NOT. NOTE(1)) GO TO 1
78      6 CALL BFECH(H,EPISLN,TWALL,TINF,ETABEL)
79      ETABEL = BLPAR(1,KTOT)
80      IF (NOTE(5)) WRITE (6,101) (K,(BLPAR(I,K),I=1,7),K=1,KTOT)
81 101 FORMAT (/5X,' ',15X,' ',37X,' ',16X,' ',17X,' ',K,' ',12X,' ',ETA,' ',16X,
82     1' ',17X,' ',15X,' ',17X,' ',THETA,' ',12X,' ',THETA,' ',12X,' ',THETA,' /
83     2'(5.7E13,5))
84      IF (NOTE(6)) WRITE (6,102) KTOT,ETABEL
85 102 FORMAT (/', KTOT =',I4/, ETABEL =',E13.8/)
86      IF (NOTE(7)) WRITE (6,103) ETABLS
87 103 FORMAT (/', ETA SUBSCRIPT DELTA STAR =',E16.8/)
88      WRITE (6) PRINF,ETABEL,ETABEL,KTOT,NOTE(24),H,TWALL,TINF,BETA,
89      1E-51*((BLPAR(I,K),I=1,7),K=1,KTOT),((C(I,K),I=1,14),K=1,KTOT)
90      IF (NOTE(1)) STOP
91      GO TO 2
92      READ (5,104) PRINF,ETABLS,ETABEL,PT01,H20VAR,HA,TWALLA,TINFA,BET
93      1A,EPISLA,((BLPAR(I,K),I=1,7),K=1,KTOT),((C(I,K),I=1,14),K=1,KTOT)
94      IF (NOTE(2)) .AND. (H20VAR) GO TO 10
95      IF (NOTE(2)) .OR. (H20VAR) GO TO 11
96 10  IF (JUL((H-A-H))<.006) .NEQ. 0 .AND. INT(((TWALLA-TWALL)+(TINFA-
97     TINF)+(BLPAR(BETA)+(EPISLN-EPISLN))),1.E6) .EQ. 0) GO TO 9
98 11  WRITE (6,117)
99 117 FORMAT (/1E-65(*1)/5A,' THE REQUIRED INFORMATION IS NOT THE SAME
100    1A2 THAT STORED IN UNIT 5.',/1X,8d(1.1)/)
101      STOP
102 9  IF (NOTE(5)) WRITE (6,101) (K,(BLPAR(I,K),I=1,7),K=1,KTOT)
103 10  IF (NOTE(6)) WRITE (6,102) KTOT,ETABEL
104 11  IF (NOTE(7)) WRITE (6,103) ETABLS
105 12  READ (5,104) PRINF,ETABEL,EPISLN,BCV
106 104 FORMAT (10.10,4L11.1,I10)
107 107 IF (NOTE(8)) WRITE (6,103) (K,(C(I,K),I=1,14),K=1,KTOT,5)

```



```

108 103 FORMAT ((I4,14E9.3))
109     IF (.NOTE(30)) WRITE (6,107)
110     IF (.NOT. .NOTE(30)) WRITE(6,108)
111     IF (.NOT. .NOTE(28)) WRITE(6,110)
112 107 FORMAT (/'* *** RESULTS FOR EQUATIONS OF LONELL ***/)
113 108 FORMAT (/'* *** RESULTS FOR EQUATIONS OF MAZZAN, OKAMURA, AND SMITH
114     1 ***')
115 110 FORMAT (* *** WITHOUT TEMPERATURE FLUCTUATIONS ***)/
116     IF (.NOTE(6)) WRITE (6,104) ANGLE,ITRMAX,EPSLN
117 114 FORMAT (* MIN ANGLE ALLOWED BETWEEN SOLN VECTORS =*:F10.4/
118     1! MAX NO. ITERATIONS PERMITTED =*,I3/
119     2! CONVERGENCE CRITERION FOR EIGENVALUES =*,E10.4)
120     HSTEP = -2.0**I
121     KMAX2 = (KMAX/2)+1
122 C ESTIMATE RE,OMEGA, AND ALFA TO USE IN E.V. CALCULATION
123     READ (5,203) MM,(REDLS(I),ARMLS(I),AIDLs(I),FREQ(I),I=1,MM)
124 203 FORMAT (I4/(4E16.0))
125     DO 3 I=1,MM
126     NOTE(21) = .TRUE.
127     RE = REDLS(I)/ETADLS
128     ALFAI = AIDLs(I)/ETADLS
129     OMEGA = FREQ(I)*RE
130     ALFAR = ARMLS(I)/ETADLS
131     IF (NEV .EQ. 1) EV(1) = CMPLX(ALFAR,OMEGA)
132     IF (NEV .EQ. 2) EV(1) = CMPLX(ALFAR,ALFAI)
133     IF (NEV .EQ. 3) EV(1) = CMPLX(ALFAR,RE)
134     IF (NEV .EQ. 4) EV(1) = CMPLX(OMEGA,RE)
135     IF (NEV .EQ. 5) EV(1) = CMPLX(OMEGA,ALFAI)
136     IF (NEV .EQ. 6) EV(1) = CMPLX(RE,ALFAI)
137     EV(2) = (1.01,0.0)*EV(1)
138     EV(3) = CMPLX(1.005*REAL(EV(1)),1.02*AI*IMAG(EV(1)))
139     CALL D1STEG(EV,ITRMAX,HSTEP,ANGLE,Y,EPSLN,PRINF,NEV,$3,P,ZDIST)
140     FREQ(I) = OMEGA/RE
141     ARMLS(I) = ALFAR+ETADLS
142     REDLS(I) = RE*ETADLS
143     AIDLs(I) = ALFAI+ETADLS
144     CR = OMEGA*ALFAR/(ALFAR**2+ALFAI**2)
145     CJ = -OMEGA*ALFAI/(ALFAR**2+ALFAI**2)
146     IF (.NOTE(6)) WRITE (6,105) ARMLS(I),AIDLs(I),REDLS(I),FREQ(I)
147     1,CR,CJ
148 105 FORMAT (* ALFAR =*,F16.8/* ALFAI =*,F16.8/* RE =*,E19.8/* FREQ =
149     1*,E16.8/* CR =*,E19.8/* CJ =*,E19.8)
150     IF (.NOTE(2) .OR. .NOT. .NOTE(21)) GO TO 3
151     KPTOT = KTOT/2+1
152     IF (.NOT. .NOTE(15) .OR. .NOT. .NOTE(30)) GO TO 5
153     WRITE(6,112)
154 112 FORMAT (*/* KPTOT,DENSITY FLUCTUATION/*/*VISCOSEITY FLUCTUATION
155     1/* THERMAL CONDUCTIVITY FLUCTUATION ABS(DENFLU) ABS(VISFLU) A
156     2BS(TCFLU)/*)
157     DO 4 K=1,KPTOT
158     TEMP = BLTMR(5,2**K-1)
159     CALL TEFAR(TEMP+1)
160     IF (.NOT. .NOTE(26)) FLUCTD(2,K) = G(2)*GP(2)*Y(3,K)
161     IF (.NOT. .NOTE(26)) FLUCTG(2,K) = (0.0+0.0)

```



```

162   FLUCTG(3,K) = G(3)*GP(3)*Y(3,K)/G(2)
163   FLUCTG(4,K) = G(4)*GP(4)*Y(3,K)/G(2)
164   IF (INT(T+ALL-TINK) .NE. 0) WRITE (6,111) K,(FLUCTG(J,K),J=2,4),
165   1(CABS(FLUCTG(J,K)),J=2,4)
166   111 FORMAT (14.6E14.8,2X,3E14.8)
167   4 CONTINUE
168   5 IF (.NOT. NOTE(16)) GO TO 3
169 C COMPUTE TERMS OF ENERGY BALANCE EQUATION FOR NEUTRAL DISTURBANCES.
170 C FUNC(1,K) = REYNOLDS STRESS PRODUCTION
171 C FUNC(2,K) = PRODUCTION DUE TO VISCOSITY FLUCTUATIONS
172 C FUNC(3,K) = PRESSURE ENERGY PRODUCTION
173 C FUNC(4,K) = DISSIPATION
174 C FUNC(5,K) = DISSIPATION DUE TO NONCONSTANT MEAN AND FLUCTUATION DEN.
175 C FUNC(6,K) = PRODUCTION DUE TO MEAN VISCOSITY GRADIENT
176   WRITE (*,114)
177   114 FORMAT (/! ENERGY PRODUCTION AND DISSIPATION TERMS FOR NEUTRAL STA
178   1BILITY (ALFAI=0.0) !/ KP RE STRESS PROD VISC FLUCT PROD PRES
179   2S PROD'!,0X,DISSIPATION!,0X,DEN DISSIP VISC GRAD PROD'!)
180   DO 6 K=1,KPTOT
181   L = 2+K-1
182   FUNC(1,K) = -BLPAR(3,L)*ALFAR*RE*REAL(Y(2,K)*CONJG(Y(1,K)))/C(1,L)
183   IF (.NOT. NOTE(30)) FUNC(1,K) = FUNC(1,K)+C(1,L)
184   FUNC(2,K) = -BLPAR(3,L)*(REAL(FLUCTG(3,K)*CONJG(Y(5,K)))/C(1,L)*#2
185   +ALFAR*#2+AIMAG(CONJG(Y(1,K))*FLUCTG(3,K)))
186   IF (.NOT. NOTE(30)) FUNC(2,K) = 0.0
187   FUNC(3,K) = -ALFAR*RE*REAL(CONJG(Y(4,K))*(#0.,#1.)*FLUCTG(2,K)*
188   #BLPAR(2,L)-CR)*C(1,L)+C(14,L)/2.*Y(1,K))
189   IF (.NOT. NOTE(30)) FUNC(3,K) = 0.0
190   FUNC(4,K) = -C(2,L)*(ALFAR*#0.*Y(1,K)*CONJG(Y(1,K))*C(1,L)*#2+
191   #CONJG(Y(5,K))*Y(5,K)/C(1,L)*#2+2.*ALFAR*#2*AIMAG(CONJG(Y(5,K))*#
192   2Y(1,K)))
193   FUNC(5,K) = #. #C(2,L)*C(7,L)*BLPAR(6,L)/C(14,L)*ALFAR*#2+(((
194   #BLPAR(2,L)-CR)*C(1,L)*#2*FLUCTG(2,K)*CONJG(FLUCTG(2,K))+C(14,L)/
195   22.)+(#2Y(1,K)*CONJG(Y(1,K))+#BLPAR(2,L)-CR)*C(14,L)*C(1,L)*#
196   3AIMAG(CONJG(FLUCTG(2,K))*Y(1,K)))
197   IF (.NOT. NOTE(30)) FUNC(5,K) = 0.0
198   FUNC(6,K) = #. #ALFAR*#2*C(2,L)/C(1,L)*(C(8,L)+C(14,L)/2.)*AIMAG(
199   #CONJG(Y(1,K))*Y(2,K))
200   IF (CR .GT. BLPAR(2,L)) GO TO 7
201   IF (CR .GT. BLPAR(2,L-2)) WRITE(6,115) K-1,K,BLPAR(1,L-2),BLPAR(1,L)
202   115 FORMAT (! THE CRITICAL POINT IS HERE WHERE I4,I5,K<#13# OR !
203   I4,I5,<#ETAB<#P4,2)
204   7 WRITE (6,116) K,(FUNC(J,K),J=1,6)
205   116 FORMAT (14.6E16.8)
206   6 CONTINUE
207   3 CONTINUE
208   END

```


MFEQN

```

1      SUBROUTINE MFEQN(H,EPISLN,TWALL,TINF,ETADLS)
2      DIMENSION Y(15),DY(15),ETAEND(4),TEST(4),B(7,701),C(14,701)
3      GN(4),GNN(4)
4      DOUBLE PRECISION Y,DY,H,ETA,X,Z,DELX,DELZ,SUMODD,SUMEVN
5      LOGICAL NOTE
6      COMMON /BLK1/ALPHA,BETA,PRINF/BLK3/G(4),GP(4),GPP(4)/BLK4/B,C/
7      BLK5/N,M,KTOT,KMAX,KMAX2/BLK8/NOTE(30)
8      EXTERNAL DIFF
9      DATA ND/2/, (ETAEND(I),I=1,2)/2.,10./, (TEST(I),I=1,2)/1.,1.E-8/
10     ,ETEST/1.0E-12/
11     X = 1.000
12     Z = -1.000
13     I = 1
14     MARK = 1
15     K = 1
16     3 ETA = 0.000
17     Y(1) = 0.000
18     Y(2) = 0.000
19     Y(3) = X
20     Y(4) = 1.000
21     Y(5) = Z
22     Y(6) = 0.000
23     Y(7) = 0.000
24     Y(8) = 1.000
25     Y(9) = 0.000
26     Y(10) = 0.000
27     Y(11) = 0.000
28     Y(12)= 0.000
29     Y(13) = 0.000
30     Y(14) = 0.000
31     Y(15) = 1.000
32     CALL AUAMS(15,H,ETA,0,Y,DY,1,DIFF)
33     GO TO (4,30), MARK
34     30 B(1,K) = ETA
35     B(2,K) = Y(2)
36     B(3,K) = Y(3)
37     B(4,K) = DY(3)
38     B(5,K) = Y(4)
39     B(6,K) = Y(5)
40     B(7,K) = DY(5)
41     C COMPUTE MEAN PROPERTY VARIATION THROUGH THE BOUNDARY LAYER
42     DO 1 I=2,4
43     GJ(I) = GP(I)*B(5,K)
44     1 GJJ(I) = GPP(I)*(B(6,K)**2) + GP(I)*B(7,K)
45     IF (NOTE(13)) WRITE (6,101) K,G(1),(G(I),GN(I)*G(I),GNN(I)*G(I),I=
46     12,4)
47     101 FORMAT (I4,10E12.7)
48     C COMPUTE MEAN FLOW COEFFICIENTS FOR DISTURBANCE EQUATIONS
49     C FOR MECH PRESSURE, SET VIS2=-2/3. FOR THERMO PRESSURE, SET VIS2 = 2.1
50     VIS2 = -2./3.
51     DVIS2 = 0.0
52     C(1,K) = 1.0/G(2)
53     C(2,K) = G(3)/G(2)

```



```

54 C(3,K) = (2.+VIS2)*(2.*GN(2)**2-GNN(2)-GN(2)*GN(3))-GN(2)*DVIS2
55 C(4,K) = GN(2)*(2.+VIS2)-GN(3)
56 C(5,K) = -GP(3)
57 C(6,K) = (2.+VIS2)*(GP(2)*(3.*GN(2)-GN(3))-GPP(2)*B(6,K))-GP(2)*
58 DVIS2
59 C(7,K) = -(2.+VIS2)*GP(2)
60 C(8,K) = -GN(3)
61 C(9,K) = -GPP(3)*B(6,K)*B(3,K)-GP(3)*B(4,K)
62 C(10,K) = -GP(2)*(1.+VIS2)
63 C(11,K) = PRINF*G(1)/G(4)
64 C(12,K) = -GNN(4)
65 C(13,K) = -2.0*GN(4)
66 C(14,K) = 2.*GN(2)
67 IF ((1.-Y(2)).LE.EPSILN .AND. Y(4).LE.EPSILN) GO TO 13
68 K = K+1
69 4 CALL ADAMS(15,H,ETA,1,Y,DY,1,DIFF)
70 GO TO (6,30), MARK
71 IF(ETA.LT.ETAEND(I)) GO TO 4
72 B11 = Y(7)**2 + Y(9)**2 + Y(8)**2 + Y(10)**2
73 B12 = Y(7)*Y(12) + Y(9)*Y(14) + Y(8)*Y(13) + Y(10)*Y(15)
74 B21 = B12
75 B22 = Y(12)**2 + Y(14)**2 + Y(13)**2 + Y(15)**2
76 C1 = -((Y(2)-1.0D0)*Y(7) + Y(4)*Y(9) + Y(3)*Y(8) + Y(5)*Y(10))
77 C2 = -((Y(2)-1.0D0)*Y(12) + Y(4)*Y(14) + Y(3)*Y(13) + Y(5)*Y(15))
78 DEM = B11*B22 - B21*B12
79 DELX = (C1*B22 - C2*B12)/DEM
80 DELZ = (C2*B11 - C1*B21)/DEM
81 IF (NOTE(10)) WRITE(6,104) ETAEND(I),X,DELX,Z,DELZ
82 104 FORMAT (F10.6,4D20.8)
83 E = (Y(2)-1.0D0)**2 + Y(4)**2 + Y(3)**2 + Y(5)**2
84 X = X + DELX
85 Z = Z + DELZ
86 9 IF(ABS(DELX/X).GT.TEST(I).OR.ABS(DELZ/Z).GT.TEST(I)) GO TO 3
87 10 IF(E.LT.ETEST) GO TO 12
88 11 IF (I .EQ. ND) STOP
89 I = I + 1
90 GO TO 3
91 12 MARK = MARK + 1
92 YEND = Y(1)
93 ETASTP = ETA
94 IF (NOTE(10)) WRITE (6,106) ETEST,E,X,Z
95 106 FORMAT ('/ MAXIMUM ALLOWABLE ERROR IN ASYMPTOTIC SOLUTION =',E13.8
96 1/' ERROR IN FINAL ASYMPTOTIC SOLUTION =',E13.8/' FINAL ESTIMATE OF
97 2:/ WALL VELOCITY GRADIENT =',D16.8/22X,'WALL TEMPERATURE GRADIENT
98 3 =',D16.8/)
99 IF (NOTE(13)) WRITE (6,107)
100 107 FORMAT (/37X,'',11X,'',23X,'',11X,'',22X,'',10X,'',/2X,'K',
101 13X,'SPEC.HT.',5X,'DENSITY',4X,'DENSITY',5X,'DENSITY',5X,'(DEN*VIS)
102 2',2X,'(DEN*VIS)',3X,'(DEN*VIS)',5X,'(DEN*TC)',3X,'(DEN*TC)',3X,
103 3'(DEN*TC)')
104 GO TO 3
105 C ENSURE KT01 IS ODD FOR STABILITY EON INTEGRATION AND ETADLS SOLUTION
106 13 IF (K/2**2 .EQ. K) GO TO 8
107 KT01 = K

```



```

108 C CALCULATE ETA SUBSCRIPT DELTA STAR = ETADLS USING COMPOSITE SIMPSONS
109 C RULE FORMULA
110   IF (1.0(TWALL-TINF) .ME. 0) GO TO 14
111   DENT11 = ETA
112   ETADLS = ETASTP + YEND
113   GO TO 17
114 14 SUMODD = 0.0
115  SUMEVN = 0.0
116  I_M2 = KTOT-2
117  I_M1 = KTOT-1
118  DO 15 K=3,IM2,2
119 15 SUMODD = SUMODD + C(1,K)
120  DO 16 K=2,IM1,2
121 16 SUMEVN = SUMEVN + C(1,K)
122  DENTINT = (C(1,1)+C(1,KTOT)+2.*SUMODD+4.*SUMEVN)*ETA/3./IM1
123  ETADLS = DENTINT-YEND+ETASTP-ETA
124 17 IF (NOTE(7)) WRITE (6,102) 1.-EPSILM,DENTINT/ETADLS
125 102 FORMAT (/1 (BOUNDARY LAYER THICKNESS (U=1,F8.7,1)/DISPLACEMENT TH
11CKNESS) =1,F12.8)
126  IF (.NOT. NOTE(12)) RETURN
127  KTOTM2 = KTOT - 2
128  YHONDM = 0.0
129  WRITE (6,103) YHONDM,B(1,1)
130 103 FORMAT (' Y/(DISPLACEMENT THICKNESS)',6X,'ETA'/2E20.8)
131  DO 18 K=1,KTOTM2,2
132 18 YHONDM = YHONDM+(B(1,K+2)-B(1,K))*(C(1,K)+4.*C(1,K+1)+C(1,K+2))/6,
133 1/ETADLS
134 18 WRITE (6,105) YHONDM,B(1,K+2)
135 105 FORMAT (2E20.8)
136  RETURN
137
138 END

```


DIFF

```

1 C      SUBROUTINE TO CALCULATE THE DIFFERENTIAL EQUATIONS
2      SUBROUTINE DIFF(ETA,Y,DY)
3      DOUBLE PRECISION ETA,Y,DY
4      DIMENSION Y(15),DY(15),GX(4),GZ(4),GN(2),GNX(2),GNZ(2)
5      COMMON /BLK1/ALPHA,BETA,PRINF/BLK3/G(4),GP(4),GPP(4)
6      TEMP = Y(+)
7      CALL TENVAR(TEMP,1)
8      DO 1 I=1,4
9      Gx(I) = GP(I)*Y(9)
10     1 Gz(I) = GP(I)*Y(14)
11     DO 2 I=3,4
12     Gx(I) = GP(I)*Y(5)
13     Gx(I) = CPP(I)*Y(5)*Y(9)+GP(I)*Y(10)
14     2 Gz(I) = GPP(I)*Y(5)*Y(14)+GP(I)*Y(15)
15     Dy(1) = Y(2)
16     Dy(2) = Y(3)
17     Dy(3) = -Gx(3)*Y(3)-(BETA*(1.0/G(2)-Y(2)**2)+ALPHA*Y(1)*Y(3))/G(3)
18     Dy(4) = Y(5)
19     Dy(5) = -Gx(4)*Y(5)-PRINF*G(1)*ALPHA*Y(1)*Y(5)/G(4)
20     Dy(6) = Y(7)
21     Dy(7) = Y(8)
22     Dy(8) = -GX(3)*DY(3)-GNx(3)*Y(3)-GN(3)*Y(8)+(BETA*(GX(2)/G(2)
23     +2.0*Y(2)*Y(7))-ALPHA*(Y(6)*Y(3)+Y(1)*Y(8)))/G(3)
24     Dy(9) = Y(10)
25     Dy(10) = -GX(4)*DY(5)-GNx(4)*Y(5)-GN(4)*Y(10)-PRINF*ALPHA*G(1)*
26     1(Gx(1)*Y(1)*Y(5)+Y(6)*Y(5)+Y(1)*Y(10))/G(4)
27     Dy(11) = Y(12)
28     Dy(12) = Y(13)
29     Dy(13) = -GZ(3)*DY(3)-GNZ(3)*Y(3)-GN(3)*Y(13)+(BETA*(GZ(2)/G(2)
30     +2.0*Y(2)*Y(12))-ALPHA*(Y(11)*Y(3)+Y(1)*Y(13)))/G(3)
31     Dy(14) = Y(15)
32     Dy(15) = -GZ(4)*DY(5)-GNZ(4)*Y(5)-GN(4)*Y(15)-PRINF*ALPHA*G(1)*
33     1(GZ(1)*Y(1)*Y(5)+Y(11)*Y(5)+Y(1)*Y(15))/G(4)
34     RETURN
35     END

```


TEMVAR

```

1 SUBROUTINE TEMVAR(TTEMP, INDEX)
2 LOGICAL L0TE
3 COMMON /BLK2/R,S,GINF(4),C2/BLK3/G(4),GP(4),GPP(4)/BLK8/NOTE(30)
4 1/BLK1/ALPHA,BETA,PRINF
5 DIMENSION A(21),B(19)
6 DATA (A(L),L=1,21)/1.4833689,0.8072501,0.3289602,0.803928,0.461590
7 11.0,2.609774,0.02361689,45.2396949,137.1963063,142.7970742,59.819762
8 23.9,28.0,31.34,2.5820196,6.7056261,3.7344471,0.5163417,73.376906,208,
9 37.74530,197.7604576,0.05,0.6261686,7.4779458/
10 DATA (L(L),L=1,19)/1.12574,-9.69137E-3,2.68530E-5,-2.42139E-8,
11 13.9663,200.9414,5.36329,2.03.12963,0.011445,374.3,1.002,1.37023,
12 28.36,-4.109,1.43429448,-9.90169,1.601932,-1.873892E-4,1.03957E-7/
13 C IF INDEX = 0 COMPUTES FREE STREAM VALUES, GINF (KAUSS & SMITH FORM
14 C COMPUTES GINF/GREF WITH REF QUANTITIES EVALUATED AT T = 32 F)
15 C IF INDEX > 0 COMPUTE PROPERTY VARIATION, G(I), AT SPECIFIED TEMP
16 C G(1) = SPECIFIC HEAT AT CONSTANT PRESSURE
17 C G(2) = DENSITY
18 C G(3) = DENSITY*VISCOSITY
19 C G(4) = DENSITY*(THERMAL CONDUCTIVITY)
20 C ALL THESE QUANTITIES ARE NONDIM. W.R.T. REFERENCE VALUES AT TINF
21 T = S*TEMP4R
22 TC = (T-1)*273.16111
23 TK = TC + 273.16
24 IF (TC .LT. 1.0) TEXP = 0.0
25 IF (TC .GE. 1.0) TEXP = EXP(-B(10)/TC)/TC**4
26 IF (.NOT. NOTE(24)) GO TO 1
27 G(1) = B(1)+B(2)*TK+B(3)*TK**2+B(4)*TK**3
28 G(2) = 1.0-(TC-B(5))*2*(TC+B(6))/B(7)/(TC+B(8))+B(9)*TEXP+TC**4
29 G(3) = B(2)*B(11)/10.0*((B(12)*(TC-20.0)+B(13)*(TC-20.0)**2)/(TC+
30 1B(14)))
31 G(4) = G(2)*(B(16)+B(17)*TK+B(18)*TK**2+B(19)*TK**3)
32 Go To 3
33 1 G(1) = A(1)-A(2)*T+A(3)*T**2
34 G(2) = A(4)+A(5)*T-A(6)*T**2+A(7)*T**3
35 G(3) = 1.0/(A(8)-A(9)*T+A(10)*T**2-A(11)*T**3+A(12)*T**4)
36 G(4) = -A(13)+A(14)*T-A(15)*T**2+A(16)*T**3
37 3 IF (INDEX .GT. 0) GO TO 4
38 DO 2 IF=1,4
39 2 GINF(I) = G(I)
40 IF (NOTE(.GT.1)) PRINF = 41.84*G(1)*G(3)/G(4)
41 IF (.NOT. NOTE(24)) PRIF = 13.66/(A(17)-A(18)*T+A(19)*T**2-
42 1A(20)*T**3+B(21)*T**4)
43 RETURN
44 C COMPUTE (D6(I)/DH)/G(I) AND (D2G(I)/DH)/G(I) WHERE H = (T-TINF)/
45 C (FINAL-TINF)
46 4 IF (.NOT. NOTE(24)) GO TO 5
47 GP(1) = (B(2)+B(3)*B(4)*B(5)*B(6)*B(7)*B(8)*B(9)*B(10)*B(11)*B(12)*B(13)*B(14))
48 GP(2) = (-B(10)-B(5))/B(3)*B(4)*B(5)*B(6)*B(7)*B(8)*B(9)*B(10)*B(11)*B(12)*B(13)*B(14)
49 110*B(14)/(TC-24.0*(10.0+11.0+12.0+13.0+14.0))
50 GP(3) = ((-B(2)*B(3)*B(4)*B(5)*B(6)*B(7)*B(8)*B(9)*B(10)*B(11)*B(12)*B(13)*B(14))
51 16.0)*(TC-1.0)+(-3.0)*12.0/3.0*(2.0+C2**2*B(2)*B(3)/(TC+B(6)))
52 GP(3) = GP(3)-(C2*(1.0+B(15)*(TC-20.0)-1.0010*(B(11)*G(2)/G(3)))*
53 10.0/(B(15)+B(14)+B(16)))

```



```

54 GPP(3) = GPP(2)+GP(3)*2-GP(2)**2-2,*B(13)*C2**2/B(15)+(GP(3)-
55 1GP(2))*C2)/(B(14)+TC)
56 GP(4) = GP(2)+(A(17)+2,*B(13)*TK+3,*B(19)*TK**2)*C2*G(2)/G(4)
57 GP(4) = GPP(2)+2,*GP(2)+(GP(4)-GP(2))+(2,+B(18)+6,*B(19)+TK)*C2
58 1*Z*G(2)/G(4)
59 GO TO 6
60 G(1) = (-A(2)+A(3)*2,*T)*S/G(1)
61 GP(2) = (A(5)-2,*A(6)+1+3,*A(7)*T**2)*S/G(2)
62 GPP(2) = (-2,*A(6)+5,*A(7)*T)*S**2/G(2)
63 GP(3) = -G(3)*(-A(9)+2,*A(10)*T-3,*A(11)*T**2+4,*A(12)*T**3)*S
64 GP(3)= 2,*GP(5)*Z*G(3)*(2,*A(10)-6,*A(11)*T+12,*A(12)*T**2)*S**2
65 GP(4) = (A(14)-2,*A(15)*T+3,*A(16)*T**2)*S/G(4)
66 GPP(4) = (-2,*A(15)+6,*A(16)*T)*S**2/G(4)
67 DO 7 I=1,4
68 7 G(I) = G(I)/GINF(I)
69 RETURN
70 END

```


ADAMS

```

1      SUBROUTINE ADAMS(H,X,ISET,Y,DY,INDEX,F)
2      DOUBLE PRECISION P,Y,YR,DYLL,DYL,DYR,C2,C3,C4,X,H
3      DIMENSION Y(15),DY(15),P(15),YR(15),DYLL(15),DYL(15),DYR
4      1(I5),C2(15),C3(15),C4(15)
5      1 IF(ISET.GT.0) GO TO 6
6      2 IF(INDEX.LE.0) GO TO 4
7      3 K = 2
8      GO TO 5
9      4 K = 1
10     5 CALL F(X,Y,DY)
11     K=1,N
12     6 GO TO (10,7,8,9,11),K
13     7 K = 3
14     GO TO 10
15     8 K = 4
16     GO TO 10
17     9 K = 5
18     10 DO 1001 I=1,N
19     1001 P(I) = Y(I) + (H/2.000)*DY(I)
20     CALL F(X+H/2.000,P,C2)
21     1002 I=1,N
22     1002 P(I) = Y(I) + (H/2.000)*C2(I)
23     CALL F(X+H/2.000,P,C3)
24     1003 I=1,N
25     1003 P(I) = Y(I) + H+C3(I)
26     CALL F(X+H,P,C4)
27     1004 I=1,N
28     1004 Y_(I) = Y(I) + (H/6.000)*(DY(I)+2.000*C2(I)+2.000*C3(I)+C4(I))
29     CALL F(X+H,YR,DYR)
30     GO TO 12
31     11 DO 1101 I=1,N
32     1101 P(I) = Y(I) + (H/24.000)*(55.000*DY(I)-59.000*DYL(I)+37.000*DYLL(I)
33     1)-9.000*DYLLL(I)
34     CALL F(X+H,P,CYR)
35     1102 I=1,N
36     1102 Y_(I) = Y(I) + (H/24.000)*(9.000*DYR(I)+19.000*DY(I)-5.000*DYL(I)
37     1+LYLL(I))
38     CALL F(X+H,YR,DYR)
39     12 X = X+H
40     DO 1201 I=1,N
41     Y(I) = YR(I)
42     DYLL(I) = DYLL(I)
43     DYL(I) = DYL(I)
44     DY(I) = DY(I)
45     1201 DY_(I) = DYR(I)
46     RETURN
47     END

```


DISTEQ

```

1      SUBROUTINE DISTEQ(EV,ITRMAX,H,ANGLE,Y,EPSLN,PRTF,NEV,$,P,Z)
2      COMPLEX Z(ALFA),PY(X),GAMMA,SIGMA,YINT,DYINT,EV,F
3      I=1000,J=1000,K=1000,L=1000,M=1000,N=1000,O=1000,P=1000,Q=1000,R=1000,S=1000,T=1000,U=1000,V=1000,W=1000,X=1000,Y=1000,Z=1000
4      LOGICAL NOTE,ADLER
5      COMMON /BLK4/BLPAR(1:C/BLK5/N:M:KTOT,KMAX,KMAX2/BLK7/ALFAR,ALFAI,
6      IR,I,OMEGA,I,LAG,I,OTE(30),
7      OI,I,S10,I,Z(3,6,351),EV(ITRMAX),P(3,3,351),KORTH(351),C(14,701),
8      IX(3),F(50),IM(KMAX2),BLPAR(7,701),YINT(6),DYINT(6)
9      EXTERNAL STAGEQ
10     KPTOT = (KTOT/2)+1
11     DJ = ITEM=1,ITRMAX
12     AGLMIN = 90.
13 C ESTABLISH INITIAL CONDITIONS AT BOUNDARY LAYER EDGE
14     IF (NOTE(14)) WRITE (6,130) ITER, EV(ITER)
15 130 FORMAT ('/ EV(1,12) = ',2E16.8)
16     DO 10 (21,22,23,24,25,26)=NEV
17     21 ALFAR = REAL(EV(ITER))
18     OMEGA = AIMAG(EV(ITER))
19     GO TO 1
20     22 ALFAR = REAL(EV(ITER))
21     ALFAI = AIMAG(EV(ITER))
22     GO TO 1
23     23 ALFAR = REAL(EV(ITER))
24     RE = AIMAG(EV(ITER))
25     GO TO 1
26     24 OMEGA = REAL(EV(ITER))
27     RE = AIMAG(EV(ITER))
28     GO TO 1
29     25 OMEGA = REAL(EV(ITER))
30     ALFAI = AIMAG(EV(ITER))
31     GO TO 1
32     26 RE = REAL(EV(ITER))
33     ALFAI = AIMAG(EV(ITER))
34     1 ALFA = COMPLX(ALFAR,ALFAI)
35     IF (ALFAR .LT. 0.0 .OR. OMEGA .LT. 0.0 .OR. RE .LT. 0.0) RETURN 9
36     2 GAMMA = CSQRT(ALFA**2+(0,1.0)*RE+(ALFA*BLPAR(2,KTOT)-OMEGA))
37     SIGMA = CSQRT(ALFA**2+(0,1.0)*RE+PRIME*(ALFA*BLPAR(2,KTOT)-OMEGA))
38     IF (NOTE(14)) WRITE (6,104) GAMMA/SIGMA
39 104 FORMAT ('/ GAMMA = ',2E16.8/10X,'SIGMA = ',2E16.8/)
40     IF (REAL(GAMMA) .LT. 0.0) GAMMA = -GAMMA
41     IF (REAL(SIGMA) .LT. 0.0) SIGMA = -SIGMA
42     IF (NOTE(26) .AND. NOTE(36)) DB = (C(10,KTOT)-C(7,KTOT))+(
43     BLPAR(4,KTOT)-CHESALFA)/C(1,KTOT)
44     IF (NOTE(26) .OR. .NOT. NOTE(36)) DB = (0,0,0,0)
45     Z(1,1,KTOT) = (1.0,0,0)
46     Z(1,1,KPTOT) = (1.0,0,0)
47     Z(3,1,KPTOT) = (0.0,1,0)+SIGMA*DL/(SIGMA**2+ALFA**2)
48     Z(1,2,KPTOT) = -(0.0,1,0)+ALFA
49     Z(2,2,KPTOT) = -(0,0,1,0)+SIGMA
50     Z(3,2,KPTOT) = ALFA**2+DB/(SIGMA**2+ALFA**2)
51     Z(1,3,KPTOT) = (0,0,0,0)
52     Z(2,3,KPTOT) = (0,0,0,0)
53     Z(3,3,KPTOT) = (1,0,0,0)

```



```

54      DO 3 J=1,N
55      Z(J,4,KPTOT) = (GAMMA*Z(J,1,KPTOT)+(0.,1.)*Z(J,2,KPTOT))+(ALFA+
56      16ALFA*1)/RE-(0.,1.)*DI/(4.*ALFA/3.+GAMMA*(ALFA+GAMMA)/(ALFA+SIGMA))*_
57      2Z(J,3,KPTOT)/RE
58      Z(J,5,KPTOT) = -((0.,1.)*ALFA*GAMMA*Z(J,1,KPTOT)+(ALFA+GAMMA)*_
59      1Z(J,2,KPTOT))+ALFA*(ALFA*GAMMA)*DI*Z(J,3,KPTOT)/(ALFA+SIGMA)
60      3 Z(J,6,KPTOT) = -SIGMA*Z(J,3,KPTOT)
61      IF (NOTE(14)) WRITE (6,108) ((Z(J,I,KPTOT),I=1,M),J=1,N)
62 108 FORMAT (' INITIAL VALUES BEFORE B.C. INTEG/12E10.4')
63      I1 = 1
64 C INTEGRATE DISTURBANCE EQUATIONS FOR ASSUMED EIGENVALUE, ORTHONORMALIZING
65 C WHEN NECESSARY OR WHERE SPECIFIED
66      DO 4 KPP=1,KPTOT
67      KP = KPTOT+1-KPP
68      IF (KP .EQ. KPTOT) GO TO 15
69      DO 10 J=1,N
70      K = 2*KP+1
71      DO 9 I=1,M
72      9 YINT(I) = Z(J,I,KP+1)
73      CALL DIFFEQ(STABEQ,DYINT,YINT,H,K)
74      DO 10 I=1,M
75      10 Z(J,I,KP) = YINT(I)
76      15 CALL ORTHCR(Z,ITER,KP,ANGLE,II,P,KORTH,AGLMIN)
77      4 CONTINUE
78      IF (NOTE(17)) WRITE (6,117) AGLMIN
79 117 FORMAT (' MINIMUM ANGLE BETWEEN SOLN VECTORS ENCOUNTERED IN ORTH,
80 1PROCESS =1,F10.6)
81      IF (AGLMIN .LT. 1.0) RETURN 9
82      5 IIEND = II - 1
83      IF (NOTE(17)) WRITE (6,107) IIEND
84 107 FORMAT (' TOTAL NO OF ORTH RECD =1,I4)
85 C EVALUATE SATISFACTION OF B.C. AT THE WALL
86      B1 = HLPAR(4,1)
87      B2 = (0.0,0.0)
88      B3 = (1.0,0.0)
89      X(1) = (1.0,0.0)
90      DENOM = (B2*Z(3,6,1)+B3*Z(3,3,1))*(Z(2,2,1)+B1*Z(2,1,1))-_
91      1(B2*Z(2,6,1)+B3*Z(2,3,1))*(Z(3,2,1)+B1*Z(3,1,1))
92      X(2) = X(1)*((B2*Z(1,6,1)+B3*Z(1,3,1))*(Z(3,2,1)+B1*Z(3,1,1))-_
93      1(B2*Z(5,6,1)+B3*Z(5,3,1))*(Z(1,2,1)+B1*Z(1,1,1)))/DENOM
94      X(3) = X(1)*((B2*Z(2,6,1)+B3*Z(2,3,1))*(Z(1,2,1)+B1*Z(1,1,1))-_
95      1(B2*Z(1,6,1)+B3*Z(1,3,1))*(Z(2,2,1)+B1*Z(2,1,1)))/DENOM
96      DO 16 I=1,4
97      16 Y(I,1) = ((1)*Z(1,I,1)+Y(2)*Z(2,I,1)+X(3)*Z(3,I,1))
98      IF (NOTE(19)) WRITE (6,112) (Y(I,1),I=1,4)
99 112 FORMAT (' Y(I,1) =1.2E10,4)
100     IF (CABS(Y(1,1)) .LT. 1.0E-25) RETURN .
101     F(ITER) = 1.0/1/Y(1,1)
102     IF (CABS(F(ITER)) .LE. EPSIN .AND. ITER .GE. 1) GO TO 7
103     IF (CABS(F(ITER)) .LT. 1.0E-16) ITER=ITER+1,ITER,CABS(F(ITER))
104     1.6 FORMAT (' F(ITER) =1.2E10,BEST OF CABS(F(ITER)) =1.E16,8)
105 C USE THIS VALUE OF ASSUMED EIGENVALUE TO USE
106     17 (ITER)=0.0
107     8 CALL EVEST(F(ITER),EV,ITER,ITER,MMILLER)

```



```

108      IF (ABS(1.-REAL(EV(ITER))/REAL(EV(ITER+1))) .GT. EPSLN .OR.
109      )ABS(1.-AIAG(EV(ITER))/AIAG(EV(ITER+1))) .GT. EPSLN) GO TO 6
110      IF (CAbs(F(ITER)) .GT. EPSLN) GO TO 6
111      IF (NOTE(.2)) RETURN
112      DO 17 I=1,3
113      17 X(I) = X(I)/CAbs(Y(4,I))
114      GO TO 7
115      C CONTINUE
116      IF (NOTE(.21)) WRITE (6,101) EV(NITR),F(NITR)
117      NOTE(.21) = .FALSE.
118      101 FORMAT (/1X'MAXIMUM ALLOWABLE NO ITERATIONS FOR EIGENVALUE EXCEEDED
119      /1X' BEST ESTIMATE OF E.V. =',2E14.8,' ATTEMPTING TO SATISFY HQMO B
120      2.C. WITH ADMITTANCE OF',2E14.8)
121      IF (NOTE(.22)) WRITE (6,113) (EV(ITER),F(ITER),ITER=1,ITRMAX)
122      113 FORMAT (13X,'EV(ITER)',25X,'F(ITER)'/(4E16.8))
123      GO TO (31,32,33,34,35,36)/NEV
124      31 ALFAR = REAL(EV(NITR))
125      OMEGA = AIAG(EV(NITR))
126      RETURN
127      32 ALFAR = REAL(EV(NITR))
128      ALFAI = AIAG(EV(NITR))
129      RETURN
130      33 ALFAR = REAL(EV(NITR))
131      RE = AIAG(EV(NITR))
132      RETURN
133      34 OMEGA = REAL(EV(NITR))
134      RE = AIAG(EV(NITR))
135      RETURN
136      35 OMEGA = REAL(EV(NITR))
137      ALFAI = AIAG(EV(NITR))
138      RETURN
139      36 RE = REAL(EV(NITR))
140      ALFAI = AIAG(EV(NITR))
141      RETURN
C EVALUATE EIGENFUNCTIONS
142      7 IF (NOTE(18)) WRITE (6,103) (J,X(J),J=1,N)
143      103 FORMAT (' VALUES OF COMBINING COEFF AT WALL:   X(1,I1,1) =',2E15.8
144      1/(38X,'X(1,I1,1) =',2E15.8))
145      CALL EGIFC4(X,Y,Z,IEND,P,KORTH)
146      IF (NOTE(20)) WRITE (6,114) ((1,KORTH(II)),II=1,IEND)
147      114 FORMAT ((1,KORTH(1,13),1=1,14))
148      WRITE (6,102) (KP,BLPAR(1,2+KP-1),(Y(I,KP),I=1,N),KP=1,KPTOT)
149      102 FORMAT (/15X,',',15X,',',/2X,',',KP',',3X,',ETA',',6X,','(RHO*PHI)',',15X,',F',
150      115X,',TE, PERTATURE',,11X,',PRESSURE',,14X,',F',,15X,',TEMPERATURE')/(14
151      2F7.4,14E10.5))
152      WRITE(6,115) (KP,BLPAR(1,2+KP-1),(CAbs(Y(I,KP)),I=1,N),KP=1,KPTOT)
153      115 FORMAT (' , , AND THEIR CORRESPONDING AMPLITUDES')/(15,F7.4,6E20.8))
154      RETURN
155      END

```


STABEQ

```

1      SUBROUTINE STABEQ(Y,DY,K)
2      COMPLEX Y,DY,ALFA,WLESSC
3      LOGICAL NOTE
4      COMMON /BLK4/BLPAR,C/BLKS/N,M,KTOT,KMAX,KMAX2/BLK7/ALFAI,1
5      RE,OMEGA,Z,CLK8/L,OTE(30)
6      DIMENS10,Y(M),Y(M),BLPAR(7,701),C(14,701)
7      ALFA = C*PLX(ALFAI+ALFAI)
8      IF (.NOT. NOTE(26)) CON = 1.0
9      IF (.NOT. NOTE(28)) COI = 0.0
10     IF (.NOT. NOTE(26)) DEN = 1.0
11     IF (.NOT. NOTE(28)) DEN = 0.0
12     WLESSC = BLFAR(Z,K)-OMEGA/ALFA
13     IF (.NOTE(30)) DY(1)=-(0.,1.)*(Y(2)+(C(10,K)-C(7,K))/DEN)*WLESSC*Y(3)
14     1)
15     IF (.NOT. NOTE(30)) DY(1) = -(0.,1.)*Y(2)
16     DY(2) = Y(5)
17     IF (.NOTE(30)) DY(3) = Y(6)*CON
18     IF (.NOT. NOTE(30)) DY(3) = (0.,0.,0.)
19     IF (.NOTE(30)) DY(4) = (0.,1.)*(-ALFA**2*WLESSC*C(1,K)*Y(1)+(ALFA/R
20     1E)*C(2,K)+(-0.,1.)*(C(5,K)-(ALFA+C(1,K))*2)*Y(1)+(C(4,K)+C(8,K)
21     +C(14,K))*Y(2)-Y(5)+(.WLESSC/DEN*(C(6,K)*Y(3)+C(7,K)*Y(6))+C(7,K)
22     3*DEN-C(5,K))*BLPAR(3,K)+Y(3))*CON)
23     IF (.NOT. NOTE(30)) DY(4) = (0.,1.)*(-ALFA**2*WLESSC*C(1,K)*Y(1)+Y(1)*
24     1ALFA/RE*C(2,K)+((-Y(5)+Y(2)*(2.*C(3,K)+C(14,K)/2.))/C(1,K)+
25     2*(0.,1.)*ALFA**2*C(1,K)*Y(1)))
26     IF (.NOTE(30)) DY(5) = ALFA*RE*(BLPAR(3,K)*Y(1)+(0.,1.)*(Y(2)*
27     1WLESSC+C(1,K)*Y(4)))*C(1,K)/C(2,K)+(ALFA*C(1,K))*2*((0.,1.)*C(4*K
28     2)*Y(1)+Y(2)+C(10,K)*WLESSC*Y(3)+DEN*CON)+C(5,K)*Y(5)+(C(9,K)
29     3*(Y(3)+C(5,K)*Y(6)+BLPAR(3,K))*CON)
30     IF (.NOT. NOTE(30)) DY(5) = ALFA*RE*(Y(1)*BLPAR(3,K)+(0.,1.)*(
31     1Y(2)*WLESSC+C(1,K)*Y(4)))*C(1,K)+42/C(2,K)+ALFA**2*(C(1,K)**2*Y(2)
32     +2*(0.,1.)*Y(1)*(C(5,K)-C(14,K)/2.))+Y(5)*(C(8,K)-C(14,K))+Y(2)*
33     3*(C(3,K)/(C(4,K)-C(8,K))-C(14,K))/C(14,K)/2.
34     IF (.NOTE(30)) DY(6) = (ALFA*RE*(Y(1)*BLPAR(6,K)+(0.,1.)*WLESSC*Y(3
35     1))*C(11,K)+Y(3)*((ALFA*C(1,K))*2+C(12,K))+C(13,K)*Y(6))/COI
36     IF (.NOT. NOTE(30)) DY(6) = (0.0,0.0)
37     RETURN
38     END

```



```

EONFCN
1      SUBROUTINE EONFCN(X,Y,Z,I1END,P,KORTH)
2      IMPLICIT COMPLEX (P-Z)
3      COMMON /ZELKS/N,M,KTOT,KMAX,KMAX2
4      DIMENSION X(N),Y(N,KMAX2),Z(N,M,KMAX2),Q(3),KORTH(KMAX2),
5      P(M,N,KMAX2)
6      II = I1END
7      KPTOT = (KTOT/2)+1
8      DO 1 J=1,M
9      1 Q(J) = X(J)
10     DO 4 K=1,KPTOT
11     IF (II .LE. 0) GO TO 3
12     IF (K .LE. KORTH(II)) GO TO 3
13     KTEMP = KORTH(II)
14     DO 2 L=1,M
15     G(L) = (0.0,0.0)
16     DO 2 J=1,N
17     2 Q(L) = Q(L) + P(L,J,KTEMP)*X(J)
18     DO 5 L=1,M
19     X(L) = G(L)
20     I1 = II - 1
21     3 DO 4 I=1,M
22     Y(I,K) = (0.0,0.0)
23     DO 4 J=1,N
24     4 Y(I,K) = Y(I,K) + Z(J,I,K)+X(J)
25     RETURN
26     END

```


GSORTH

```

1      SUBROUTINE GSORTH(Z,P,K)
2      COMPLEX P,S,T,Z
3      LOGICAL NOTE
4      COMMON /BLK5/N,M,FTOT,KMAX,KMAX2/BLK8/NOTE(30)
5      DIMENSION S(3,3),W(3,3),T(3,3),Z(N,M,KMAX2),P(N,N,KMAX2)
6      DO 10 J=1,N
7      DO 2 I=1,M
8      2 T(J,I) = (0,0,0,0)
9      IF (J .EQ. 1) GO TO 6
10     JSTOP = J - 1
11     DO 5 L=1,JSTOP
12     S(J,L) = (0,0,0,0)
13     DO 4 I=1,M
14     4 S(J,L) = S(J,L) + CONJG(Z(L,I,K))*Z(J,I,K)
15     DO 5 I=1,M
16     5 T(J,I) = T(J,I) - S(J,L)*Z(L,I,K)
17     DO 7 I=1,M
18     7 T(J,I) = T(J,I) + Z(J,I,K)
19     W(J,J) = 0.0
20     DO 8 I=1,M
21     8 W(J,I) = W(J,I) + CONJG(T(J,I))*T(J,I)
22     W(J,J) = SORT(W(J,J))
23     IF (S(J,J) .LE. 1.0E-20) RETURN
24     DO 9 I=1,M
25     9 Z(J,I,K) = T(J,I)/W(J,J)
26     IF (NOTE(2)) GO TO 16
27     DO 15 L=1,N
28     10 IF (L .EQ. 11,13,14)
29     11 P(L,J,K) = (0,0,0,0)
30     DO 12 LI=L,JSTOP
31     12 P(L,J,K) = P(L,J,K)-S(J,LI)*P(L,LI,K)/W(J,J)
32     GO TO 15
33     13 P(L,J,K) = CMPLX(1.0/W(J,J),0,0)
34     GO TO 15
35     14 P(L,J,K) = (0,0,0,0)
36     15 CONTINUE
37     16 CONTINUE
38     RETURN
39     END

```


EVEST

```

1      SUBROUTINE EVEST(F,ITERMAX,EV,ITER,NITR,MULLER)
2      DIMENSION F(ITERMAX),EV(ITERMAX)
3      IMPLICIT COMPLEX (A-H,P)
4      LOGICAL MULLER,AVG
5      COMMON /BLK/NOTE(30)
6      11 IF (ITER .LT. 3) GO TO 6
7      AVG = .FALSE.
8      MULLER = .FALSE.
9      NITR = 1
10     DO 5 ITR=1,3
11     IF (CABS(F(ITR)) .LE. CABS(F(NITR))) NITR = ITR
12     5 CONTINUE
13     GO TO 7
14     6 IF (CABS(F(ITER)) .LE. CABS(F(NITR))) NITR = ITER
15     IF (CABS(F(ITER)) .LE. 5.0E-3) AVG = .FALSE.
16     IF (ITER .NE. NITR) AVG = .TRUE.
17     IF (NOTE(25)) WRITE(6,104) NITR,CABS(F(NITR))
18     104 FORMAT (' CABS(F(:,I2,:)) = ',E16.8)
19     7 Z1 = AIMAG(F(ITER-2)*CONJG(F(ITER-1)))
20     Z2 = AIMAG(F(ITER)*CONJG(F(ITER-2)))
21     Z3 = AIMAG(F(ITER-1)*CONJG(F(ITER)))
22     S = ABS(REAL(EV(ITER))/AI AG(EV(ITER)))
23     IF (S .GT. 1.0E3 .OR. S .LT. 1.0E-3) GO TO 9
24     IF ((Z1**2+Z2**2+Z3**2) .LE. 1.E-15 .AND. .NOT. MULLER) GO TO 8
25     9 EV(ITER+1) = (Z1*EV(ITER)+Z2*EV(ITER-1)+Z3*EV(ITER-2))/(Z1+Z2+Z3)
26     IF (AVG .OR. ITER.EQ.3) EV(ITER+1) = (EV(ITER+1)+EV(NITR))*(.5,.0)
27     MULLER = .FALSE.
28     RETURN
29     8 IF (ITER .EQ. 3) GO TO 2
30     1 IF (CABS(F(ITER)/F(ITER-1)) .LE. 10.0) GO TO 2
31     EV(ITER+1) = EV(ITER) + (EV(ITER)-EV(ITER-1))/2.0
32     IF (NOTE(27)) WRITE (6,103)
33     103 FORMAT (' DIFFERENCE BETWEEN F(ITER)'S TOO LARGE TO USE MULLER.')
34     RETURN
35     2 H1 = EV(ITER) - EV(ITER-1)
36     H1M1 = EV(ITER-1) - EV(ITER-2)
37     EI = H1/H1M1
38     OI = 1.0 + EI
39     G1 = F(ITER-2)*EI**2 + F(ITER-1)*DI**2 + F(ITER)*(EI+DI)
40     RAD = CSQRT(G1+12*4.*F(ITER)*DI*EI*(F(ITER-2)*EI+F(ITER-1)*DI+F(ITER)))
41     DENO1 = G1+RAD
42     G1 RAD = G1 - RAD
43     L1 (CABS(DENO1) .LT. CABS(G1RAD)) DENOM = G1RAD
44     IF (CABS(DENO1) .LE. 1.0E-20) GO TO 4
45     E1P1 = -2.0*F(ITER)*DI/DENOM
46     3 H1P1 = EI*E1P1
47     E1(ITER+1) = EV(ITER) + H1P1
48     IF (NOTE(27)) WRITE (6,101) EV(ITER+1)
49     101 FORMAT (' MULLER'S METHOD REQUIRED FOR THIS ITERATION. EV(ITER+1) = '
50     11*Z(16.8)
51     MULLER = .TRUE.
52     RETURN
53

```



```
54      4 E1P1 = (1.0,0.0)
55      IF (NOTE(27)) WRITE (6,102)
56 102 FORMAT (' E1P1 SET EQUAL TO 1.0')
57      GO TO 3
58      END
```


ORTHCR

```

1      SUBROUTINE ORTHCR(Z,ITER,K,ANGLE,IJ,P,KORTH,AGLMIN)
2      COMPLEX P,Z,S
3      LOGICAL NOTE
4      COMMON /SNS/ N,MRKTOT,KMAX,KMAX2/BLR0/NOTE(30)
5      DIMENSION Z(N,N,KMAX2),P(N,N,KMAX2),KORTH(KMAX2),S(3,3)
6      IF (K .EQ. 1) GO TO 6
7      2 IF (ANGLE .GE. 90.0) GO TO 6
8      C DETERMINE ANGLE BETWEEN SOLN VECTORS
9      DO 4 J=1,N
10     S(J,J) = (0.0,0.0)
11     DO 3 I=1,N
12     3 S(J,I) = S(J,J) + CONJG(Z(J,I,K))*Z(I,J,K)
13     4 S(J,I) = CSRT(S(J,J))
14     DO 9 L=2,N
15     JJ = L-1
16     DO 9 J=1,JJ
17     S(J,L) = (0.0,0.0)
18     DO 5 I=1,N
19     5 S(J,L) = S(J,L) + CONJG(Z(J,I,K))*Z(L,I,K)
20     GAMMA = ACOS(CABS(S(J,L))/(S(J,J)*S(L,L))))
21     GAMMA = GAMMA*57.29578
22     AGLMIN = AMIN1(AGLMIN,GAMMA)
23     IF (NOTE(29) .AND. ITER .EQ. 1) WRITE (6,101) J,L,K,GAMMA
24 101 FORMAT (' ANGLE BETWEEN SOLN VECTOR',I2,',',I2,',',I2,' AT KP ',I4,
25   1' IS ',F9.4,' DEGREES.')
26     IF (GAMMA .LE. ANGLE) GO TO 6
27     9 CONTINUE
28     RETURN
29     6 CALL GSORTH(Z,P,K)
30     KORTH(IJ) = K
31     IJ = IJ+1
32     RETURN
33     END

```


DIFFEQ

```

1      SUBROUTINE DIFFEQ(F,DY,Y,H,K)
2      COMPLEX DY,Y,P,C2,C3,C4
3      COMMON /SLKS/N,M,K10T,KMAX,KMAX2
4      DIMENSION DY(1),Y(1),C2(6),C3(6),C4(6),P(6)
5      CALL F(Y,DY,K)
6      DO 1 I=1,M
7      1 P(I) = Y(I) + (H/2.0)*DY(I)
8      CALL F(P,C2,K-1)
9      DO 2 I=1,M
10     2 P(I) = Y(I) + (H/2.0)*C2(I)
11     CALL F(P,C3,K-1)
12     DO 3 I=1,M
13     3 P(I) = Y(I) + H*C3(I)
14     CALL F(P,C4,K-2)
15     DO 4 I=1,M
16     4 Y(I) = Y(I)+(H/6.0)*(DY(I)+2.*C2(I)+2.*C3(I)+C4(I))
17      RETURN
18      END

```


APPENDIX E

The Computer Program in Operation - Selection of Numerical Parameters

The numerical program developed to solve the stability problem outlined in Chapters II and III is written in FORTRAN V language and evaluated on a Univac 1108 digital computer. Just as discussion of the complete problem has been divided into two categories (mean and disturbance), so too is the computer program:

- (1) Solution of the mean flow equations in real, double-precision arithmetic, and then calculation of the variable coefficients required for solving the disturbance equations;
- (2) Solution of the eigenvalue problem in complex, single-precision arithmetic and subsequent manipulation of the eigenfunctions to compute Reynolds stresses, dissipation, etc.

Operation of all or part of these two elements is regulated by a series of input logical variables.

In addition to the parameters (or eigenvalues) which explicitly characterize the formulated stability problem (α_R , α_I , w_∞ , Re , and of course T_w , T_∞ , and M), there are also adjustable parameters which implicitly characterize its numerical solution (e.g., step size, orthonormalization criterion, specification of boundary layer edge, etc.). Since the latter govern the ability to accurately and efficiently determine the former, discussion of the program's operation will be developed around the optimum selection of these numerical parameters.

To better illustrate the difficulties associated with making such a selection, numerical examples are calculated for each parameter for the same typical "eigenvalue" with fixed:

$$T_w = 90^\circ\text{F}, T_\infty = 60^\circ\text{F}, M = 0, \alpha_I = 0, \text{ and } Re = 7000.$$

Table E.1 demonstrates the sort of results obtained for the same fixed parameters and with: $h_d = .0175$, $\Omega = 88^\circ$, $\eta_{\max} = 10$, and $\eta_\delta = 5.7925$ ($\bar{u}_\delta = .999020$).

α_R	$\omega_\infty \times 10^6$	Comments
.123764	3.72957	Including fluctuating temperature field but without density fluctuations.
.121905	3.66240	Without fluctuating temperature field but with all mean fluid properties variable in disturbance equations.
.122347	3.68283	Including <u>all</u> mean and fluctuating quantities, equations (2.37 - 2.40)
.118809	3.56218	Without fluctuating temperature field but with variable mean viscosity only (Wazzan, et.al equation (1.2) [3 - 6]).
.119928	3.60135	Wazzan's equation using property variation described by Kaups and Smith [7] (see Figure B.7).

TABLE E.1 The Influence of Included Disturbance Quantities and Chosen Property Variation on an Eigenvalue Calculation.

E.1 Boundary Layer Edge, η_{\max} and η_δ

Two distinct length scales must be specified to accurately solve the eigenvalue problem: η_{\max} , the finite value of the independent variable, η , at which the mean flow's asymptotic boundary conditions (eqns. (2.21a)) are assumed to be approximately satisfied; and η_δ ($\eta_\delta < \eta_{\max}$), arbitrarily selected boundary layer edge where asymptotic disturbance flow conditions are satisfied. For computational purposes, there is no reason to suggest that the two need be the same. While the former is associated with obtaining accurate mean velocity and temperature profiles, the latter determines where these profiles may be truncated for the eigenvalue problem without appreciably degrading the accuracy of its solution.

The practical capability for determining the proper η_{\max} , however, is contingent upon utilization of an efficient means for calculating the initially unspecified, mean-flow, wall boundary conditions, $\bar{u}'(0) = F''(0)$ and $H'(0)$. The effectiveness of the particular method used in this investigation [18] for finding these conditions is demonstrated by the example in Table E.2 where

$$T_w = 90^\circ\text{F}, T_\infty = 60^\circ\text{F}, M = 0, h_m = .02, \eta_{\max} = 10.$$

Iteration	n	STEP	$F''(0)$	$H'(0)$
Guess			1.0	-1.0
1		2	0.63890603	-0.80589459
2		10	0.45716795	-0.71569664
3		10	0.46637891	-0.71328643
4		10	0.46639972	-0.71321361
5		10	0.46639971	-0.71321361
6		10	0.46639971	-0.71321361

TABLE E.2 Convergence History of Unknown Mean Flow Boundary Conditions, $F''(0)$ and $H'(0)$.

With 0.55 seconds required for the first iteration, approximately 2.78 seconds/iteration thereafter, and six iterations, both convergence to values of $F''(0)$ and $H'(0)$ with better than eight-place accuracy (for the specified fluid property variation, of course), and calculation and allocation to storage of all mean-flow coefficients needed for solution of the disturbance equation can be accomplished in less than twenty seconds (see Table E.3).

Final selection of n_{\max} is determined by observing the value for which an increase in this parameter fails to make a discernable change in $F''(0)$ and $H'(0)$. It is reasoned that values of n_{\max} greater than this one will not alter the mean flow profiles (thus, the variable coefficients for the disturbance equations) and so must represent an unnecessary expenditure of computational effort and time.

The results of such an η_{\max} search for the mean wall temperature and velocity gradients considered in this study are presented in Table E.3. In all cases, $F''(0)$ and $H'(0)$ were unchanged for $\eta_{\max} \geq 10$. Thus, noting that the time required to solve the mean flow equations and compute disturbance equation coefficients varies only slightly over the η_{\max} range considered, accuracy rather than economy governed the selection:

$$\eta_{\max} \equiv 10.$$

This value ensures satisfaction of asymptotic conditions (eqn. (3.4)) to order (10^{-18}) . Due to its importance in calculating the eigenvalue, the influence of η_{\max} on η_{δ}^* is also displayed in Table E.3. As a basis of comparison, it may be noted that the value of $F''(0)$ for the unheated, flat plate case agrees well with Howarth's value of $F''(0) = .33206$ [9, p. 129].

The primary considerations for selecting η_{δ} were founded in attainment of an accurate eigensolution and reduction of running time and storage requirements (known a priori to be relatively large when eigenfunction recovery is required [20]). Although the time restriction could be relaxed somewhat if the information were needed badly enough, storage limitations (150,000₈ for the Univac 1108 computer) could not. To evaluate the effect on the eigenvalues of using a "truncated" mean flow solution, the example shown in Table E.4 was calculated with: $T_w = 90^\circ F$,

η_{\max}	$F''(0) = \bar{u}'(0)$	$H'(0)$	η_{δ}^*	E (defined by Eqn.)	Time Required (sec)
<u>$T_w = 60^\circ F$</u>					
6	.33255559		1.7152416	.52436x10 ⁻⁵	13.8464
7	.33209439		1.7203045	.43557x10 ⁻⁷	15.3772
8	.33205907		1.7207617	.13211x10 ⁻⁹	16.7630
9	.33205738		1.7207868	.14727x10 ⁻¹²	17.7298
10	.33205733		1.7207876	.60392x10 ⁻¹⁶	18.8970
11	.33205733		1.7207876	.91101x10 ⁻²⁰	20.9158
<u>$T_w = 90^\circ F$</u>					
6	.46680267	-.71341605	1.5112973	.19198x10 ⁻⁵	14.6256
7	.46642702	-.71322750	1.5142917	.12898x10 ⁻⁷	16.1574
8	.46640087	-.71321419	1.5145365	.31727x10 ⁻¹⁰	15.2932
9	.46639974	-.71321362	1.5145486	.28695x10 ⁻¹³	17.0454
10	.46639971	-.71321361	1.5145491	.95693x10 ⁻¹⁷	18.9308
11	.46639971	-.71321360	1.5145491	.25249x10 ⁻¹⁹	19.7002
<u>$T_w = 150^\circ F$</u>					
6	.74345286	-.78390563	1.2098509	.35870x10 ⁻⁶	14.5934
7	.74320905	-.78382177	1.2111477	.17598x10 ⁻⁸	14.5190
8	.74319434	-.78381662	1.2112361	.31693x10 ⁻¹¹	15.8284
9	.74319379	-.78381642	1.2112399	.21000x10 ⁻¹⁴	16.9238
10	.74319378	-.78381642	1.2112400	.68194x10 ⁻¹⁸	17.7392
11	.74319378	-.78381642	1.2112400	.17341x10 ⁻¹⁸	19.3116

TABLE E.3 Influence of η_{\max} on computed values of $F''(0)$, $H'(0)$, and η_{δ}^* .

$T_w = 200^\circ F$

6	.96336141	-.83923358	1.0362211	.11659x10 ⁻⁶	12.3970
7	.96318694	-.83918394	1.0369269	.47597x10 ⁻⁹	13.5738
8	.96317728	-.83918114	1.0369723	.71388x10 ⁻¹²	14.8100
9	.96317695	-.83918104	1.0369741	.39403x10 ⁻¹⁵	16.5640
10	.96317694	-.83918104	1.0369741	.68671x10 ⁻¹⁸	18.4704
11	.96317694	-.83918104	1.0369741	.61905x10 ⁻¹⁸	18.5082

$T_\infty = 60^\circ F$, $M = 0$, $h_m = .02$

TABLE E.3 Continued

$T_\infty = 60^\circ F$, $M = 0$, $h_d = .02$, $\Omega = 45^\circ$, $Re_\delta^* = 7000$, $\alpha_I = 0$ (lower branch without density fluctuations).

η_δ	\bar{u}_δ	# Steps	# Ortho-normalizations	Time/ Iteration	α_R	$\omega_\infty \times 10^6$
7.00	.999959	351	102	11.1514	.123762	3.72956
6.70	.999903	336	102	10.7356	.123765	3.72957
5.80	.999038	291	99	9.5320	.123817	3.72989
4.68	.990055	235	96	7.6570	.124466	3.73420
3.14	.900150	158	91	5.1472	.134641	3.83808

TABLE E.4 Influence of the Arbitrarily Specified Boundary Layer Edge, η_δ , on the eigenvalue computation.

Note that consideration of additional segments of the boundary layer does not appreciably change the number of ortho-normalizations required, suggesting that most of them are required in the region near the wall. It does, however, require more

integration steps and so more time per iteration. Unfortunately, due to storage and time limitations, it is more difficult to ascribe a definite value to η_δ (also the case for the disturbance equation step size, h_d) than for η_{\max} . Even using the maximum allocated storage ($h_d = .02$ and $\eta_\delta = 7.0$), variations in the eigenvalue are still slightly greater than their indicated six place accuracy.

Since even four place accuracy is adequate to clearly delineate between calculations with and without temperature fluctuations (see example in section 3.4), it is sufficient to specify

$$\bar{u}_\delta = .999$$

as the position at which the boundary layer may be truncated for stability calculations.

Greater accuracy than that indicated in Table E.4 is restricted by both storage and the interdependence of η_δ and h_d in the program; when h_d must be reduced, so too must η_δ according to the relationship $h_d > \eta_\delta/350$.

E.2 Step Size, h

Perhaps no other parameter more critically governs the accuracy and efficiency with which a solution is numerically calculated than does the step size. If it were chosen too large, the fourth order Runge-Kutta and Adams-Moulton integration schemes (with truncation errors proportional to h^5) would be basically inaccurate, rapid changes of the dependent variables (such as in the thermal boundary layer for large Pr) would be obscured, and (most importantly for this analysis) between consecutive steps, for a given αRe , linear independence of the solution vectors may be destroyed beyond accurate restoration by the orthonormalization procedure, independent of the Ω specified (see section 3.4.3). If chosen too small, not only would integration time and storage be prohibitively large, but error propagation, enhanced by the increased number of mathematical operations required, would contaminate the solution sooner and thus require more frequent orthonormalization within a given interval (see section 3.3),

Thus, to solve the disturbance equations, the selected h must be very closely related to the specified values of αRe and Ω . Since accurate convergence is ensured only by giving the orthonormalization procedure a chance to work effectively, as αRe increases, h should be decreased and Ω increased. In mapping out a stability contour, the point at which convergence difficulty can be anticipated is preceded by a limited range of smaller αRe in which the number of iterations required for convergence is greatly

increased and more importantly, the minimum angle encountered between solution vectors drastically drops to less than 1° . At or beyond this point, convergence could be obtained only by decreasing the step size. It is interesting to note that similar difficulties were encountered by Mack [24, p.283] (in a scheme not using orthonormalization), but at much smaller values of αRe .

In contrast, for the numerical values calculated using the fourth order system of Wazzan, et.al [3], no such difficulty was found. One possible explanation can be advanced by considering the examples given at the beginning of section 3.4. For the sixth order system (that is, the problem as formulated in this study but without density fluctuations), the minimum angle encountered during the boundary layer integration was 36.40° , whereas for the fourth order system (Wazzan's equations) it was 78.21° . Since the region in which significant thermal fluctuations exist is much smaller than that of the velocity fluctuations, it can be expected that the step size accordingly must be smaller for the sixth order system to maintain the same degree of orthogonality as for the fourth.

Since the Runge-Kutta integration scheme requires information at half-step intervals, the mean equations are integrated with a step size, h_m , half that of the one used to solve the disturbance equations, h_d , (i.e., $h_m = h_d/2$). This permits the program to calculate the required variable, mean-flow-dependent coefficients for the latter exactly for all points.

An example illustrating some of the points discussed above is given in Tables E.5 and E.6 for: $T_w = 90^\circ\text{F}$, $T_\infty = 60^\circ\text{F}$, $M = 0$, $\eta_{\max} = 10$, $\bar{u}_\delta = .999$, $\Omega = 45^\circ$, $\text{Re}_\delta^* = 7000$, $\alpha_I^* = 0$ (lower branch without density fluctuations).

h_m	$\bar{u}'(0)$	$H'(0)$	η_δ^*
.01	.46639971	-.71321361	1.5145491
.02	.46639971	-.71321361	1.5145491
.03	.46639972	-.71321358	1.5145490
.04	.46639973	-.71321352	1.5145489
.05	.46639977	-.71321341	1.5145489
.06	.46639982	-.71321321	1.5145487

TABLE E.5 Influence of Step Size, h_m , on the Unspecified Wall Temperature and Velocity Gradients, $\bar{u}'(0)$ and $H'(0)$.

h_d	#Steps	Time/ Iteration(sec)	#Orthonor- malizations	α_R	$\omega_\infty \times 10^6$
.01675	347	11.1042	103	.123819	3.72996
.02	291	9.5320	99	.123817	3.72989
.03	194	6.4763	94	.123812	3.72967
.04	146	5.0016	78	.123797	3.72917
.05	117	4.0280	67	.123774	3.72834
.06	98	3.3430	59	.123741	3.72718

TABLE E.6 Influence of the Step Size, h_d , on the Computed Eigenvalue.

From these calculations ($\alpha Re = 866.6$), it appears that at least four place eigenvalue accuracy is obtainable by using $h_d < .03$. Note that this choice also ensures eight place accuracy of the mean flow solution (for the specified property variation). For results given in Chapter IV, a step size of $h_d = .02$ or smaller was used.

E.3 Orthonormalization Angle, Ω .

As previously indicated (section 3.3), the orthonormalization criterion used for this study is a specified minimum angle permitted between complex solution vectors. (A comparison of relative magnitudes of the vectors also could have been used [39]). If this angle were chosen too large (e.g., 90° as for Wazzan, et.al. [3]), aside from an increased integration time, the extensive matrix manipulation required for the orthonormalization procedure could be expected to introduce errors in the solution [39]. Alternatively, if it were chosen too small, then linear independence of solution vectors could be so degraded that insufficient resolution would remain to accurately reestablish an orthonormal basis.

Since the parametric group αRe appears exponentially in the exact solution to the disturbance equations outside the boundary layer (see equations (3.11 - 3.15)) or inversely as a coefficient multiplying the highest order derivative term (see equations (1.2 - 1.4)), it can be anticipated that as αRe increases, so too should the rate at which the solution vectors linear independence

degenerates. It follows, then, first that for the specified Ω , the number of orthonormalizations required must also increase. Secondly, as Ω is increasing to accommodate the larger value of aRe , so too should the percentage of orthonormalized integration steps, ranging from zero when $\Omega = 0^\circ$ to one hundred when $\Omega = 90^\circ$. These observations are substantiated by Figure E.1 and Table E.7.

Care must be exercised to ensure that Ω is chosen sufficiently large that the resolution of solution vectors is not lost between successive integration steps just before the orthonormalization criterion is violated. That is, if the smallest angle between solution vectors at one step is greater than Ω , but less than Ω at the next, this minimum angle must still be large enough to enable reformation of the orthonormal basis. When degeneration of orthogonality is sufficiently rapid to require orthonormalization at consecutive steps, it can be expected that the minimum angle between solution vectors (and thus convergence capability) would cease to be a function of Ω and become one of the step size instead, as indicated in Figures E.1 and E.2.

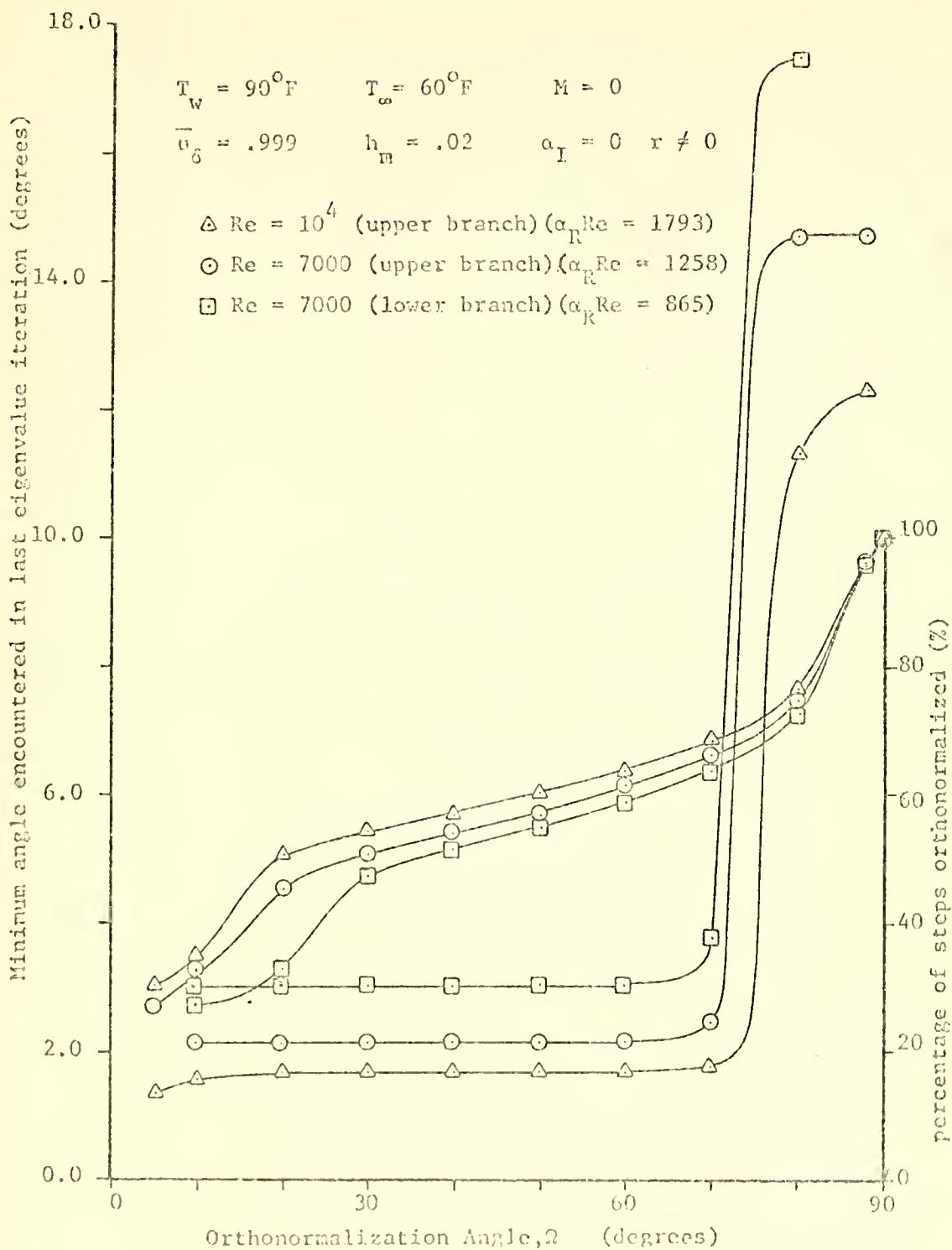


Figure E.1 Influence of the Orthonormalization Angle, Ω , on the number of orthonormalizations required per iteration and on the minimum angle encountered in the last boundary layer integration.

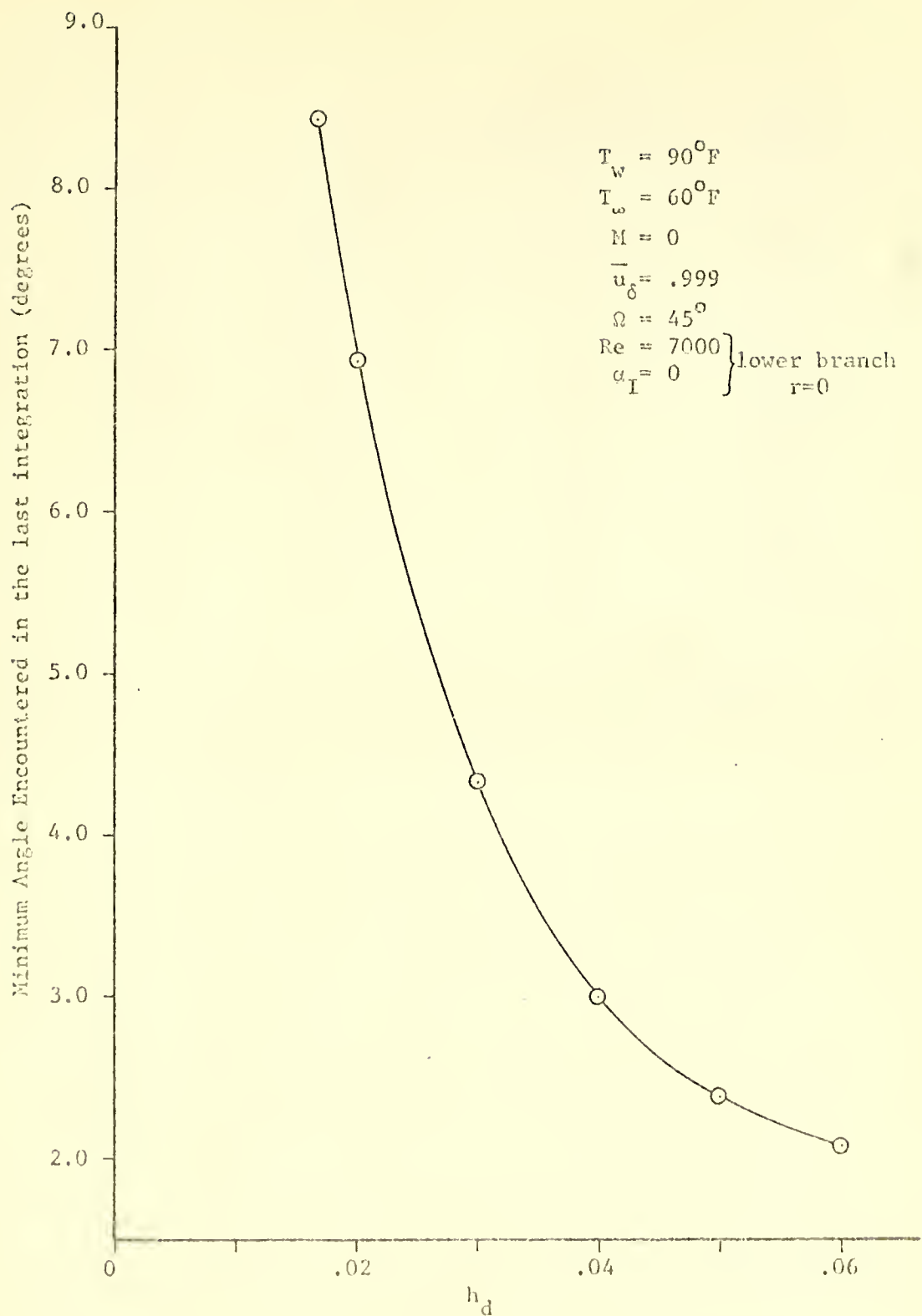


Figure E.2 Influence of the step size on the minimum angle encountered between solution vectors on the last eigenvalue iteration for a specified Ω .

Ω	a_R	$\omega_\infty \times 10^6$	Number of Orthonormaliza- tions required	Minimum Angle
5	.179330	3.70852	44	1.3547
10	.179330	3.70852	50	1.5390
20	.179330	3.70852	74	1.6808
30	.179330	3.70852	79	1.6808
40	.179330	3.70852	83	1.6808
50	.179330	3.70852	88	1.6808
60	.179330	3.70852	93	1.6808
70	.179330	3.70852	100	1.7733
80	.179330	3.70852	112	11.3345
88	.179330	3.70853	140	12.3368
90	.179330	3.70853	146	not computed

where $Re = 10^4$, $a_I = 0$, $h_d = .04$, $\bar{u}_\delta = .999$ (upper branch, $r \neq 0$)

TABLE E.7 Influence of Orthonormalization Angle, Ω , on Computed Eigenvalue.

On the basis of these calculations, it would seem that although the minimum angle between solution vectors is profoundly affected by the specified orthonormalization angle in some regions, the computed eigenvalue is not. Further, in the intermediate range of Ω , there is a region in which the number of required orthonormalizations is significantly less than for $\Omega \approx 90^\circ$ and where this number varies only slightly with Ω . Naturally, such a reduction translates as a significant savings in required program running time. For example, for the $Re = 7000$ (upper branch) calculation shown in Figure E.1, the time required

to complete eigenvalue convergence (in seven iterations) is reduced from 36.9 to 34.4 seconds by specifying Ω equal 50° rather than 88° , still with almost six-place accuracy. Thus, selection of Ω apparently can be based primarily on computational economy; that is, it is chosen to reduce the number of computer manipulations and program storage requirements.

Since these results are typical of others found during the course of this study, it is felt that the selection

$$\Omega = 45^\circ$$

represents a good balance between accuracy and efficiency. To note in passing, this choice is also compatible with the results of Gersting and Jankowski [20].

E.4 Eigenvalue Estimates, α , ω , and Re

As indicated in section 3.3, three eigenvalue estimates are required to start either of the root-finding schemes used in this study (i.e., that of Wazzan, et.al. or Muller). To trace out a contour in parameter space, the first eigenvalue estimate, ev_1 , is taken from the lower branch of the stability curves of Wazzan, et.al. [4] near the minimum critical Reynolds number (see for example Figure 4.4). This procedure is employed for two reasons. First, since the present investigation represents a departure from the Wazzan results due to the inclusion of a fluctuating temperature field and consideration of all fluid property variation, it would

seem that these should give the best available initial estimate. Second, as the difficulty of solution increases with increasing αR (due to problems associated with degeneracy of the orthogonality of solution vectors, etc.), an eigenvalue on the new contour is chosen for which solution should be easiest (see also discussion by Mack [24, p. 280]).

The second and third eigenvalue estimates are arbitrarily chosen as $ev_2 = 1.01 ev_1$ and $ev_3 = 1.005 ev_{1R} + 1.02 ev_{1I}$. With the three initial eigenvalue estimates thus specified, the three corresponding boundary layer admittances, Y_o , can be calculated.

The plane fitting technique of Wazwan, et.al. is used first, conditionally followed by that of Muller. That is to say, only when all the following criteria are violated will the latter be utilized:

$$(1) \quad 10^{-3} < \left| \frac{ev_{jR}}{ev_{jI}} \right| < 10^3$$

(2) from the denominator of a_o

$$\begin{aligned} & \left| \left[(Y_{oj} Y_{o(j-1)*})^2_I + (Y_{o(j-2)} Y_{oj*})^2_I \right. \right. \\ & \left. \left. + (Y_{o(j-1)} Y_{o(j-2)*})^2 \right] \right| < 10^{-15} \end{aligned}$$

- (3) Muller's method was not used in computing the preceding estimate. (It was found that consecutive application of this method gave poor convergence.)

In general, this scheme worked well, ensuring six place accuracy within five to eight iterations (depending on the accuracy of the initial guess). At first, to ensure uniform convergence (after the first three arbitrary estimates, $ev_1 \rightarrow ev_3$), an estimated "eigenvalue" obtained by either method was first averaged with the most accurate one previously calculated (i.e., that one which gave the smallest value of $|Y_o|$) before reevaluating the stability equations. However, since this procedure was found to increase (by as much as 50%) the number of iterations required for convergence, it was modified to average only when the condition of uniform convergence was violated (i.e., when the condition $|Y_{o(j-1)}| > |Y_{oj}|$ was not satisfied). When Muller's method was used alternately as discussed, it was found to be very effective, usually refining the "eigenvalue" estimate so as to reduce $|Y_o|$ by several orders of magnitude. Thus, the net result is an iteration scheme which ultimately but sporadically converges, often in a nonmonotonic fashion.

An example of the convergence is given below for $T_w = 90^\circ F$, $T_\infty = 60^\circ F$, $M = 0$, $\Omega = 50^\circ$, $h_d = .04$, $\bar{u}_\delta = .999$, $Re = 7000$, $\alpha_L = 0$, $\alpha_R = .12233$, $\omega_\infty = 3.6821 \times 10^{-6}$ (lower branch including density fluctuations, $r \neq 0$).

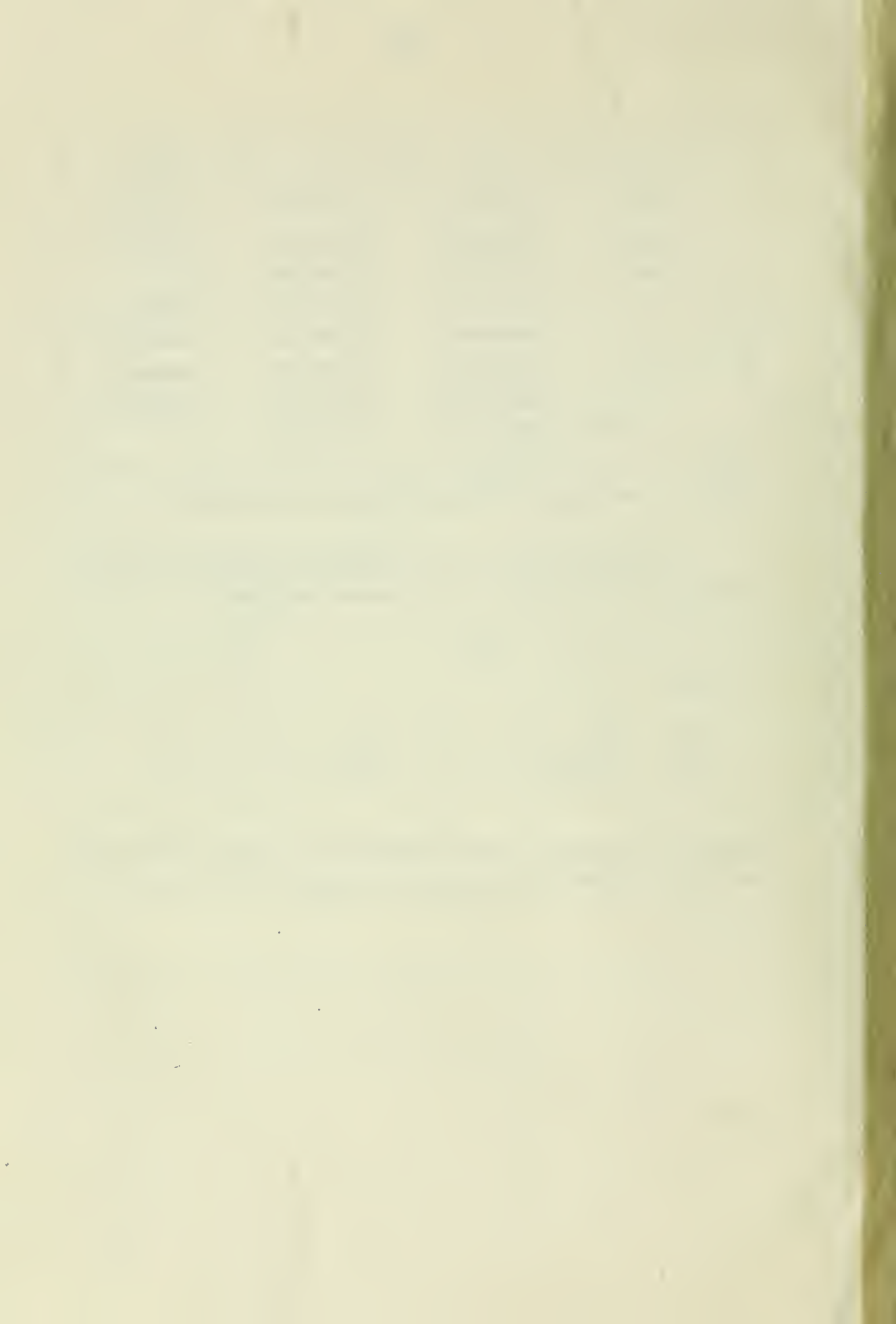
Iteration	$\bar{\alpha}_R$	\bar{w}	$ y_o $
Guess 1	.081212293	.017239455	.432x10 ⁻¹
Guess 2	.082024415	.017411849	.342x10 ⁻¹
Guess 3	.081618354	.017584244	.139
1	.081367993	.017209441	.176x10 ⁻¹
2	.080728449	.017008234	.332x10 ⁻³
3	.080769324	.017018352	.323x10 ⁻⁴
4	.080769138	.017018221	.311x10 ⁻⁶
next estimate	.080769140	.017018221	

TABLE E.8 Convergence History of an Eigenvalue Search

In keeping with previous discussion of obtainable and required accuracy, iteration was terminated when both

$$\left| y_o \right| \quad \text{and} \quad \left| 1 - \frac{ev_{jR}}{ev_{(j+1)R}} \right| \quad \text{and} \quad \left| 1 - \frac{ev_{jI}}{ev_{(j+1)I}} \right| \quad \left. \right\} < 10^{-5}$$

This criterion usually ensured "eigenvalue" accuracy to six places and "zero" wall boundary conditions of order (10^{-7}) or less.



Thesis
L865

Lowell

146221

Numerical study of
the stability of a
heated water boundary
layer.

17 JAN 74

DISPLAY

Thesis
L865

Lowell

146221

Numerical study of
the stability of a
heated water boundary
layer.

thesL865
Numerical study of the stability of a he



3 2768 002 12690 6
DUDLEY KNOX LIBRARY